INVESTIGATIONS OF FLOW AND PRESSURE IN SILOS DURING FILLING AND DISCHARGING IN PRESENCE OF INSERTS

By

Songxiong Ding

A thesis submitted for the degree of

Doctor of Philosophy

December 2004

To my family

ABSTRACT

This thesis is mainly concerned with the study of flow and pressure in silos during filling and discharging. It describes the numerical and experimental studies undertaken to investigate the effects of filling modes and inserts on the flow and pressure in silos.

The numerical investigations were performed using two different finite element codes: SILO from Sweden and the commercial Abaqus Code. Finite Element (FE) models were developed to simulate a progressive filling process, and used to investigate the development of filling pressures along the walls of a steep hopper and a shallow hopper. Two filling modes were simulated: a concentric filling mode and a distributed filling mode. The FE results obtained were compared with the predictions from classic theories, and for the case of the shallow hopper, also with the results measured in large scale experiments.

The investigation of the effect of inserts on silo flow using the FE code SILO shows that the insert converts the discharge pattern from funnel flow to mass flow in a silo with a modest inclination hopper. Parametric study further exhibited that a combination of a careful positioning of the insert and a reduction of wall friction between the solid and hopper walls would improve the silo discharge pattern in a silo with a shallower hopper. The residence times of tracers were measured to identify the flow pattern in the experiments with a double cone insert and compared with the numerical predictions.

Measurements carried out in a full scale axi-symmetric silo with a 45° hopper showed that a loss of pressure symmetry started during filling even though the pile

formed appeared to be axi-symmetrical. An installation of the double cone insert led to a slight increase of filling pressure and its unevenness at the transition level. During discharge, the normal pressure increased substantially in a small region close to the transition in the hopper, but decreased considerably in the lower part of hopper. The presence of an insert was found to increase the flowing zone during discharge, but with a risk of increasing loss of symmetry in the flow and pressures.

DECLARATION

The candidate hereby declares that this thesis entitled "Investigations of flow and pressure in silos during filling and discharging in presence of inserts" has not been, either in whole or in part, previously submitted for a degree in this or other institutes, and the work presented in this thesis is original.

The candidate has published following papers related to the thesis during the course of research.

1. S. Ding, S. R. de Silva and G. G. Enstad, 2003, Effect of Passive Inserts on the Granular Flow From Silos Using Numerical Solutions, *Particulate Science and Technology*, 21, 211-226.
2. S. Ding, G. G. Enstad and S. R. de Silva, 2003, Development of load on a hopper during filling with granular material, *Particulate Science and Technology*, 21, 259-270.
3. S. Ding, M. Wojcik, M. Jecmenica, and S. R. de Silva, 2003, Loads on walls and inserts in mass-flow silos, *TASK QUARTERLY* 7 (4), 525-538.
4. S. Ding, G. G. Enstad, 2003, Stress distribution in the material and development of loads on the wall during hopper filling, *TASK QUARTERLY* 7 (4), 512-524.
5. S. Ding, G. G. Enstad and F. O. von Hafenbrädl, 2004, Measurement of double cone inserts effects on the loads along a full-scale silo, *POWTEC 2004*, Nuremberg, Germany, March 15-19.
6. S. Ding, G. G. Enstad, 2003, FE approach to the sensitivity of load on a hopper to the filling method and process with granular material, *Proceedings of IMECE'03 ASME International Mechanical Engineering Congress & Exposition,* Washington, D.C., USA, November 16-21.
7. S. Ding, G. G. Enstad, 2003, Effect of feeding rate on the loads measured along the wall of a full-scale hopper during filling, *The Sixth Conference on Measurement and control of Granular Materials*, Shanghai, China, Aug. 20-22.
8. S. Ding, G. G. Enstad, M. Wojcik and F.O. von Hafenbrädl, 2003, Measurement of filling and discharging loads in a full scale hopper, *The 4th International*

Conference for the Conveying and Handling of Particulate Solids, Budapest, May 27-30.

9. S. Ding, 2002, Numerical prediction of flow patterns and loads on walls and inserts in a silo, *Particle Technology UK Forum IV*, AIChE, The University of Leeds, England, April 11-12 (Extensive abstract).
10. S. Ding, J. Y. Ooi and M. J. Rotter, 2002, FE investigations of the effects of a passive insert on flow patterns in silos, *15th International Congress of Chemical and Process Engineering "CHISA 2002"*, Aug. 25-29.
11. S. Ding, J. Y. Ooi, and M. J. Rotter, 2002, Simulations of silo discharge flow patterns and predictions of loads on walls and inserts, *15th International Congress of Chemical and Process Engineering "CHISA 2002",* Aug. 25-29.
12. S. Ding, M. Jecmenica, M. Wojcik, 2001, Finite element predictions of loads on walls and insert in a gravity flow silo, *Scandinavia Abaqus Users' Conference*, Gåteberg, Sweden, Sept. 21-22.
13. S. Ding, G. G. Enstad, M. Jecmenica, and S. R. de Silva, 2001, Simulation of a Double Cone's effect on granular material flow in silos, The *7th international conference on bulk material storage, handling and transportation,* Newcastle, Australia, Oct. 25-29.
14. S. Ding, F. O. von Hafenbrädl, G.G. Enstad, M. Jecmenica, 2001, Observations on the change from funnel to mass flow in silos by means of a double core, The *7th international conference on bulk material storage, handling and transportation* Newcastle, Australia, Oct. 25-29.

Signed: [redacted]

Songxiong Ding

Conference for the Conveying and Handling of Particulate Solids, Budapest, May 27-30.

9. S. Ding, 2002, Numerical prediction of flow patterns and loads on walls and inserts in a silo, *Particle Technology UK Forum IV*, AIChE, The University of Leeds, England, April 11-12 (Extensive abstract).
10. S. Ding, J. Y. Ooi and M. J. Rotter, 2002, FE investigations of the effects of a passive insert on flow patterns in silos, *15th International Congress of Chemical and Process Engineering "CHISA 2002"*, Aug. 25-29.
11. S. Ding, J. Y. Ooi, and M. J. Rotter, 2002, Simulations of silo discharge flow patterns and predictions of loads on walls and inserts, *15th International Congress of Chemical and Process Engineering "CHISA 2002"*, Aug. 25-29.
12. S. Ding, M. Jecmenica, M. Wojcik, 2001, Finite element predictions of loads on walls and insert in a gravity flow silo, *Scandinavia Abaqus Users' Conference*, Gåteberg, Sweden, Sept. 21-22.
13. S. Ding, G. G. Enstad, M. Jecmenica, and S. R. de Silva, 2001, Simulation of a Double Cone's effect on granular material flow in silos, The *7th international conference on bulk material storage, handling and transportation,* Newcastle, Australia, Oct. 25-29.
14. S. Ding, F. O. von Hafenbrädl, G.G. Enstad, M. Jecmenica, 2001, Observations on the change from funnel to mass flow in silos by means of a double core, The *7th international conference on bulk material storage, handling and transportation* Newcastle, Australia, Oct. 25-29.

Signed:

Songxiong Ding

ACKNOWLEDGEMENTS

This PhD project has been carried out on a "home and away" base, a special arrangement between the University of Edinburgh (UOE), Scotland and the University College Telemark (UCT), Norway arching over the North Sea. Such an arrangement was initiated by the late Prof. De Silva at UCT and achieved by Prof. Rotter at UOE. The author is grateful for their efforts to set up such a platform for him to stage in.

The author is greatly indebted to his supervisors Dr. Ooi, Prof. Rotter at UOE and Profs. Enstad and De Silva at UCT for their consistent encouragement, inspiring guidance, and commanding strategy at some crucial moments. The author values very much the friendship thereby developed.

The author was sponsored by POSTEC (POwder Science and TEChnology), a department at Telemark Industrial R&D Centre, Porsgrunn, Norway, where the author spent most of his time during his candidature. He is thankful for this financial support.

The author wishes to thank the staff at POSTEC. Their efforts to make all the facilities required available and functional in time are very much appreciated. Many thanks go to Mr. M. Wojcik, a Marie Curie scholarship fellow, and Dr. M. Jecmenica, a staff at the UCT, for their assistance in setting up the facility and conducting experiments.

The interests of Dr. R. Royles at EOU in reading the manuscript in its preparation, and his valuable comments and suggestions are gratefully acknowledged.

The author would like to thank friends and colleagues at the Institute for Infrastructure and Environment at UOE. In particular, many thanks are due to Dr. Z. J. Zhong, Dr. T. Hong and Mr. B. Chun and Ms Y. P. Zhang; their friendships made the author's stay in Edinburgh quite memorable.

Special thanks reserve for my family, the lovely children in particular. To them the author dedicates this thesis.

CONTENTS

1 OVERVIEW AND SCOPE

1.1 Introduction

Bulk solid storage is a fundamental part of materials handling in many industries, such as mining, food processing and chemical engineering. For such industries, silos or bunkers are designed and built as a vital part. A silo is often constructed in either metal or concrete. In appearance it looks rather simple, but usually involves a large capital expenditure.

It might well seem that a silo is simple. The bulk material (solids) is filled into a silo from the top, and left in the silo until it is discharged through an outlet in the bottom. The simplest enduring theory to describe the mechanics of the material in a silo was devised by Janssen (1895). It explained how the pressure exerted on silo walls from particulate materials changes with depth and is strongly affected by wall friction. Unlike a hydrostatic distribution, an asymptotic condition is approached at great depth: the horizontal pressure in the lower part of a tall silo is only a small fraction of the value for a similar water container. As a result of wall friction which transfers vertical load from the stored material and induces vertical compression forces in the wall, the compression force in the wall progressively increases, even at great depth.

Following understanding of this phenomenon, simple structural systems were used for silos: silos were designed for quite small internal pressures. However, as economic development progressed from the 1950s onwards, taller and larger silos were needed to store larger quantities of material. The simpler silo design ideas, adequate for small silos, were assumed to apply to these large structures, but many failures resulted.

Serious damage to many silo structures (Fig. 1.1) began and continue to be very common in all countries of the world (Rotter, 2001). The rate of silo failures is far

higher than other engineered structures, estimated to be between 100 and 1000 times that of buildings. Jenkyn and Goodwill (1987) concluded that over 1000 structural failures occur in silos in North America every year: many of these failures were in metal silos, but this may reflect the proportion of silos built in each construction material. The failure record in Europe is less well documented, but there is extensive evidence that the failure rate may be quite similar.

Fig. 1.1 Modern silos and an example of structure damage

Except for the failure of structure, problems of reliable solids flow occur very frequently. These are dominated by material arresting, flooding or segregating. These phenomena usually cause economic losses far in excess of the cost of the silo facility itself, because the arresting or degrading of the solids feed stream results in an entire plant being shut down or becoming less economic.

The failures and the economic losses led to more serious and systematic silo research at the beginning of the 1960s. Much effort was expended on both the functional and structural design of silos. As a result, some solid achievements have been made: notable amongst these are the criteria for mass and funnel flow, which are widely used in silo functional design (Jenike, 1964, 1987; Drescher, 1991, 1992, 1998).

Because of the complexities involved, however, serious problems continue to occur, and new phenomena emerge that were rarely mentioned before, producing new challenges and difficulties for researchers and designers. The difficulties mainly lie in the following areas:

1. There is great variety in the mechanical behaviours and characteristics of bulk solids, and

2. The interactions between the bulk solids and walls result in quite complex effects, particularly when geometric imperfections in the walls, zones of local polishing, and the flexibility of the structure affect the stresses in the solid.

Neither of these areas is well understood yet: the scientific understanding of solids in silos remains poor, despite several decades of energetic research. As a result, questions concerning solids flow during silo discharge, the loads induced by the solids on the walls of a silo after filling or during discharge, and the relationship between the flow and loads, all still present great challenges and require further investigation. Research on silos is a big task indeed.

1.2 Challenges in silos

It is well known that the silo pressure pattern and magnitude both usually change from filling to discharging (Ketchum 1907; Pieper and Wenzel, 1964). These changes cannot be predicted without knowledge of the flow patterns that develop during solids discharge. The flow patterns themselves may depend on the manner in which the silo is filled (Sugden, 1980; Zhong at al., 2001). A filling mode may be brought under control (for instance by a device to force concentric filling of the silo), but even then the flow pattern during discharge is still hard to predict.

1.2.1 Challenges in securing stable flow of solids

It is the objective of all silo designs to obtain a reliable and controllable flow of particulate solids in any handling process and to secure the safety of the silo structure. If the silo is poorly designed, the following effects in solids flow often occur (Jenike,

1964; Rotter, 2001):

1) No flow takes place when the outlet is opened. A stable arch is formed above the outlet which prevents flow (Fig. 1.2 (a)). This may happen both with fine powders and coarse solids and is generally attributed to the development of cohesion in the solid or to mechanical arching;

2) The flow stops after a while. Only the bulk solid which is located vertically above the outlet flows out while the remaining bulk solids (material in the dead zones) form stable vertical walls thus creating a 'rat-hole' or 'pipe'(Fig. 1.2 (b)); or

3) The flow is erratic.

Methods to try to overcome the problems of arching or rat-holing include the use of aeration, vibration, air cannons and hammers. The stored cohesive solid does not always start to flow as desired, and sometimes it either compacts even more or discharges in an uncontrolled manner ("floods"). Unreliable flow often occurs when fine solids (powder) forms and arch which then collapses and picks up air during the dynamic event, becoming aerated and leading to flow similar to that of a fluid, which produces flooding. The fine solid then similarly to a liquid: it may pass through most small openings, and it may be very difficult to control the flow (Fig. 1.2 (c)).

If the rate of discharge can be controlled, with solids flow in either mass flow or funnel flow, other problems may also arise (e.g. segregation). Mass flow is defined as a flow pattern where the bulk solid is all in motion within the silo whenever the silo is discharged. Funnel flow is defined as any pattern which is not mass flow (Jenike, 1964). Some segregation usually occurs under funnel flow conditions; and its prevention is largely addressed by the adoption of mass flow silo geometries and careful filling procedures if segregation must be avoided.

The flow pattern in a funnel flow silo remains a major topic for research because asymmetries in the flow pattern can increase the unpredictability of the flow, and can also endanger the silo's structural integrity. Reliable methods of predicting the details

of the flow pattern, based on high quality experiments, are badly needed.

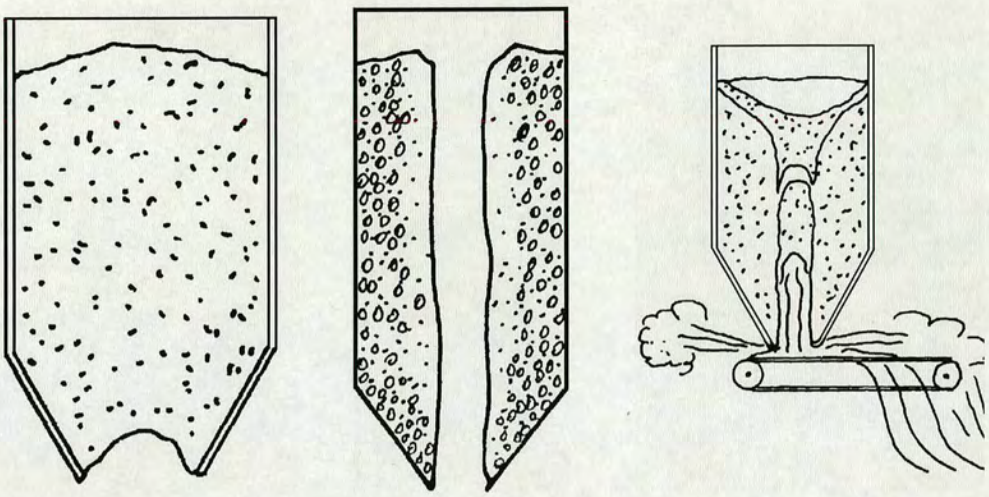

(a) Arching (b) Rat-holing (c) Flooding

Fig. 1.2 Typical examples of silo functional problems

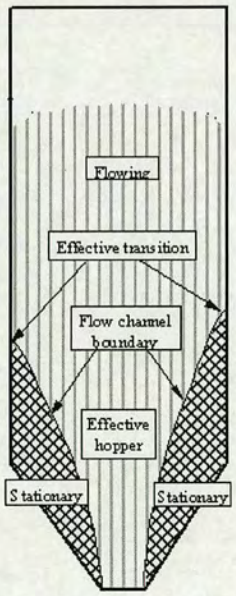

Fig. 1.3 The flow channel boundary (FCB) in a funnel flow silo (Rotter, 2001)

The principal challenge in predicting the flow pattern in funnel flow is to establish the shape of the flow channel boundary (Rotter, 2001). This boundary is defined as the interface between flowing and stationary solid as illustrated in Fig. 1.3. The point at

which this boundary strikes the silo wall is termed the 'effective transition'. Many experimental observations of the flow channel boundary have described the flow boundary as non-linear, often becoming steeper away from the orifice.

1.2.2 Challenges concerning the loads on silo walls

Accurate determination of the loads on silo walls is not only important to ensure the structural integrity of a silo and the requirements of feeders or other discharge equipment below the silo. It is also necessary to design the silo geometry for functional purposes. For example, calculations to determine the size of the outlet opening for reliable flow (Roberts, 1987; Rotter, 2001) require that the stresses generated with the bulk material and exerted on the silo walls are found, since these determine the cohesion that will develop during storage and thus control the incidence of arching. The minimum outlet size B for a given hopper half angle θ and wall friction μ depend on the flow properties of the solid and the stresses developing in the individual silo.

The pressures on silo walls during emptying are very different from those after filling. Filling pressures are usually close to the pattern of the Janssen distribution, though the magnitude of the lateral pressure ratio is often uncertain, and may vary a little from one filling to another. The pressure distribution during discharge or flow is generally more complex. Theories that describe the pressures on silo walls during symmetrical mass-flow emptying are now better established than those for funnel-flow, but there remain many large discrepancies even between the mass flow predictions. Much further work is needed before the effects of different material properties on these pressures are fully understood.

Many experimenters, from the earliest times (Ketchum, 1907), have observed that increased pressures, commonly referred to as "overpressures", occur on silo walls during discharge. Some experimenters have reported that these pressures may be up to three times greater than the Janssen filling pressure at the same position, but there is some doubt about the significance of these observations (Rotter, 1995, 2001). It is not clear whether these large pressures occurred over a large area, or whether the equipment used to make the measurements gave a reliable indication of the true state

in the bulk solid. These overpressures are typically largest shortly after the start of the discharge, when the silo is still virtually full to capacity, but when a flow channel has fully developed. This is not a state that can truly be realised, as the silo is never full by the time the flow channel has developed, but as the design condition, it is known as the "Full Condition" (Rotter, 2001). Most research studies and design treatments attempt to address this condition.

It is also widely believed that overpressures in funnel flow silos occur during discharge principally near the point where the flow channel boundary intersects the silo wall (effective transition). In mass flow, it is widely believed that the high pressure point is at the top of the mass flow hopper (transition).

High pressures are however not in themselves necessarily a serious danger to silo structure provided they remain symmetrical (Rotter, 2001). High pressure must be seen in the context of the structural form and the way in which the structure carries loads. For this reason, local low pressure can be more damaging than very high but symmetrical pressure (Rotter, 1998, 1999).

Munch-Andersen and Nielsen (1990) and Ooi et al. (1990) reported an unsymmetrical pressure distribution around the circumference at a given height following symmetrical filling. This suggests that geometric imperfections in the silo wall and variations in wall roughness may both have an important influence on either the flow pattern or the pressure distribution.

Loss of symmetry can also be attributed to a loss of homogeneity in the solid, leading to anisotropic behaviour, which is developed by the initial packing during filling (Nielsen, 1998). Thus, unless the mechanism of packing is understood, the mechanics of these solids cannot be modelled. The sensitivity of granular materials to the stress history and the role of geometrically imperfect boundaries present other complications in interpreting experimental observations and understanding the mechanics of silo pressure and flow regimes.

Because there is a serious lack of precision in predicting the geometry of the flow

channel in funnel flow, the wall loads also cannot be defined with precision. Large displacements of the stored granular solid occur whenever a silo is discharged. Measurements of the pressures during flow, combined with visual observations of flow patterns and control tests on solids, have revealed several phenomena contributing to pressure variation during flow (Roberts, 1993; Roberts and Wensrich, 2002). Not only are the pressure variations time-dependent within a single silo, but significant systematic differences are found between one silo and another, even when the two are superficially identical and contain similar materials (Nielsen, 1998). One serious result is that silo pressures may often be quite unsymmetrical even in symmetrical silos (Ooi at al., 1990), and this is one of the most dangerous phenomena for the safety of silo structure (Rotter et al., 1986; Rotter, 1999).

1.3 Strategy to improve the solids flow and reduce silo wall loads

1.3.1 Mass flow or funnel flow

Mass-flow presents some obvious advantages: mass-flow guarantees complete discharge of the silo contents at flow rates that are generally predictable. It is a 'first-in, first-out' flow pattern: that is, the first material to enter the silo is the first to be discharged, so that ageing of stored material is not a problem. When successfully designed, a mass-flow silo can re-mix bulk solids which may have segregated during the filling of the silo.

However, mass flow also presents some disadvantages. A steep smooth hopper is needed, which means that the silo must be quite tall, bringing a serious cost penalty. Wear of the silo walls may also be a problem when abrasive solids are stored. The height required to achieve a reasonable capacity may lead to particle degradation on impact during filling.

The main disadvantages of funnel flow are that the flow may be erratic with a tendency to form stable pipes which stop the silo from discharging. When flow does occur, segregation may take place. Funnel flow is often thought to be an undesirable flow pattern for cohesive or deteriorating bulk solids.

Nevertheless, under funnel flow the bulk solid protects the silo walls from wear. Because funnel-flow silos are characterised either by their squat hopper geometry or their flat bottoms, they store more material than a mass flow silo of the same overall height and diameter. The advantages of reduced headroom, reduced capital expenditure and reduced wear make it an attractive solution provided measures can be taken to overcome the disadvantages outlined above.

1.3.2 The use of inserts

As noted above, both funnel-flow silos and mass-flow silos have their own advantages and disadvantages. For different applications, different flow patterns should be chosen and silos designed accordingly. Many silo problems are related to the flow pattern that develops during discharge, and controlling the flow pattern in a silo is often the key to solving a functional problem. For example, by changing a silo from funnel flow to mass flow, segregation can be reduced or eliminated when the silo is discharged. Methods of changing funnel flow silos into mass flow silos require investigation. The commonest method is to make the hopper steeper or to choose a smoother hopper wall material. However, such methods are not always practical, and furthermore, they usually cost a great deal to implement in existing silos. Other methods, including transformation of a funnel flow geometry into an expanded flow silo (Fig. 1.4) and the introduction of inserts into the hopper therefore deserve investigation (Fig. 1.5).

An expanded-flow silo, shown in Figure 1.4, is often the ideal solution to the dual requirements of storing more material within a given height, and maintaining the reliable discharge characteristics (Roberts, 1987). However, some observations of expanded flow silos in service (Fig. 1.4, right) suggest that stagnant zones may still exist, so the solution is not complete.

Inserts were used (Johanson and Kleysteuber, 1966; Johanson, 1970) for the purpose of blending material. Later, they were also exploited to obtain mass flow (Johanson, 1982; Carson and Royal, 1992), to eliminate segregation and reduce flow problems. Many silos have hoppers with wall angles of 60° to the horizontal. Even with such steep hopper angles, some of these still do not function as mass flow. As a result,

problems such as rat-holing, flooding and segregation, which are commonly associated with funnel flow, frequently occur. By taking an existing hopper and installing a successfully designed insert, it may be possible to cause a funnel flow conical hopper geometry to function as if the slope was at 75° to the horizontal. Thus an appropriate insert may change the solids flow from funnel flow to mass flow. For instance, the cone-in-cone insert (Fig. 1.5), marketed by Jenike & Johanson Inc and by J. R. Johanson Inc. allows the annular region to perform in mass flow when the hopper wall inclination to the horizontal is lower than would be required otherwise.

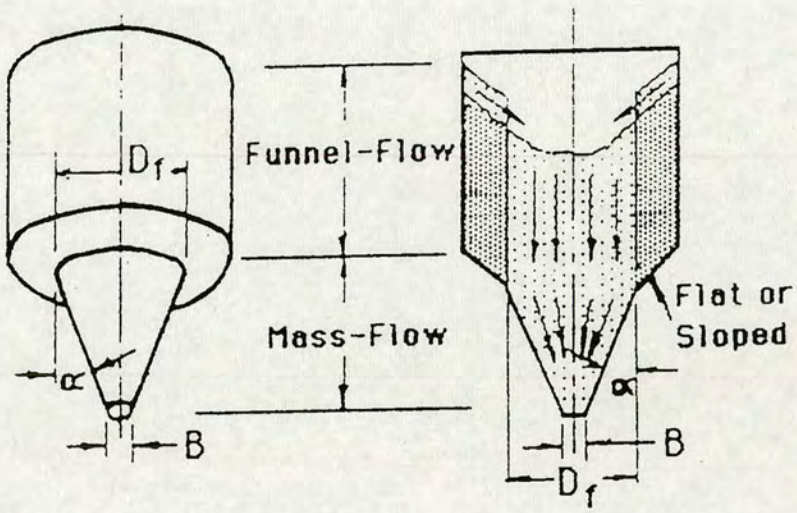

Fig. 1.4 The expanded silo (Roberts, 1987)

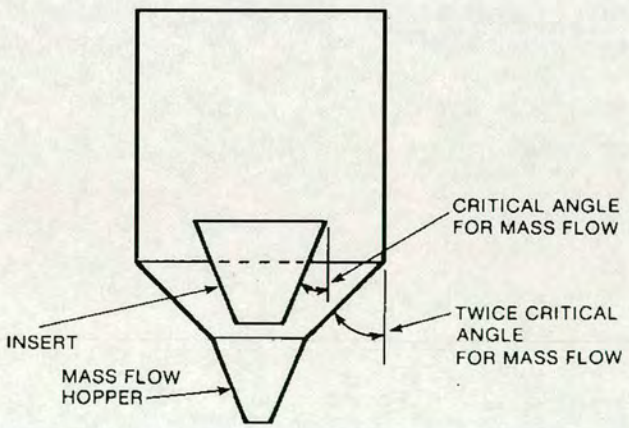

Fig. 1.5 The cone in cone insert (Johanson, 1982)

Even if this ideal outcome cannot be achieved, the insert may transform a narrow

funnel flow zone into a much wider flow. When this is done, the stored bulk solid must flow around the insert, producing an increased flow zone. Under some circumstances, both an improvement in the flow pattern and a reduction in segregation can be achieved by the use of an insert.

1.4 Background and scope of the thesis

1.4.1 Background to the thesis

Investigations of the behaviour of granular and particulate bulk solids in silos date back to Roberts (1884), Janssen (1895) and Ketchum (1907). It was already evident by 1910 that the Janssen (1895) theory provided a reasonably good prediction of the pressures which occur after filling, that larger pressures were sometimes encountered during discharge, and that eccentric discharge could cause high unexpected pressures. However, in some respects, the progress of knowledge has been rather difficult ever since; major progress in terminology and definition does not appear to have occurred until the work of Jenike and his colleagues (1961). Much progress in silo conceptual development may be credited to Jenike (1964). The experimental and theoretical investigations of Jenike and his co-workers (Jenike, 1961, 1962, 1964, 1967,1968, 1969; Jenike, Johanson and Carson, 1973) had, in both theoretical and experimental investigations, a great influence on many studies afterwards.

In the context of silo pressure theories, many different analytical models have been proposed. These models mostly adopted rather simplified plastic models and assumed that the granular material is an isotropic homogeneous continuous single phase. With such simplifications, continuum mechanics could be used for theoretical analyses. Some considerable achievements were obtained: the criterion widely used to predict a mass or funnel flow for functional design purposes (Jenike, 1961, 1964, 1987; Drescher, 1992, 1998).

These simplified models, mostly using only a plastic treatment of the solid, were quite inadequate to represent observed behaviour in experiments. As a result, most for structural engineering design is based on Janssen's theory with empirical adjustments for the conditions of discharge (ACI, 1989; ACI 313, 1991; Eurocode ENV 1991-4,

1995; Rotter, 2001). The mismatch between the simple theories and the results of experiments has also led to many attempts to find better models, most of which involved the same homogeneous isotropic continuum assumption, but with more complex non-linear continuum models to represent the solid. With the arrival of these more complex models, purely algebraic methods appear to be rather limited; computational modelling represents a powerful tool and has been used to cope with the new challenges. However, it does have a major disadvantage that the solid must be characterised by many more parameters, many of which are difficult to measure. For engineering design, it is necessary to know the properties of the solid, so much more experimental development on property measurement will be needed before these models can be used in practice (Rotter, 1998).

The last two decades have seen many attempts to develop computational models to represent the behaviour of granular materials in silos. To date computational models present an opportunity to resolve some problems met in past research work. The most commonly used, and currently the most useful method is the finite element method (FEM) (Rotter et al., 1998; Rotter, 1998).

The FEM, based on continuum mechanics, has become well established in silo research. Eliminating many approximating assumptions, it can provide a description of a problem that take many details into account, and a great variety of silo problems can be studied. Calculations starting from the bulk material at rest up to the initiation of flow are possible. In principle, there seem to be few restrictions concerning the silo geometry and the bulk material, only a question of computer speeds and capacity, as well as better constitutive laws of bulk material behaviour. Nevertheless, it may be noted (Rotter, 1998) that FEM cannot represent the filling process, but must assume the properties and geometry of the filled solid *a priori*, and the anisotropic and inhomogeneous character of bulk solids (Hartlen at al., 1984; Nielsen, 1998) has not yet been addressed significantly at all.

In a finite element analysis, the analysis may be static or dynamic, and may be carried out using either a Lagrangian formulation (Bishara, 1977; Ooi and Rotter, 1990; Wu and Schmidt, 1992; Anand and Gu, 2000; Martý´nez etc. 2002), an Eulerian

formulation (Huassler and Eibl, 1984; Karlsson, 1996), or a mixed Eulerian-Lagrangian formulation (Wieckowski et al., 1999; Ding et al., 2002; Socolaret et al., 2002). Some of these analyses may also be conducted using an advanced commercial package such as Abaqus (2002, 2003), but mostly they have been the result of research on computational mechanics by researchers who wrote their own codes in Fortran or C specifically for the analysis of granular materials (Rombach, 1998). The computer facility and resources at the Institute for Infrastructure and Environment at the University of Edinburgh and at POSTEC (a research centre belonging to the Telemark Technological R&D Centre, University College Telemark, Norway), where the author undertook most of his candidature, provide unique opportunities. The FEM package Abaqus, available at both establishments, and an FEM code called SILO (Karlsson, 1996; Karlsson et al., 1998) which the University College Telemark acquired from Karlsson at Luleå University, Sweden, are both used in this thesis to carry out investigations into the behaviour of solids in silos .

The above describes both algebraic and computational studies of granular solids pressures and flow. However, these always need to be verified against experimental studies which measure the real behaviour of solids. Silo flow and pressure measurements have always been carried out to improve our knowledge of silos, and most current design is simply based on this experimental database. The behaviour of solids in silos are complex, so silo tests are vital to verify any theoretical predictions. Since the earliest tests on model silos in the late 19^{th} century (Ketchum, 1907), many silo tests have been carried out. The majority of these were on model silos in laboratories rather than on full scale silos, and most involved only pressure measurements: few scientific measurements of flow were made.

The objective of pressure measurement is to determine the forces exerted on the walls and bottom of the silo during filling and discharge. Two methods are available for the determination of these forces:

- Local direct measurement of the normal and tangential stresses applied by the solids, using pressure cells. These measurements are rather difficult to perform without serious error (Askegaard et al., 1971) and the cells must satisfy very

strict conditions (Askegaard and Andersen, 1982; Askegaard, 1986). Furthermore, it is not clear what may be happening between the locations of the pressure cells, and the proper size of the pressure cell to measure a "mean" local value is not so easy to determine.

- Measurement of the strains in the silo wall using strain gauges or other similar devices. This method encounters two main problems: the effects of temperature variations and temperature gradients can induce strains that may be of the same order of magnitude as those due to the internal pressure; and the rigorous deduction of the pressures acting on the structure from these strain readings requires a major computational effort (Chen et al., 1998).

Pressure cells mounted in the silo wall have been most widely used for wall pressure measurements in previous studies.

Experiments to study granular solids flow can be divided into three groups: those to study the flow mechanisms, those to distinguish the flow pattern, and those to determine the solids moving paths and velocity fields. These studies have often concerned the effects of various parameters that control the flow. The opaque character of most bulk solids limits the possibilities for making useful observations of the internal movement within a mass of solid, but observations of the top surface profile are often misleading. Simple examinations of abrasion, scouring and polishing signs along the walls are sometimes used, but these are unreliable indicators of the behaviour in the full condition and can only provide a little information about the flowing regions of solid. Studies of the internal flow field in silos represents a tough challenge, so some ingenious techniques, such as the radioactive pill tracking technique and tracer residence time measurements, have been specifically devised for specific measurement circumstances.

In theory, the results of model tests can be translated to full-scale results. However, the reliability of such translations is in doubt. The question of scale effects was thoroughly explored by the Danish silo research group in the late 1970s and early 1980s (Nielsen and Kristiansen, 1979; Hartlen et al., 1984; Munch-Andersen and Nielsen, 1986;

Nielsen, 1998). They determined that scale effects can be very pronounced: many of the conclusions previously drawn from laboratory models were seen to be irrelevant to industrial installations. The extrapolation of observations made in laboratory models to full scale industrial silos remains most uncertain, despite the fact that most of what is currently known about silos has been obtained from laboratory models. However, for reliable information, it is necessary to carry out experiments at either full scale or pilot scale, the latter being similar to a small full scale silo.

Scientific measurements of flow patterns in full scale silos were rare until the full scale silo experimental project carried out at the University of Edinburgh in the 1990s (Rotter, et al., 1995). In this project, many experiments were conducted to measure solids flow patterns and wall pressures in two full scale silos. The technique of residence time measurement of radio tags seeded into the solid was adopted to measure flow patterns, and the strain gauges were mounted on the silo steel wall to measure strains (from which the pressure regime was deduced). Some sophisticated statistical work was undertaken to deduce the wall pressures, and the results of residence time measurements were subjected to many different interpretative processes to infer the solids flow pattern.

The silo battery shown in Fig. 1.6 was erected alongside the POSTEC Hall at the Telemark Technological R&D Centre (Tel-Tek), Porsgrunn, Norway during the period of the author's candidature. It consisted of a cylindrical silo and a rectangular silo, each with a 50 m^3 capacity. This initiative established a pilot scale silo research test facility, capable of undertaking large pilot scale experiments with both flow pattern instrumentation and pressure measurement capability.

For that purpose, a pressure measurement system was set up. It consisted of pressure transducers and a data logger. The pressure transducers were designed for both normal pressure and frictional traction measurements. They were mounted at designated locations on the silo walls – down a generator line and on one circumferential line just below the transition. The pressures exerted on the pressure transducers both after filling and during discharge were measured in this newly-built silo battery, and interpreted as loads on the silo wall. To implement the residence time measurement

technique for flow pattern measurement, an apparatus to seed radio markers in the solid during filling, and instruments to detect the markers radio signals during discharge, are still being constructed. They will be used in future tests to identify the flow pattern during silo discharge.

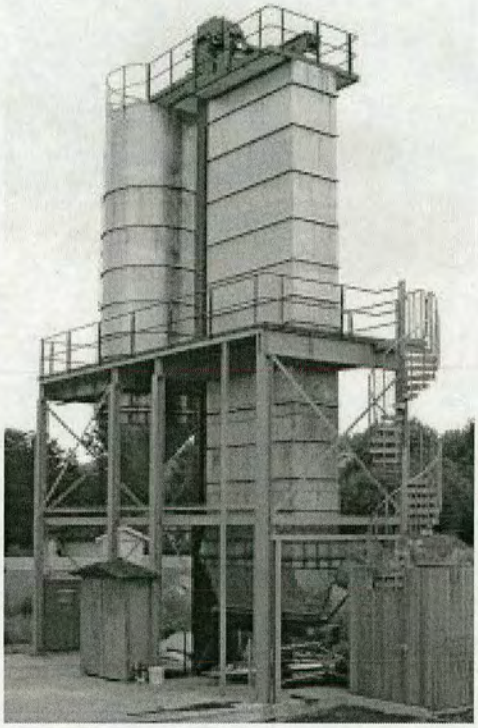

Fig. 1.6 The silo battery at POSTEC

Several types of flow promoting inserts have been investigated experimentally at the POSTEC Department of the Tel-Tek for some years now. These experiments were performed in model silos. When the pilot scale silo battery is completely ready, it is anticipated that larger scale experiments will be carried out to investigate the effect of inserts on flow during silo discharge, and on the pressure exerted on the silo walls after silo filling and during discharge.

1.4.2 Scope covered in the thesis

This thesis is concerned with the computational modelling and experimental studies of pressures on the silo wall during filling and discharge, and of the flow in a silo during discharge. It includes:

1. Numerical and experimental investigations of the development of pressure on the walls of a hopper with different filling methods (Chapter 3);

2. The use of computational methods to explore the effects of an insert on the solids flow during silo discharge (Chapter 4); and

3. Experimental measurements on the effects of inserts on the silo wall pressure and its distribution on the silo wall during filling and discharge (Chapter 5).

The subject matter of each of the following chapters may be briefly summarized as follows.

A literature review relevant to the topics included in the thesis is presented in Chapter 2. Starting with a "framework" on which most previous studies were based, a review of the main analytical achievements in the fields of solids flow and pressure are presented. This is followed by short descriptions of the dynamic phenomena (velocity and stress discontinuities and fluctuations) occurring during silo discharge. Various numerical methods used to predict the silo flow and wall pressures are also discussed. Attention is then turned to studies of experiments conducted for the measurement of both solids flow and silo wall pressures. The flow pattern observation techniques adopted in solids flow measurement are first reviewed and commented; the methods and achievements of silo pressure measurements are then presented and discussed. Finally the use of various inserts to enhance the discharge pattern of the stored solid is also covered in this review; it ends by highlighting the influence of an insert on the pressure distribution on the silo wall.

The commercial advanced finite element software package Abaqus (2002, 2003) is employed in Chapter 3 to develop a model that tries to represent the "progressive filling" of a hopper to simulate the process silo filling. This contrasts with previous research which mostly used the complete "switching on" of gravity on the whole stored mass. FEM models are devised to explore the effect of progressive filling in the first half of this chapter. In these computational models, the solids are filled into a steep hopper progressively with either a "distributed" or a "concentric" filling mode

(these being represented by different geometries for the top surface). This steep hopper had an apex half angle of 15°, with a ϕ 2400 mm upper edge and ϕ 400 mm outlet. The pressure distribution induced by both filling modes on the wall of this steep hopper is then presented. The predictions are compared with results calculated using classical algebraic theories for hopper pressures. In the second half of Chapter 3, the progressive filling model is again used to simulate the filling of a shallow hopper under concentric filling. This shallow hopper had an apex half angle of 45°, with a upper edge diameter of ϕ 2520 mm and a ϕ100 mm outlet. Experiments are also conducted on a shallow hopper of the same geometry. Comparisons between the computational predictions and the experimental measurements are presented.

Chapter 4 begins with an attempt to create a model with Abaqus to simulate a hopper discharge process by exploiting its mixed Lagrangian-Eulerian formulation. It transpired that there is a fatal error in the code for this relatively recent innovation in Abaqus, which is difficult to overcome. Effort was then shifted to the use of the finite element code SILO (Karlsson, 1986; Karlsson et al., 1998). It uses an Eulerian formulation and was able to simulate the solids flow in a steady state discharging process. In this chapter, this program was used to investigate the effects of several inserts on the flow. Some parametric investigations were also carried out to provide clues concerning the optimum location of a double cone insert. Experimental measurements were made in a laboratory scale silo of the residence times of markers that were seeded into the particulate material. These experiments were conducted to provide some validation of the computational simulation results.

The numerical models created in this thesis are confined to a two dimensional axisymmetric framework. It is currently beyond the capacity of these models to address the issues of loss of symmetry in the flow pattern observed in the experiments conducted in previous chapter. In Chapter 5 experimental studies are described to examine a question concerning asymmetry in the flow and the wall pressures in an axisymmetric silo when a double cone inserts is either present or absent.

Preliminary experiments were conducted first in a pilot scale silo. This pilot silo had a

cylinder diameter of ϕ 2520 mm and was 1500 mm in height, with a 45° conical hopper (the top and outlet of the hopper were ϕ 2520 mm and ϕ 100 mm in diameter). It was fitted with a double cone insert; the configurations between the insert and the silo were based on the numerical modeling findings obtained in the previous chapter. The wall pressure was measured using pressure transducers mounted at chosen locations on the silo wall. The filling loads were measured under concentric filling. Surface movement observations were used as an indication of the flow pattern during discharge, and the discharge pressures were measured. From the results, assessments of the effects of a double cone insert on the pressure distribution on the walls were made. These focused on the influence of the double cone insert on the load symmetry in the process of silo filling and discharge.

Experiments were then carried out in the larger pilot scale axisymmetric silo. This silo has a cylinder diameter of ϕ 2520 mm and is 7800 mm in height, with the same hopper as the earlier pilot scale silo. A configuration which performed best in the preliminary tests is chosen as the configuration between the double cone insert and this larger silo for further investigation in a silo battery. Tests parallel to those conducted in the smaller pilot scale silo were performed, and the issues of asymmetry of load distribution on the wall of the silo were further addressed.

Chapter 6 summarises the conclusions drawn from the studies of the previous chapters.

In the Appendices, key information relevant to the topics presented in the main text is provided. Appendix A presents the classical theories developed for calculations of pressure distributions in the processes of filling and discharge on the walls of hoppers. These formulas are used in the main text for the purpose of comparisons (Chapters 3 and 5). A brief description of the principle used in the pressure transducers and the calibration results are also given in Appendix B.

2 LITERATURE SURVEY

2.1 Introduction

Flow of granular material through silos, and the pressure on the walls of silos induced by the material during filling or in storage or in discharging, have been the topics of extensive theoretical and experimental research. The achievements are quite worth celebrating and well reflected in a great number of theoretical and experimental papers worldwide, even though there is still a long way to go.

The concern on flow mainly focuses on securing the operational adequacy in order to get an uninterrupted flow and reliable discharge, concentrating on required discharge rates and prevention of impediments to the flow. The interest in the issue of pressure is on the structural safety in order to ensure the strength of the silo body during various handling phases. These activities were interwoven, for instance, Jenike (1961), Spencer (1964) and Pariseau (1970) employed a failure criterion (Mohr-Coulomb) to determine the stress distribution within a static granular material, by which both the velocity field of material and the pressure on the wall were possible to be approximated from the known stress distribution.

In this chapter, a review relevant to this thesis is to be presented to cover the recent development and achievements.

2.2 Silo flow analysis

The flow of granular material through storage silos, and hoppers in particular, has its importance because of the direct involvements into many processes. Bad or unstable flow of solids can cause enormous financial losses if the flow of the solids is interrupted when the solid is to be extracted. Studies of flow patterns can be dated back to the earliest study of Ketchum (1907). He made brief reference to the differences in

flow geometries. However, major progress did not appear to have occurred until the work of Jenike and his colleagues in the early 60s last century.

2.2.1 Analyses framework

Considerable experimental effort has been dedicated to measuring and classifying the various types and shapes of the flow region as functions of bin/hopper geometry and height of material (Rajchenbach, 2000). They show that, upon opening the outlet, a dilation zone propagates upwards in the material. Depending on the geometry of the bin and the roughness of the walls, this zone assumes either a shape of a narrow plume or spreads over the entire width of the container. Often, localized dilation bands form from wall to wall; the density in this zone is distinctly lower than in the surrounding material, as is clearly seen in radiographs (Fig. 2.1) (Michalowski, 1987; Dresches, 1998). Except near the outlet, the boundaries of the plug-type zone are nearly vertical, and the zone widens laterally and may eventually reach the walls. The results obtained indicate complexity and time variability in the flow patterns, and this is affected further by particle size, angularity, bulk density, and material/wall interface friction.

When considering flow in silos, in hoppers in particular, Baxter and Behringer (1989), Ristow (2000) defined such a flow as either slow or fast flow, depending on the parameters of both material and hopper and material position in the silo. For instance, the material at the outlet is likely to be in rapid flow regime. Other material higher up in the hopper is moving slowly, and elsewhere within the hopper, the granular material may be stagnant. The material on surface at the top may show an avalanching behaviour.

Generally the slow flow is characterised by low deformation and small inertial forces; the solid particles behave as conglomerate and exhibit solid-like properties; during flow, the internal stress are generated only by normal and friction forces. The fast flow is interpreted as high deformation and large inertial forces. The particles lose their contacts and are subject to short impulsive collisions and overriding, and behave more like dense fluid; during flow, the internal stress occur due to both normal and friction forces between particles and impacting. Both fast and slow flow are energy-dissipated.

To describe the behaviour of the material during slow flow, continuum models are usually implemented, and of the material in fast flowing, the models treating the characteristic of individual particle are usually created and applied.

Fig. 2.1 Shear band shown in radiograph indicates the fact of unsteady state in silos (Michalowski, 1984; Drescher, 1998)

Litwiniszyn (1958) and Mullins (1972, 1974) recognised the discrete nature of the particulate medium and employed a stochastic approach to describe the discharge of a hopper. In this approach, it is assumed that the particles flow by falling into the space vacated by the departing particles in the layer beneath. The velocity profiles will depend on geometric factors alone and will be independent of the stress distribution. Nedderman and Tuzun (1987, 1979, 1995)proposed a variant of this method known as kinematic model. By applying the condition of continuity in incompressible flow, they derived a governing partial differential equation which led to solutions valid both in the converging flow zone and in a plane strain, flat-bottomed silo.

In contrast with the approach of discrete individual particles, Jenike (1961,1964) and Drescher (1998) argued that, neglecting the influence of contained gas on particle flow, and collisional effects characteristic of rapid flow similar to that in chutes flow, granular solid flow in silos can be considered as a one-phase material flow. With these simplifications, either the methods considering only the methods of continuum mechanics or the kinematics of particles, form the framework of the majority of

theoretical analyses.

With the framework, numerous mathematical models have been proposed for flow of granular or powder-like material as reviewed by Rajchenbach (2000). Rajchenbach summarised that the materials display numerous physical properties which remain poorly understood. There is, as yet, no single model which is widely accepted to account for behaviour of all real materials, under all practical or experimental conditions. For instance one can cite internal stress fluctuations, strain localization, non-Newtonian rheology exhibiting either intermittent avalanches or continuous flow regimes, size segregation or spatial pattern creations. All these phenomena have no equivalent in the classical solid- or liquid-state physics.

Approaches to the flow in silos are however currently carried out by some simplified model based on plasticity theory. Within the plasticity simplifications, further assumptions usually made to account for the deformations of granular solid in silos are the Mohr-coulomb theory and alike. The Mohr Coulomb theory assumes that slip planes will appear inside the bulk as soon as the internal state of stress overpasses the Coulomb criterion of failure. There are several other theories for the description of the velocity field, one well-developed theory is the double-shearing theory that was formulated in and developed by Spencer (1992, 2001).

Unsteady flow in bins and hoppers is usually set-up by in-homogeneities in the flow pattern. Theoretical work aimed at describing or predicting the flow have dealt primarily with the steady state flow. Steady flow may develop in loosely packed materials in tall bins or in shorter bins when the material is continuously supplied from above; smooth walls and round particles enhance steady flow further. A number of dynamic and steady-state analyses described by Drescher (1998) indicate that this steady-state assumption is a good engineering approximation for most practical purposes.

2.2.2 Silo flow mode and pattern

2.2.2.1 Solid flow patterns in silos

Jenike and his colleagues (1961 - 1973) made a large number of observations of flow in silo models, and gave the definitions of mass flow and funnel flow which are widely used today.

In mass-flow, the bulk solids are in motion at every point within the silo whenever material is drawn from the outlet (Fig. 2.2(a)). There is flow of bulk solids along the walls of the upper parallel section of the silo and the hopper (the lower converging section of the silo). In general, the velocity is fairly similar at all points in the vertical cylindrical part of the silo. Mass flow is generally regarded as desirable to ensure a smooth even supply of solid with little danger of flow interruption, or loss of effective storage capacity.

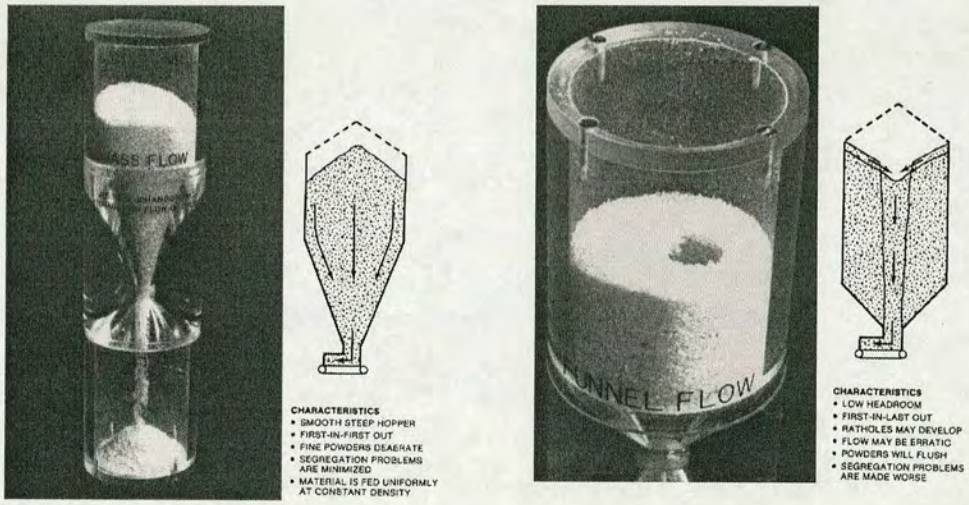

(a) Mass flow

(b) Funnel flow

Fig. 2.2 Modes of flows in silos (Johanson, 1982)

Funnel-flow is characterised by the bulk solid sloughing off the solid surface and discharging through a vertical channel which forms within the material in a silo (Fig. 2.2(b)). A central zone of moving solid develops above the outlet, and usually expands outwards towards the silo walls. After much of the solid is withdrawn, some of the

solid which was originally stationary may start to move, forming a wider flowing zone than before. Funnel flow occurs when the hopper walls are rough and the angle of inclination to the vertical is too large.

2.2.2.2 Mass flow or funnel flow

The derivation of the criterion for mass flow originated from Jenike (1962,1987) and Johanson (1964). They assumed that, because of the large shearing deformations developing during discharge, the granular material can be regarded as incompressible rigid-perfectly plastic, with yield condition containing one parameter: the effective angle of internal friction. They presented an exact solution for a particular plastic stress field in hopper called a radical stress field under steady state. They demonstrated that in conical hoppers there exists a critical combination of material effective friction angle, wall friction, and hopper half-angle beyond which the radial field cannot be constructed. This critical combination was taken as a criterion limiting the occurrence of mass flow.

Jenike's theory is based on the assumption of mass flow; and he showed that the bound for mass-flow in conical hoppers is given by

$$\alpha=\frac{1}{2}\{\pi-\cos^{-1}(1-\sin\delta)/2\sin\delta)\}-\beta,$$

where β is $\frac{1}{2}\{\phi_w+\sin^{-1}(\sin\phi_w/\sin\delta)\}$,

α is the hopper half-angle,

δ is the effective angle of internal friction,

ϕ_w is the wall friction angle.

For large hopper angles, and high wall friction angles, no solution exists; funnel flow must take place.

For plane-silo, the bound between mass and funnel flow are much less critical than for conical hoppers. In plane-flow hoppers, much larger hopper half-angles are possible which means that the discharging bulk solid will undergo a significant change in direction as it moves from the parallel to the converging hopper section.

The hopper angle, the wall friction and the effective angle of internal friction , as mentioned above, are the three most important parameters which determine whether the material in a silo will be discharged in mass-flow or funnel-flow. Jenike presented charts for the prediction of these flow patterns; they are summarised in Fig. 2.3.

The position of the limiting line depends slightly on the effective angle of internal friction δ. The abscissa and ordinate are the hopper angle α, and the wall friction angle, ϕ_w respectively. The mass flow and funnel flow regions are then separated by a limiting line. It is worth mentioning that the half-angles for plane-flow are up to 12° larger than the corresponding angles for conical hoppers.

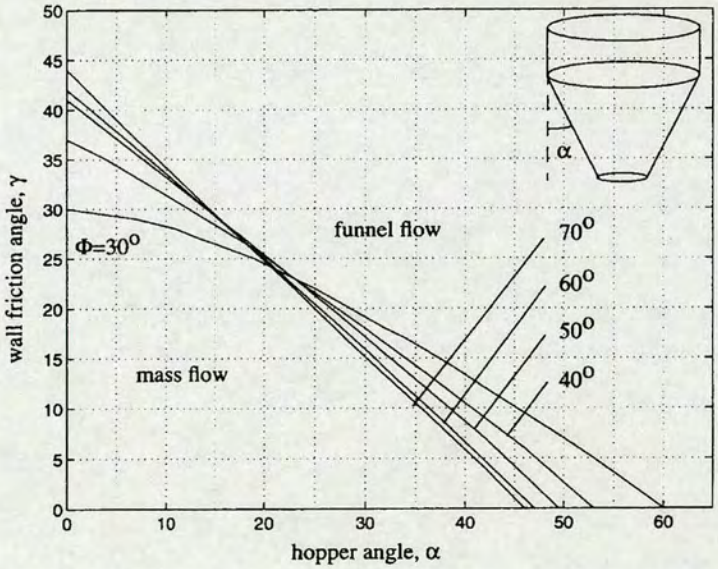

a. Jenike's chart for axi-symmetric silo

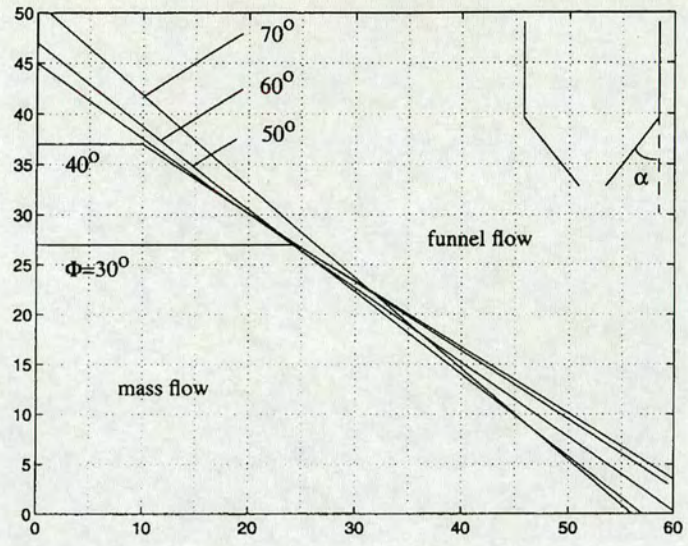

b. Jenike's chart for plane flow silos

Fig. 2.3 The Jenike chart (Jenike, 1964)

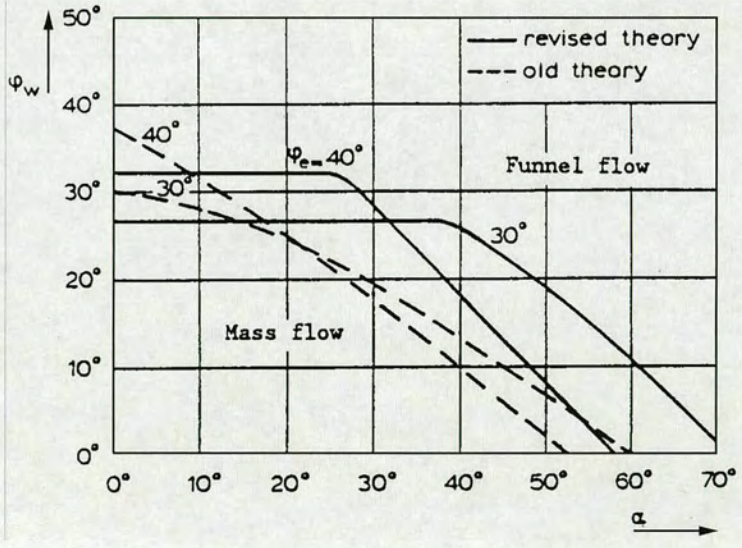

Fig. 2.4 Comparison between Jenike's original and revised theories for mass- and funnel flow limits (Jenike, 1987)

In 1987 Jenike presented a new theory for the limit between mass flow and funnel flow. This theory uses the Drucker-Prager yield criterion instead of the Mohr -

Coulomb yield criterion. In other words, the difference is that the former is based on the condition that the velocity becomes zero at the wall, while the latter is based on the fact that the stress becomes zero along the centre line of the hopper. As a result, this improved theory increases the mass flow region, and at the same time, shows two different flow patterns. A comparison between the original and revised limits is shown in Fig. 2.4.

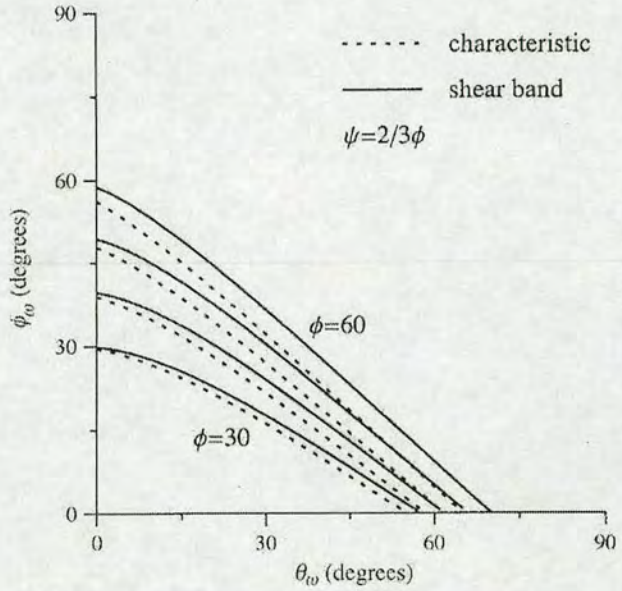

Fig. 2.5 Region of mass/funnel flow (the solid line derived from shear band theory, while the dash line from characteristic theory (Drescher, 1998))

Drescher also proposed a mass/funnel flow criterion based directly on the orientation of shear bands in hoppers (1991,1992, 1998; Drescher, etc. 1978, 1995). Experimental observations of the onset of flow indicate that in mass flow the shear bands emanating from the edges of an outlet propagate towards the opposing walls and undergo successive reflections. In funnel flow, on the other hand, the shear bands propagate towards the adjacent walls. The vertical orientation of the bands, corresponding to plug flow, is regarded as separating mass and funnel flow. The analysis of the limiting plastic state of stress at the wall to the outlet leads to the following criterion that must be satisfied for mass flow:

$$\tan\varphi_w = \frac{\sin\phi\cos(2\theta_w - \psi)}{1+\sin\phi\sin(2\theta_w - \psi)}$$

where: φ_w is the wall friction angle;

ϕ is the friction angle at shear band initiation;

θ_w is a critical hopper half—included angle beyond which the radium field cannot be constructed; and ψ is the corresponding dilatancy angle as show in Fig. 2. 5 as an example when $\psi=2/3\phi$ holds.

2.2.2.3 Predictions of FCB in funnel flow silos

Stagnant dead zones are a characteristic of funnel-flow. Flowing solid slides past stationary solid zones which forms an effective hopper. The boundary between flowing solid and stationary solid is called the flow channel boundary (FCB) (see Fig. 1.3).

Several authors (Lenczner, 1963; Brown and Richards, 1965) observed the presence of a curved flow channel boundary taking shape in model tests during discharge. Deutsch and Clyde (1967) demonstrated that the rigid block /rupture surface flow pattern can also occur in funnel flow silos. They believed that it is a fundamental mechanism as it occurs across a wide range of vessel diameter to material diameter ratios. They also proposed, following Johanson (1964), that these flow patterns represent a steady-state phenomenon for much of the period of discharge from the silo. Some research was conducted to predict the FCB.

2.2.2.3.1 FCB prediction by the kinematic model

Since the kinematic theory was firstly presented by Litwiniszyn (1958), a number of workers have carried out kinematic modelling of granular solid flow. Mullins (1972) formulated the kinematic theory using similar method of stochastic mechanic with different assumptions. Nedderman & Tuzun (1987,1992, 1995), Tuzun & Nedderman (1979) proposed a variant of this method. They all arrived at essentially the same governing equation although different assumptions were made in each case.

Nedderman & Tuzun (1992) assumed that if the two particles in the lower layer have different velocities, there will be a tendency for the upper particles to move side-way towards the faster falling particle. Tuzun & Nedderman (1979) put forward the very simple proposition that the horizontal velocity is a linear function of the horizontal gradient of the vertical velocity. Applying the condition of the continuity in incompressible flow to this proposition led to their governing partial differential equation. Tuzun & Nedderman (1979) exploited a solution valid in converging flow zone, and a more general product solution in plane strain, flat-bottom silo.

Continuing their research into discharge of glass from plain strain silos, Tuzun & Nedderman (1982) directed their work towards an investigation of the flow channel boundary. Long time exposures were used to measure the extent of the flowing region of solid in their experiments (1979). They found that FCB as assessed from the experiments corresponded closely with the theoretical velocity contour of 1 particle diameter per second and with streamline that bounded 99% of the total flow.

The applications of the kinematic theory were restricted to planar or semi-infinite silos until Graham et al. (1987) exploited a standard serious solution to solve the basic kinematic differential equation for discharge through a point orifice of an axi-symmetric silo. They obtained a theoretical prediction of the vertical velocity field, and developed a graphic method to determine the kinematic constant from experimental residence time data of particle on the centreline. By integrating down a particle trajectory, they calculated the residence time of each particle.

Clearly, only in very few special cases can standard solutions be exploited. For more general cases such as the silos with irregular geometry or silos with eccentric or multiple outlets, an analytical solution no longer exists. To extend the application scope of the kinematic theory, Watson (1993, 1995) implemented the kinematic theory in a finite element program.

Despite the simplicity in the kinematic theory, the outcomes indicate that this approach is viable when applied to the free flow of a dilated, smooth granular solid. However it is unable to analyse incipient flows of very frictional and consolidated granular solids.

As reviewed and explained by Rotter and Zhang (1995), the kinematic approach assumed that the velocity field is completely independent of stress, any effects of inter-particle frictions or wall friction are excluded. The emphasis is on solving the equations for velocities and fluxes in the granular solid mass rather than for pressure and stresses. They concluded that this model cannot be used to predict the existence of a truly stagnant zone.

2.2.2.3.2 FCB prediction by plasticity theory

The methods based on the concepts of plasticity, as pioneered by Jenike (1961), can in principle predict the existence of the stagnant zone. In plasticity theory, the material behaviour is assumed to be independent of silo strain rate. For the materials consisting of hard, dry and cohensionless particles, the assumptions that the stresses and the strains are independent are generally valid. Many granular materials have been idealised as plastic materials.

Unfortunately, there is no reliable method for predicting the shape of the stagnant zone boundaries. Cleave (1993) found that the flowing zone predicted by Jenike's radial velocity field is far narrower than that observed in practice. Although later Jenike (1987) gave a wider flowing zone, this is not confirmed experimentally either (Cleave, 1991; Cleave and Nedderman, 1993). Furthermore, many observations of batch discharge show that the position of the stagnant zone boundary changes slowly with time.

Gardner (1966) assumed that the solid in the flow channel was in a state of plastic equilibrium and used the method of characteristics to solve the equilibrium and plasticity equations for a continuum. His theoretical prediction of the FCB was found to be in good agreement with experiments. Takahashi and Yanai (1973) developed an analysis for sliding flow in flat-bottom concentrically discharging planar silos. Like Gardner (1966), they used the method of characteristic and assumed a Mohr-Coulomb solid. Tuzun and Nedderman (1982) demonstrated that the FCB predicted by Gardner gave geometrically similar FCB as the silo width varied.

Spencer and Hill (1992, 2001) implemented the non-dilatent double-shearing theory into the equations of motion in gravity silo flow. The stress generated in such flow is assumed to be governed by the Coulomb-Mohr yield condition. With this model, a coupled system of partial differential equations were obtained and several simple exact solutions were examined. These solutions give rise to the flow patterns. These patterns are similar to those observed in funnel-flow in the discharge of rectangular and circular cylindrical silos and hoppers. The solution also predicts the existence of rat-hole.

The plasticity model seems a simple appropriate approach to analyse incipient flow of granular solid. However, since the plastic behaviour of dilated, free-flowing granular solids is not yet well defined, there is a considerable mismatch between most theoretical predictions and experimental observations. This method is now drawing less attention than other numerical techniques which can give a more realistic representation of the solids behaviour.

2.3 Classical theories for pressure distributions

2.3.1 Analytical method

Several classical methods were fully exploited in a monograph by Drescher (1991). These methods are the limit state methods, the differential slice methods. A rigid-plastic model assumption allows these analytical analysis to be applied to certain problems related to storage and flow of bulk material. However they are not universal and have quite limited applicability.

Limit state methods have been developed primarily for analysing geo-technical problems. Their application to problems of storage and flow of bulk material was demonstrated by Jenike (1964), Johanson (1964), Savage(1979), Horne & Nedderman (1978), Wilms and Schwedes (1985).

Limit state methods are not concerned with deformations that may develop in a material at the limiting state of stress. From the equations that describe the rigid-perfectly plastic solid only the yield condition is utilised. In this regard, solutions obtained by these methods are incomplete. A complete solution for a rigid-perfectly

plastic sliding requires not only determination of stress, but also of velocities. Nonetheless, the knowledge of stresses that develop within a bulk material stored or discharged from a bin or hopper permits direct evaluation of wall stresses and thus, bin-load.

2.3.2 Filling

Many classical theories are available for predicting the static pressures in silos after initial filling (Janssen, 1895; Walker, 1966; Walters, 1973; Jenike et el, 1973; Reimbert, 1976, 1987; Enstad, 1981; Rotter, 2001). Most of these theories were devised from plastic equilibrium considerations on the basis of different simplifying assumption. Discussions of these theories and fuller descriptions may be found elsewhere (Arnold et al., 1980; Ooi and Rotter, 1990; Roberts, 1989; Rotter, 2001).

A typical Janssen prediction for filling pressure against the wall is shown in Fig. 2.6. Janssen (1895) assumed that the ratio of horizontal pressure against the wall to the mean vertical stress in the stored solid (the lateral pressure ratio k) is invariant with depth in the silo, but he did not define it. Koenen (1895) proposed that the Rankine (1857) as reviewed by Nedderman (1992) active pressure ratio should be used for this quantity. Most of the other theories for silo pressure attempted to find better means of predicting this single quantity. These authors adopted the Janssen pressure distribution as a basis. Jaky (1948) proposed that k should be given by $k=1-\sin\phi$, a relationship originally suggested for silos, but which is still widely used in the field of soil mechanics. The parameter ϕ in this expression is the solid's internal friction angle. Piper and Wenzel (1963), Pieper (1969) adopted this too. Walker's (1966) deduced k by assuming that the material adjacent to the wall is sliding down the wall and is at active failure. Walters (1973) extended Walkers analysis to include non-uniformity of the vertical stresses and assumed that all the solid is at active failure. Jenike et al. (1973) empirically proposed k = 0.4 and Homes (1972) similarly suggested k = 0.45 for most common solid. Ooi and Rotter (1990) showed that under storing conditions, much of the solid is not at failure, so the lateral pressure ratio k can approximately be elastic value for a solid confined within an elastic shell, $k = \nu/(1-\nu+\alpha)$, in which ν is the Poisson's ratio and α is the relative stiffness parameters.

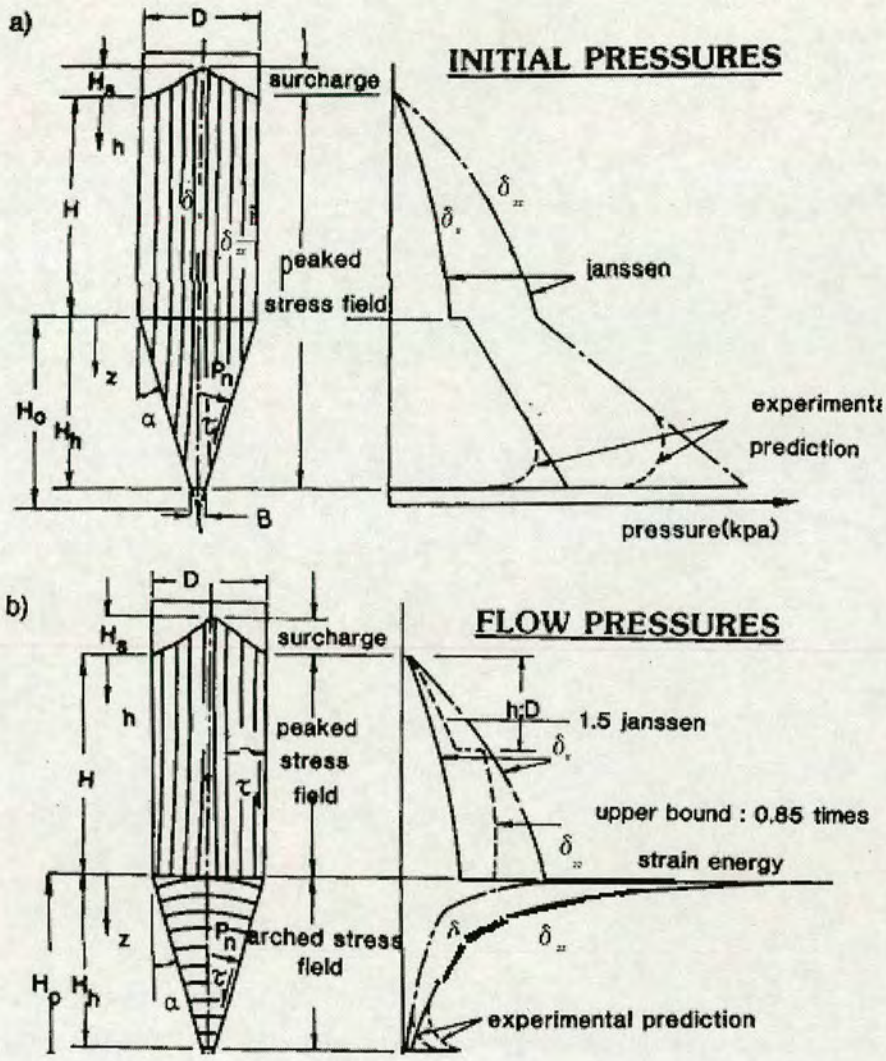

Fig. 2.6 Pressure distribution in a mass flow silo (Roberts, 1986)

Reimbert (1976) produced an alternative solution to the Janssen differential equation by curve fitting experimental results within the confines of the equation, thus effectively allowing k to vary between zero at the surface and the value of Rankine active pressure ratio at great depth. Some comparisons of this solution with Janssen have been made (Briassoulis 1987, 1991; Reimbert, 1987).

2.3.3 Discharge

The pressure distributions in a silo when the bulk solid is being symmetrically discharged are more unpredictable than those after filling. Attempts to describe them and to produce satisfactory rules have included such phenomena as switch pressures

and local patch pressure (Rotter, 1988, 1990, 1991). Nanninga (1956) attempted to explain the higher pressures during flow in terms of a 'switch' from an active plastic stress field after filling to a passive field during discharge (Fig. 2.6 (below)). This idea was extended by Jenike and Johanson (1968), Jenike et al. (1973), Walker (1966) and Walters(1973), but is by now largely discredited. Walter's theory (1973) predicted much higher pressure than those observed experimentally. Jenike minimum strain energy theory (Jenike et al., 1973; Mclean and Arnold, 1976; Arnold et al., 1980) gained some acceptance, but the theory is still poorly understood (Rotter, 1990). McLean (1984) made a simple but unsubstantiated proposal when he suggested that cylindrical wall pressure under funnel flow should not exceed static filling values.

If the discharge is eccentric to the silo axis, the problem is much more complicated. A few theories have been proposed for the design of silos under eccentric discharge (Jenike, 1967; Wood, 1983; Rotter, 1986). However, there have been many serious failures involving eccentric discharge, so most codes specifically excluded it. Existing experiments lead to a wide range of alternative descriptions and there is little consistency between the theoretical treatments. Codes which do include eccentric discharge treat it very differently (AS 3774, 1990; ACI313, 1989). This has led to great confusion amongst silo designers.

Many other factors such as wall imperfections and in-homogeneities in the silo cannot be dealt with by the classical theories. They are known to be important. Numerical methods represent on the other hand a powerful tool to cope with these effects.

2.4 Pulsation in gravity discharge from silo

Gravity flow in silos may occur a cyclic or pulsating-type flow. It may be caused by changes in density during flow and by varying degrees of mobilisation of the internal friction and boundary wall friction (Roberts et al., 1991; Roberts, 1996, 1999; Roberts and Wensrich, 2002). Several authors have studied the subject of pulsating flow of bulk solids in bins and silos (Shinohara et al., 1968; Kmita, 1985, 1991, 1992; Firewizc, 1988; Baxter, 1989; Michalowski, 1987, 1991; Drescher, 1992, 1998; Tejchman, J., & Gudehus, G., 1993; Wensrich, 2002, 2003). The studies showed that

the velocity and stress distribution of bulk solid in silos and the pressure distribution exerted by the material on the silo walls are far more complex than those reviewed earlier.

2.4.1 Velocity and stress discontinuity in silo

One of the characteristic features of mass flow in plane (wedge-type) hoppers is the occurrence of zones of localized deformation in an otherwise continuous field of flow (Drescher, 1998). These have been given the name shear bands, rupture zones or (strong) velocity discontinuity lines, and they can be detected using various measuring techniques, notably stereo photo radiography as shown in Fig. 2.1 (Michalowski, 1984, 1987, 1991; Drescher , 1992, 1998).

Experiments of gravitational flow through a hopper (Michaloski, 1987, 1991) have been carried out and revealed similar phenomena. The common features for most of the results published is the appearance of narrow zones with large velocity gradients within the flowing material, usually interpreted as velocity discontinuity surfaces. Large shearing strain is accompanied by dilation of the materials. The velocity of particles experience a rapid variation across the rupture surface, hence they are often interpreted as velocity discontinuities.

Using X-rays Baxter and Behringer (1989) visualized wave-like patterns emanating from the outlet of a two dimensional wedge-shaped hopper. Brown and Richards (1965) explained the density fluctuations during the outflow with non-random dilatant waves but their experiments with single layer had limitations due to irregular sticking to the plate.

Plug flow experiments (Waters and Drescher, 2000) indicated that with discharge progressing, the vertical shear bands tend to move laterally outward thus widening the region of flow. This was seen in radio-graphs, indicating clearly a boundary between the dense and dilated material.

Tuzun and Nedderman (1979, 1982) declared that the experiments showed no

evidence of velocity discontinuities in the flow of a coarse granular material. He argued that if the velocities are indeed a result of the stress distribution, it is hard to imagine circumstances in which a continuous velocity field would result from a discontinuous stress field.

Baxter (1993) also measured the stresses acting on the walls of a 3-D hopper with an inclination angle of 45° during discharge of sand. He observed a power law decay in the spectrum of the time dependence of the normal stress.

2.4.2 Investigations into the velocity and stress fluctuation

The mechanics of the formation and propagation of shear bands remain poorly understood. Only a limited number of theoretical analyses have been performed to explain and predict their occurrence (Cutress & Pulfer 1967; Pariseau 1969, 1970; Drescher *et al.,* 1978; Michalowski 1984, 1987, 1991; Pitman 1986).

The first attempts to investigate bands of localized deformation in hoppers hinged on constructing the kinematic counterpart to the (quasi) static solution for a rigid-perfectly plastic, pressure dependent (Mohr-Coulomb or Drucker-Prager) model of granular material. Drescher (1998) concluded that "This is done by tracing the velocity characteristics net related to the stress field through the flow rule. As the equations governing the kinematics are linear, strong velocity discontinuities coinciding with the velocity characteristics are permissible. The location of the discontinuities, and the magnitude of velocity jumps, can then be determined if the stress field is continuous and the velocity boundary conditions are known. These are seldom uniquely defined, however, and additional assumptions are necessary to arrive at a solution. This is because the flow of granular materials in hoppers is usually driven by gravity and not by prescribed movement of a boundary, as is the case of extrusion through wedge-shaped dies. Accordingly, the solutions obtained are used for explaining experimental observations rather than for predicting the actual pattern or type of flow. This is illustrated clearly in papers by Pariseau (1970) and Michalowski (1987), with the examples of characteristics net and velocity discontinuities shown in Fig. 2.7. A direct numerical integration of the governing static and kinematic equations has also been

performed (Pitman, 1986), and shows strong in-homogeneities in the velocity field which can be interpreted as the occurrence of localized deformation".

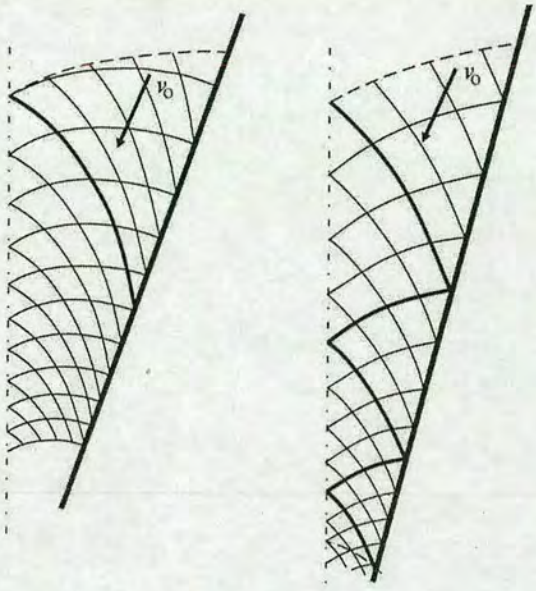

Fig. 2.7 Velocity characteristic and velocity discontinuities (Michalowski, 1987)

Mathematical analysis of the fundamental equations also show that exact steady-state flow is seldom realised. There are usually some oscillations in flow velocities and, hence, also in stresses. In mass-flow hoppers, oscillation is slight; the situation is different in funnel flow. For instance Horne and Nedderman (1978) used the method of characteristics (MOC) to calculate the stress distribution in two-dimensional hoppers. Their extensive stress analysis showed that, especially in the case of a convergent flow where a passive state of failure will occur, the stress field is intersected by many discontinuities. They found that stress discontinuities were propagated through the region, with stress varying in a saw-tooth manner about the radial stress field prediction. The amplitude of the stress discontinuities was comparable with the mean stress throughout the hopper and hence there was no convergence towards the radial stress field.

Assuming that the stress distribution was given by the radial stress distribution (Jenike, 1962), Nedderman (1996) imposed various velocity boundary conditions and did some calculations for a wedge-shaped geometry. They found that weak velocity

discontinuities were present throughout the hopper, giving velocities which oscillated about the radial stress field solution. The magnitude of the oscillations was comparable with the magnitude of the mean velocity.

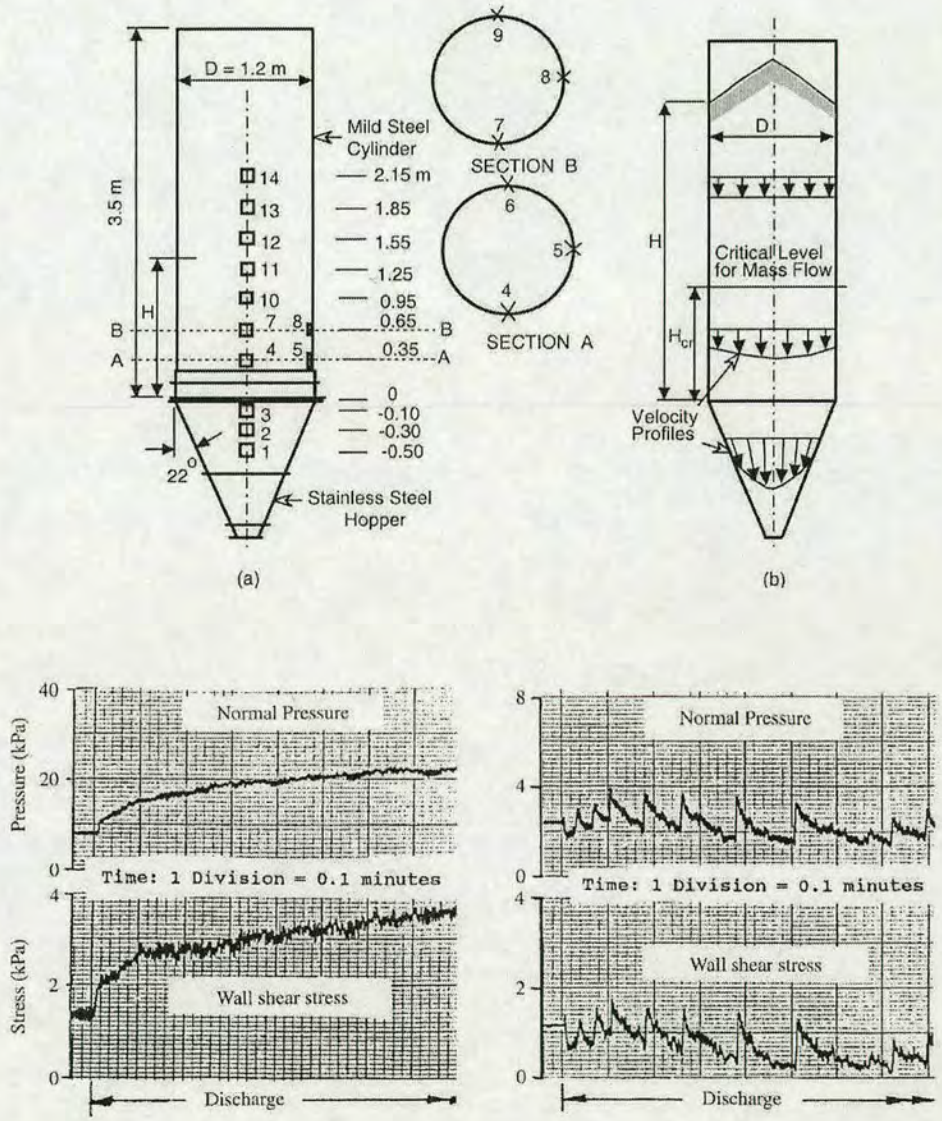

Fig. 2.8 Samples of normal pressures and shear stress in a silo pulsation (a) results from location 5; and (b) results from location 14 (Roberts, 2002)

The formation and propagation of the shear band and rupture contribute to the 'slip-stick' motion mode in a tall silo, and result in the pulsation (Roberts, 1996, 2002 (Fig. 2.8); Wensrich, 2003; Schwedes, 2003). Pulsating flow has been studied by several authors. Shinohara et al. (1968) recognised the existence of a dynamic arch and studied

the flow of both sand and glass beads. He noted that the location of the arch was higher for glass beads than for sand, and derived an expression to predict the frequencies of the pulsating flow. Firewicz (1988) proposed an improved solution to that presented by Shinhara et al.(1968).

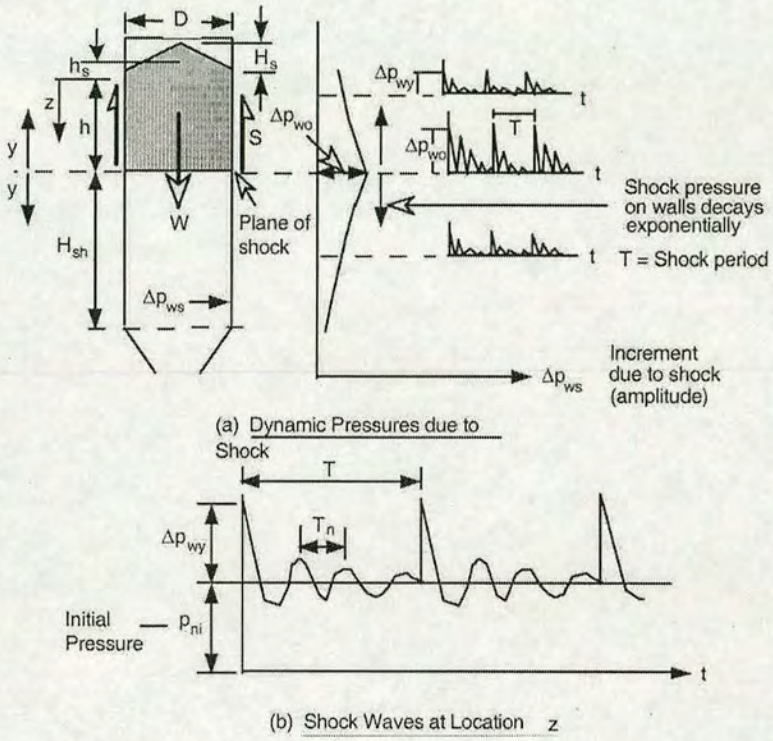

Fig. 2.9 Dynamic loads induced in a silo (Roberts, 2002).

Roberts studied the influence of the pulsation on the pressure on the silo walls (Fig. 2.9). Wensrich and Roberts (2000) considered a series of coupled sliding masses to model the slip-stick motion at the boundary surface. From the slip-stick material movement mode, they set up a 'Multi-mass system'(Roberts, 1996, 2002) and put forward a silo dynamic model. It was applied to predict the propagation of the pressure shock wave in silos. From Fig. 2.9, one can see that the pulsation makes the pressure distribution more complex; and may well trigger an un-symmetric pressure distribution in a symmetric silo.

2.5 Numerical prediction of velocity and stress in silos

2.5.1 Introduction

Due to the limitations of classical theories, numerical methods were gradually introduced in the early 1960s and many advances have been made ever since. The method of characteristics was first applied to flow of material in a hopper by Jenike (1961) to validate his radial stress theory: further studies of both filling and discharge continued until the 1980s (Horne and Nedderman, 1976; Wilms and Schwedes, 1985). Pitman (1986) used the finite difference method to solve the partial differential equations for the stress and velocity fields in hoppers. A few attempts have also been made to apply the boundary element method for stress calculations in silos.

A considerable effort in many countries has been put into developing computational models for the behaviour of granular solids in silos since the early 1960s. Two main types of computational model (finite elements method (FEM) and discrete element method (DEM)) are widely used to predict the responses of granular solids in silos (Bishara and Mahmoud, 1976; Jofriet *et al.*, . 1977; Mahmoud & Abdel-Sayed 1981; Eibl & Rombach 1988; Häussler & Eibl 1984; Runesson & Nilsson 1986; Askari & Elwi 1988; Ooi & Rotter 1989, 1990; Schmidt & Wu 1989; Wu & Schmidt 1992; Aribert & Ragneau 1990; Tejchman & Gudehus 1993; Tejchman, 1996, 1999, 2001; Ragneau *et al.*, . 1994; Wieckowski & Klisinski 1995; Karlsson *et al.*, . 1998; Sanad, et al., 2001; Keiter and Rombach , 2001; Gunies et al., 2001; Chen et al., 2001; Ayuga et al., 2001). With the rapid increase in computing power, the finite element method has dominated the field through its versatility and ability to model complex geometries and material properties. While the use of finite elements to model the solid as a continuum is still increasing, the behaviour of individual particles is also being studied using the discrete element method.

2.5.2 The numerical methods

2.5.2.1 The method of characteristics

The method of characteristics is a mathematical tool for solving partial differential

equations by transforming them along the characteristics into ordinary differential equations. Starting with the differential equations governing equilibrium and introducing a yield locus for the material, it is possible to derive a system of two hyperbolic differential equations that describe the stress field in the material. The method of characteristics predicts discontinuities in the stress field in many practical situations.

Horne and Nedderman (1976) used this method to calculate limiting stress distributions in two-dimensional vertical-sided bins. Wilms (1985) performed extensive calculations with this method. The results agreed well with Janssen's theory for the vertical section of the silo, though the assumption of horizontally uniform vertical stress is incorrect.

This method has been extensively used to find both filling and flowing stress fields in hopper. It has been useful in understanding stress fields near singularities in hoppers. Some researchers (Gardner, 1966) used this method to study the stress field at the transition between the vertical walls and the sloping hopper walls.

The method depends however on solids being in a plastic state. This is a condition which is rarely true after filling, and of doubtful value for parts of the solid during discharge sometimes. It is therefore seriously limited.

2.5.2.2 The boundary element method

The boundary element method was proposed as early as the FEM. It involves numerical solution of a set of integral equations that connect the boundary, or surface, tractions to boundary displacement. Unlike FEM, the BEM is based on the solution of integral rather than differential equations. Only the boundary or the surface of the body is discretised into a number of elements. Thus the number of dimensions in the problem is reduced by one, and the computational effort is greatly reduced. Wu and Schmidt (1992) applied the boundary element method to silo stress calculations and compared the results with observed filling and flow pressure in silos and hoppers.

2.5.2.3 Discrete elements

The Discrete Element Method is a relatively new technique for simulating moving granular particles. Different terms such as Discrete Element Methods (Cundall, 1971), "Molecular Dynamics" (Ristow and Herman, 1993), " Distinct Element method" (Thornton, 1989) and " Granular Dynamics" (Poschl, 1992) have been used for this method.

It was first proposed and developed by Cundall (1971) for rock mass problems and later applied to granular materials by Cundall and Strack (1979). It is based on the use of an explicit numerical scheme in which the interactions between a finite number of particles is monitored contact by contact and the motion of the particles is modelled particle by particle. Newton's equation as of motion for each particle effectively replace the equilibrium equations used in continuum mechanics, and the model of inter-particle contacts replace the constitutive model. The algorithm of DEM is based on the finite difference formulation of the equation of motion and avoids the inversion process for stiffness matrices (Cundall and Hart 1992). Such an algorithm enables quite a number of particles to be handled in a simulation.

The discrete element method has been extended by many authors in recent years (Cundall, 1971, 1978, 1979; Thornton, 1989, 1991; Bardet, 1993; Schewedes and Feise, 1993). While most researchers are concerned with spherical particles, a few studies (Hogue, 1991; Posscjl, 1992) with non-spherical particles have been undertaken. The normal and shear stiffnesses between two particles are generally represented by a contact model which consists of a spring and a friction slider (Bardet, 1993).

Even with such an idealised model, discrete element enables the investigation of the micro-mechanics of granular materials in a way that can not be achieved with the continuum approach since they handle particles properties directly. The calculated flow patterns in model silos are consistent with experimental work, even though the calculated stresses in the silo fill are only qualitatively in agreement with measured ones (Langston et al., 1996, Luding et al., 1996, Ristow, 1997).

Difficulties in the discrete element approach lie in the process of simulating real granular materials where almost an infinite number of particles with various shapes are assembled. When using the discrete element approach, it is inevitable to model granular material as idealised assemblies of particles. At present, the number of particles which can be considered is still very small, e.g. 20,000, which is only a tiny portion compared with the huge number of particles in a real situations. The huge computational effort required to monitor a useful number of particles makes this method very difficult to use practically. They certainly belong to future methods on investigations of flow behaviour in silos.

2.5.2.4 Finite element methods

The finite element method has experienced enormous growth in both theoretical development and applications (Zienkiewicz, 1991, 2001). Since having been adopted , it is certainly the most popular and powerful tool for silo pressure research.

The finite element method is often used to study macroscopic phenomena such as the flow behaviour of granular solids and the pressure exerted on silo walls. In this method, the granular solid is treated as a continuum and follows some prescribed behavioural laws based on classical mechanics combined with generally complex constitutive models.

2.5.3 The applications of finite element method

2.5.3.1 Filling, discharging pressure and silo-structure interaction

Many attempts have been made to calculate silo filling pressures using finite elements. Bishara and Mahmoud (1976), Jofriet, (1977), Eibl and Rombach, (1987), showed that there was a good agreement between Janssen's theory and finite element predictions. Mahmound (1981) modelled the interaction between solids and a flexible wall in shallow grain bins. They adopted the hyperbolic stress-strain model for the stored sand, and found some agreement with experimental measurements. Bishara and his co-workers studied many problems, beginning with silage, to determine the effect of solids behaviour in cylindrical silos. They devised non-linear bulk modulus and shear

modulus response from materials tests on coarse and fine materials and modelled a concrete silo wall with elastic hoop elements. The predicted wall pressure were similar to those of the Janssen and Reimbert theories. Aribert and Gagneau (1990) used a perfectly plastic and a more complicated (Wilde, 1979) model for their constitutive laws. Zhang and his co-worker (Zhang et al., 1986, 1987, 1989) also carried out many finite element studies to predict static and thermal pressure in grain bins.

Although all of these studies used complex material characterisation, the correlation between their experimentally observed pressure and theoretical predictions was generally not close and only a limited range of the relevant parameters was studied. Ooi and Rotter, Rotter et al. (1990, 1991, 1998) however used a comparatively simple elastic finite element model with wall friction characteristics. The results show that the key non-linearity in filling pressure is the wall friction, not the material constitutive model. A wide range of parametric studies for wall flexibility was also presented.

The effect of wall flexibility was first studied by Ooi and Rotter (1990). By the studies of a squat silo they showed that the wall flexibility can be best presented by a parameter and that, in practice, only very few designs for squat silos lie in the range where wall flexibility influences the wall pressure if the system is entirely symmetrical.

Other studies explored different aspects of solid-wall interaction using finite elements. Rahim (1989) analysed a cylindrical concrete silo and concluded that imperfections in the silo wall have very little effect on the internal forces in the silo wall if the wall pressures are independent of the wall geometry. However, the effect of wall imperfections on the wall pressure was not investigated. Askegaard et al. (1990) used finite elements to estimate the measuring error caused by stiffness of a pressure cell mounted in a thin wall and concluded that serious measuring errors will occur if the cell thickness is slightly different from that of the wall. A recent finite element study of wall-solid interaction (Ooi and She, 1996) shows that geometric imperfections in the wall may have a very significant effect on the wall pressures in thin-walled squat silos.

While many researchers adopted complicated stress-strain relationships to analyse the

wall stress distribution, Askari and Elwi (1988) adopted a simple technique using a double iterative scheme over friction and the perfect elastic-plastic bulk material model. The material was assumed to be no-tension Drucker-Prager elastic-perfectly plastic. By simulating incipient flow conditions in strong materials, a switch load was simulated at the opening of the outlet. The effect of load history was included by applying gravity in stages to the bulk material during filling (Link and Elki, 1990).

A few studies have explored the effect of a switch stress at the transition on the silo structure. These have generally shown that symmetrical switch stresses are not very serious in steel structure (Rotter, 1986; Teng and Rotter, 1991), provided the loading remains symmetric. Unsymmetrical loading conditions lead to much more serious conditions for a cylindrical wall (Rotter, 1983; Ansourian, 1983, Rotter, 1986, 1987; Holst et al., 1999, 2000).

The most serious unsymmetrical distribution is that arising from eccentric discharge of the solids, which has caused many failures. Some attempts have been made to predict the very different structural effects of these loads in concrete (Emanuel, 1983) and steel silos (Rotter, 1986a). Ibrahim and Dickerson (1983) performed a two dimensional finite element analysis of a horizontal slice in a concrete silo for powdered coal with eccentric discharge. Core flow was assumed, with the horizontal pressure in non-flowing material taken from Janssen values. This work was carried forward by later papers (Emanuel, 1983 a and b). The bending moments in a concrete silo wall can be predicted, but they are very sensitive to the assumed stiffness of the stationary solids, which make them difficult to apply in practice.

The existence of the stiffness of solids also increases the buckling strength of a metal silo very significantly (Rotter, 1980, 1990; Zhang and Ansourian, 1990; Knoedel, 1992). The analysis of shell buckling with the effects of granular solid restraint added to those of geometrical imperfections and internal pressurisation is a very complicated problem, and requires much further work.

2.5.3.2 Solid flow and discharge

The stress and velocity fields during flow of granular materials has also been a field of much finite element activity. Häussler and Eibl (1984) developed an elegant Eulerian Formulation to simulate the silo discharge process. The granular bulk material was considered to satisfy a complex elastic-plastic-viscous law, and the velocity and stress fields in mass-flow silos were calculated using finite difference in time. They obtained the transition velocity and the stress fields with the bulk material for the beginning of discharge and noted that the strong stress re-distributions caused an increased wall pressure. Progressively improved models have been developed, until a complete simulation of the filling and discharge processes is now possible with realistic material behaviour, density variations, and varied boundary conditions (Ruckenbrod and Eibl, 1993).

In an attempt to model the FCB in funnel flow, Watson and Rotter (1995) invoked the kinematic model propounded by Litwiniszyn (1963), Mullins(1979) and Tuzun (1979). They defined the stagnant zone boundary to be the positions at which the velocity was equal to 1% of the centreline velocity at the same height. With this assumption the results appear to be satisfactory to predict the FCB. However, they did not attempt to adapt the kinematic model for the unsteady state and as a consequence of both these features, they found only qualitative agreement with their batch experiments.

Based on the Eulerian approach, Karlsson et al. (1996, 1998), Runesson and Nielsen (1986) built a model to investigate the emptying of silos and the effect of an insert on the silo flow pattern. The motion of the granular material subject to gravitational forces is modelled as the motion of an elasto- plastic fluid. This model has been successfully used to show the difference between funnel flow and mass flow (Karlsson, 1996), and the effects of several kinds of insert on the flow patterns (Ding et al., 2001, 2002). The shortcoming is that some of the parameters used lack a clear physical meaning and restricts the general applications of this model.

Wieckowski et al. (1999) analysed the flow of granular material in the process of discharging by means of the particle-in-cell method. The mechanical behaviour of the

material was described as elasto-plastic solid with the Drucker-Prager yield condition and non-associative flow rule. They adopted an approach of an arbitrary Lagrangian-Eulerian formulation, and overcame the main obstacle related to mesh distortion. By doing this, the entire process of silo discharging was analysed, and the dynamic problem was also explored by the use of the explicit time-integration scheme.

Assuming that the wall friction will decrease in a region with high flow velocities, Ruckenbrod and Eibl (1993) simulated the dynamic pulsation in a silo fill during flow. Tejchman and Wu, 1997; Gudehus and Tejchman (1993) showed that many mechanisms of granular mass in silos at the onset of quasi-static mass flow could realistically be described with polar elastic-plastic and polar hypo-plastic approach. Based on this general constitutive model, various aspects of cohesionless materials have been investigated, e.g. shear banding (Tejchman and Wu, 1997; Tejchman and Bauer, 1996). Using the same approaches with an additional consideration of inertial forces, Tejchman and Gudehus (1993) and Tejchman and Wu, 1997; Tejchman and Bauer, 1996; Tejchman (2000) successfully described the onset of dynamic flow in a silo with controlled and free outlet velocity, and the formation of shear zones, stress fluctuations and the interaction between the material and the roughness of the walls.

Although the finite element method is powerful and has produced many satisfactory predictions, it has some serious shortcomings when modelling silo discharging. In continuum mechanical analysis of granular material, the determination of a constitutive model is the most difficult process. A constitutive model based on continuum approaches usually includes a lot of material constants, which have no clear physical meanings; while in discrete element approaches, the particle arrangement is modelled explicitly. The ambiguous characters of the material constants based on continuum approaches may have their origin in the implicit expression of the geometry of a packed assembly of particles. It has also difficulties in simulating the unsteady-state flow. With the continuum treatment, the finite element method is not capable of predicting rupture zones and flow boundaries.

2.6 Flow and pressure measurement

2.6.1 Introduction

Silo flow and pressure measurements have always been carried out. The majority of such measurements were on model silos in laboratories rather than on full scale silos; and pressure measurements were more often carried out than flow measurements.

In theory, results of model tests can be translated to full-scale results. However, the reliability of such translations is in doubt. The question of scale effects was thoroughly explored by a Danish silo research group in the late 1970s and early 1980s as reviewed by Nielsen(1998), using a full scale concrete grain silo, together with large a laboratory model and a small centrifuge model. They asserted that the scale effects were very pronounced: many of the conclusions previously drawn from laboratory models were seen to be irrelevant to industrial installations. It is therefore necessary to carry out full-scale experiments.

It has long been recognised that the pattern of solids flow in a silo has a strong influence on the pressures exerted by the solid on the walls (Ketchum, 1907; Jenike, 1964; Nielsen and Andersen, 1982; Zhong et al., 2001). The silo wall pressure can not be predicted properly without knowledge of the flow pattern. Lack of information of the solids flow pattern will make it difficult to interpret the results of the pressure measurements. A full-scale silo flow measurement should be carried out prior to the pressure measurements.

2.6.2 Silo flow measurement

2.6.2.1 Flow pattern observation and measurement

The study of flow patterns in discharging silos presents several fundamental problems to the experimenters. Firstly, the majority of granular solids are opaque in nature, so the experimenters cannot look into the bed of solids. Very little information can be gained from direct visual observation of the free surface. Even if the walls are made of transparent material, only the flow adjacent to the walls can be studied. Secondly, the

method by which the silo has been filled affects the subsequent flow pattern. If it is necessary for free surface to be levelled, for example, to position marker particles, it may affect the flow pattern. Thirdly, effects such as vibration and time storage may also influence the flow pattern. The study of the internal flow fields in silos is seldom a simple affair. Many ingenious methods have been devised to chart the internal events in a discharging silo.

2.6.2.1.1 Observation of horizontal layers of dyed solid

In this technique, horizontal layers of visually-detectable solid are placed adjacent to a transparent wall in a plane-strain apparatus during filling. The subsequent deformation of these layers is then observed. Unless the silo is filled in a distributed manner, some levelling of the free surface is necessary. Munch-Anderson and Nielsen (1990) have shown that the stacking arrangement effects the flow patterns and so this levelling may have an influence. The visually-detectable solid is usually either a sample of the granular solid that has been dyed or a similar granular solid of a different colour. In either case, the layers contain grains that have essentially the same properties as the bulk solid. In this experimental technique, the problems associated with the retarding effect of the front wall are pertinent. Litwinszyn (1963), Gardner (1966) and Jenike and Johanson (1962) are amongst many who have used this technique. The results obtained are generally of a qualitative nature since it is not possible to determine the trajectory of any particles except those adjacent to the transparent front wall. This method is only applicable for plane silos.

2.6.2.1.2 Direct visual observation through transparent silo walls

Another visual observation technique was employed by Carson (1991). They carried out flow experiments on flat-bottomed, cylindrical model silos. The walls were made of transparent Plexiglas, so they could visually determine the boundary between flowing and stationary solid. By assuming a linear zone of stationary solid, they plotted flow channel angle against the circumferential angle. Their experiments were carried out on silo models which were full, two-thirds full and on third full, and discharged either concentrically or eccentrically. They found that the flow channel closely

followed a radial path from the outlet to the cylinder wall. The flow channel boundary, as observed through the wall, however, was neither distinct nor stable for most of the solids they tested. They also reported very little correlation between the flow channel angle and measured material properties such as the angle of internal friction.

Similar experiments on steeper flow channels in sand under eccentric discharge were conducted by Fitz Henry (1986). The deduced flow channel form was found to have very non-linear vertical boundaries. This flow channel boundary shape may be dependent on properties of the solid being stored which were not measured.

2.6.2.1.3 Photographic techniques

Photographic techniques are one of the most common methods used to study the behaviour of flowing granular solid and are often in conjunction with observation of the movement of horizontal layers of dyed solid. Photographic technique have been employed by many researchers using transparent plane-strain silos (Pariseau, 1970; Bosley et al., 1969; Tuzun and Nedderman, 1979, 1982). Either high-speed photography or long exposures are often taken.

It is assumed that flow behaviour observed adjacent to the front wall is representative of the behaviour throughout the bed. However, several researchers (e.g. Brown and Richards, 1965; Cleaver, 1991) have reported that the front wall exerts a retarding force on the flow. This must be taken into account somehow when velocities are calculated, as these velocities will almost certainly be less than those occurring at similar positions with the bed. However, it is not easy to devise a satisfactory technique to account for the retardation caused by the transparent wall (Watson, 1993).

Brown and Richards (1965) and Gardner (1966) took photographs of the flow through the transparent front walls of their plane-strain model silos. Careful scrutiny of these photographs reveals a surprising point of contra flexure in these flow channel boundary. It seems possible that stationary zones start to curve into the flow field near the outlet. This phenomenon cold, however, be caused by frictional effects against the front wall.

Tuzun and Nedderman (1979) are amongst those to have used cine filming to determine particle trajectories. Polynomials describing the position of a tracer particle with time were then fitted to the tracer trajectories. On differentiation, these polynomials yielded the horizontal and vertical velocities at any point at any time in the trajectory

Long time exposure were used by Gardner (1966) and Tuzun and Nedderman (1982) to determine the positions of the flow channel boundary. Gardner laid horizontal layers of dyed solid in the silo during filling. Flow was allowed to proceed until steady-state conditions were achieved. The flow channel boundary was defined in this study as the edge of the stationary solid, and its location was assessed by measuring the extent of the remaining horizontal layers of the dyed solid.

By using an exposure time of 0.5 seconds whilst photographing their discharging planar silo, Tuzun and Nedderman (1982) observed that some particles appear blurred whilst others (those that moved at less than one particle diameter per expose time) were in focus. In this way, they could determine a flow exposure time of 1 sec, the flow channel boundary altered giving the appearance of a large flowing region. They reported that these boundaries were also velocity contours. They did not, however, increase the exposure time beyond 1 sec to investigate further shift in the observed flow channel boundary.

Photographs are occasionally used to investigate flow in full scale facilities. The concept is that photographs of the surface of the solid give an indication of the flow pattern. Whilst it is true that a developing depression in the surface of the solid must indicate that solid is flowing down a channel at this point, many anecdotal descriptions of this technique suggest that little can be learned about the pattern of flow lower down in the solid.

2.6.2.1.4 Radiographic techniques (X rays)

In the radiographic technique, lead shot tracers, which are opaque to X rays, are seeded into a silo bed during filling. Because the X-rays must be able to penetrate the solid

and be detected on the far side, this technique can only used in thin non-metallic plane-strain models. It is therefore very susceptible to errors caused by friction on the side wall, through which the observation must be made.

The flow is halted at frequent intervals during the discharge and the apparatus exposed to an X-ray source. The resulting X-ray photograph shows the positions of the trace particles. By comparing successive X-rays, velocities can be calculated. This method is relatively rarely employed, presumably because of the expensive equipment required and the restricted size of the apparatus. Lee et al. (1974), Cutress and Pulfer (1967) and Drescher et al. (1978) are amongst those to have used this technique. Voidage changes, which often coincide with rupture surfaces, are the most important phenomena which can be detected with the X-ray exposure.

2.6.2.1.5 Tomographic techniques

Tomographic techniques form another class of radiation-based methods in which the position of tracers is determined by their radiation emission rather than by radiation transmission, as in the case of X-rays (Bemrose et al., 1988; Beynon et al., 1993; Parker et al., 1993; Seville et al., 1995). One of these techniques, termed Positron Emission Particle Tracking (PEPT), uses radio-labelled particles which emit a positron, which in turns gives rise to matched γ-ray pairs. Positron-sensitive detectors serve to locate the tracer position by triangulation. PEPT has been used in the investigation of flow characteristics in a multiphase granular medium (Seville, 1995). Whilst the technique is useful in some ways, it is very restricted in that up to now, only one particle can be traced at a time, and the cost involved is very high. This technique is naturally not suitable for measuring the solid flow pattern in full scale silos.

2.6.2.1.6 Radio pill tracking technique

The radio pill tracking technique involved following a miniature radio-transmitter as it passes through a model silo. Handley and Perry(1965, 1967), Perry (1975, 1976) and Rao and Venkateswarlu (1973) are amongst those to have employed his technique. Perry and his co-workers carried out the most comprehensive study using cylindrical radio pills of length 25 mm and diameter 8.8 mm. In an attempt to measure the stresses

in the granular solid, some pills were fitted with a pressure sensitive diaphragm. The pills were placed within axi-symmetrical model silos filled with fine sand. The signals from the radio pills were received by an aerial adjacent to the wall.

Since the radio pills were much larger than the mean particle diameter, the problem of segregation must be addressed when analysing the results. Later work by Arteaga and Tuzun (1990) can be used to demonstrate that segregation was not a problem in the observations of Perry et al.(1975, 1976). However, the major drawback in the work of Perry is the short range over which the radio can be detected. For reliable detection, the radio pills must never be more than about 50 mm from the wall, so the technique is restricted to very small models.

2.6.2.1.7 Bed splitting techniques

In the bed-splitting technique, horizontal layers of dyed granular solid are introduced into the silo during filling. After an appropriate period of flow, the discharge is halted. The bed of granular solid is then immobilised. The most common immobilisation technique is to pour in a fixing medium which fills the space between the granular particles and then solidifies, rending the particulate solid rigid. Brown and Richards (1965) and Novosad and Surapati (1968) used molten paraffin wax and Chatlynne and Resnick (1973) used a polyester resin as the fixing medium. The solidified granular solid can be sliced up to several the internal deformation of the coloured layers.

In their experiments with sand in a plane-strain mass-flow hopper, Brown and Richards (1965) reported that the velocity profiles were unsymmetrical about the vertical centreline and that the flow rate generally increased with distance from the end of face. However, the maximum flow rate did not occur in the central section of the hopper.

Brown and Richards also made measurements of the 'angle of the approach'. This angle β, was defined as the angle of the flow channel boundary, near the exit, made with the vertical. In plane-strain silos, the angle of approach was measured from direct observation through the transparent end face. In axi-symmetrical silos, large numbers

of tracer particles were initially seeded in layers into the silo at known positions. From a study of the particles that were left in the silo after a few seconds of discharge, an estimate of the angle of approach could be made. The angles of approach were measured for different solids in three flat-bottomed silos of different geometries:

- discharge through an edge slot adjacent to a side wall in a planar silo (this angle of approach was designated β_e).

- discharge through a central slot, parallel to the side walls, in a planar silo (β_c).

- discharge through a central circular orifice in the base of a cylindrical silo (β_3).

They found that all these angles fluctuated, but in general $\beta_e > \beta_c > \beta_3$. They showed that the geometry of the silo has an influence on the angle of approach.

Giunita (1969) investigated the position of the flow channel boundary in an axi-symmetric model silo. By continuously replenishing the top surface, steady-state conditions were allowed to develop. A different method of the fixing technique described above was then used to split the flow field. After fitting a semi-circular lid, the silo was rotated through 90^o about the horizontal axis. A vacuum shovel was then used to remove the uppermost half-cylindrical section, thus exposing the longitudinal plane of symmetry. Although it was Giuntia's intention to study the flow channel boundary in only flat-bottomed silos, his apparatus included a conical hopper of a smaller diameter than the cylindrical silo and so perhaps a reliable comparison with other results from flat-bottomed silos cannot be made.

Takahashi and Yanai (1973) used a technique similar to Giunta's to measure the flow pattern and void fraction of 4 mm diameter glass, silica and alumina spheres during flow through a vertical pipe. They reported a central constant-velocity region and a peripheral shear region where the velocities fell abruptly.

Although bed splitting techniques allow the flow patterns in true three-dimensional silos to be investigated, the results are generally only of a qualitative nature since

trajectories are unknown. A further disadvantage of the fixing technique is that it is both time –consuming and labour-intensive.

2.6.2.1.8 Indicator bars passing through penetrations in the silo wall

The most common current method used by practising engineers to investigate solid movement in a full scale industrial installation is to drill a series of holes in the silo wall at different heights, and to insert a bar through each hole into the solid (Levison and Munch-Andersen, 1993). During discharge, the bar is seen to move if the solid inside is moving, and in careful studies, the rotational velocity of the bar about the hole can be used to estimate the local velocity of the moving solid. By placing such bars an many heights, the boundary between the moving and stationary material in a semi-mass flow silo can be detected.

However, the technique has many disadvantages. The movement do not measure a real velocity since the bar's rotation means slow translation near the wall, but more rapid translation further inside. Second, the bar must be repeatedly installed as flow progresses, involving much human interactions with no potential for automation. Thirdly, the movement of the bar only indicates the flow of solid against the wall, so events deeper in the silo are undetectable. Fourthly, many penetrations must be made into the wall to achieve the goal. These penetrations may be permitted by silo owners with serious flow problem, but those who are undertaking the study with prevention of problems rather than cure of known difficulties in mind are rarely enthusiastic about drilling holes in their silos.

2.6.2.1.9 Residence time measurements

In this technique, the time taken for tracers to travel through the bulk from an initial known starting position to the outlet is measured. This technique lends itself very conveniently to the analysis of flow in truly three-dimensional systems. The resources needed to implement this technique are few and inexpensive and the method is simple but time consuming.

In circumstances where mass flow occurs and small asymmetries are not of concern,

streamline and velocity fields can be assessed from residence time. A stream function analysis can be used. Velocity distributions can only be calculated if either the trajectory of the particle or a constant bulk density is assumed. With the latter assumption, contours of equal time may be fitted to the residence time data and stream function values may then be evaluated. Streamlines are calculated by numerically differentiating these stream functions (Cleaver, 1991). Smallwood and Thorpe (1980) continued the analysis to calculate velocity fields. This technique works well in mass flow regions, but is much more difficult to apply to funnel flow.

Cleaver (1991) reported that the stream function analysis was very sensitive to error in the experimental results from this mass-flow silo. In the funnel experiments described by Waston (1993), many tracer particles remained stationary for considerable period until the flow point reached them. Therefore, the measured residence times of these tracers do not represent the time that the trace was in motion. This phenomenon renders such residence time data unsuitable for stream function analysis.

Different methods of placing the tracer particles into the silo have been employed. Smallwood and Thorpe(1980), Murfitt (1980), Graham et al. (1987), Nedderman (1988) and Cleaver (1991) used a permanent positioning tube to introduce tracer particles into discharging silos. Cleaver (1991) showed that the presence of a positioning tube in the flow field caused the subsequent movement of the tracer particle to be impeded. For most accurate results, therefore, the tubes must be retracted after positioning the tracer particle. Tracer particles were dropped from the marked positions at the top of the silo onto a pre-flattened free surface by van Zanten et al. (1977). The accuracy of this method of positioning the tracer particles is in doubt because burrowing of the tracers is unknown.

A drawback of this residence time technique is that the positioning of tubes and recovery of tracers in full scale silos may be hampered by problems of access. The question of segregation of the markers must also be addressed.

In addition, interpretation of the observations made using residence time measurements under funnel flow conditions is not at all straightforward, and numerical processing of

the results to identify the changing flow channel boundary is still in its infancy.

The residence time technique can be used in full scale industrial installations, and is the adopted method in a full scale research project in the University of Edinburgh (Rotter et al., 1995, Chen, 1996).

2.6.2.2 Flow tests in small-scale models

Most tests of flow are applied in small-scale models. However, results of flow tests in small-scale models have limited and uncertain relevance to real installations. This is mainly due to the lower stress level in solids because they are a direct function of gravity forces acting on the solids. Another uncertainty concerns the influence of the shear zone along the wall on the flow because this zone has more influence in a small-scale model than it has in a real scale silo. Further more, the possible effect of the particle size on the test has to be mentioned. The particles' size has to remain small in comparison with the dimensions of the model. These and other factors influence the flow behaviour of the solid, and because of this the chance of arching, and the segregation of the solid is influenced.

2.6.2.3 Flow pattern measurement in full-scale silos

Measurements of flow patterns in full scale silos are rarely done. Observations usually rely on visual records of the top surface profile, together with signs of abrasion, scouring and polishing of the wall. From these, the regions of flowing solids are approximately deduced, though often it is not easy to ascertain whether the same flow pattern always occurs and whether it changes from time to time during the discharge. Flow pattern measurement in full-scale level was not achieved until the work carried out by the Silos and Particulate Group at the University of Edinburgh (Rotter et al., 1995; Ooi et al., 1998).

The technique they used was the residence time technique: placement of markers and automated measurement of the residence time of the markers. Rotter et al. (1995) conducted a series of experiments in which a massive quantity of residence time observations were made in two full-scale silos. The silos were seeded with radio

frequency tags which were placed in a systematic pattern using a specially designed deployable seeding device. Up to 300 radio tags were placed in known positions at up to nine levels (see Fig. 2.10). The residence time was assessed in terms of the amount of solid remaining in the silo at the instant when each marker passed through the outlet.

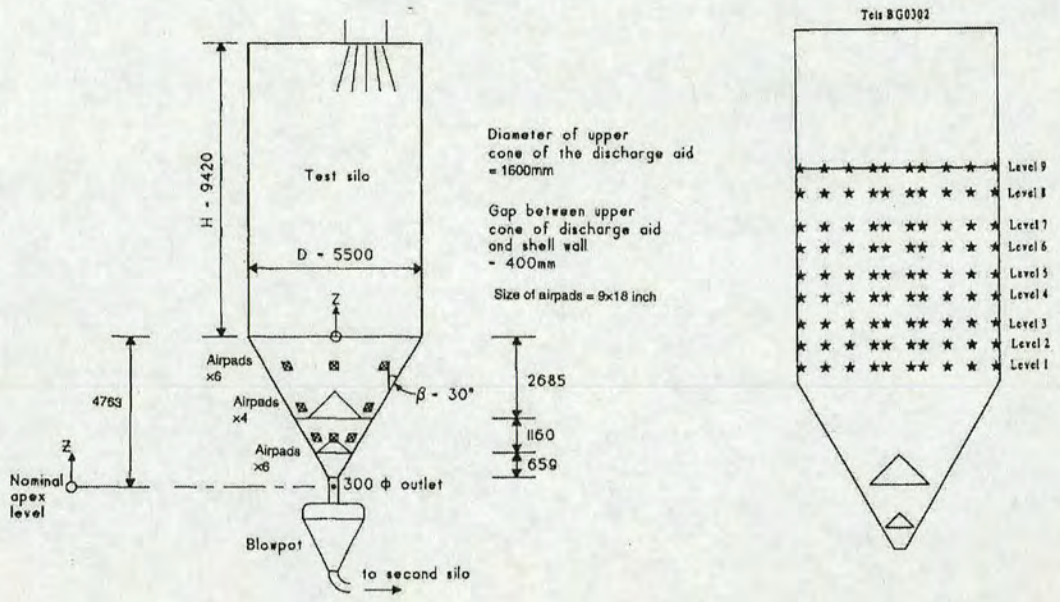

Fig. 2.10 A full-scale silo used for measuring the flow pattern with the residence time technique (left); 300 hundred radio tags (markers) were carefully seeded in position in 9 levels in the tests (Rotter et al., 1995; Ooi et al., 1998)

The location of each marker is very important, since there is no independent means of verifying where the marker was placed once it has been covered by additional bulk solid. Thus the chosen technique had to ensure that (a) the marker was correctly identified at the time of placement, and (b) it was placed in exactly the intended location. Rotter et al. (1995) used markers which were carefully identified by colour and number coding, and which were precisely placed using a placement template with the silo.

The chief challenges in full-scale flow pattern measurement lie in making direct observations, the expense of conducting full-scale studies, the constraints of operational need of the plant, and the critical importance of making reliable observations.

2.6.3 Silo pressure measurements

Experimental investigations into the pressure on silo walls have been undertaken since the test of Roberts (1882, 1884), which preceded Janssen's (1895) theory. A huge number of tests have been conducted by a great variety of researchers, so that a full review is well beyond the scope of this report. The literature is much larger than for solids flow, so a limited review is given here.

The early experiments on silos are reported in detail by Ketchum (1907). From his review, it could already be established that the Janssen (1895) theory provides good predictions of the pressure which occur on filling, that larger pressure were sometimes encountered during discharge, and that eccentric discharge could cause unexpected high pressures.

A number of major studies influenced the development in the field of silo pressures since Ketchum. These may be chosen as the studies of Pieper's large experimental group in Braunschweig (Pieper and Wenzel, 1963; Pieper, 1969), the experimental and theoretical investigations of Jenike and his co-workers (Jenike, 1961, 1964, 1967; Jenkie and Johanson, 1968, 1969; Jenike, Johanson and Carson, 1973), and the experiments of Deutsch and Clyde (1967). The full scale, model scale and centrifuge studies of the Danish group under Askegaard and Nielsen (Askegaad et al., 1971; Nielsen and Kristiansen, 1979, 1980; Nielsen, 1983; Nielsen and Andersen, 1982; Hartlen et al., 1984; Askegaard and Munch-Andersen, 1985; Munch-Andersen and Nielsen, 1986, 1990) must also be mentioned, and there were many other important studies as described below.

Askegraard and Munch-Andersen (1985) paid special attention in description of their shear cells installed in a medium-scale model silo. The cells were used to measure normal pressure and shear stress in the tests of both central filling and central and eccentric discharge of barley. It was found the wall friction coefficient were higher in filling (0.58) than that in discharge (0.43).

Rowe (1959) measured wall stresses using a strain gauge pressure cell in a 10m

diameter, 30m high reinforced concrete silo containing cement. Air slides were used to extract the material. Rowe concluded that the pressures measured in silos were not predicted well by Janssen's theory.

Turitzin (1963) summarised much of the early work in Russia and France on the measurement of stresses that arise during discharge from silos. He concluded that lateral pressures during filling are generally less than those during emptying.

Walker and Blanchard (1967) measured wall pressures in pilot scale hoppers with up to 5 tonne capacity. Conical hoppers with 3, 15, 39 and 45 degree half angles and pyramid shaped hoppers with 15, 30 and 45 degree half angle were used. Experiments were performed using coal as the test material. A water filled football bladder connected to a pressure transducer was also used to measure internal pressures within the material. The stress fields during discharge were found to be very different from those set up after filling. For the steeper smoother hoppers, the resulting pressures showed good agreement with Walker's theory. The bladder is , however, an extremely unreliable method of measuring pressures in a still solid such as coal.

Aoki and Tsunakawa (1969) measured wall pressures in small mass flow hoppers and found that Walker's theoretical approach agree with the experimental results well. Aoki and Tsunakawa later summarised much other Japanese work on silo loads. They found that Janssen's theory produced good estimates of the pressure in a 530 mm diameter model bin (1972).

Sugita (1972) measured the wall pressure in a 7 m diameter, 28 m high reinforced concrete bin containing wheat using diaphragm type gauges. Flow in the bin was described as funnel flow, though no measurements were made. Static pressure were nearly equal to the values given by the Jassen theory. Pressure during discharge were very much higher and showed a maximum part of the way up the cylindrical silos. Sugita related his full scale silo pressure measurements to the flow pattern he observed in small model bins.

Smid (1975) used the model cylindrical silo, previously used for flow experiments by

Novosad and Surapati (1968) to investigate wall pressures in silica sand. Experimental results for the pressures after filling were in good agreements with predictions based on Janssen's theory. Novosad and Surapati (1968) found internal or core flow during discharge. Smid noticed the measured stresses oscillated during discharge.

Wright (1980) reported an investigation carried out in 1961 of the pressure in a 300 ton capacity reinforced concrete coal bunker. The bunker was approximately 21 m high with two rectangular compartments each 8 m wide and 4.5 m long. The flow regime in the hoppers was mass flow. Pressures recorded using strain gauge diaphragm pressure were significantly higher than excepted, particularly during discharge near to the hopper transition.

Blight (1983) measured pressures in a 20 m diameter steel maize storage bin using mercury-filled strain-gauged diaphragm pressure cells. The profiles of the maize surface in the bin was determined by dropping a tape from the top of the bin. The height of the material in the bin fluctuated during the measurement period as a result of normal transfer of grain in and out of the bin. Rusting of bin walls at the bottom identified the extent of dead material in the base of the bin. Blight reported an increase in lateral pressure at the effective transition where the flow changes from parallel to convergent flow.

Blight et al. (1983) measured the strain in the hoop reinforcing of a concrete silo during rapid filling with raw meal of cement. The silo was 43 m high with a diameter of 15 m. When the fine powder is rapidly loaded into the silo it entrains a large proportion of air. The pressure exerted on the silo walls at any depth is made up of the pressure in the entrained air and that exerted by solid particles. As the air escapes from the powder the pressure distribution changes. These authors suggested that the maximum pressure could be predicted reasonably accurately by solving Janssen's differential equation with special allowance for consolidation of the stored solids.

In pilot scale hoppers approximately 2 m in diameter, Murfitt and Bransby (1982) found that the total stresses during discharge approached the hydrostatic distribution.

Suzuki et al. (1985) measured the stress distribution at the wall and frictional loss at the transition in small and medium sized silos. The found that the lateral and vertical stress distributions at the wall were as predicted by the Janssen theory and that the stress distribution during discharge in the hopper could be predicted by Walter's (1973) modification of the method of differential slices.

Blight (1987, 1988) measured the strains in walls of a free-standing cylindrical steel silo. The silo diameter was 20 m and it was 40 m high. Discharge was through 24 extractor cones situated around a central deflector cone. Although the flow pattern during discharge was concentric, wall loads were radically non-uniform during discharge. The author suggested that variations in wall friction caused the non-uniformity. Horizontal pressures increased during discharge resulting in a reduction in the wall load. They noted that temperature has a significant effect on wall loads during further investigations with the silo.

Blight made pressure measurements on a number of large silos. He believed that much of the early work on pressure measurements in silos was seriously flawed (Blight, 1986). He used strain gauge diaphragm pressure cells to measure the pressure in 20 m diameter, 54 m high concrete walled coal silo (Blight, 1986). The coal in the bottom of the silo formed a conical hopper with the wall 60 to 70 degrees to the horizontal. His interpretations of the experiments indicated that the horizontal pressure in the silo increase linearly with depth.

Brown et al. (1996, 2000) did a series of experiments on a square funnel-flow un-stiffened steel silo. The material used was free-flowing granular solids. They found that the pressures across the face of each wall were non-uniform. High pressure were seen to develop near corners and low pressure near the centre of the wall. This pattern is thought to be caused by the wall flexibility, together with the square shape. They also found that changes in the stiffness of the wall affects the pressure distribution around the circumference of a rectangular silo. Further experiments showed that the wall pressure at any level in a rectangular silo are systematically non-uniform (Rotter et al., 2002).

Zhong et al. (2001) monitored the sensitivity of silo flow and wall stresses to the filling method. They found that small changes in the filling process have a very marked effect in the solid flow pattern under concentric conditions. This change of flow pattern will effect the silo pressure distribution; at worst, this change will lead to a great variation and marked asymmetry of the wall stresses during the discharge. This loss of symmetry is so strong that it is probably more important than any symmetrical overpressure.

2.7 Influence of inserts

2.7.1 Introduction

Inserts are used to alter the solid flow patterns; the original purpose was for blending material and reducing segregation through theirs influence on flow in silo (Johanson and Kleysteuber, 1966; Johanson, 1970, 1982; Wilms, 1986, 1992). Studies were carried out to find the possibility of changing a funnel flow silo into mass flow with the aid of inserts. The influence caused by the use of inserts on the silo wall pressures, the stress distribution within the granular material and the loads on inserts were also investigated (Johanson and Kleysteuber, 1966; Tuzun and Nedderman, 1983; Polderman et al., 1985; Strusch et al., 1993; Antes et al., 1995; Strusch and Schwedes, 1998).

2.7.2 Types of inserts

Various inserts have been invented for various goals by different researchers through the world. According to their geometrical features, they can be classified into two groups. The cone-shaped insert and hopper-shaped insert are typical.

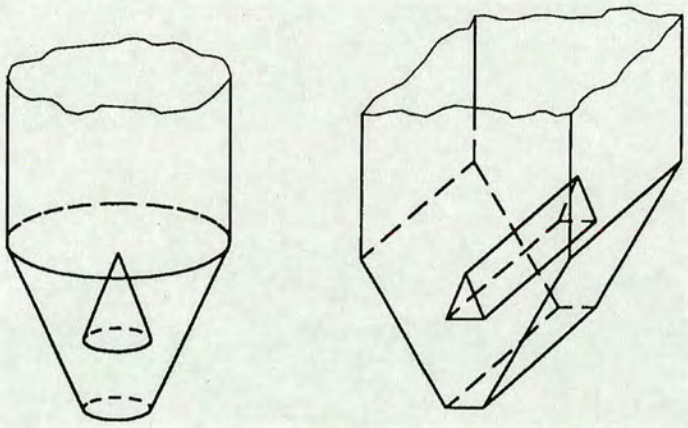

Fig. 2.11 Cone-shaped inserts (Roberts, 1986)

Cone-shaped inserts (e.g. Fig. 2.11) are usually wedge-shaped or conical. The sloped walls have to be considered in the same way as hopper walls, and therefore they have to be designed for mass flow in order to avoid flow problems. A double –cone shaped insert is an alternative to such single cone inserts.

The original hopper shaped insert was known as the Cone-in-Cone (see Fig. 1.5). It was originally proposed by Johanson (1966), and was used to make blending more efficient. The cone-in cone controlled flow patterns and can make typical funnel flow hoppers into mass flow without excessive headroom. Theoretically, the cone-in-cone can principally be extended to many such inserts within the outer hopper, but little work has been done on testing this theory.

LynFlow inserts (Bates, AJAX Equipment), are fitted to the inclined hopper walls by welding or bolting. The technique is versatile, in that different designs can be employed to counter segregation, provide homogenisation of the contents, accelerate the de-aeration fine powders in a fluidised condition and secure more stable density of the discharging material than is given by conventional flow channels.

2.7.3 Applications of inserts

Application of inserts to silos has effects both on the flow and the loads. A brief account is given below about its the status quo.

2.7.3.1 Influence on flow in silos

2.7.3.1.1 Eliminating segregation

Principally segregation can be reduced /eliminated only if mass flow occurs. One of the most extensive uses of the BINSERT has so far been the elimination of segregation problems. Very often, material segregates upon entering the silo, and re-mixing of the segregated material is expected during discharge. This can be accomplished simply by causing a uniform flow pattern in the silo. Using an insert can change the material flow from funnel-flow to mass-flow. As a result, the material, with the aid of an insert, will be discharged in a uniform flow pattern -- in this process the segregated material is re-mixed.

2.7.3.1.2 Blending and homogenisation

In addition to their use in counteracting segregation, inserts can also be used for blending and homogenisation. In fact, the major purpose of the BINSERT was to make blending more efficient. With careful design, the average relative velocity of the flow channels inside and outside the insert can be controlled by the velocity profile produced at the bottom of the insert. This is useful. For example, if a mass flow cone is attached at the bottom, then a more rapid velocity will occur through the inside cone than through the outside annular region. This can be used in blending / homogenising solids in the silo. Whereas when a vertical section is imposed between the bottom of insert and a mass flow hopper or feed device, a uniform flow pattern can be achieved causing uniform velocity throughout the silo and the hopper. This is useful in preserving the homogeneity of the blend during the final discharge. The arrangement also provides for flexibility. By making the length of the vertical section variable, continuous change in flow pattern can be achieved from uniform to a maximum velocity gradient. This allows a fine tuning of the hopper if it is to be used for blending. It also allows a change from blending /homogenisation mode to the plug flow mode during final discharge.

2.7.3.1.3 Promoting mass flow in conical hoppers

Throughout industry there are a lot of silos whose hoppers have wall angles of 60° to the horizontal; but some of these silos, even with such steep hopper angles, still do not work as mass flow silos. As a result, problems such as rat-holing, flooding, flushing, and segregation which are associated with funnel flow frequently occur. By taking such an existing hopper and installing a properly designed insert, it is possible to cause an otherwise funnel flow cone to act as the equivalent of a cone that is sloped 75° from the horizontal. That is to say, the insert can change material flow from funnel to mass flow. For instance, the cone-in-cone, marketed by Jenike & Johanson Inc and J. R. Johansan Inc (1966, 1982) allows the annular region to mass flow at wall inclinations greater than would be possibly required otherwise.

If this ideal result does not happen, narrow funnel flow zones can at least be expanded with the aid of an insert. In such operations, the bulk solid has to flow around the insert. As a result, an increased flow zone occurs. Furthermore, under some circumstances, an improvement in the flow conditions can be achieved if the insert is designed carefully; and under other favourable circumstances segregation can also be reduced. Nevertheless, care is necessary and the insert must not give rise to arching. Cone-shaped inserts have also been used to promote mass flow in axi-symmetric silos. They effectively transform the flow pattern to that of a plane flow silo, hence allowing one to benefit from the fact that mass flow in plane flow occurs at angles up to 12° greater (to the vertical) than in axi-symmetric flow. Once again, however, one has to be aware of the possibility of arching between the insert and the hopper walls.

2.7.3.1.4 Enhancing flow rates

The cone-shaped inserts can be used to inject gas into the bulk solid. The injected-gas flows into the void below the insert and then permeates the bulk solid. This makes the material looser and flow easier. This technique can be used in cooling bulk solids as well.

2.7.3.2 Influence on wall stress distributions in silos with inserts

2.7.3.2.1 Pressure measurements on the wall

Measurements of wall normal stresses on silos with inserts have been carried out by Theimer (1974) and Nothdurft (1976). Their measurements show an increase in the wall normal stress at the level of the insert during filling and during discharging.

Tuzun and Nedderman (1985) placed wedge-shaped inserts and square inserts in a tall silo of rectangular cross-section. The flow patterns were photographed through the float glass front wall of the silo. Wall normal and shear stresses along the side-walls of the silo were measured. They observed that the presence of an insert affected the wall stress distribution in different ways during filling and during discharging. During filling, the wall stresses at the level of the insert were generally larger than those observed without inserts. By contrast, during discharging, the wall stresses at the level of the insert were less than those without inserts. Considering the flow pattern observations around the insert, they said that the observed disturbance of the flow field around the insert is coupled with peak values of the wall stresses measured at the level of the insert.

Kroll (1975) measured no increase in the wall normal stress at the level of the insert. He measured the horizontal stress within the bulk solid with the help of a stress measuring cell, which was moving together with the bulk solid during the discharge. He detected an increase in the horizontal stress at the level of the insert. He concluded from his measurements that the bulk solid between insert and silo wall is deformed in a similar way to that in the hopper section.

Scholz (1988) measured an increase in the wall normal stress at the level of the insert during the filling and during discharging in the case of an insert positioned in the vertical section of the silo. He observed no increase in the wall normal stress for an insert positioned in the hopper section.

Strusch and Schwedes (1995) studied the possibility of distributing the silo wall stress by use of a triangular insert. A preliminary numerical model was made to show qualitative results. Different shape and size of insert were implemented in their program. Karlsson (1996) also did similar studies when investigating a cone-in-cone's effects on the flow pattern. However, the results were still premature.

Northdurft (1976), Strusch et al. (1993, 1995) showed that an asymmetrically installed insert within a silo led to an asymmetric flow pattern with completely asymmetric wall stress distributions and asymmetric insert loads. Enstad et al. confirmed that putting the inserts axi-symmetrically in to an axi-symmetrical silo was very important to use inserts, otherwise it will make the material flow skewed during discharge (1997, 1998).

2.7.3.2.2 Reduction of over-pressures

Inserts in silos are among a number of means used to influence the flow pattern and to relieve the feeder. The change in the flow pattern leads to a change in the stresses in a silo.

The reduction of the wall stress below the insert results from the fact that the insert takes up a part of the vertical load. That is not difficult to imagine. What proportion of the load the insert takes from the wall shear stress will be briefly discussed later. On the other hand, however, the wall stress change at the level of the insert is a bit complex to explain. Briefly, the space between the wall and the insert form a space which is similar to the hopper; so it can be concluded that the bulk solid between the insert and the silo wall is deformed in a similar way to that in the hopper section. That is to say, a radial stress field appears between insert and the silo wall. The pressure at the level of the insert is then distributed based on the way along which the narrowest section between the insert and the wall is the 'outlet'. As a result the position of the peak of pressure moves upwards, while the magnitude of the peak pressure decreases on account of the insert partially sharing the weight of the material.

Placing the insert symmetrically inside the silo is very important, otherwise it will well maybe lead to serious consequences. Kroll (1975), Scholz (1988), Johanson and Kleysteuber (1966), Tsunakawa and Aoki (1975), Polderman et al. (1985) measured the vertical load on inserts in silos. The measured vertical insert loads are significantly higher than the loads which result from Janssen's formula of the vertical stress of wall stress in the vertical section of a silo.

2.7.3.2.3 Use of inserts to control loads on feeders

Inserts have not only been used to modify the flow pattern, but can also be adopted to reduce the load on the feeder and the corresponding power requirements as well. Roberts (1990) employed this idea in the case of an apron feeder. Investigations were carried out involving the use of both longitudinal and transverse, triangular-shaped inserts. Preliminary tests showed that while the longitudinal insert produced some load control, it was not as effective as the transverse insert.

As there are practical difficulties in using longitudinal inserts which limit their application, further tests were confined to the transverse insert. The position of the transverse insert was varied, and the loads on the feeder recorded. As expected, the reduction is more pronounced for the initial filling or start-up torque since the load is influenced by the surcharge head in the hopper. This is not the case for the flow load and running torque. The advantages of using an insert to control the initial loads is clearly demonstrated.

2.7.4 Loads on inserts

Inserts will also take up the loads of the weight of material and may reduce the burden on the silo wall. Tests (Strusch and Schwedes, 1998) revealed that the proportion the insert takes varies greatly according to the different handling processes, as well as the insert position in the silo and the size of the insert itself.

3 LOADS ON THE WALLS OF CONICAL HOPPERS AFTER FILLING

3.1 Introduction

The hopper part of a silo has been a subject of extensive experimental and theoretical research. The hopper supports the majority of loads induced by the stored material, and is usually subject to a biaxial tension (Rotter, 2001). It is well known that the load acting on the hopper walls varies between the condition after filling to that during discharge.

The manner in which the hopper is filled has been shown to have an effect on the way that the stored material is discharged (Munch-Andersen and Nielsen, 1990; Zhong *et al.,* 2001; Rotter, 2002). The process of filling is a process in which solid is piled up from a loose surface flow (Khakhar, 2001; Baxter and Yeung, 1999). Within the pile, a distribution of stresses, anisotropic in character, develops (Ristow and Herrmann, 1995; Edwards and Mounfield, 1996; Wittmer et al., 1996, 1998; Socolar et al., 2002). This stress field transmits loads to the wall as filling progresses. After filling is complete and discharge begins, a shift in the stress state is expected to occur within the stored solid, followed by further stress field evolution during the process of discharging. The stress field during discharge transmits forces and exerts loads on the hopper walls. The stress field during discharge depends on the stress pattern and packing arrangement before discharge commences. An accurate determination of the conditions produced in the granular solid by the end of filling is critically important.

The theories that aim to predict the pressures exerted on hopper walls must first be traced back to those for the vertical walls of silos. For a vertical wall, the classical theoretical approach was the analysis of Janssen (1896). This theory was based on two assumptions:

1) the ratio between the average vertical stress on a horizontal section and the average horizontal pressure on the wall is constant throughout the entire height of the vertical wall; the value of this ratio depends on whether the stress state that the stored material is in, which has often been simplified into either an active state or a passive state; and

2) the wall friction coefficient μ is constant throughout the entire height of the silo.

Although the parameters of bulk unit weight and wall friction angle are directly measurable, the value of lateral pressure ratio in Janssen's theory is less clear. As a result many different authors later attempted to produce extensions or modifications of Janssen's theory in which the lateral pressure ratio was able to be determined from the failure properties (e.g. internal friction angle) of the solid. These theories mostly assumed some types of active failure for the solid after filling, and passive failure during discharge. Unfortunately, the simplest of such theories produced filling pressure predictions that were too low, and discharge pressure predictions that were far too high, when compared with experiments. As a result, many such theories were developed over the last five decades, but none has yet gained widespread acceptance: indeed it can be shown that they must all be wrong, since the experimental results are rather different in character from these predictions.

Computational modelling offers a powerful tool to explore hopper pressures and has been used here to obtain more convincing descriptions. In the last two decades, many attempts have been made to develop computational models to represent the behaviour of granular stored solid in silos. The two main methods used are the finite element method and the discrete element method.

The finite element method (FEM) is often used to study macroscopic phenomena such as the stress regimes within the granular stored solid and the reaction of the wall to the pressure exerted from the granular stored solid. The granular stored solid is represented as a continuum with an appropriate constitutive law, usually based on a semi-empirical interpretation of static tests on small samples of the granular stored solid. The FEM

analyses have been conducted using programs written specifically for the analysis of silos, or by using available commercial packages such as Abaqus.

In this chapter, the finite element method was used to investigate the development of stresses within the stored solid in a hopper and the wall loads on the hopper during filling. To simulate the filling process, the zones representing the granular stored solid were partitioned into layers, upon which fine meshes were defined. The interaction between the granular stored solid and the hopper wall was modelled using Coulomb friction. The meshes representing the stored solid and the corresponding wall interaction were suspended at the beginning of analysis. Steps were taken to reactivate the suspended mesh and wall interaction in a designed sequence layer by layer to model the progressive filling process. In addition and for comparison, an analysis in which gravity was 'switched on' for the entire mass of solid in the hopper was also conducted. These two types of analysis are later referred to as 'progressive filling' and 'switch-on'.

A constitutive law widely used for granular material was adopted as described below.

The finite element package Abaqus was used to set up the FEM models. The models were first applied to a hopper with a steep inclination angle, and then to a hopper with a fairly flat (shallow) inclination angle. The predictions of classical theories for the pressures acting on the wall of the hopper are compared here with the numerical predictions. Experiments designed to validate the predictions for the shallow hopper were also conducted and the comparison is shown.

3.2 Predicted pressures in a hopper with a steep inclination angle

3.2.1 Hopper Geometry

The hopper was assumed to be quite steep in the first study, following the same approach as classical theory adopted. Its geometry, shown in Fig. 3.1, was axi-symmetric with a height of 2400 mm, an upper edge diameter of 2400 mm and an outlet diameter of 400 mm. The wall was assumed to be made of stainless steel with a thickness of 6 mm.

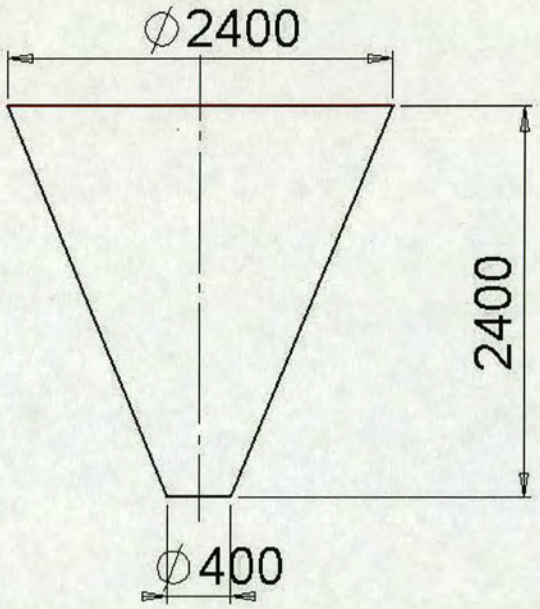

Fig. 3.1 The geometry of the hopper with a steep inclination angle (dimension in mm)

3.2.2 Classical approach

Many theories have been proposed for the distribution of pressures in a conical hopper. The differential slice method, originally used by Janssen (1895) for vertical walls, was modified and adopted by for instance Walker (1966), Walters (1973), Enstad (1981) and Rotter (2001) to derive theories to describe pressure distributions in conical hoppers. These theories may be suitable for both filling and flow conditions; a brief review in Appendix A gave emphasis to the filling condition to be consistent with the main topic to be studied in the present chapter.

3.2.3 Finite element numerical approaches

3.2.3.1 Introduction

Both finite element and discrete element techniques have been used for many problems involving granular bulk solids. Granular bulk solids, as stored in silos, exhibit more complex behaviour than fluids or solids. They exhibit shear strength and can support forces without time-varying deformation, but at failure they flow with large deformations. These conditions cause major difficulties for both the finite element method and the discrete element method.

The discrete element method seems a more natural choice for a realistic representation, but it places huge demands on computing resources even for small and over simplified problems. In a large international comparison project, 10,000 circular particles were used in a 2D model of a planar silo, but a realistic full scale three dimensional problem might require as many as 10^{13} particles, many orders of magnitude outside the current limit. Such particles are usually complex shaped, and difficult to represent individually (Rotter et al., 1998; Goodey et al., 2003). This project also showed that it is currently very difficult to deduce appropriate properties that represent individual particles well and also to derive practically useful pressures from the output.

By contrast the finite element method has an advantage in setting up the model by the application of stored solid constitutive laws (the challenge is shifted to finding an appropriate stored solid model), with dramatic simplification. The wide availability of commercial packages has enhanced the practical application of the finite element method, and led to many robust programs capable of very complex modelling. It offers a choice for the analysis of practical silo problems. In the present study, filling pressures are investigated using the finite element method and modelling the granular bulk solid as a continuum, adopting an appropriate constitutive law.

3.2.3.2 Geometries for stored solid formed from distributed filling or concentric filling

The axisymmetric conical hopper shown in Fig. 3.1 was used for further analysis. An attempt was made to model two different possible filling processes. The filling of this hopper was made either by a distributed filling mode, or by a concentric filling mode (Zhong et al., 2001). Under the distributed filling, the granular stored solid rained down evenly over the whole surface, forming a flat surface profile in the hopper. By contrast, under the concentric filling, the stored solid was deemed to fall on the axis of the conical hopper, piling up into a cone at the repose angle. The regions for these two models are illustrated in Fig. 3.2.

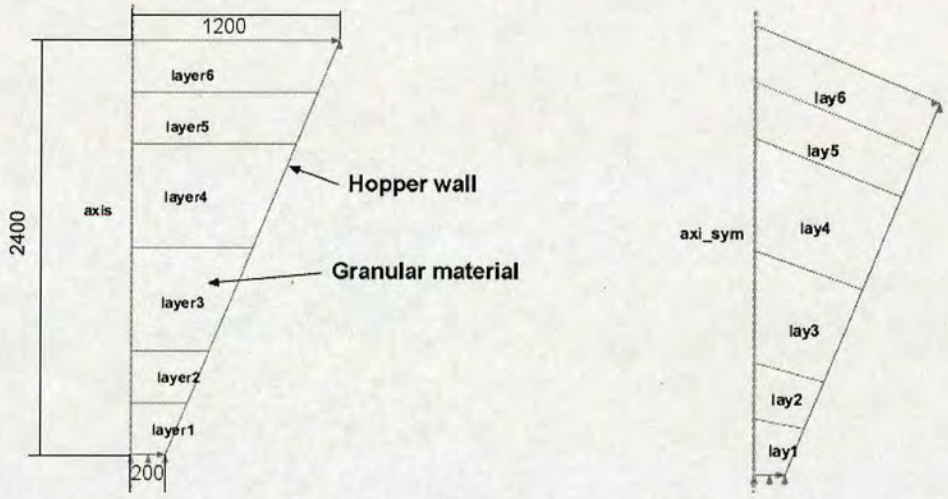

a) distributed filling b) concentric filling

Fig. 3.2 Geometry for the hopper and stored solid with different filling processes

3.2.3.3 FEM Formulation

Using the geometries described above, finite element models were devised following the standard procedure provided by Abaqus (2003) to model the hopper wall, the granular stored solid and the contact interaction between the granular stored solid and the wall. In each model the region as shown in Fig. 3.2 was discretised. An axisymmetric shell element was defined for the wall, and a continuum axisymmetric element for the granular stored solid. They together formed the element domain. Within this domain, the hopper was constrained both horizontally and vertically at its top edge and horizontally at its bottom edge; in addition, the edge node of the granular stored solid at the outlet was also constrained vertically. The other edges were set free. The loading on the granular stored solid was due to its weight; the hopper structure was assumed to be weightless.

In a finite element model, the behaviour of each stored solid involved is characterised by using an appropriate material constitutive law. The wall of the silo was simply modelled as an elastic material. The search for a precise model for the granular solid material is, however, still a challenge and has not been resolved satisfactorily. Granular materials display various behaviours and the mechanical description of such assemblies is an old but still open problem. A general feature observed both in

experiments and in simulation is the very heterogeneous and anisotropic character of the force network arising from the inter-granular contacts (Ristow and Herrmann, 1995; Edwards and Mounfield, 1996; Wittmer et al., 1996, 1998; Vanel and Clement 1999; Kolb et al., 1999; Socolar et al., 2002). Recently, strong interest has developed in both the engineering and physics communities to try to develop a new understanding from a description of such granular contacts and force distribution to a macroscopic description of the stress-strain relations (Kolb, et at. 1999).

In the present investigation some classical and well established models were adopted. The stored solid in the silo was assumed to be a single phase solid, and was modelled approximately as an elastic-plastic frictional material. Under this model, the major parameters involved were the Young's modulus E_p, Poisson's ratio ν_p, the bulk density ρ, granular material internal friction angle φ and its friction angle with the wall of hopper ϕ_w. More details will be presented in each specific applications later.

The interaction between the granular stored solid and the silo wall depends on the material properties of the hopper wall and the granular stored solid. It could be quite complicated. For instance a slip-stick behaviour is observed quite often during wall friction measurements, as summarised by Schwedes (2003). Modelling such a mechanical interaction can be quite complex, and is still a great challenge (Heege et al., 1995; Kolb et al., 1999; Evesque and Adjemian, 2002; Pfiste and Eberhard, 2002). In the current study, the interaction between the contacting surfaces of the hopper and the granular stored solid was modelled through a simplified constitutive model of Coulomb friction. A constant friction coefficient μ was assumed.

3.2.3.4 Modelling of the filling process

It has always been a challenge to simulate a process such as a silo filling process. In a real process of filling, the granular stored solid is fed usually from the top and falls into the container. As the volume of the stored solid increases, the edges of this volume change. There have been several attempts to try to simulate the silo filling process. For instance, in discrete element method (DEM) calculations, the filling process (Holst et al., 1999; Rotter at al., 1998) was simulated by first seeding a hopper with particles,

which were allowed to fall through a centrally located orifice at a fixed height above the silo floor. This method of numerical modelling the process has been proven not currently feasible due to the huge number of particles required to be realistic. To model the filling process using the finite element method, the volume of the object is usually required to be defined first. Hence, it is common practice to define a finite element mesh to represent the whole stored solid, and then apply the load as gravity to the whole region (described here as 'switch-on'). It turns out to be a process of consolidation without initial stresses within the stored solid rather than a process of progressive filling. For closer representation of a filling process, several attempts have been tried, such as progressively increasing the density of the stored solid, or incremental 'progressive filling' with a small preloading in the stored solid or incrementally applying body weight over the total volume of the stored solid (Rombach, 1991; Ooi and She, 1997; Rotter *et al.,* 1998; Holst *et al.,* 1999; Keiter *et al.,* 2001; Guines *et al.,* 2001; Sanad *et al.,* 2001; Goodey *et al.,* 2003)

In the present study, the volume of the object was meshed, the stored solid properties and the loads defined, and then the meshes and the contact interactions involved were deactivated and suspended. The suspended layered mesh was reintroduced one layer at a time in a designated sequence. Corresponding to the reintroduction of each layer of elements, the load and the contact associated with that layer would be activated again. Through this procedure of reintroducing each layer of elements and reactivating of the corresponding load and contact, the progressive filling process was believed to be simulated. This approach is not exactly equivalent to the true process of filling; but it is clear that the finer the layering, the closer the approach will be to a real filling process.

However, the aim in the current attempt was to try out whether such an operation of suspension and reactivation was acceptable. For that purpose, a partition technique was utilized to divide the region of granular stored solid as shown in Fig. 3.2 a as an example. The region was divided firstly into two parts of equal thickness. Each of these two parts was subdivided again into two parts, giving four layers with the same thickness. The layer at the bottom and the layer at the top were again subdivided, resulting in six layers in total.

3.2.3.5 Filling modes: distributed or concentric filling

As described above, a distributed filling mode is presented by the mesh shown in the left hand side diagram in Fig. 3.2, and a concentric filling mode shown in right hand side diagram. In both cases, no initial velocity was implemented, so the impacting effect during filling was not taken into account. There was also no initial stress in any of the layers when they were reintroduced; so the filling of each layer was in fact a process of consolidation without initial stress within the stored solid.

3.2.4 Numerical simulation result and analysis

3.2.4.1 Determination of model parameters and convergence test

The determination of material parameters relates to the model adopted. For the wall, it was made of stainless steel, and was regarded as elastic. The Young's modulus E_w = 2.0 x 10^{11} Pa and the Poisson's ratio ν_w= 0.3 were assumed. The granular material was modelled as an elastic-plastic material, with the Drucker-Prager hardening / yield law. Under this model, the parameters involved were the Young's modulus E_p, the Poisson's ratio ν_p, the bulk density ρ, the internal friction angle φ, and the friction angle ϕ_w with the wall of the hopper.

The bulk density was an important parameter since the gravity loading was defined through the density. It makes the material deform, and together with the Young's modulus E_p, the Poisson's ratio ν_p and the internal friction angle φ, have an influence on the numerical convergence. Convergence tests were carried out after setting the stored solid bulk density to ρ = 1000 kg/m^3, and the Poisson's ratio ν_p to 0.3 (SAA, 1990; Hjelmestad and Taciroglu, 2000; Qu et al., 2001). Convergence was achieved when the Young's modulus E_p was higher than 5.5 × 10^4 Pa. The ratio between the Young's modulus and cohesion was assumed to be 11. The parameters, chosen to represent the stored solid, were assumed based on parameters used in Abaqus manual as summarized in Table 3.1.

Table 3.1 Constitutive model for the granular stored solid and parameters used

*material, name=POW	Keyword to define a name for material
*density 1000.,	Keyword to implement the density kg/m^3
*Drucker Prager 55., 1., 35.	Keyword to implement the material model The material angle of friction in meridional plane, ratio of the flow stress in tension to that in compression and the dilation angle in meridional plane (Hibbitt, 2003).
*Drucker Prager hardening 50000., 0. 55000., 0.02 60000., 0.025 70000., 0.03 120000., 0.035 100000., 0.05	The same as above; the true stress and strain
*elastic 550000, 0.3	Keyword to implement E_p (Pa) and ν_p
*friction 0.5	Keyword to implement the interaction as a friction

Two preliminary tests were carried out with different Young's moduli in the condition of 'switch-on' loading with concentric filling conditions. Neither the mesh nor contact interactions were suspended or removed, the loading was added throughout the whole region of the granular stored solid in one step. It was found that when the two different values of Young's modulus were used larger deformations occurred when the Young's modulus and yielding /hardening parameters were lower. However, the stress distribution field that developed within the granular stored solid was very similar (Fig. 3.3). To avoid possible numerical problems associated with very large deformations of the mesh, the higher value of Young's modulus and the hardening parameter were used throughout the rest of the analysis.

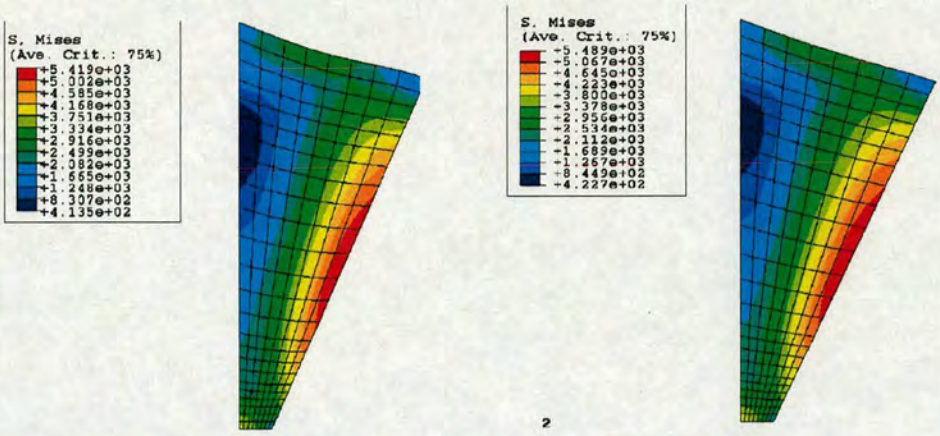

a) Lower E_p = 55000 Pa Higher E_p = 550000 Pa

Fig. 3.3 Contours of von Mises stress field developed under 'switch-on' loading

3.2.4.2 Simulations for a distributed filling mode

3.2.4.2.1 Stress distributions within the stored solid

3.2.4.2.1.1 Stresses under a "switch-on" filling process

First, the predictions for switch-on loading are shown. The stresses in a rectangular coordinate system are shown in Fig. 3.4 along horizontal lines through the centre of each layer for the shear stress σ_{xy}=S12, the vertical stress σ_{yy}=S22 and the horizontal stress σ_{xx}=S11.

3.2.4.2.1.2 Stresses under progressive filling process

Under progressive filling, each layer was activated starting from Layer 1 as described above. The stored solid in Layer 1 was first consolidated with no initial stress, and stresses developed in this region. When the elements from Layer 2 were reintroduced, the stored solid in Layer 2 underwent the same process as the stored solid in Layer 1 in the first step. The stored solid in Layer 1 would be consolidated further under the loads from Layer 2, producing further stress development. The stress development is shown in Fig. 3.5 for the shear stresses S12, the vertical stresses S22 and the horizontal stresses S11 along the same lines as those in the last section at the end of filling.

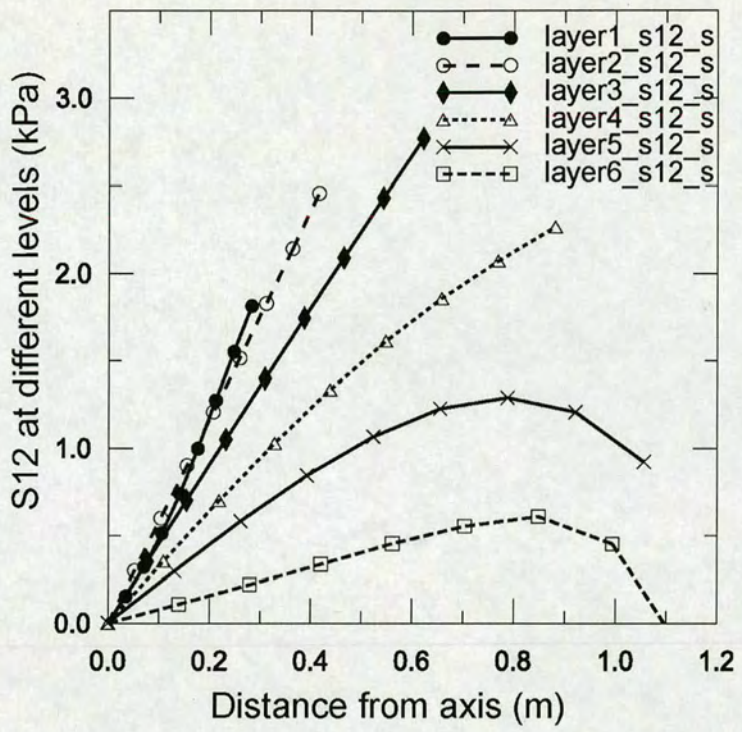
layer1_s12_s
layer2_s12_s
layer3_s12_s
layer4_s12_s
layer5_s12_s
layer6_s12_s
S12 at different levels (kPa)
3.0
2.0
1.0
0.0
0.0
0.2
0.4
0.6
0.8
1.0
1.2
Distance from axis (m)

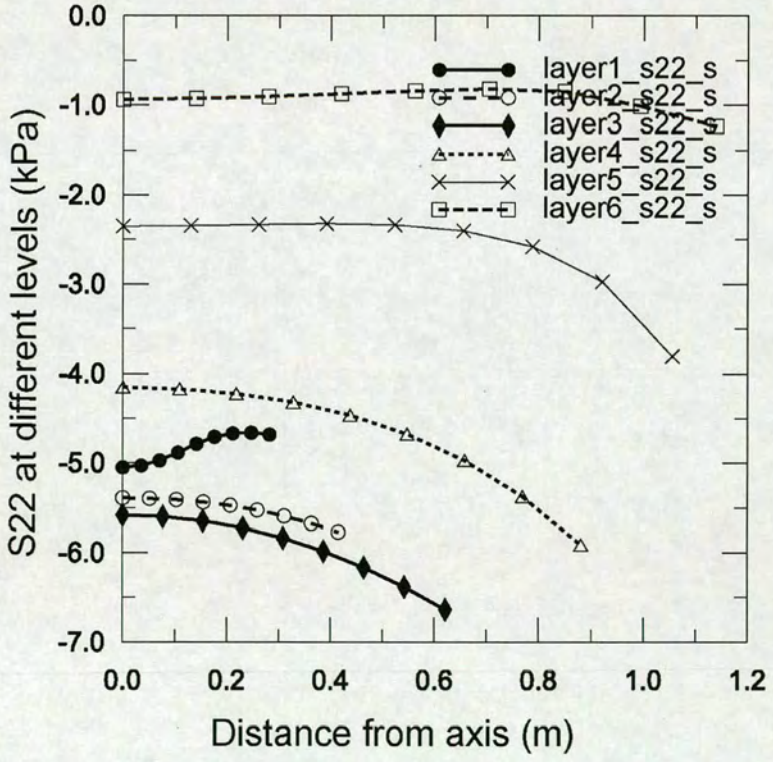
layer1_s22_s
layer2_s22_s
layer3_s22_s
layer4_s22_s
layer5_s22_s
layer6_s22_s
S22 at different levels (kPa)
0.0
-1.0
-2.0
-3.0
-4.0
-5.0
-6.0
-7.0
0.0
0.2
0.4
0.6
0.8
1.0
1.2
Distance from axis (m)

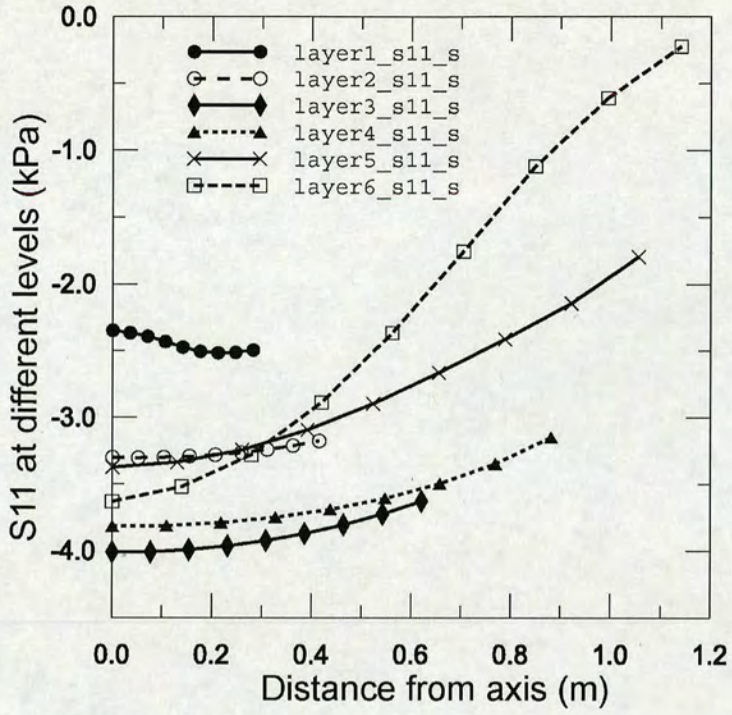

Fig. 3.4 Stresses on horizontal lines at the mid-height of each layer under switch-on filling

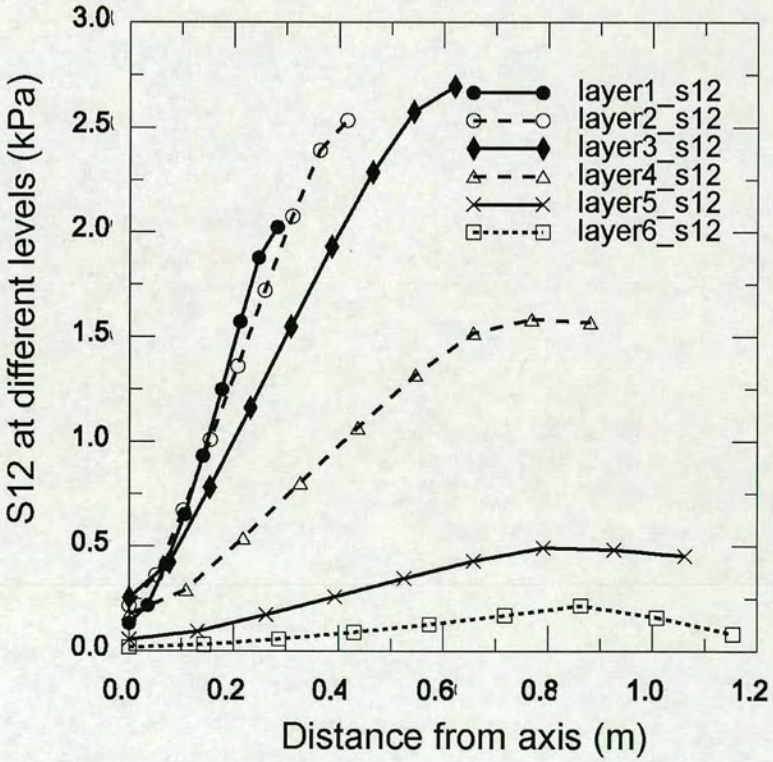

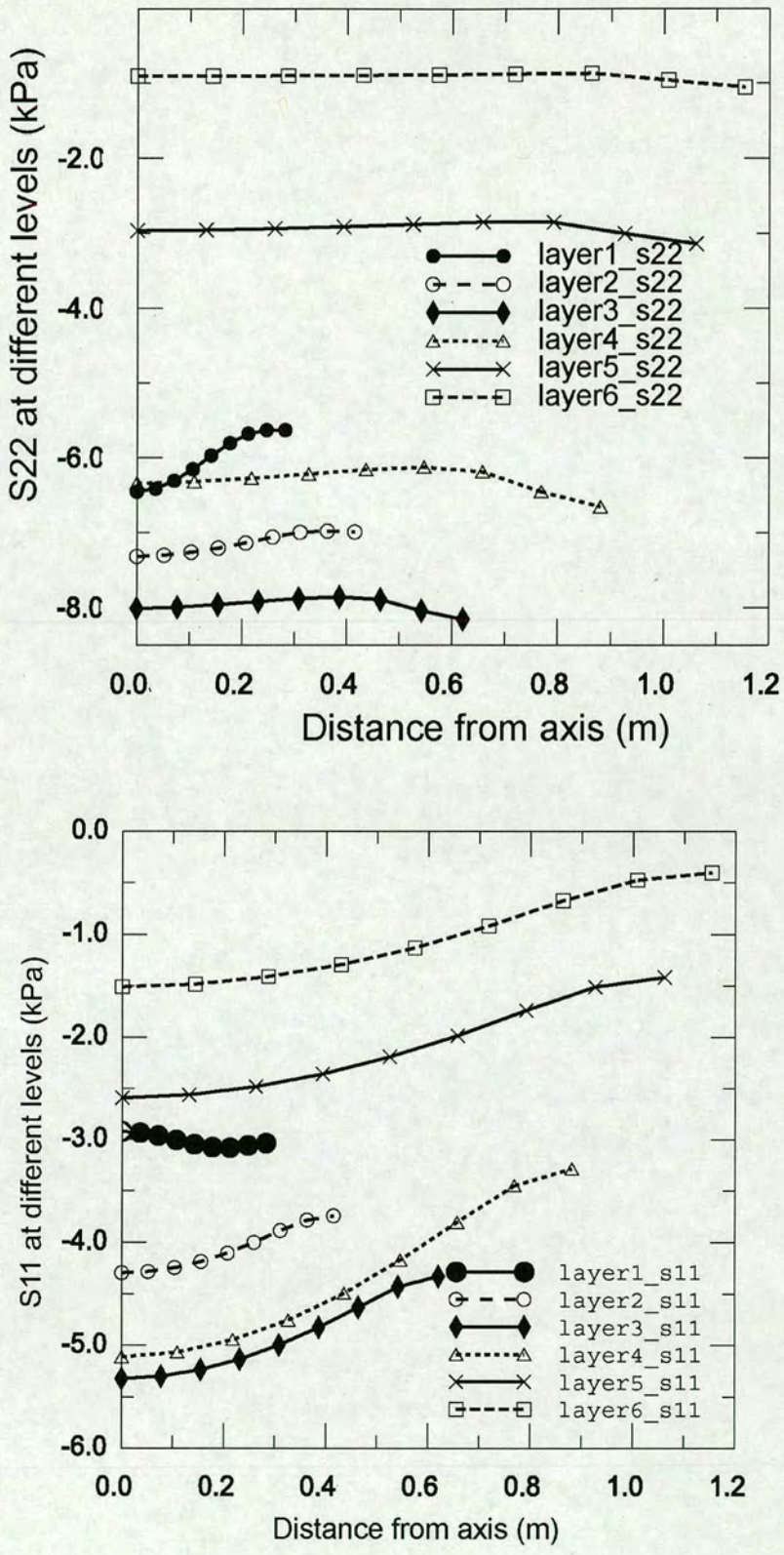

Fig. 3.5 Stresses along the mid-height of each layer under progressive filling

3.2.4.2.2 Pressures along the hopper walls

The pressures acting on the hopper walls are explored in this section. Some studies related to the application of different stored solid models and different finite element meshes are also discussed. However the majority of numerical analyses were carried out using linear elements. This is because only linear elements are valid in the further investigations of discharging reported in the next chapter (Hibbitt, 2003).

3.2.4.2.2.1 A modelling of the progressive filling process and the forces exerted by the stored solid

When elements are in contact under loading, normal forces and frictional shear forces or frictional tractions are generated across interacting surfaces between the wall and the stored solid. The resultants of the normal pressures and frictional tractions between the contacting surfaces of stored solid and wall are interpreted as loads on the walls. The normal force is regarded as normal pressure on the wall, and the shear force as frictional traction distribution on the wall.

When Layer 2 to Layer 6 of the finite element mesh were suspended, only the contact surfaces of Layer 1 and the wall were active. This interaction generated pressures and frictional tractions within this contact region. After that, Layer 2 was reactivated in the second stage of filling, and the contacts between Layer 2 and the corresponding wall surface were added back. The contact interactions were between the contacting surfaces of Layer 1 and Layer 2 and the wall. This new interaction brought about contact pressures and frictional tractions on the surface of a region covering Layer 1 and Layer 2. This process was repeated until all the layers were activated. The development of the filling pressure on the hopper walls thus obtained are shown in Fig. 3.6 for normal pressure on the wall, and in Fig. 3.7 for frictional traction on the wall surface.

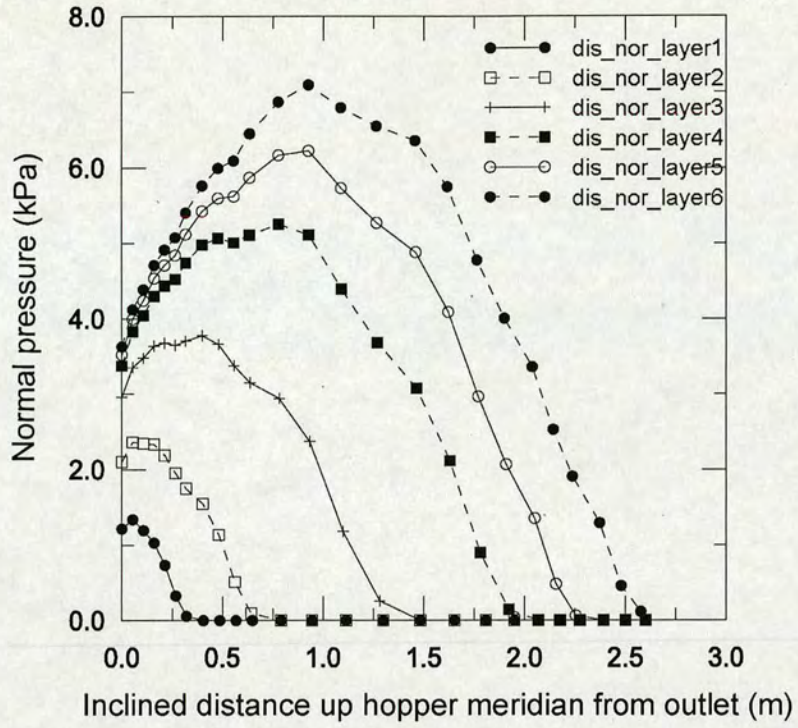

Fig. 3.6 The development of normal pressure on the hopper walls during filling

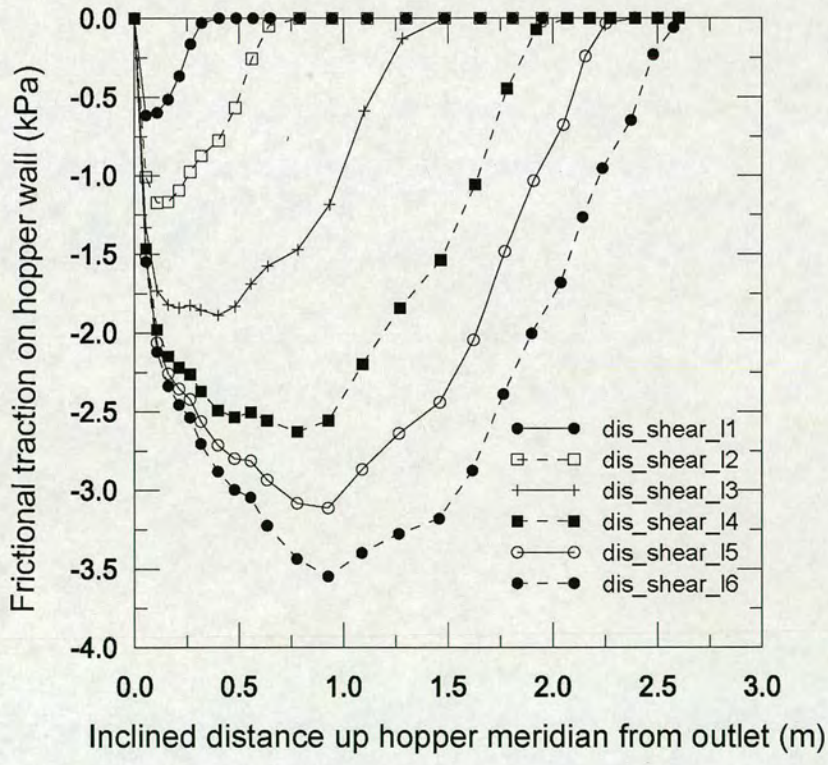

Fig. 3.7 The development of frictional traction along the hopper walls during filling

3.2.4.2.2.2 Application of different stored solid models

The field of finite element modelling was dominated at one time by the development of complex, sophisticated constitutive models as reviewed by Nielsen and Weidner (1998).

Several different well known constitutive laws for the behaviour of the stored solid are presented in the Abaqus package. These include

- Mohr–Coulomb plasticity (mc);
- Drucker–Prager plasticity (dp); and
- Drucker–Prager plasticity with creep (dpc)

For the simple axisymmetric filling case, Ooi and Rotter (1989) explored both Drucker-Prager plasticity and simple linear elasticity. They showed that even linear elasticity could give quite credible predictions for filling conditions because the behaviour is dominated by wall friction and Poisson phenomena. Their further work (Ooi and Rotter, 1991) showed that linear elastic material filled into a hopper exerts pressures that are very similar to those predicted by classical plasticity theories which assume that all the material is at yield.

The Mohr–Coulomb plasticity model defines the plastic behaviour, namely a yield criterion and a flow rule. The Drucker–Prager criterion is similar to the Mohr–Coulomb criterion, with one of the differences in that the defined yield surface is curved in deviatoric stress space, which improves the performance numerically. These two granular solid plasticity models are similar to the metal plasticity models: Tresca for Mohr–Coulomb and von Mises for Drucker–Prager. In addition, the Drucker-Prager creep model was also trialled. All of these are based on the plasticity theory, and fuller descriptions of these models can be found in some standard references including the Abaqus manuals.

In the first case of analysis, the material constitutive law used was the Drucker-Prager model. In the second case the Mohr-Coulomb model and the Drucker-Prager creep model were used for the purpose of comparison.

These three models all require the adoption of an elastic law. Therefore the basic parameters are still the Young's modulus E_p, the Poisson ratio ν_p, the wall friction angle ϕ_w and the stored solid internal friction angle φ. They were all given the same values. The stored solid internal friction angle φ needs to be converted in order to be suitable for the format adopted in Abaqus. The ratio between the Young's modulus and cohesion was still 11. The same plastic hardening/yielding parameters were used (see Table 3.1).

Figure 3.8 shows the predictions of the development of normal pressure on hopper walls during filling. One can see from this figure that these models did not generate any noticeable difference in wall pressures predicted.

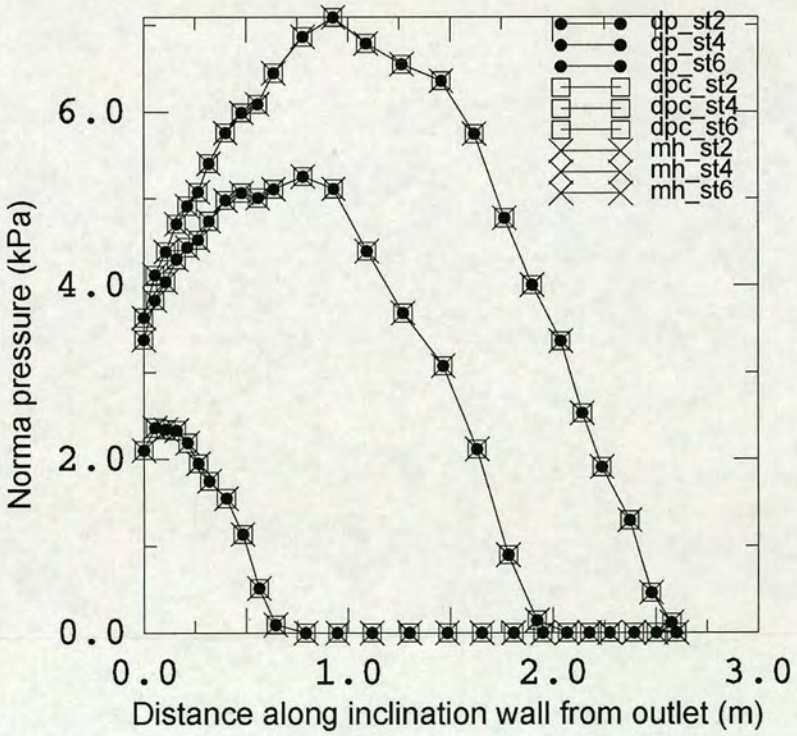

Fig. 3.8 Effect of material models on normal pressure on the hopper walls

3.2.4.2.2.3 Application of linear and quadratic meshes

It is necessary to investigate how the finite element mesh affects the outcome in a finite element analysis. In this section, both meshes with linear and quadratic elements were designed for the hopper wall and the stored solid. Using the Drucker-Prager model for the stored solid, and choosing the same material parameters, parallel analyses were again carried out and the predictions of three stages of filling are shown in Fig. 3.9.

From Fig, 3.9, one can see the effects of adoption of first order or second order element are very limited.

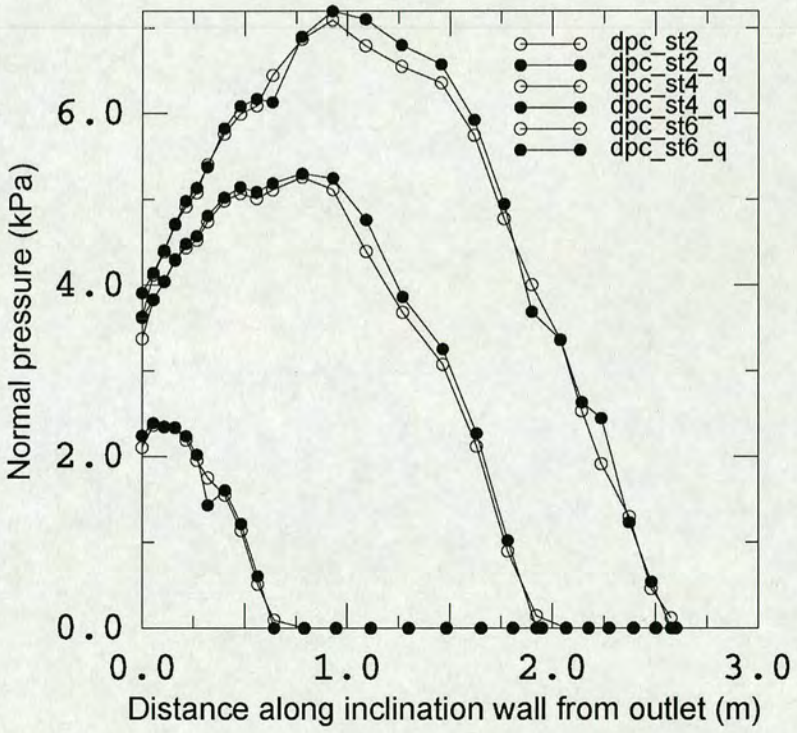

Fig. 3.9 Comparison of linear (open symbols) and quadratic (filled symbols) meshes for wall pressure prediction

3.2.4.2.3 Development of loads on the hopper outlet during filling

The next investigation focused on the development of pressures on the hopper outlet. The pressures near the outlet is useful for the design of discharging feeders.

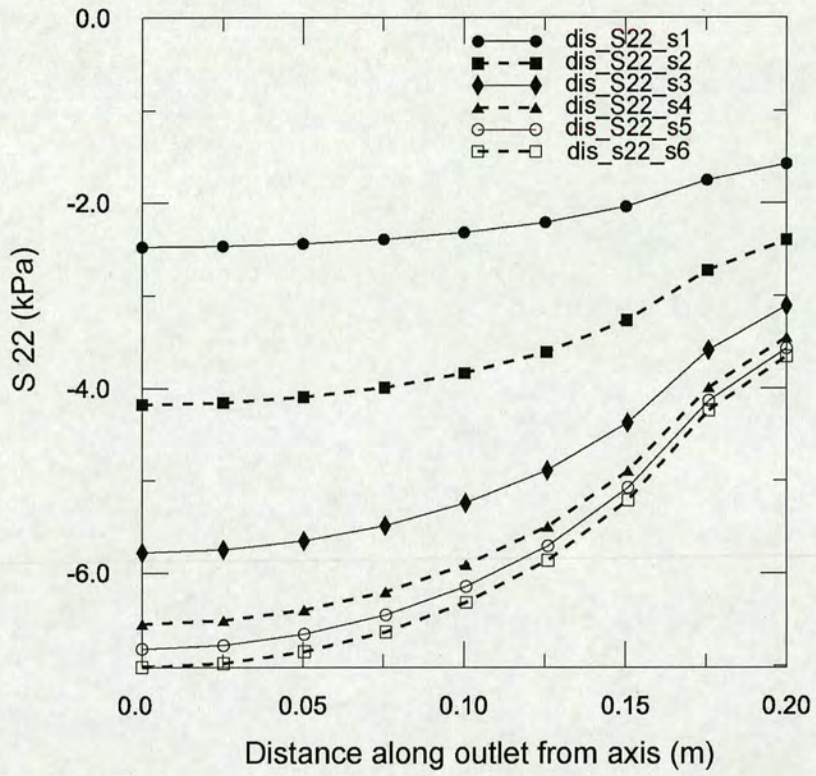

Fig. 3.10 Development of the vertical stress S22 on the outlet

In this investigation, the outlet was modelled as closed by constraining the outlet vertically. When the stored solid was filled into the hopper, it could not pass through the outlet, but would consolidate instead due to its gravity. Stresses would develop within the stored solid. The vertical stresses S22 at the interpretation points along the outlet line are treated as the pressures acting on the outlet. As filling progressed, these pressures increased in magnitude, as shown in Fig. 3.10.

3.2.4.3 Investigation of filling loads under concentric filling

3.2.4.3.1 Stress distribution within the stored solid

3.2.4.3.1.1 Stresses in the stored solid after "switch-on" filling

The same process as in section 3.2.4.2.1 was carried out for the conditions formed by concentric filling. Figure 3.11 shows the shear stress S12, the vertical stress S22 and

the horizontal stress S11 along the mid-height of each of the six layers of the mesh.

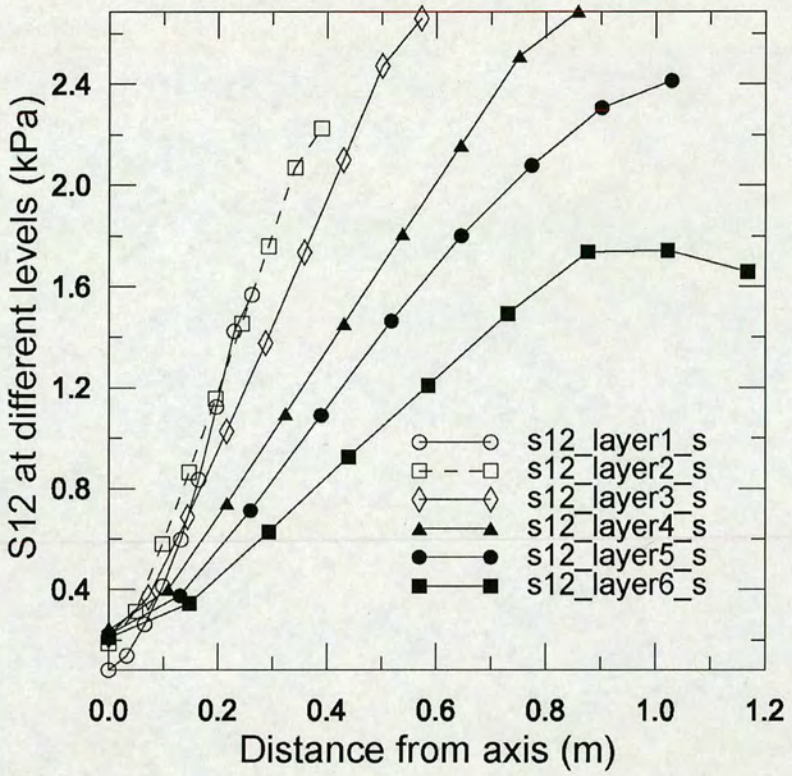

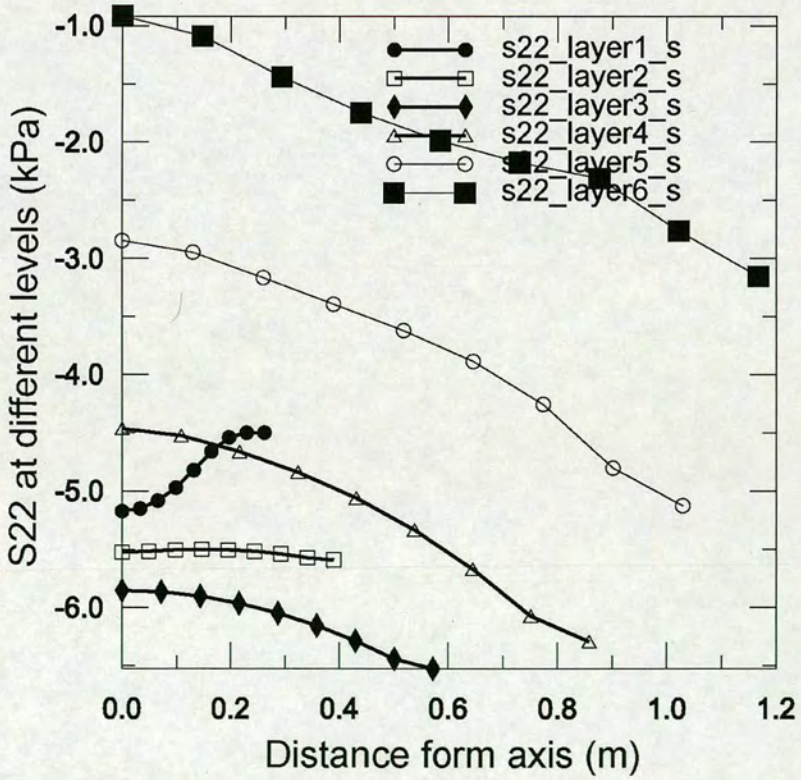

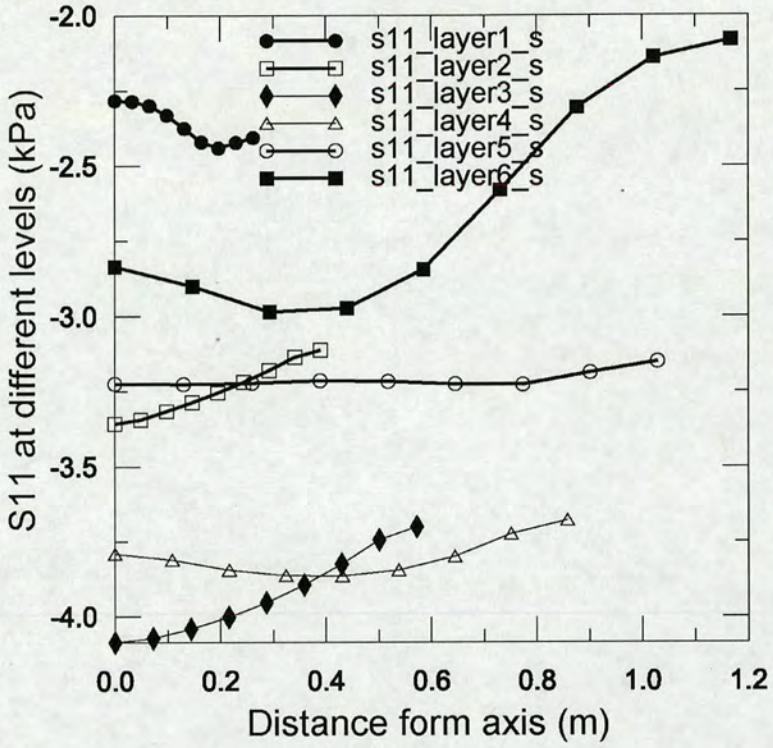

Fig. 3.11 Stresses on horizontal lines at the mid-height of each layer after switch-on filling

3.2.4.3.1.2 Stress development within the stored solid under a progressive filling process

Again the same process, outlined in Section 3.2.4.2.1, was applied and the development of stresses within the stored solid was investigated. Figure 3.12 shows the shear stress S12, the vertical stress S22 and the horizontal stress S11 along the same horizontal lines in each layer as described in the previous section.

3.2.4.3.2 Development of loads on the hopper walls

The development of loads on the hopper walls under concentric filling was investigated. Based on the findings in section 3.2.4.2.2, only the Drucker-Prager model and linear elements were employed. The predictions are shown in Fig. 3.13 for normal pressure on the wall, and in Fig. 3.14 for frictional traction on the wall.

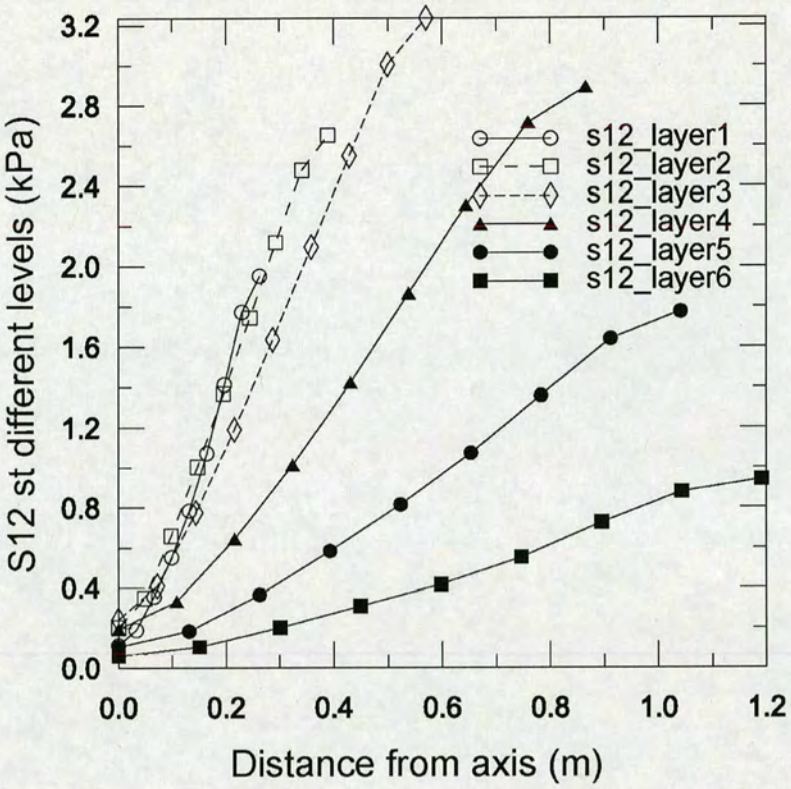
S12 st different levels (kPa)
Distance from axis (m)
s12_layer1
s12_layer2
s12_layer3
s12_layer4
s12_layer5
s12_layer6
3.2
2.8
2.4
2.0
1.6
1.2
0.8
0.4
0.0
0.0
0.2
0.4
0.6
0.8
1.0
1.2

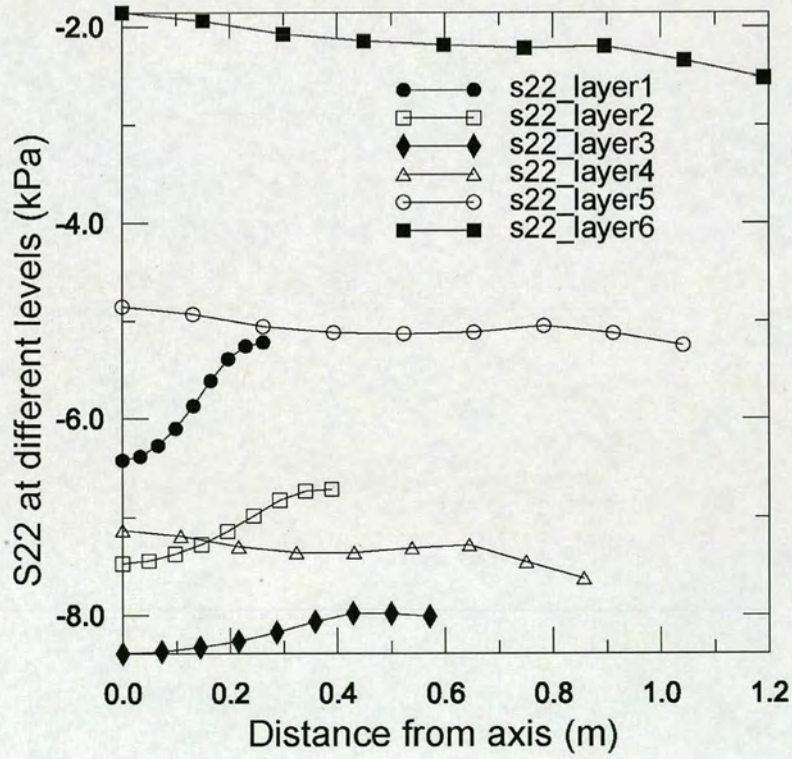
S22 at different levels (kPa)
Distance from axis (m)
s22_layer1
s22_layer2
s22_layer3
s22_layer4
s22_layer5
s22_layer6
-2.0
-4.0
-6.0
-8.0
0.0
0.2
0.4
0.6
0.8
1.0
1.2

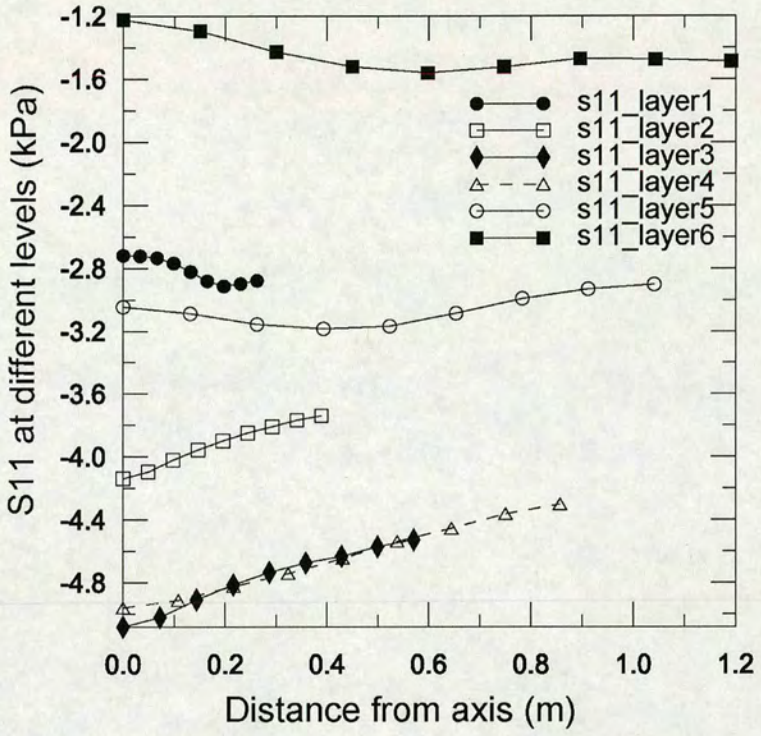

Fig. 3.12 Stresses on horizontal lines at the mid-height of each layer after progressive filling

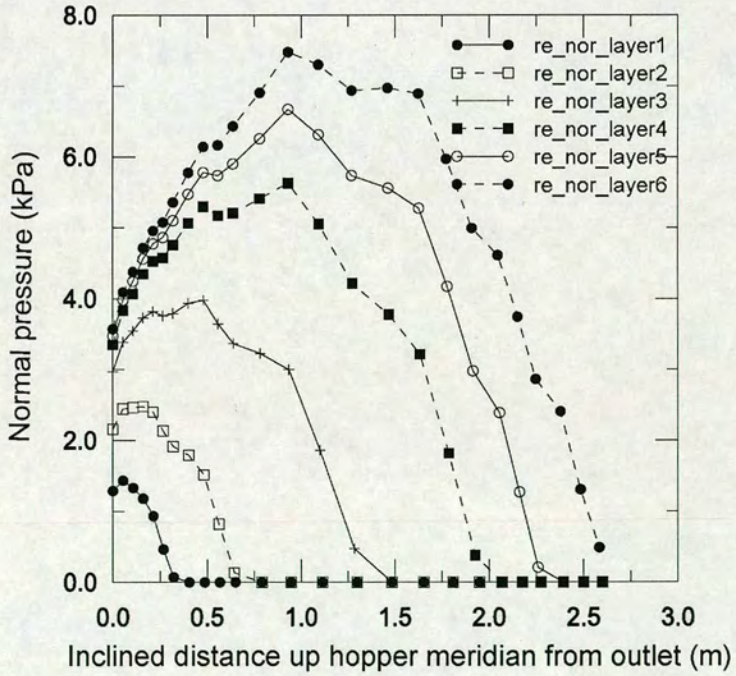

Fig. 3.13 Development of normal pressure acting the walls of the hopper

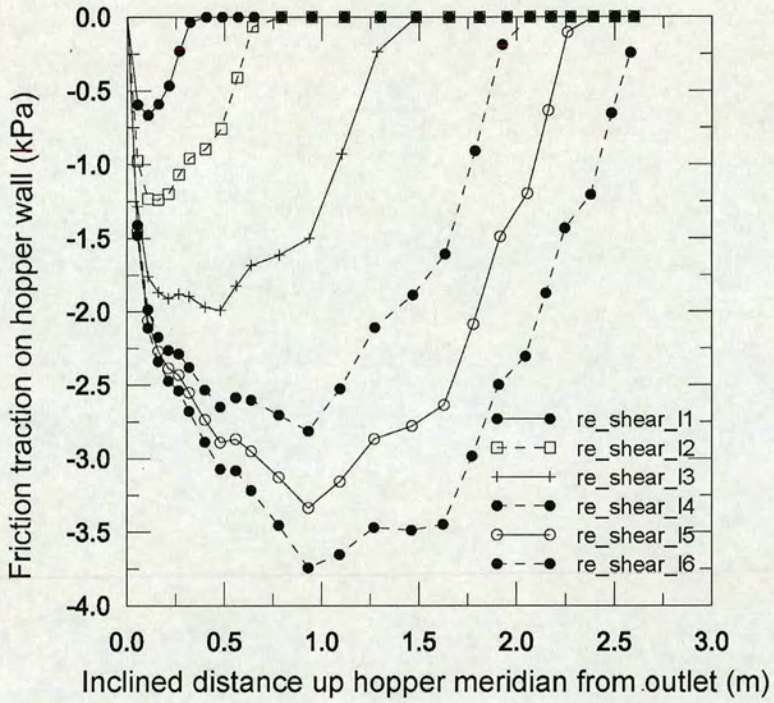

Fig. 3.14 Development of frictional traction distribution on the walls of the hopper

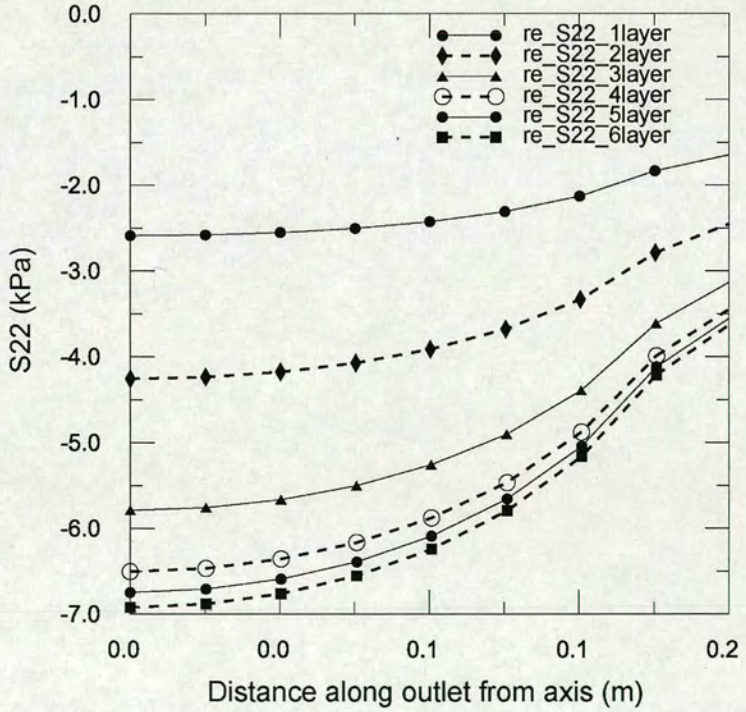

Fig. 3.15 Development of the vertical stress S22 at the hopper outlet under concentric filling

3.2.4.3.3 Development of loads on the hopper outlet during filling

The Drucker-Prager model and linear elements were used in the investigation. The vertical stresses S22 at the interpretation points along the outlet line were interpreted as the pressures acting at the outlet. They increased in magnitude with progressing filling as expected. Such pressure developments are shown in Fig. 3.15.

3.2.4.4 Discussion and comparison

3.2.4.4.1 Effects filling processes on stresses

From Figs 3.4 and 3.5 and Figs. 3. 11 and 3.12, it is clear to see that the maximum vertical stress S22 and the maximum horizontal stress S11 did not occur at the bottom, but lie somewhere in the region of Layer 3 instead, irrespective of whether the stored solid was placed by distributed or concentric filling, switch-on filling or progressive filling.

Under the switch-on case for both distributed filling and concentric filling modes, the vertical stress S22 in each layer increased (becoming more negative) from the central axis to the wall for Layers 2 to 6, but was highest at the central axis in Layer 1. Under progressive filling, the vertical stress S22 also increased slightly away from the axis in Layers 4 to 6, but was clearly highest at the axis in Layers 1 and 2.

For the distributed filling calculation, the horizontal stress S11 was higher near the axis in all layers except Layer 1, irrespective of whether switch-on filling or progressive filling was used. For the concentric filling calculation, S11 showed less clear tendencies, but were higher near the axis, but appeared to be the opposite in other regions for both switch-on filling and progressive filling.

The shear stress S12 along the horizontal lines through Layers 1, 2 and 3 was more or less the same. Layer 3 had the highest normal stress level: this may be important in an evaluation of where arching is mostly likely to form, since the higher normal stress on filling can induce a higher cohesive strength.

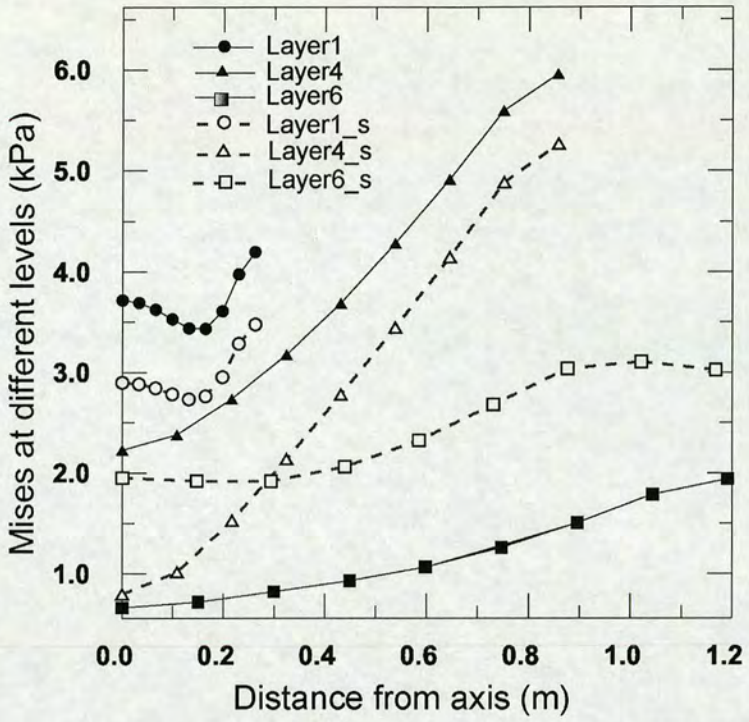

Fig. 3.16 Comparison of the von Mises stresses developed under different filling procedures

Looking closer at the stress distributions shown in Figs 3.4 and 3.5 and Figs 3.11 and 3.12, one finds also that the stresses developed differently from the switch-on filling to the progressive filling. The comparison for the von Mises Stress is shown in Fig. 3.16 as an example. One can see that the stresses developed under the progressive filling were higher than those developed in switch-on filling in the lower part of the hopper, but were lower in the higher part of the hopper. In the switch-on filling, the stored solid seemed to be "hung up", and higher stresses might develop in the higher part compared with the corresponding values developed in the progressive filling; while in the progressive filling, there were less "hanging up" effects, and the stresses mainly developed in the lower parts. This complied with the pressures developed on the outlet and the wall as shown in Fig. 3.18 later on.

3.2.4.4.2 Effects of filling modes on the load prediction

From Fig. 3.6 and Fig. 3.13, one can see that the maximum normal pressure acting on the walls, from the very beginning of the filling, was not at the outlet for both the

distributed filling and the concentric filling. The maximum normal pressure increased in magnitude and moved upwards with the development of the filling process, and was located in a position around 2/5 of the length of wall from the outlet when the filling was finished. The normal pressures acting at the outlet increased in the process of filling, but tended to approach a constant value. Based on the parameters assumed in the present study, it was about half of the maximum normal pressure acting on the walls.

Figures 3.7 and 3.14 show the development of the frictional traction on the surface of the hopper wall. It followed the same pattern as the normal pressure, with the position of the maximum frictional traction moving upwards with the filling process, and ended at a location around 2/5 of length of the wall from the outlet.

One feature for the frictional traction distribution was that the frictional traction drops to zero at the outlet. That was caused by the boundary condition adopted in the analysis. Since the node at the end was fully constrained, the stored solid cannot have any movement or movement tendency at that position, resulting in the frictional traction being zero. In other parts, there existed relative movement between the stored solid and the wall, the frictional traction thus developed.

The ratio of the frictional traction to the corresponding normal pressure at any location is defined as the 'mobilised friction coefficient' (Rotter, 2001). The mobilised friction coefficient on the walls at the end of filling is shown in Fig. 3.17 for the distributed filling (a) and the concentric filling (b). One can see that in this steep hopper, wall friction was fully mobilised everywhere except very close to the outlet. At the junction between the hopper and outlet, there can be no relative sliding, so the friction is unable to be mobilised. But this effect turns out to occur in only a very small region, so small that the general pattern of hopper pressures is unaffected by the small loss of mobilised friction. This pattern of friction mobilisation in steep hoppers matches the model of Rotter (2001), which has been adopted into the European Standard (EN 1991-4, 2004) for pressures in hoppers in 2002.

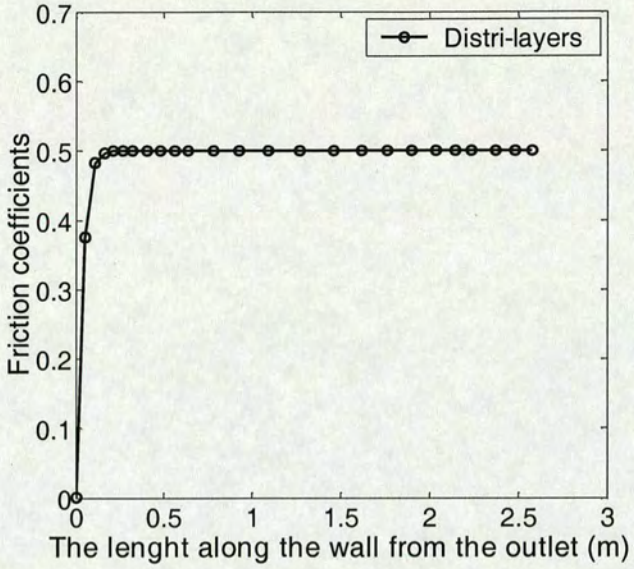

(a) for distributed filling

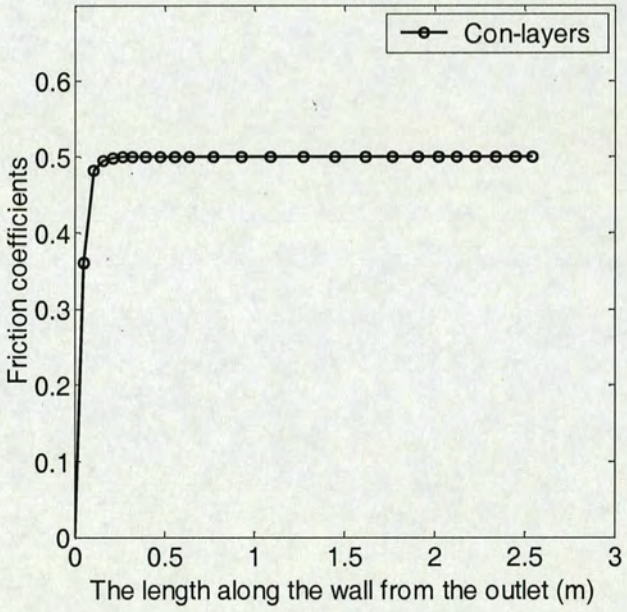

(b) for concentric filling

Fig. 3.17 Mobilised wall friction coefficient

From Fig. 3.10 and Fig. 3.15, one can see that the development of the pressures on the outlet followed the same pattern for both filling modes. They steadily increased in magnitude when the hopper was filled, but they moved asymptotically towards a final value. It is interesting to note that the pressures developed faster in the area close to

central axis than in the area close to the hopper wall, and increased quickly at the beginning of filling. In the partition operation described in Section 4, the Layers 1, 2, 5 and 6 were designed with the same thickness. The thickness of Layers 3 and 4 were doubled. One can see that the same thickness of Layer 2 had less contribution to the pressure on the outlet than the Layer 1 did. The same applied to Layer 3 and Layer 4, Layer 5 and Layer 6. One can conclude that the further the stored solid was from the outlet, the less effect it had on the pressures on the outlet.

Looking closer at the pressures in Fig. 3.10 and Fig. 3.15, one can find also that in the beginning of the filling, the pressures on the outlet for distributed filling were lower than those for concentric-filling, but were higher when the filling was finished. Fig. 3.18-a shows a comparison of the development of such pressures in a process of filling, even though the differences were small. A simple assessment might suppose that the opposite would be true since there is less stored solid in the hopper when it is filled by distributed filling than when it is concentrically filled. This investigation shows that different filling modes can lead to unexpected effects.

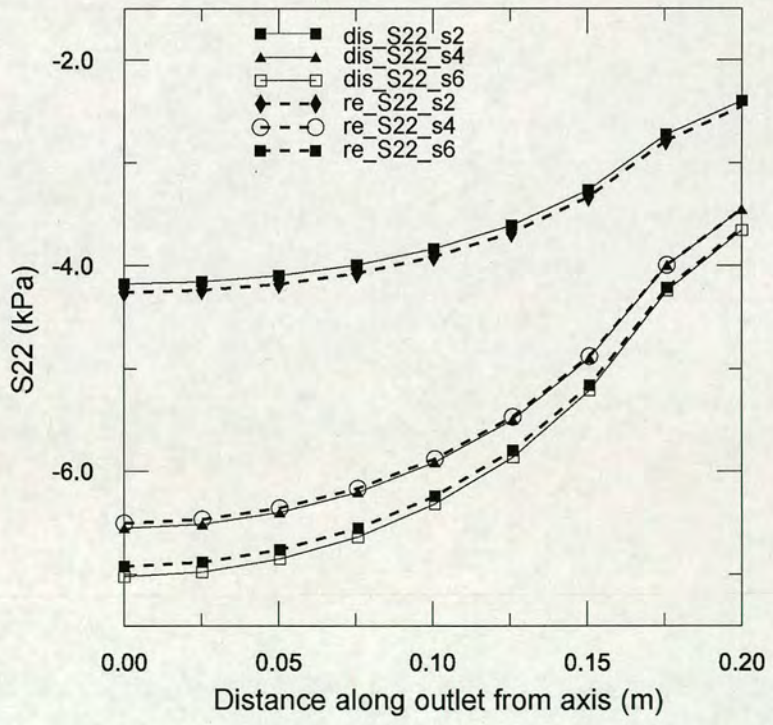

a) on the outlet

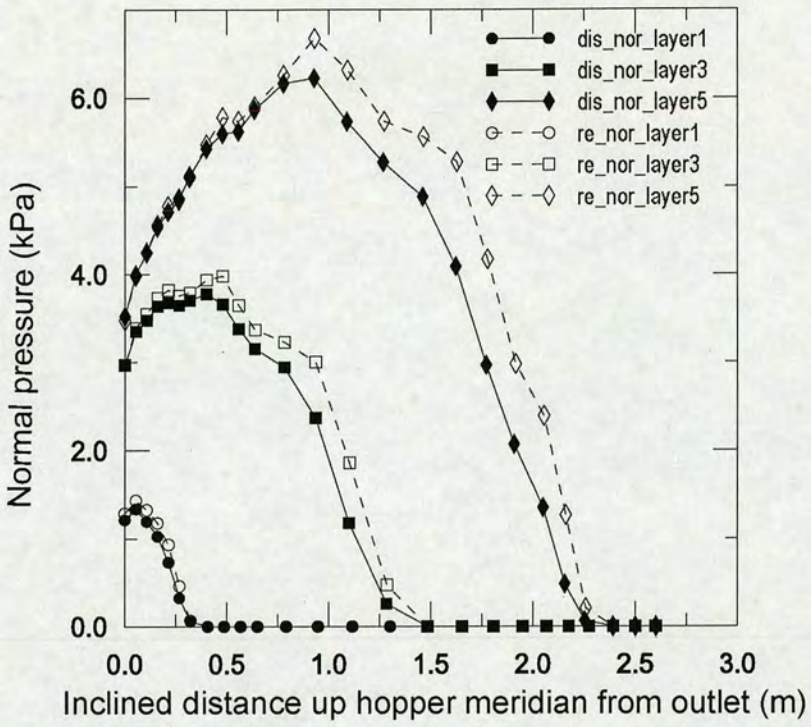

b) on the wall

Fig. 3.18 Pressures arising from different filling modes

A comparison of normal pressures on the wall of the hopper for distributed filling and concentric filling is shown in Fig. 3.18-b. It shows that the pressure on the upper part of the wall is higher for concentric filling than for distributed filling. This result is consistent with the fact that the hopper holds more granular stored solid after concentric filling so is naturally subject to higher pressures than for a distributed filling. However, these comparisons are for a common upper boundary of the contact between the stored solid and the silo wall, and not for a common equivalent surface (Rotter, 2001), so the comparison may need to be treated with caution.

3.2.4.4.3 Effects of filling processes on loads

The analyses of loads on the wall and outlet so far followed the same progressive filling process for both filling modes (distributed and concentric). To find out what effect the filling process produced, different filling processes were investigated by comparing the predictions of switch-on filling and progressive filling. Investigations were first carried out with the distributed filling mode, and then by concentric filling.

One advantage of such separate investigations is that the mass of granular stored solid involved is the same for both situations.

As an example, the loading induced by a filling process of switch-on (Ding et al., 2003) was extracted. Figure 3.19 (a) shows the predictions of normal pressures on the hopper wall under this switch-on loading when the stored solid was filled in a distributed filling mode, along with the pressures for the last stage of the progressive filling (Fig. 3.6). Figure 3.19 (b) shows similar predictions for the concentric filling case, extracted from the preliminary test in Section 3.2.4.1, along with the predictions of the last stage of progressive filling shown in Fig. 3.13.

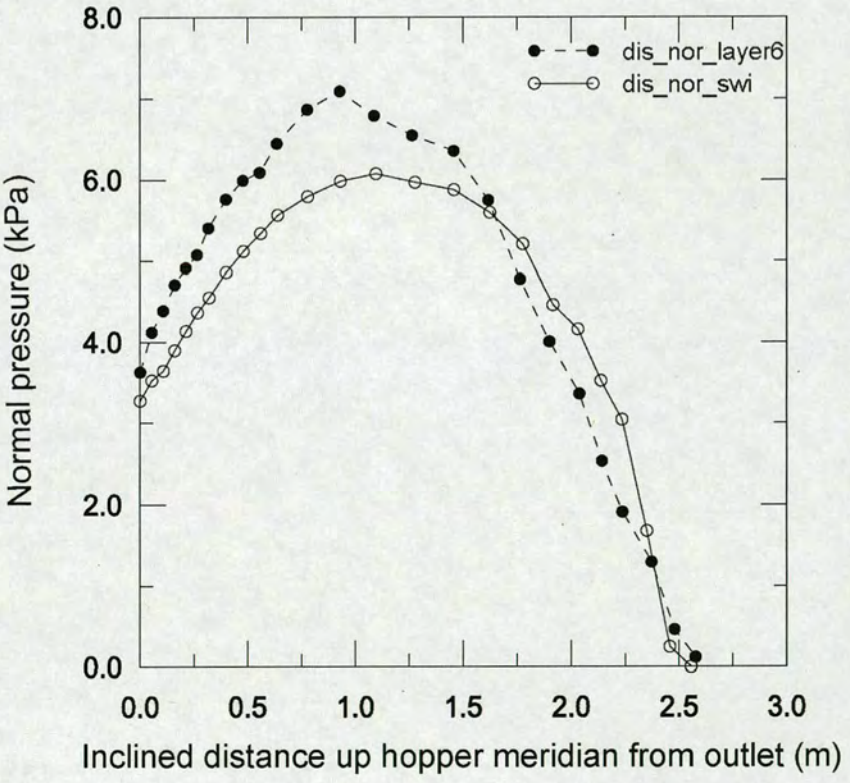

a. Distributed filling

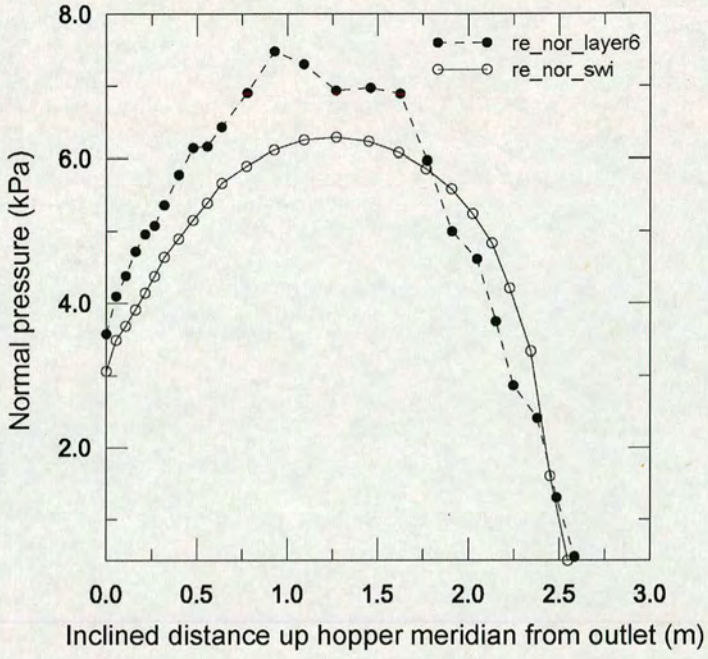

b. Concentric filling

Fig. 3.19 'Switch-on' loading effects of the contact pressure on the hopper wall

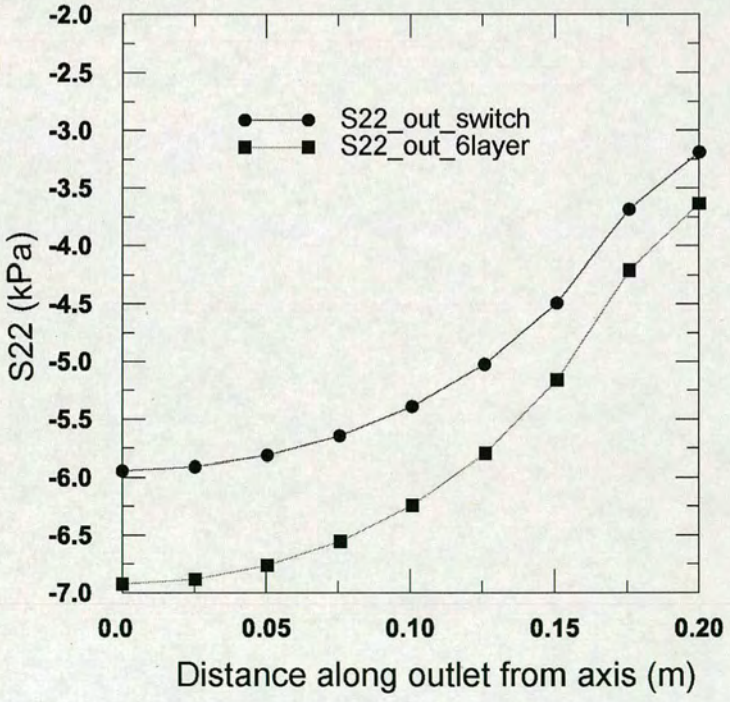

Fig. 3.20 Vertical stresses on outlet with different filling processes for a concentric filling

From Fig. 3.19, it is clear that some differences are produced by the different filling processes. Switch-on filling decreased the maximum contact pressure and moved the location of the maximum pressure upwards. On the higher parts of the hopper wall, switch-on filling raised the normal pressure, whilst in the lower part the normal pressure was reduced. These changes are compatible with the changes in vertical stresses on the outlet shown in Fig. 3.20.

In Fig. 3.20, the vertical stresses on the outlet from the preliminary tests for higher Young's Modulus as shown in Fig. 3.3 b, which used 'switch-on' filling, and the same stresses in the last step of filling as shown in Fig. 3.15, are depicted together for the concentric filling condition. One can see clearly that the vertical stresses on the outlet from the switch-on filling process were lower than those from the progressive filling process.

3.2.4.4.4 Some comparisons with the classic theoretical predictions

Some theories have been proposed for the distribution of pressures in conical steep hoppers. Some typical theoretical predictions are briefly reviewed (see Appendix A), and used here to compare with the predictions thus far obtained.

Comparisons were carried out for the pressures on the walls. As an example, the normal pressures for distributed filling are shown in Fig. 3. 21(a) for progressive filling and switch-on filling, along with the theoretical predictions calculated for the distributed filling condition. Figure 3.21 (b) shows parallel predictions: the normal pressures are those for concentric filling for progressive filling and switch-on filling.

From Fig. 3.21, one can see some differences exist between the theoretical predictions, while the predictions from the finite element analyses from both the progressive and switch-on filling have the general form proposed by Walters (1973), MacLean (1984) and Rotter (2001), though the predictions of Rotter's theory seem to be closest and lie between the two FE curves.

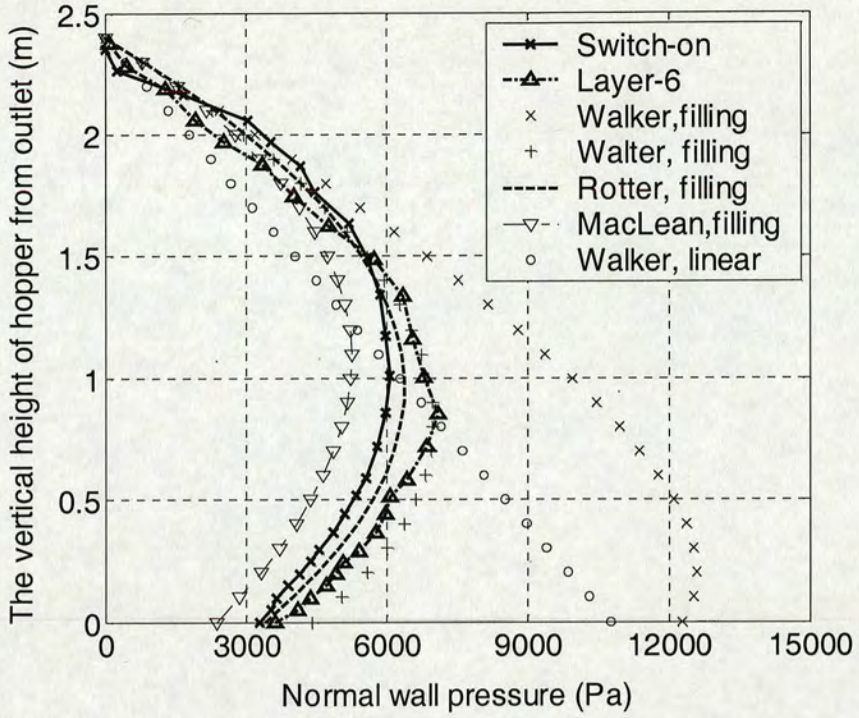

a. Distributed-filling

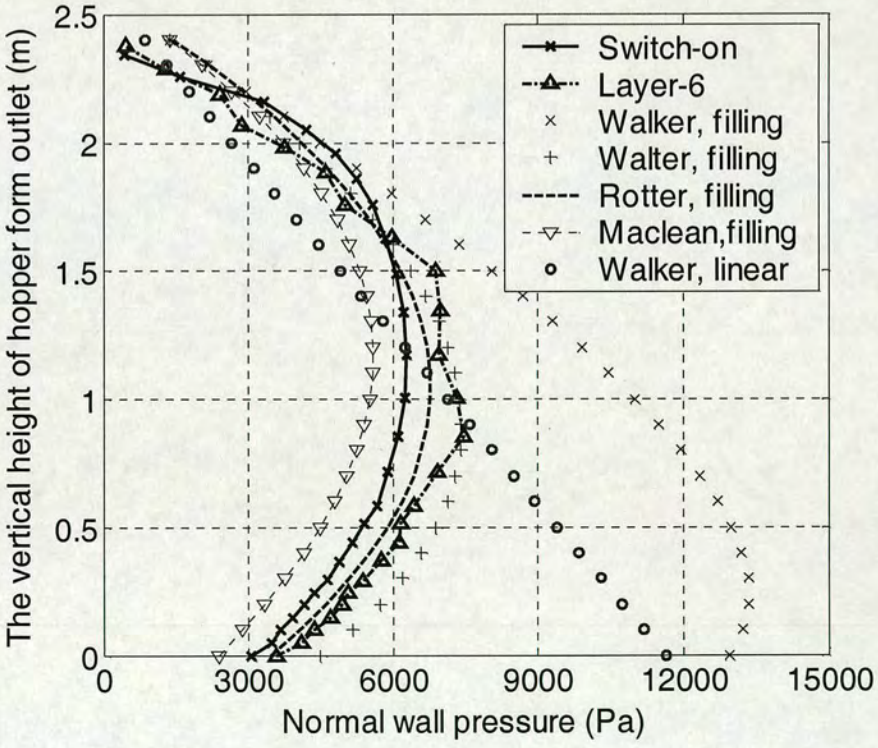

b. Concentric-filling

Fig. 3.21 Comparisons of pressure distribution by different approaches

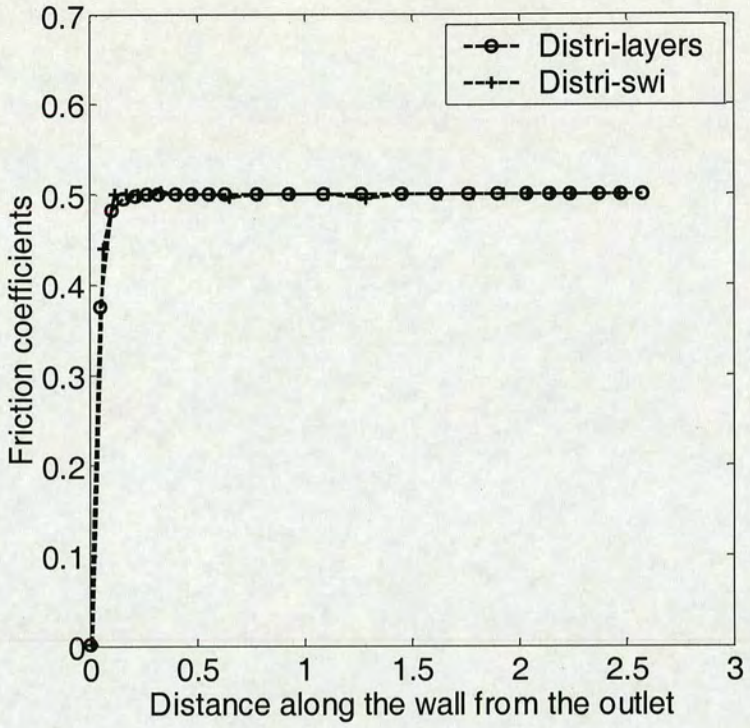

(a) Distributed filling

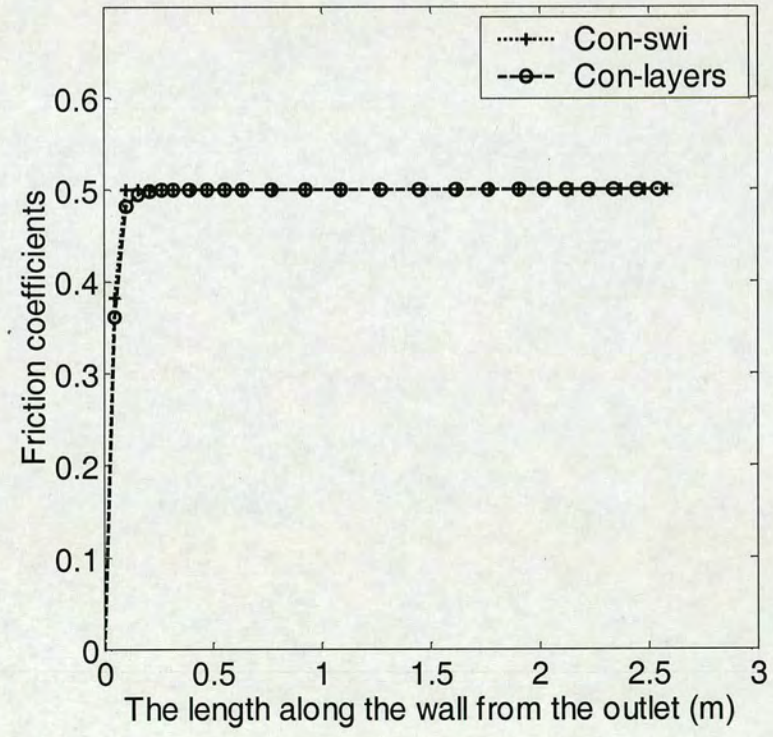

(b) Concentric filling

Fig. 3.22 Comparisons of the mobilised friction coefficient for both progressive and switch-on filling

Differences predicted from finite element analyses by the different filling processes are also noticeable. Compared with switch-on filling, progressive filling increased the maximum contact pressure and moved the location of the maximum pressure downward. In the lower part of the hopper wall, the normal pressures rose; and in higher the part, the normal pressures reduced.

The shear stress on the wall (frictional traction) develops almost completely for both progressive filling and switch-on filling as shown in Fig. 3.22, matching the proposal of Rotter (2001) for steep hoppers.

The progressive filling approach has been proven to be feasible as a finite element approach to simulate a filing process. The results obtained showed, however, no convincing advantages over the conventional switch-on filling approach conducted on the steep hopper. Further study is to carry out by this progressive filling to investigate the load developments along the walls of a shallower hopper, and thereby explore the advantages and disadvantages of this progressive filling approach as a finite element approach to simulate a filling process.

3.3 Predicted pressures in a hopper with a shallow inclination angle

3.3.1 The geometry of the objectives to be investigated

A silo with a shallow hopper may need to be used when the headroom available is limited. In such a circumstance, it is possible to design a silo with a shallow hopper to retain the silo's capacity provided the issue of segregation is not challenging. A further reason might be protection of the wall against damage by abrasion by the stored solid during flow.

A hopper with quite a low inclination was investigated in this part of the study on the development filling loads. The geometry of this hopper is shown in Fig. 3. 23. It was an axisymmetric conical hopper with a 45° half angle, 1210 mm in height, with an upper diameter of 2520 mm and a 100 mm diameter outlet. It was made of stainless steel plate, with a thickness of 6 mm. This represents the hopper of the full scale silo battery at POSTEC, and was designed to investigate the effects of inserts on both solids flow and wall pressures.

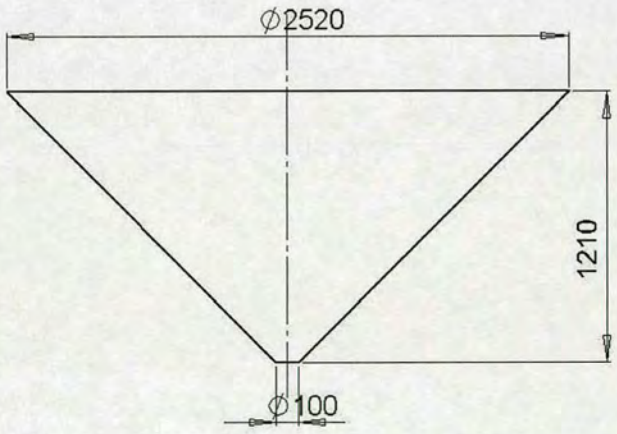

Fig. 3.23 Geometry of the shallow hopper (dimensions in mm)

The stored solid was assumed to be filled into the conical hopper from a certain height in the centre, piling up as an axisymmetrical cone with a repose angle as a result of concentric filling. The geometry formed is illustrated in Fig. 3.24.

The investigation was carried out by finite element analysis, since few of the classical theories provide comparisons for shallow hoppers (Jenike et al., (1973) and Rotter (2001) being the two known exceptions). Experiments were conducted for validation purposes.

3.3.2 Numerical approaches

3.3.2.1 Finite element formulation

A finite element mesh was developed for the shallow hopper and its stored solid. In this formulation, the wall of the hopper was fixed both horizontally and vertically at the top edge and constrained horizontally at the lower edge. The outlet was closed. The wall was assumed weightless. The stored solid properties and boundary conditions were defined. The loading on the stored solid was solely due to gravity. The interaction between the wall and stored solid was defined by the wall friction coefficient of the interface at their contacting surfaces.

An operation was carried out to partition the region of stored solid. This region was divided firstly into two parts along the middle line parallel to the repose line; the two newly formed parts were again divided respectively in the same way along their middle. The stored solid region consisted now of four layers with the same thickness though these had very different volumes. Each of them was further divided along the middle. As a result, the stored solid region was eventually divided into eight layers as shown in Fig. 3.24.

To simulate the hopper filling process, the technique used in section 3.2 was used again. Both the wall and the stored solid were meshed, with an application of mesh refinement to the stored solid in the region of the outlet. The meshes, stored solid loads and the contacting interactions between the stored solids and walls were inactivated and suspended at the beginning of the analysis. They were reactivated in a different sequence, and the filling was assumed to be simulated.

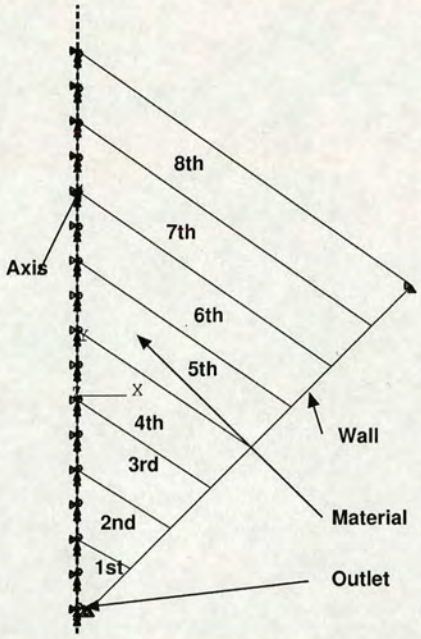

Fig. 3.24 Domain of the finite element formulation

As seen in Fig. 3.24, the zones representing the stored solid were divided into eight layers with an inclined surface profile for each layer. By the reintroduction of meshes and the reactivation of loading and contact interactions progressive, a concentric filling was regarded as achieved. In such a concentric filling, no initial velocity was implemented, indicating that the impacting effects during filling were not taken into account. There was also no initial stress in any of the layers when they were reintroduced, so the filling of each layer was in fact a process of consolidation without initial stress within the stored solid.

3.3.2.2 Determination of parameter and convergence test

The determination of material parameters to represent the stored solid depends on the model adopted. The major parameters required in this model were: the Young's modulus E_m, the Poisson's ratio ν_m, the specific weight of the sand γ (the bulk density ρ), the internal friction angle of the sand φ . The chosen Young's modulus E_m and Poisson's ratio ν_m were taken from Hjelmstad and Taciroglu (2000). The Poisson ratio ν_m was derived from the conventional description of lateral pressure ratio k (Jaky, 1948) as:

$$k = 1 - \sin\varphi$$

combined with the lateral pressure ratio from elasticity theory, Ooi and Rotter (1990) specialised

$$k = \nu_m / (1 - \nu_m)$$

for thick walled containers, which gives

$$\nu_m = \frac{1 - \sin\varphi}{2 - \sin\varphi}$$

when combining together. This relationship was also quoted by (Qu, 2000). The other properties were measured in the laboratory and are listed in Table 3.2.

Table 3.2 Constitutive model and relevant parameters implemented

The density ρ (kg/m^3): 1370	*The internal friction angle φ (degree): 36*
The elastic modulus E_m (Pa): 155000	*The wall friction angle ϕ_m (degree): 21.8*
The Poisson ratio ν_m : 0.26	*MOHR COULOMB (degree, Pa): 36.0, 0*

The wall was made of stainless steel, and was regarded as elastic. A Young's modulus $E_w = 2.0 \times 10^{11}$ Pa and a Poisson's ratio $\nu_w = 0.3$ were adopted.

3.3.2.3 Loads on the walls: from switch-on filling, six-layer to eight-layer filling

The pressures on the hopper walls were investigated using both switch-on filling and progressive filling. For switch-on filling, all elements in the eight layers were reactivated at the same time. As a result, the pressures at the contacts between the wall and stored solid were reintroduced all together. This represents stored solid consolidation without any initial stress within the stored solid. During this consolidation, the contact interaction between the stored solid and walls was interpreted as pressure on the hopper wall. The predicted distributions are shown in Fig. 3.25a for the normal pressures and in Fig. 3.26a for the frictional traction distribution on the wall.

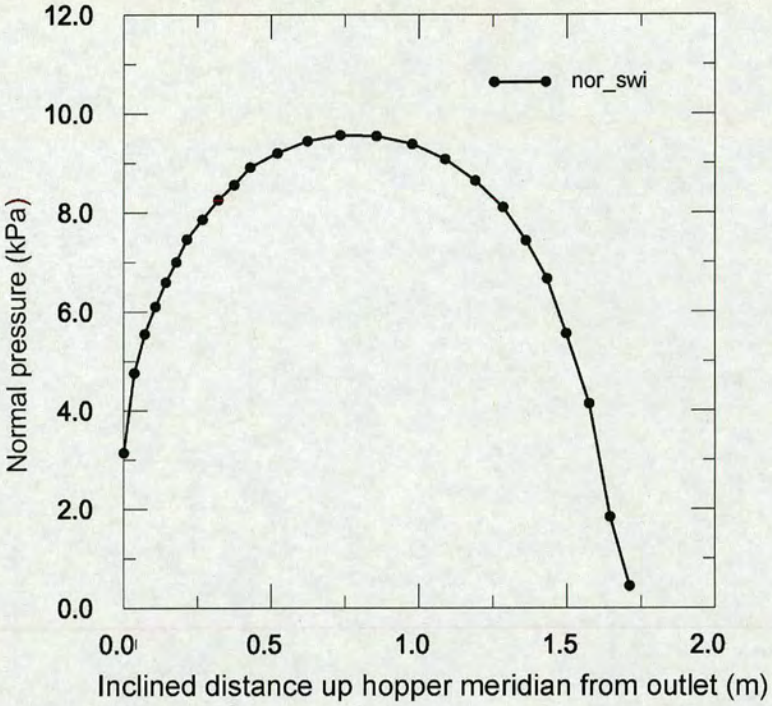

(a) Switch-on filling

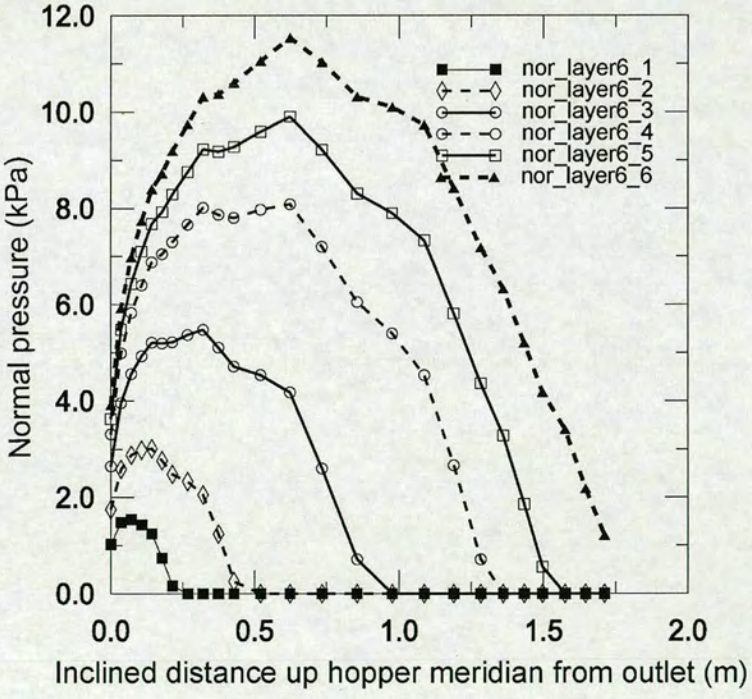

(b) Six layer filling

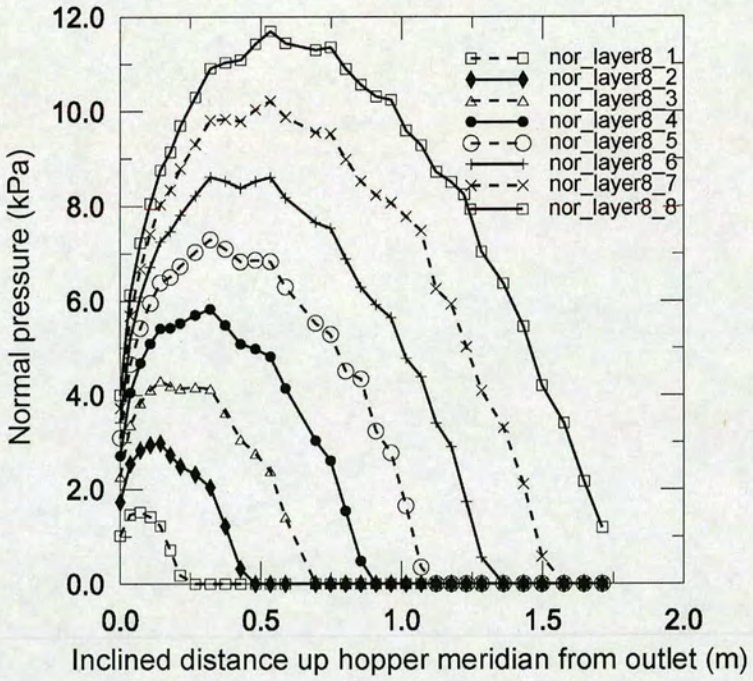

(c) Eight layer filling

Fig. 3.25 Normal pressure developed on the walls

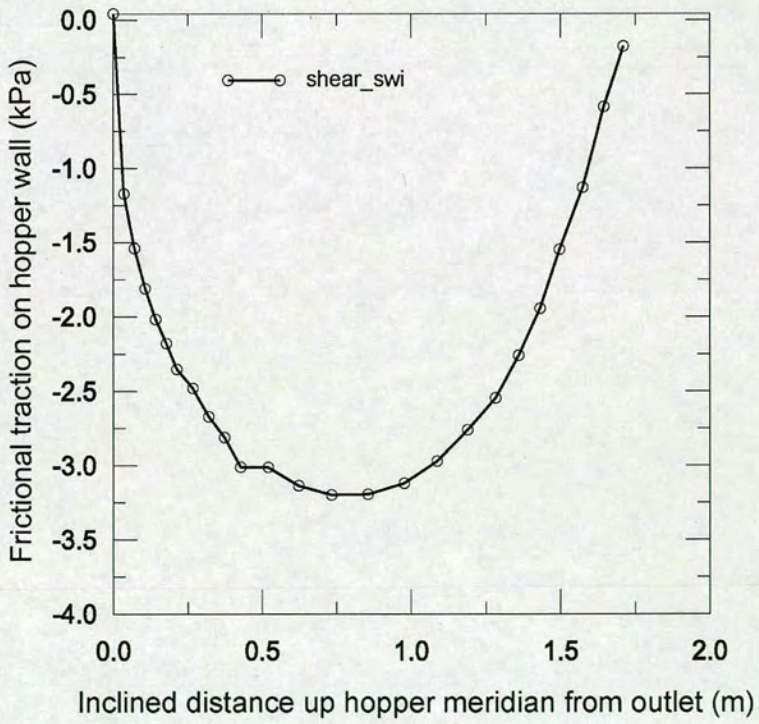

(a) Switch-on filling

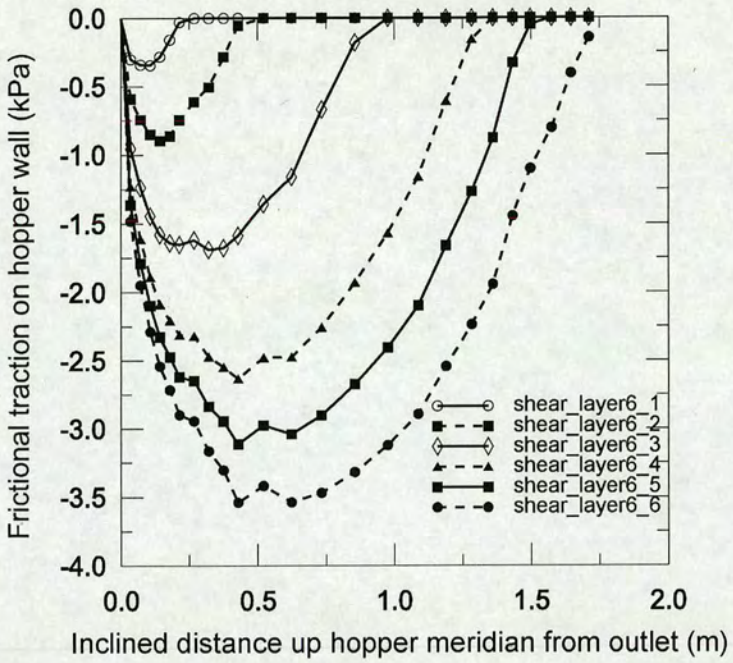

(b) Six layer filling

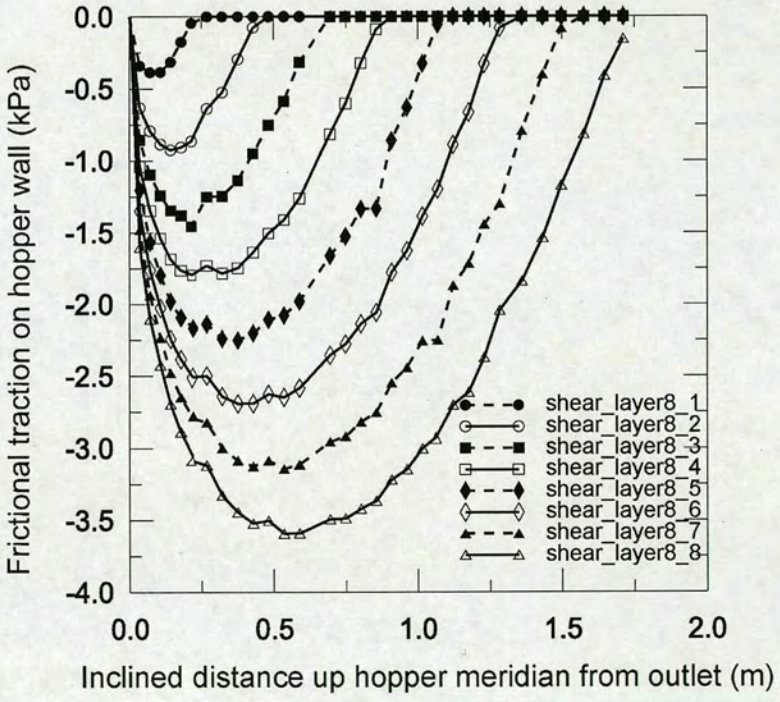

(c) Eight layer filling

Fig. 3.26 Frictional traction distributions developed on the wall

Under progressive filling, a six layer procedure and an eight layer procedure were

carried out. In the six layer approach, the reactivation of elements was in the sequence of Layer 1, Layer 2, Layers 3 and 4, Layers 5 and 6, Layer 7 and Layer 8. In the eight-layer approach, the elements were reactivated in order from Layer 1 to Layer 8, one layer at a time. When the elements of a layer were reintroduced, the contact between the stored solid and wall was reactivated. Figure 3.25 shows the development of the normal pressure on the walls induced by stored solid from the six layer procedures (Fig. 3.25b) and from the eight layer procedure (Fig. 3.25c), while the development of the frictional traction distribution on the wall is shown in Fig. 3.26.

As the modelling changed from switch-on to progressive filling, the maximum normal pressure increased in magnitude and moved downwards (Fig. 3.25). The differences between the predictions from different filling models are very clear. With switch-on filling, the maximum normal pressure is located at around 3/7 of the height from the outlet, but progressive filling increases both the value of the maximum normal pressure and moves its location downwards towards the outlet, so that it is located at around 2/7 of the hopper height at the end of filling. With more layers, this location moves downwards lower. With this change from switch-on to progressive filling, the normal pressures on the wall also increase on the lower part of the wall and decrease on the higher part on the wall.

The frictional traction again drops to zero at the outlet junction (Fig. 3.26), for the same reasons as for steep hoppers (Fig. 3.14). In the rest of the shallow hopper, frictional tractions were unlikely to be fully mobilised, and worth investigating.

It may be recalled that the full wall friction coefficient was developed in the steep hopper (Fig. 3.22). The quantitative distinction between steep and shallow hoppers was first proposed by Rotter (1999), based on arguments concerning the stress state that should exist in the hopper. These arguments were not, at that time, supported by finite element calculations, so it is valuable to check to see whether the present calculations support his theory or not.

Rotter (1999) proposed that the hopper would be shallow if:

$$\tan\alpha > \frac{1-k}{2\mu}$$

where α the half hopper angle, k the lateral pressure ration and μ the wall friction coefficient.

In a shallow hopper, the full wall friction coefficient is not expected be mobilised under consolidation of the solids during filling. Rotter (2001) proposed that the effective hopper wall friction coefficient (μ_{eff}) would be:

$$\mu_{eff} = \frac{1-k}{2\tan\alpha}$$

where k is the vertical wall lateral pressure ratio, often quoted as being between 0.3 and 0.4 for many solids (Koenen, 1895; Walker, 1966; Jenike, 1964), but for computer comparisons, it should be taken as (Rotter, 2001):

$$k = \nu_m / (1 - \nu_m)$$

ν_m the Poisson ratio. Here, the value was taken from this equation (see Table 3.2), giving k = 0.35. Using this value, and the hopper half angle α = 45°, this hopper is predicted to be shallow according to Rotter's criterion, so the wall friction is not expected to be fully mobilised. Further, the predicted effective mobilised friction coefficient is found to be μ_{eff} = 0.325. By contrast, the full wall friction coefficient was 0.4 (μ = tan 21.8°).

The mobilised wall friction coefficient at each point was determined from the finite element analysis as the ratio of frictional traction to normal pressure at each point, and is shown in Fig. 3.27 for the three different models of switch-on, and two progressive filling analyses. Irrespective of the filling modelling, the effective mobilised friction is seen to be substantially constant throughout the hopper, which was assumed by Rotter (2001).

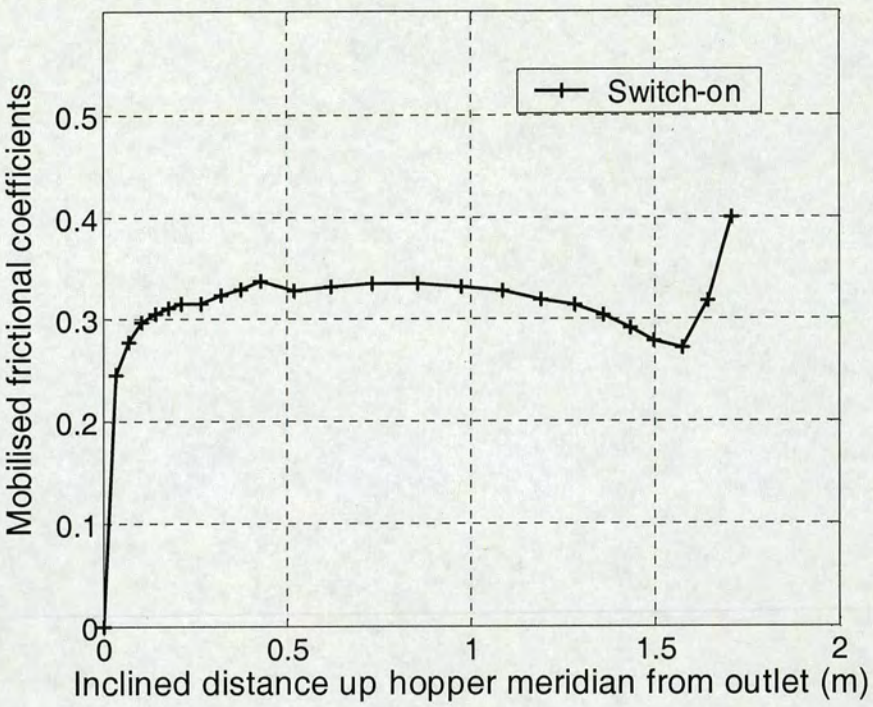

a.) Switch-on filling

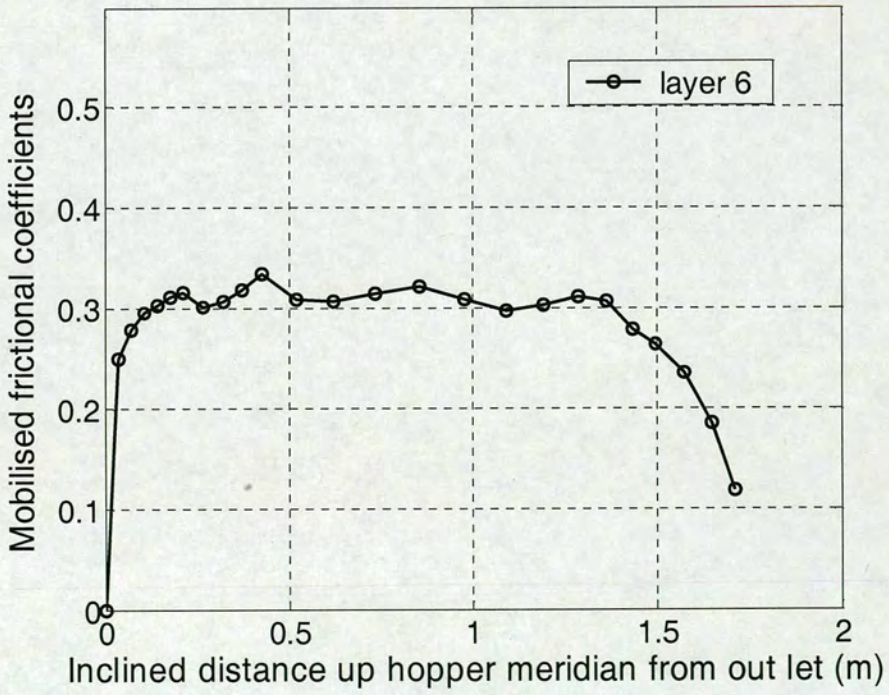

b.) Six layer filling

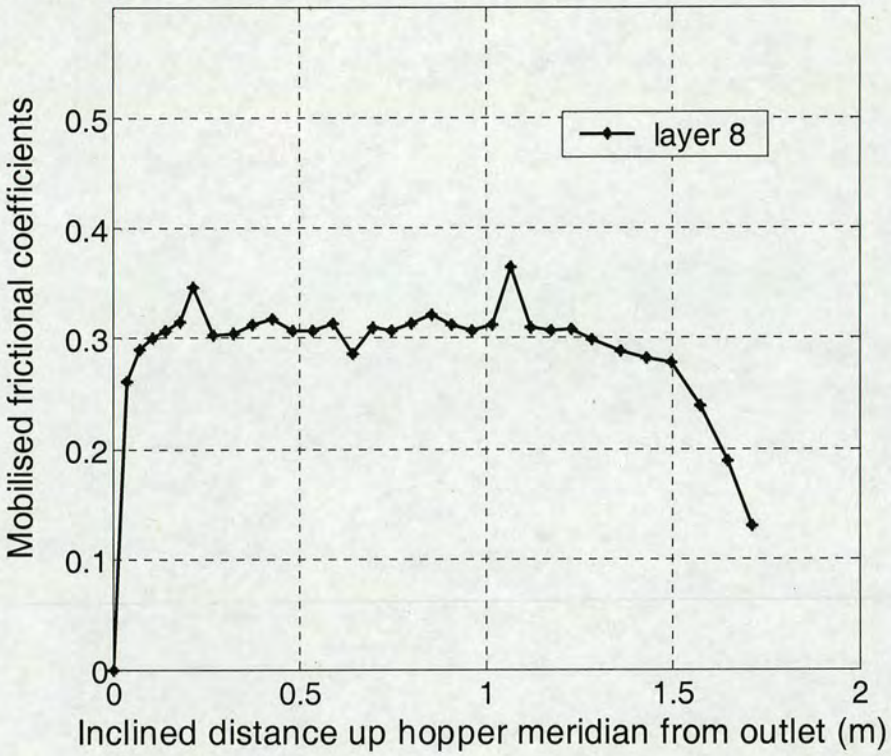

c.) Eight layer filling

Fig. 3.27. The mobilised frictional coefficients

It is also evident from Fig. 3.27 that the full wall friction coefficient was nowhere developed, thus confirming the description of this hopper as shallow. When the filling process is modelled as switch-on, a local high value of mobilised friction is predicted near the top of the hopper, but this is evidently dependent on the entire mass in the hopper sliding down simultaneously, and may also depend on the model used for the wall friction (may depend on the deformation required to develop the wall friction completely). However, this local high value is not matched by either of the progressive filling calculations, which show the opposite tendency. In the rest of the hopper (except very near the outlet), the predicted mobilised friction for the three filling approaches are all in good agreement each other, and in close agreement with the prediction of Rotter (1999, 2001) for the effective friction coefficient (μ_{eff}).

There are pronounced peaks for 8 layers filling (Fig 3.37 - c); these peaks are also noticeable in the 6 layer fillings (Fig. 3.37 - b). It is found that these peaks locate in

positions corresponding to position where the layers interface, and must be relevant to the interaction between the contacting surfaces of one layer solids with its adjacent layer solids. It is worth further investigating.

3.4 Experimental studies

3.4.1 Purpose of the experiments

In this section, observations of pressures on the wall of a full scale hopper are reported. These experiments provide evidence to test the validity of the numerical investigations carried out in section 3.3.

3.4.2 Setup and the stored solid used

3.4.2.1 Overview

The experimental arrangement, sketched in Fig. 3.28, was used to perform the experiments. The complete apparatus consisted of three parts: the materials handling system, the test hopper and the data acquisition system. The materials handling system included a solids feeding unit and a solids discharging unit. The data acquisition comprised pressure transducers mounted on the hopper wall, a data logger / A-D converter called Hydra and a PC.

3.4.2.2 The materials handling system

The feeding unit consisted of a small hopper or funnel and a crane. It was used to carry out concentric filling of sand into the test hopper. A small extra funnel, which was 400 mm in height, with a ϕ 400 mm upper edge and a ϕ 50 mm outlet, was placed above the test hopper, with their two axes aligned. The sand was carried by crane and fed into this small funnel, and then discharged into the test hopper through its outlet. The feeding rate was quite stable, measured at around 300 kg/min.

The discharging unit was simply a collecting bag and a forklift. The bag was put under the outlet of the hopper and when full, removed by a forklift. The outlet of the test hopper was controlled using a plate valve. It was designed for free discharge with a flow rate of around 580 kg/min when the outlet was fully open, and could be interrupted by a closure plate.

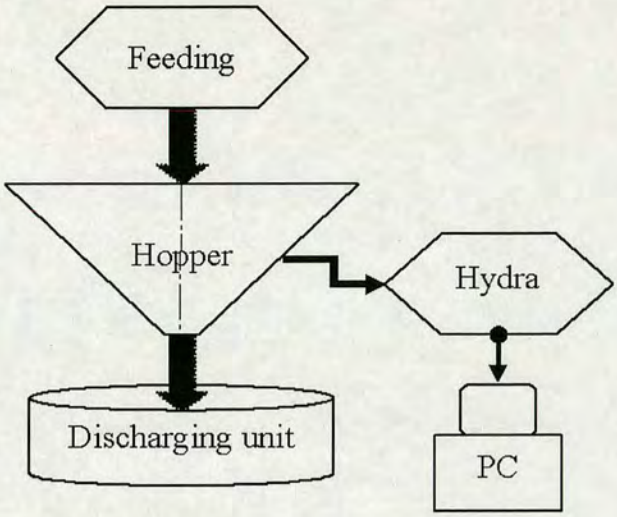

Fig. 3.28 Schematic view of the experimental setup

3.4.2.3 The test hopper

The key part of the apparatus was the test hopper, which is shown in Fig. 3.29 a. The experiment was chosen to be at a fairly large scale, so that it is best described as pilot scale, since it is a little small to be claimed as full scale. Nevertheless, this size of hopper is sufficiently close to full scale for the scale effects that other researchers have found to be relatively unimportant. The hopper was an axisymmetric conical hopper with the geometry shown in Fig. 3.23. It had a short cylinder above it 300 mm in height. Both the cylinder and the test hopper itself were made of stainless steel of thickness 6 mm.

The cylinder was used to prevent the stored solid from overflowing during filling. It was also designed and reinforced to reduce the effect of supports on the experimental observations. It had two circular annular plate rings, each of thickness 10 mm, at the transition and at its upper end. The space between the rings was strengthened with 16 vertical ribs (small plates). The ribs were distributed evenly around the circumference and welded to the outer face of the cylinder along the generating lines, and the rings (Fig. 3.29 b). It was planned that the cylinder should be a rather stiff structure, with its lower ring resting symmetrically on a rectangular frame which itself was supported on four legs (NB: the supporting points of the Ring 2 on the frame were between the generators lines of transducers. Although this design was not checked to explore the

effects of loss of symmetry, it was believed that the support structure was stiff enough to make the experiment effectively axisymmetric.

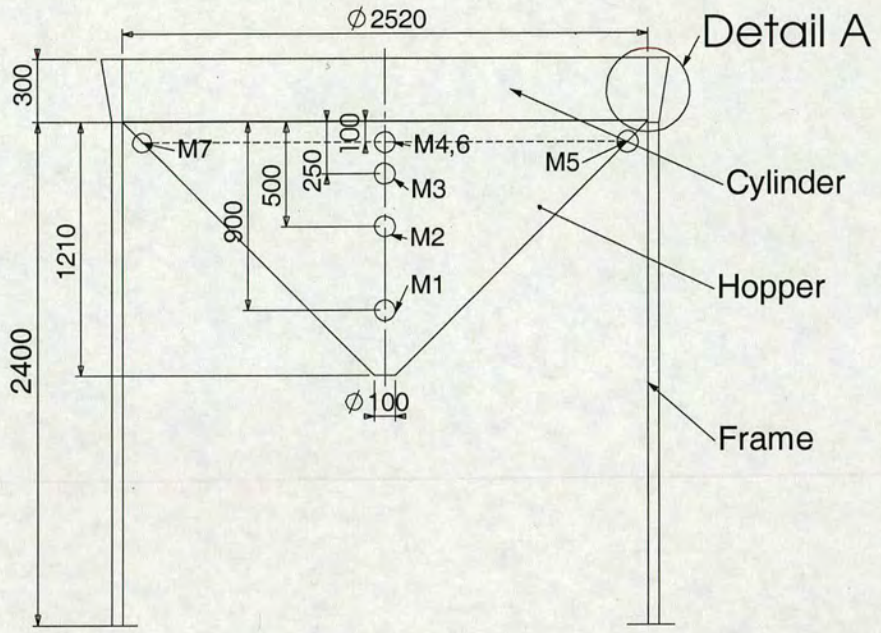

a) Experimental hopper, short cylinder and support NB: M4 diametrical opposite of M6; M5 diametrical opposite of M7

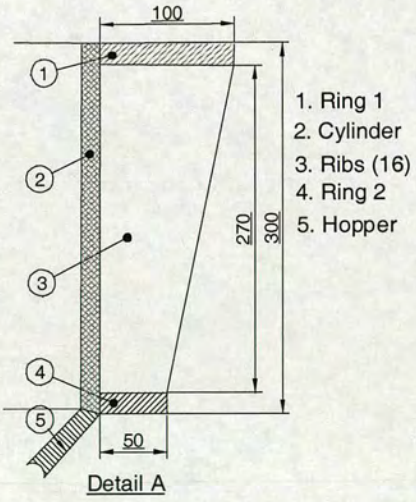

b) Detail of cylindrical section

Fig. 3.29 Geometry of hopper and locations of pressure transducers (dimensions in mm)

3.4.3 Pressure measurement system

3.4.3.1 Overview

Pressure transducers, illustrated in Fig. 3.30, were used to determine the total normal and frictional forces applied to a several areas of the hopper wall. These transducers were named M1 to M7, and were mounted in the wall of the hopper. The small gap between the disc of transducers and the hopper wall were sealed using silicon paste. In response to the pressures exerted, the pressure transducers generated electronic signals which were scanned by Hydra at a frequency of around 1 Hz, amplified and transferred to the PC based on the setting up of calibrations.

3.4.3.2 Pressure transducers and calibration

The pressure transducers were specially designed for silo pressure measurement. They were able to measure both the normal force (WW) and frictional force (FF) applied to the transducer face (Fig. 3.30). It was manufactured by DEKA Sensor & Technologie GmbH, Teltow, Germany. The reader is referred to Deka (2002) for specifications of the transducers.

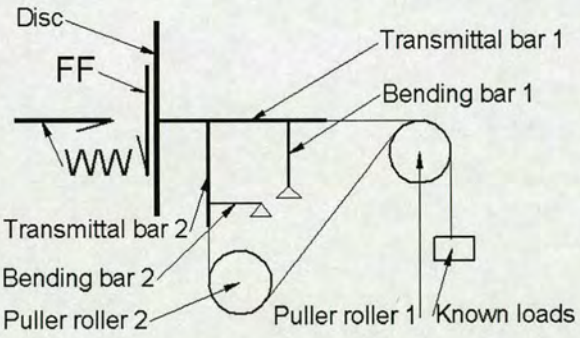

Fig. 3.30 Principle of transducer and method of calibration

The measurement principle is illustrated in Fig. 3.30. The disc of the transducer was cut from the wall of the test silo, with a diameter of ϕ 120 mm. The forces exerted on the disc were transmitted to the bending bars by the transmittal bars, perpendicular to and parallel to the disc respectively. Upon the force transmission, the bending bars, with attached strain gauge sensors, bend elastically and the changes in resistance of the

sensors is observed using the data logging system. The strength of the signal was deemed to vary linearly with the force on the transmittal bar, and some checks of this linearity were made.

The accuracy of the pressure transducer readings depends on the installation technique, the disc geometry and the bending bar stiffness (Askegaard, 1986). During installation, great care was taken to ensure that the disc was installed in the position it was originally taken from, i.e., the surface of disc was fitted into the same surface of the hopper wall. However, the protrusion of the disc into the hopper was not quantified.

The stiffness of the bending bars was deemed very stiff (for the given size of discs). It was well acknowledged that the displacement and rotation of the pressure cell face have a very important influence on the accuracy on the readings. For the given size of the discs, it was deemed that the bending bar was very stiff so that the displacement of disc under the loads to be measured was very small. However, the stiffness was not measured during this project. The effects of such a displacement on the measurement results are currently subject to further investigations.

Based on the transducer principle, calibrations for the normal force and the friction force on each transducer were carried out carefully and separately according to the instructions specified by the supplier. The results are shown in Table B.1 (see Appendix 2 or Wojcik et al. (2004) for detail). It showed that the maximum error was 5.3 % on M4 for the friction force component, and this precision was deemed acceptable.

3.4.4 The mechanical properties of the stored sand

The stored solid used was dry sand. It had a bulk density of 1370 kg/m^3 with a particle size distribution ranging between 0.6 mm and 2 mm. It was a free flowing material. The repose angles were measured at the laboratory, 35.8° for the dynamic state and 36.1° for the static state. The friction angle with the hopper wall was 21.8° ($\mu = 0.4$) as measured by the Jenike shear cell.

3.4.5 Load measurements

3.4.5.1 Concentric filling

The filling method may have an effect on the wall loads, and may also indirectly cause other effects when the silo is discharged. In these experiments, only concentric filling was carried out using the filling unit.

The sand was carried in bulk bags by a crane. Five bags, equivalent to 5000 kg of sand, were used to fill the test hopper. It was carefully done to ensure that the sand was fed into the hopper axisymmetrically. Three similar filling tests were carried out with this sand. Among the fillings carried out, the maximum difference of the measured distances between the edge of the piled cone and the top edge of the hopper was 20 mm at the end of the filling. This difference were typical around 5-15 mm. The fillings were therefore considered to be very close to axisymmetric. The pressures developing in the hopper were therefore also assumed to be close to axisymmetric, so that measurements down a single generator should be sufficient to describe the full wall pressure distribution.

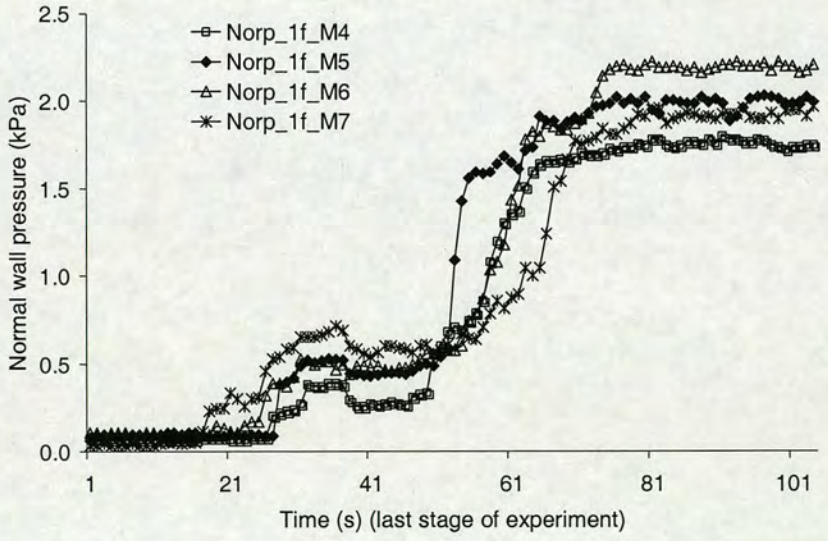

Fig. 3.31 Development of pressures on the four transducers around the periphery at the top of the hopper, during the last stage of concentric axisymmetric filling (Test 1)

3.4.5.2 Load development during filling

The extent to which the pressures differed from axisymmetry can be assessed by

considering the four transducers that were placed at the same level M4, M5, M6 and M7. Figure 3.31 shows an example of the loads development during one of the fillings at its last stage (Test 1). From this record, it is clear that although the filling process was closely axisymmetric, the pile that formed was not quite so, with M5 slightly ahead of the others and M7 slightly behind. The pressures at the end of filling vary by approximately ±12%. The observations described later should be interpreted with this potential variation or scatter in mind.

The pressure on each of the four transducers M1 to M4 down the hopper meridian were measured throughout the filling process. An example of the record for the transducers is shown in Fig 3.32, where the normal pressures for Test 2 are shown. The instants when the stored solid reached the levels at which the transducers M2, M3 and M4 are highlighted, together with the readings at the end of filling.

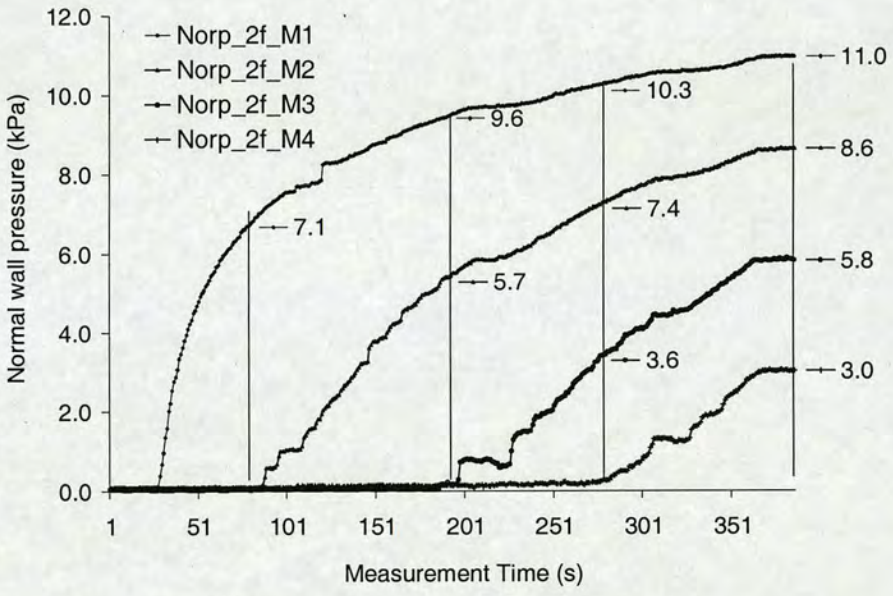

Fig. 3.32 The development of normal pressure during a filling (Test 2)

Samples of measured pressures were read from the data collected by Hydra and are shown in Fig. 3.33 for all three tests. Each figure shows the pressures on the transducers M1, M2, M3 and M4 for four different stages: where the stored solid was progressively filled up to levels of M2, M3, M4 and the level at the end of filling.

At each set of measurements shown in Fig. 3.33, the shear force on each transducer (M1 to M4) was also measured. In Fig. 3.34, the ratio of the shear force to the normal force on each transducer is shown as a measure of the mobilised friction at that stage and that position. These ratios are seen to be rather stable, though well below the full friction coefficient for sand on stainless steel.

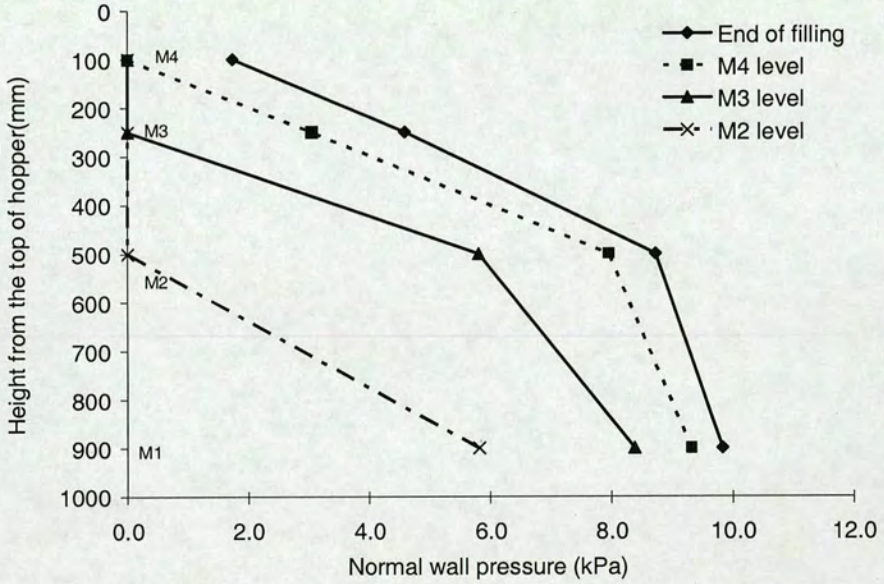

(a) Test 1

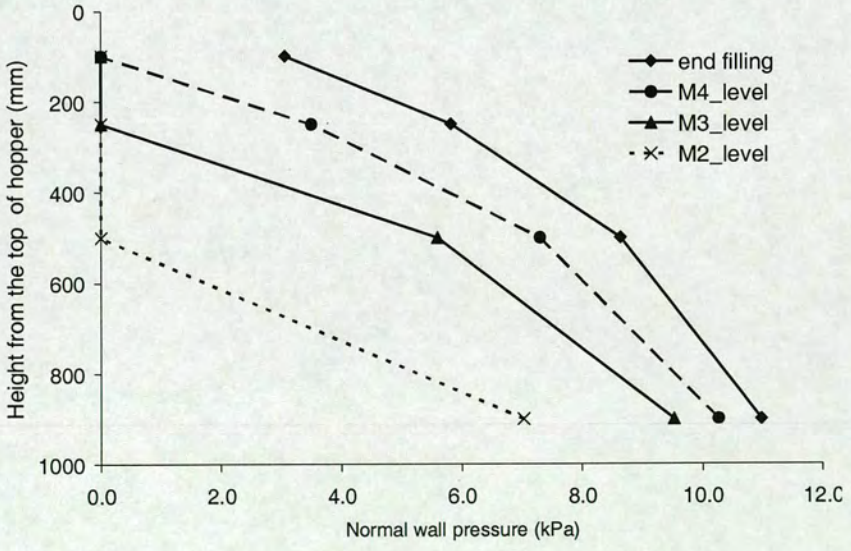

(b) Test 2

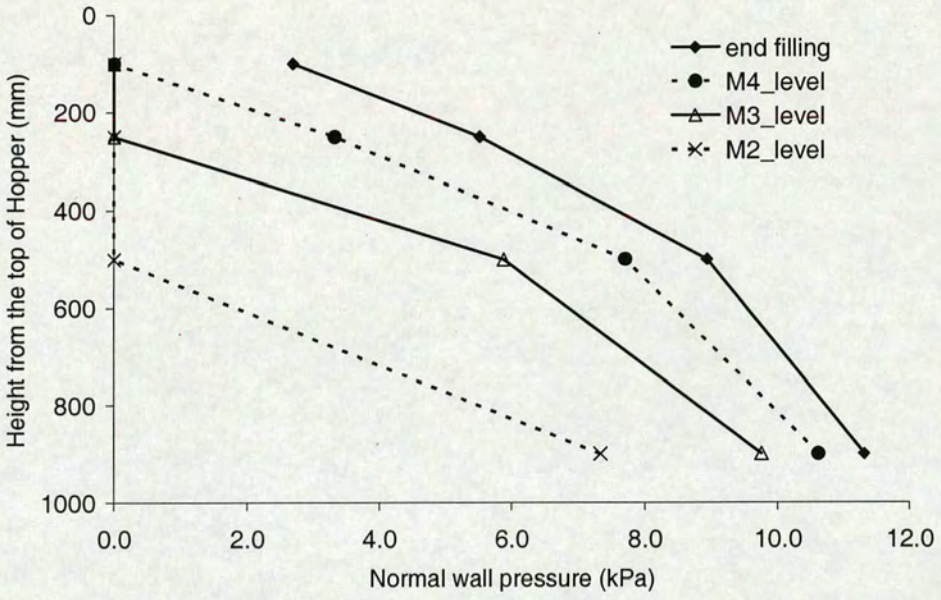

(c) Test 3

Fig. 3.33 Development of pressures on transducers during single fillings

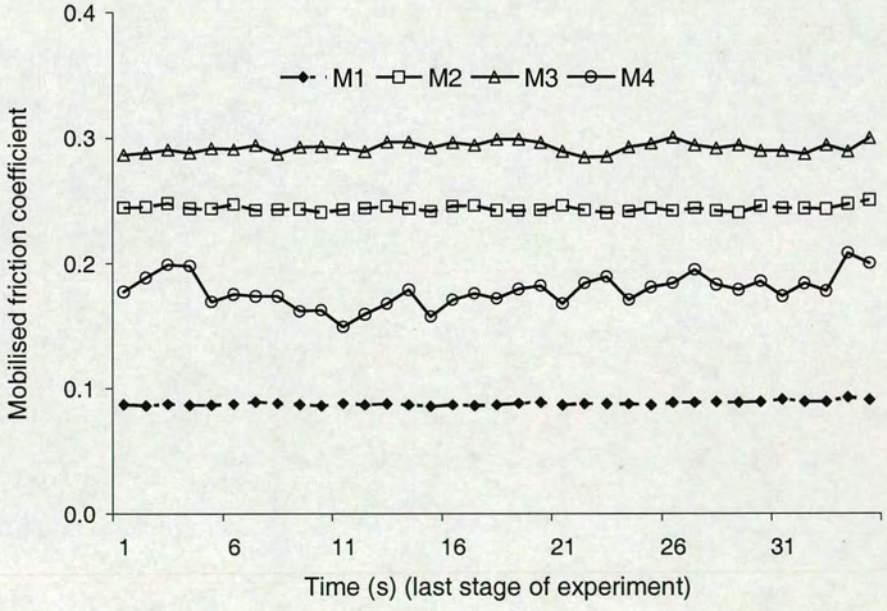

(a) Test 1

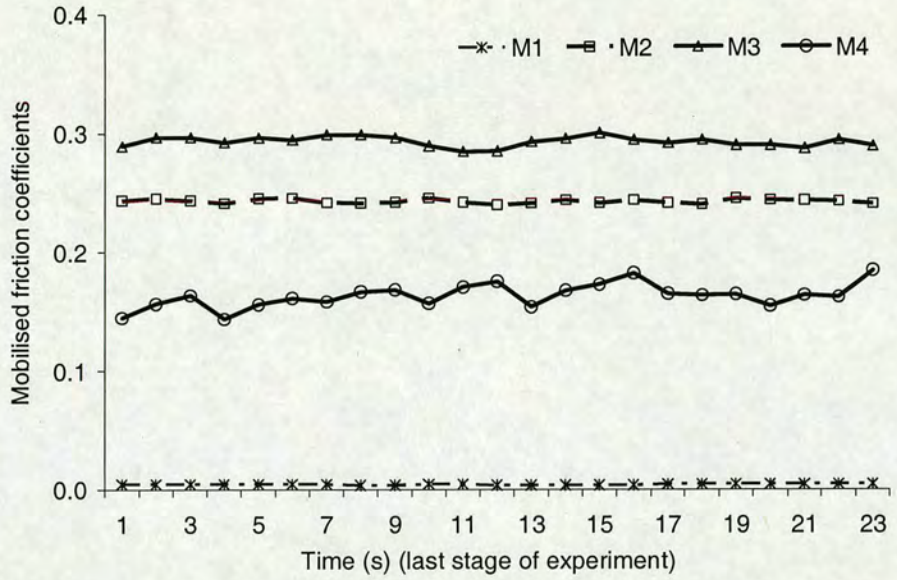

(b) Test 2

Fig. 3.34 Mobilised friction coefficients at the final stage of filling in tests

NB Results for Test 3 were similar to Test 2 and are omitted. During Test 2 and Test 3 transducer M1 was faulty.

3.5 Experimental validation of the numerical predictions

3.5.1 Some comparisons with the classical theoretical predictions

The theories proposed (see Appendix A.1) were general for the distribution of pressures in conical steep hoppers. For a hopper as shallow as the one in the present study, Rotter (2001) asserted that the hopper pressure may be evaluated using these theories but by adopting the effective hopper wall friction coefficient (μ_{eff}). This μ_{eff} has been addressed fully in Rotter (2001), and was cited earlier at section 3.3.2.3; its value was 0.325 for the condition in the current study.

Comparisons similar to those in Fig. 3.21 were carried out for the distribution of pressures on the walls of this shallow hopper. The results are shown in Fig. 3. 35 for the finite element predictions from both progressive filling and switch-on filling, along with results calculated by the algebraic models.

From Fig. 3.35, one can see that the agreement were understandably poor between the predictions by the algebraic models (except Rotter's) and the predictions by the finite element analyses from both the progressive and switch-on filling. It is a matter of validation by the results from the experiments.

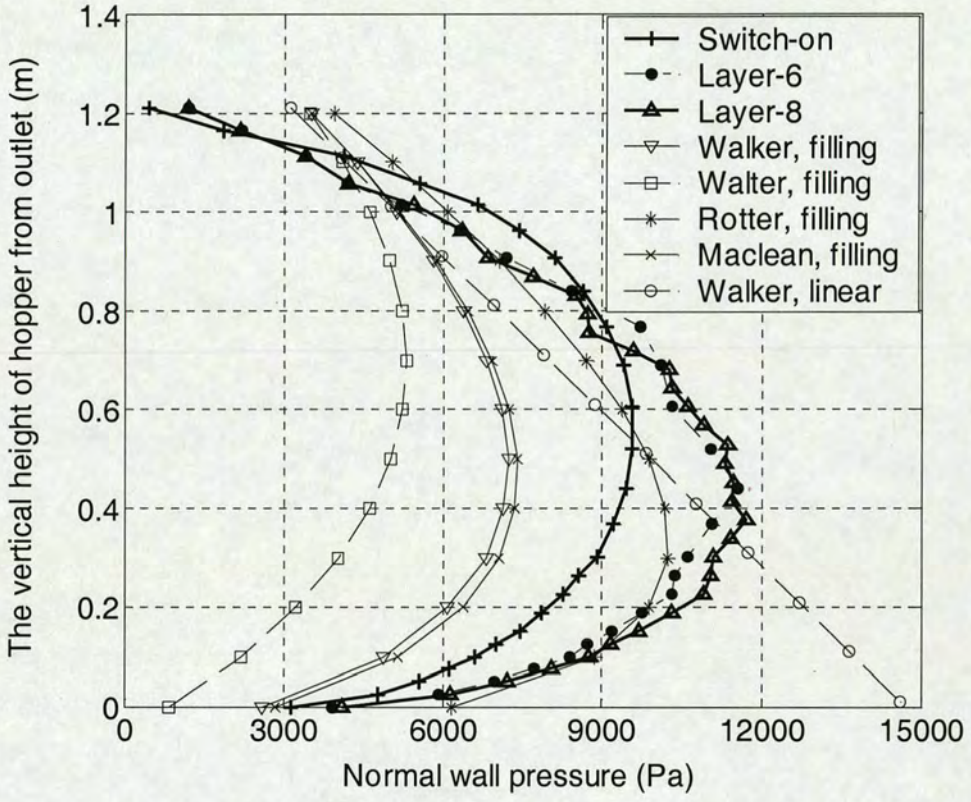

Fig. 3.35. Comparisons of pressure along the walls of shallow hopper by different approaches

3.5.2 Relationship between computation and experiment

So far, both experiments and computational predictions have been described in relation to pressures on the walls of a shallow hopper. The properties of the sand used in the experiments were measured and used in the computational predictions. Thus the experiments and calculations are directly comparable in that:

1) The computations related to a hopper with the same geometry as the experiments.

2) The stored solid in the experiments was fed into the hopper with a concentric filling, and this arrangement was modelled in the calculations.

3) At the end of filling, the stored solid in the hopper was capped by a nearly axisymmetric cone with a repose angle 36°, which was also modelled in the calculations.

4) The properties for the stored solid adopted in the finite element calculations, such as density and the internal friction angle, were taken for the sand used in the tests.

5) The wall friction coefficient measured for sand on stainless steel was adopted in the calculations ($\mu = 0.4$).

Thus, the calculations should relate well to the experimental observations if the theoretical work provides a good model for the experiments.

3.5.3 The comparison of observed and calculated pressures

The first comparison is made here between the normal pressures measured in the tests at the end of filling and the predictions obtained from the FE calculations. The measured pressures are the normal pressures on the transducers M1, M2, M3 and M4. The locations of these pressure transducers were shown in Fig. 3.29, and may be identified by the distances of each up the meridional generator from the outlet. These distances are 0.43 m, 1.00 m, 1.36 m and 1.57 m. The numerical predictions for the pressures at these locations at the end of filling from the three FE calculation procedures are shown in Fig. 3.26. The experimental and computed pressures are compared in Fig. 3.36.

In general, the experimental observations are in quite good agreement with the FE predicted pressures obtained by modelling progressive filling. Referring back to prediction by Rotter's theory as in Fig. 3.35, it also provided verifications of Rotter's theory for a shallow hopper: the power of the adoption of the effective hopper wall friction coefficient (μ_{eff}).

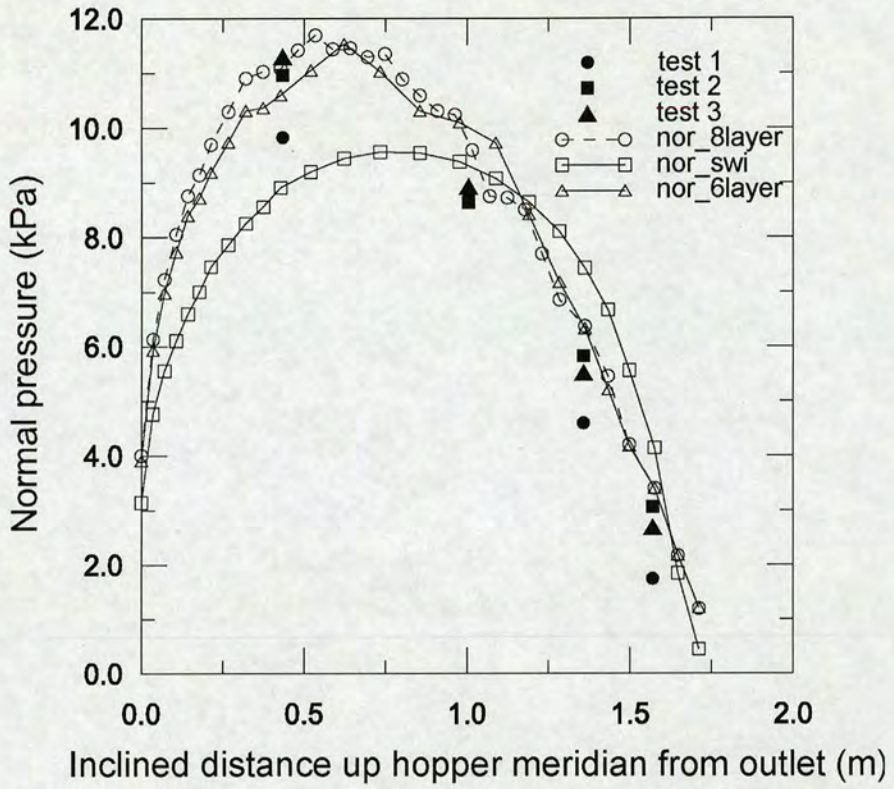

Fig. 3.36 Comparisons of experimental and numerical pressure at the end of filling

The differences among the predictions from the finite element analyses by the different approaches were previously noted: compared with switch-on filling, progressive filling increases the value of the maximum normal pressure and moved its location downwards towards the outlet; the normal pressures increased in the lower part of the wall and decreased in the higher part on the walls. The experimental observations, though limited in number, tend to support the idea that these differences are well modelled in the calculations of progressive models, and that there is a close relationship between observed and calculated values.

The next comparisons were made between the normal pressures measured when the stored solid was filled up to certain defined levels, which could be compared with the layers used in the FE progressive filling process.

In the FE analyses the stored solid was divided into layers, the six-layers and the eight-layer divisions were used in these studies. The filling process was simulated by adding the layers back in designated sequences, and the normal pressure developments were

investigated.

Diagrams showing the normal pressure distributions with the thickness of stored solid were obtained as shown in Fig. 3.25 (b) and (c). In the diagrams, the normal pressures were specified by the layers' thicknesses of stored solid. Here, the same diagrams can be used as a prediction of the pattern of normal pressure when the hopper is only partially filled. For instance from the diagram in the Fig. 3.25 (b), the value of the normal pressure on the wall should be at the middle between normal_layer6_2 and normal_layer6_3 when the stored solid is filled to 0.75 m.

Table 3.3 Normal wall pressure measured on the transducers when sand reached at several designated levels

Levels of material			m2	m3	m4	Final
The normal pressures (kPa)	filling 1	M1	5.36	7.72	8.59	9.83
		M2	0	5.35	7.33	8.73
		M3	0	0	2.81	4.59
		M4	0	0	0	1.74
	filling 2	M1	6.47	8.86	9.50	10.97
		M2	0	5.25	6.78	8.63
		M3	0	0	3.27	5.82
		M4	0	0	0	3.06
	filling 3	M1	6.76	8.99	9.78	11.31
		M2	0	5.41	7.10	8.93
		M3	0	0	3.06	5.51
		M4	0	0	0	2.70

It was difficult to identify the normal pressure in the experimental measurements to correspond to the stored solid layer thickness at an arbitrary instant from the data obtained by the data logger during the tests. However, it was possible to do so when the stored solid reached the levels where the transducers were located as listed in Table 3.3. Comparisons were therefore made between the pressures measured at the instants when the stored solid reached the levels of transducers of M2, M3 and M4, and the corresponding predicted values were identified in the diagrams of Fig. 3.25. Such results are shown in Fig. 3.37 (a) for the case of the six-layer diagram and in Fig. 3.37 (b) for the one of the eight layers diagram.

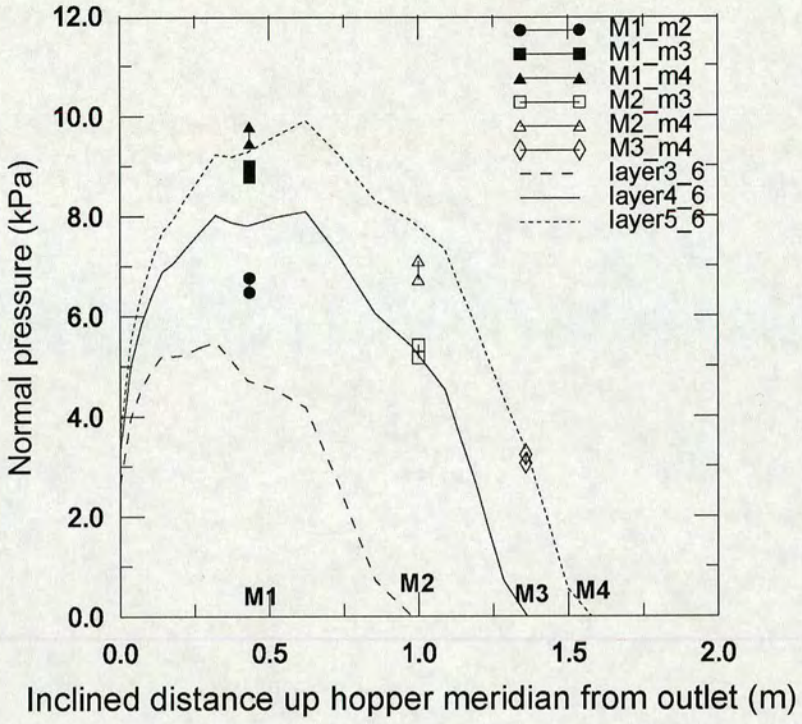

(a) Six layers

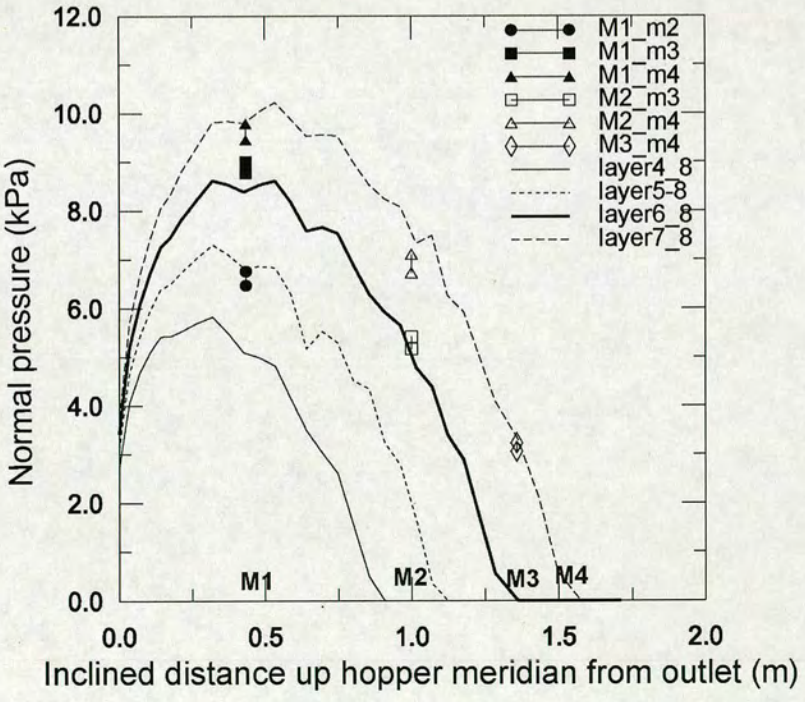

(b) Eight layers

Fig. 3.37 Comparisons of normal experimental and numerical pressure in the process of fillings

From Fig. 37, it is evident that when the stored solid reached the level M2 (1.0 m), the FE predicted pressures at the location of M1 by the eight-layer approach was closer to the experimental observations (of Tests 2 and 3) than by the six-layer approach. When the stored solid reached the level M3 (1.36 m), the experimental observations at location M1 were closer to the FE predicted pressure by the eight-layer approach than by the six-layer approach. For location M2, the two approaches appeared to make no difference, both fitting well with the experimental observations. When the stored solid reached the level M4 (1.57 m), the FE-predicted result on location of M1 by the eight-layer approach was higher than the experimental observations, whereas the FE-predicted result on location of M1 by the six-layer approach appeared be lower than the experimental observations; at the location of M2, the numerical predictions appeared to quite similar and higher than the experimental observations in both approaches, while on the location of M3, the FE predictions agreed with the experimental observations well for both progressive filling models.

Further comparisons concerned the developed wall friction, and were carried out using the ratio of the frictional traction to the normal pressure predicted in the numerical investigation and the ratio of friction force to normal force measured in the experiments. From Fig. 3.38, it can be concluded that the full friction coefficient has not been fully mobilised in this shallow hopper (as predicted by Rotter (2001)).

The transducers measured both normal force and shear force. The ratio between them measured by each transducer was taken as the mobilised friction coefficient at the location of that transducer. The extracted results for this comparison are shown in Fig. 3.38.

The full wall friction coefficient for the sand on this surface is μ =0.4, so Fig. 3.38 demonstrates clearly that this value was nowhere achieved, and the whole hopper develops only part of the potential frictional shear. However, it is also clear that the extent of this frictional development is quite closely matched between the experiment and the FE calculations, and the effective wall frictions proposed by Rotter (2001); the value itself is rather stable throughout the hopper.

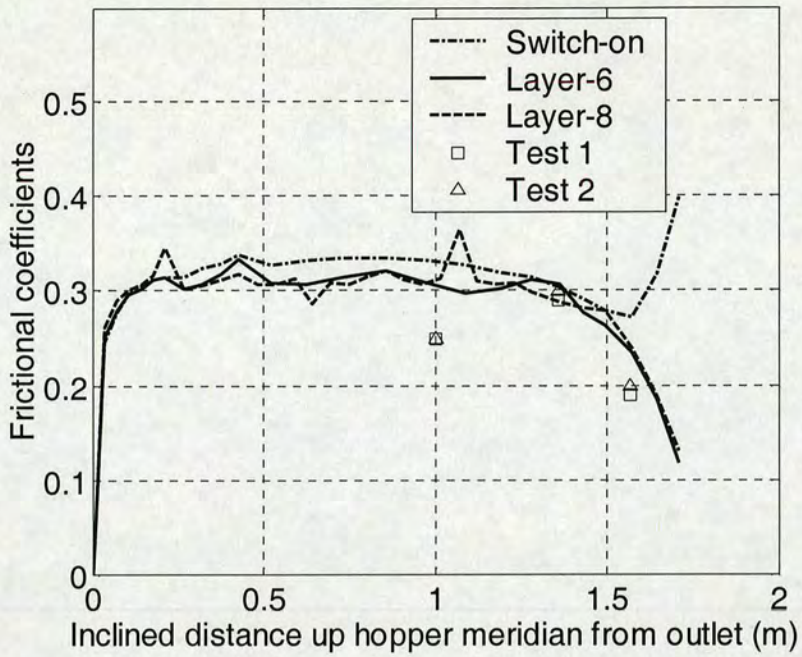

Fig. 3.38 Comparisons of experimental and numerical friction coefficients at end of filling

Two discrepancies can be seen. First, when the filling process is modelled by switch-on, there is a zone near the top of the hopper which is predicted to have a higher level of mobilised friction: this is not matched by the progressive filling calculations or by the experiments. Second, the two experiments show a rather low mobilised friction along the wall. Further investigation are needed to address this differences.

3.6 Conclusions

This chapter has described both experiments and calculations in relation to the filling of a steep and a shallow hopper made from stainless steel. The experiments have been described in detail and a number of deductions have been made directly from them. But the chief goal of the experiments has been to provide confidence that the finite element calculations of filling pressures are reliable. The relatively close match between the experiments and calculations by progressive filling have amply justified the more extended use of the FE calculations to explore a wider range of features of hopper pressures.

The FE calculations have been used to explore two important questions: what is the role of the progressive filling process on the pressures developed on the hopper wall; and what different in hopper pressures arises if distributed filling is used in place of concentric filling. These two questions have been extensively explored for the steep and shallow example hoppers. It is evident that progressive filling makes a significant difference to the pressure pattern, and that the experimental evidence supports the progressive filling calculation. The differences between the distributed and concentric filling were less marked, and open to differences of interpretation because it is not possible to simultaneously satisfy the conditions of a common top wall contact for the two cases, as well as a common total mass of stored solid (common equivalent surface).

4 PRELIMINARY INVESTIGATIONS INTO THE EFFECT OF INSERTS ON FLOW MODES

4.1 Introduction

The flow patterns during silo discharge have been the subject of extensive theoretical and experimental activities world wide. It has long been recognised that the loads exerted on the wall during silo discharge are unpredictable without knowledge of the flow pattern. Also, the flow pattern itself is still difficult to predict.

Two kinds of flow pattern are widely recognised, namely mass flow and funnel flow. Mass flow is a flow mode by which every particle in a silo is in motion once discharge starts. Funnel flow is a flow mode where stationary zones exist in certain parts of a silo, most likely above the hopper walls. As a result, there is a flow channel boundary between the flowing and static solid. Still the prediction of the locations of such boundaries is not addressed well. Nevertheless, the expected location of the flow channel is sometimes used in practice, when for example the abrasiveness of a stored material must be taken into account seriously.

Both flow modes have advantages of their own. However, a mass flow generally is superior to a funnel flow. For instance the importance of avoiding flow disruptions and quality variations, which are associated mostly with funnel flow, often requires a mass flow rather than a funnel flow in silo design. Based on the material properties, it is feasible already to design a mass flow silo.

Usually a mass flow silo requires a quite steep hopper. Compared with a silo with a shallow hopper, a mass flow silo with a steep hopper either will reduce the storage capacity when the headroom available is limited, or will require more space if the storage capacity has to be maintained. The ratio between the capital expenditure and the storage capacity will be higher for a silo with a steep hopper than one with a

shallow hopper. In many situations the headroom available is limited. In such circumstances, silos with steep hoppers can only have restricted capacity. Quite often too, a silo designed to perform in mass flow may turn into a funnel flow silo after a certain period of service, or possibly when being used to store a different material.

Therefore considerable efforts have been expended in order to obtain mass flow in a silo with a reasonably flat hopper. In practice, some retrofits have also been made to convert a silo with quite flat hoppers from a funnel flow into a mass flow. Putting an insert in a certain position in a silo is one of the common practices in such activities (Jenike, 1964; Jansson, 1968). Therefore it is desirable that a prediction be found to indicate whether such an insert functions in the manner expected or not for a given application. However, one must admit that no perfect method has yet been developed to carry out such a prediction.

A description is given in this chapter of numerical and experimental investigations into the effects of inserts on flow patterns. The numerical investigations were obtained using a computer program called SILO (Klisinski, 1989, 1996; Karlsson, 1996). The experiments were conducted in a small scale silo to measure the residence time of tracers seeded within the material.

4.2 A Lagrangian-Eulerian approach to the discharge

4.2.1 Arbitrary Lagrangian-Eulerian approach

As in the attempts described in Chapter 3 to model a process of filling, it has also been widely recognised that it is a complicated procedure to model silo discharging processes using FEM formulations. During silo discharge, the amount of material left inside the silo decreases, and the boundaries of the stored body of solid are changing. At the outlet, the material is discharged either freely or under control, so a fixed boundary could be prescribed and an Eulerian approach is favourable. While in other regions, the edges are changing as the material moves and a Lagrangian approach is necessary. To cope with such a process fully, an arbitrary Lagrangian-Eulerian formulation approach is preferable.

4.2.2 Finite element formulation

To be both simple and representative, the steep hopper described in Chapter 3 was used. The region of material was formed by concentric filling, and the same geometries as those of Fig. 3.2(b) were assumed. They consisted of the physical models, on which the incorporation of the arbitrary Lagrangian-Eulerian approach (ALE) would be based.

In order to achieve an ALE approach, a new finite element model was developed to represent the wall and bulk solid by modifying the models created earlier in the simulation of the filling process. In this new model, the settings for the wall remained the same as at section 3.2.3 in Chapter 3, i.e. the top edge was constrained both horizontally and vertically, and the bottom edge only horizontally. It was modelled as an elastic material with a Young's modulus of 1.0×10^{11} Pa and a Poisson's ratio of 0.3, but was regarded as weightless. While the setting for the material properties was the same as those listed in Table 3.1, some modifications to the boundaries were necessary.

The modification involved firstly an application of an adaptive mesh to the region of material to replace the material meshes. Further modifications included some operations on its edges. In this new approach, the edge of the material at the outlet was constrained to have zero movement; in addition, an adaptive mesh constraint and an Eulerian surface region type were applied to the solid at the outlet. By making these changes, the meshes at the outlet were fixed, but the material could flow through those meshes. A Lagrangian surface region type was applied to the other edges to ensure that the edges of the mesh follow the movement of the material as indicated in Fig. 4.1.

Adopting the above steps, the next modelling challenge was to decide how to prescribe an initial condition of stress within the material. Such stresses are necessarily developed during filling and remain during storage. In the present study, an attempt was made to import the stresses developed in the six layer filling approach as the initial stress condition.

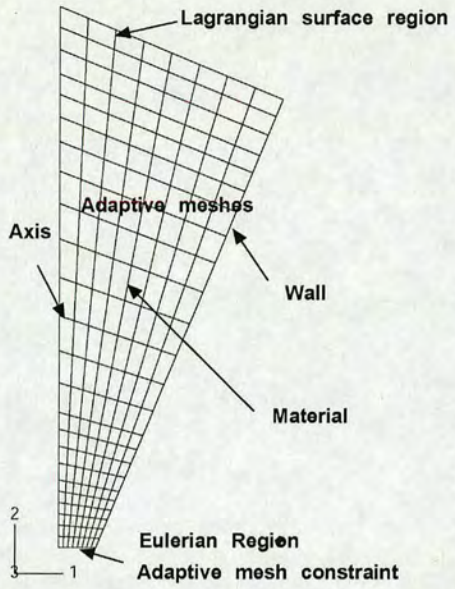

Fig. 4.1 Model design for an arbitrary Lagrangian-Eulerian approach

4.2.3 An unfortunate failure

A Lagrangian-Eulerian analysis was initiated. However, the process to import the stress distribution from the simulation results of the layer by layer filling were not successful because "a floating-point invalid operation" error was encountered during the importation. The author alerted and reported this error to the ABAQUS company. Over a period of several months of consultations, it transpired that the error was difficult to correct within the existing software, and would be addressed in a forthcoming version.

4.3 Application of the Program SILO

4.3.1 Background

For some years now, the POSTEC Department of the Telemark Technological R&D Centre has undertaken experimental investigations of several types of flow promoting inserts. It has been shown that it is difficult to provide unequivocal guidelines on exactly where the inserts should be placed for optimum effects.

A theoretical method is necessary. So far, however, analytical efforts to describe silo flow patterns are suitable only under certain circumstances. There is scarcely any analytical method available for more complex silo geometries: for example, the use of

an insert inside a silo. It is then necessary to turn to a numerical modelling approach in the hope of finding a solution.

Collaborations were initiated by POSTEC in 1986 in order to develop a computational program which would be capable of predicting flow behaviour around inserts. This program was called SILO. The achievements in the use of this program included estimation of whether a silo would display funnel or mass flow; but some challenges remain and it is uncertain whether it is capable of accurately describing flow around inserts.

The results of some numerical investigations into flow patterns and the effects of several inserts on the flow patterns will be presented. These were all obtained using the program SILO . The modelled silo was a laboratory model for flow observations, and the inserts were a cone-in-cone insert, a double-cone insert and an inverted cone insert. Investigations were carried out with different configurations of the silo and the inserts. Based on the simulation results, the program SILO was assessed for its ability to predict the effects of inserts on flow patterns.

4.3.2 The main features of the SILO code: Basic considerations

The program SILO was based on the finite element method and written in FORTRAN. The key features are summarised by the authors Klisinski (1989, 1996) and Karlsson (1996).

4.3.2.1 Methodology and approaches

In the program SILO, an Eulerian approach is adopted based on a continuum model. This approach has been proven to have some justifications in dealing with the macroscopic behaviour of granular material, and provides a possibility of investigating material movement around inserts. In this approach, it is required to fix all the edges of the objective body. As mentioned above, it is reasonable to fix the boundary at the outlet. To retain the upper surface in a stable position requires that material is refilled back into the top of the silo at the same rate as that of discharge from the outlet. Such an operation is usually carried out in a silo that is used for mixing or re-cycling and is also often performed in silo experiments where steady state conditions are sought.

Under such conditions, the discharge process does not empty the silo, but a process of steady state discharge is achieved. Since the present work focuses on the flow around an insert , this steady state condition is acceptable.

4.3.2.2 Equilibrium equations

For an Eulerian formulation, the basic equations to describe the material movement confined to a region are the equations of motion. The general form of the equations (Klisinski, 1989) are

$$\mathbf{div}\ \boldsymbol{\sigma} + \rho\mathbf{B} = \rho\mathbf{a}$$

$$\mathbf{a} = \partial\mathbf{v}/\partial t + (\nabla\mathbf{v})\,\mathbf{v}$$

where ρ is the bulk density of the material, **B** the gravity acceleration, **a** the acceleration, and **v** and $\boldsymbol{\sigma}$ are the unknown velocities and stresses.

These equations govern the motion of a continuum in a fixed region whose boundaries will be prescribed with different conditions. In the present study, the surface tractions are the friction between the material and the wall, and the friction between the material and the inserts. At the outlet, assuming that the material is discharging freely, the boundary is treated as frictionless. These boundary surface stresses are given as

$\sigma_{ij} = \sigma_{ii} \tan\phi_w$ along the wall or inserts

$\sigma_{ij} = 0$ at the outlet and upper surface

where ϕ_w is the angle of friction between material and the surface concerned, σ_{ii} is the normal stress and σ_{ij} is the shear stress.

4.3.2.3 Constitutive law

Within a continuum model framework, the silo discharge process may be further approximated as a plastic flow. The selection and implementation of a material constitutive model to account for the deformations of granular solids held in silos is always a difficult question and different researchers have taken quite different views. In the present study, an elasto-plastic continuum model, using the Mohr-Coulomb

yield condition, is adopted. Admittedly, it may be a very coarse approximation, but it has not yet been shown that a more complicated model is required.

When subjected to pressure, this elasto-plastic material will yield plastically after undergoing an initial, limited, elastic deformation. The plastic deformation process, associated with large deformations, is described in terms of the strain rate

$$d\varepsilon = d\varepsilon^{el} + d\varepsilon^{pl}$$

where: $d\varepsilon = \frac{1}{2}\left(\frac{\partial v_i}{\partial x_j} + \frac{\partial v_j}{\partial x_i}\right)$ is the strain rate

which will at first obey an elastic deformation rate $d\boldsymbol{\varepsilon}^{el}$ given by

$$d\boldsymbol{\varepsilon}^{el} = (\mathbf{D}^{el})^{-1} : d\boldsymbol{\sigma}$$

in which D^{el} is the stiffness matrix that contains the shear viscosity μ and bulk viscosity κ, and will then follow a plastic deformation rate $\dot{\varepsilon}_{ij}^{pl}$ governed by the flow rule:

$$d\,\varepsilon^{pl} = \lambda \frac{\partial G}{\partial \sigma}$$

where λ is a scalar constant, and G is the plastic potential.

The plastic potential G follows the Flow Rule. In the present work, a non-associated flow rule is adopted, suitable for granular material, and the plastic deformation $\dot{\varepsilon}_{ij}^{pl}$, in a steady flow where the material is incompressible, is governed by the Mohr-Coulomb yield condition with the dilation angle φ:

$$\dot{\varepsilon}_{ij}^{pl} = -\frac{1}{2}\tan 2\varphi \left(\frac{\partial v_i}{\partial x_j} - \frac{\partial v_j}{\partial x_i}\right)$$

where the dilation angle φ may be observed from the angle 2φ shown in Fig. 4.2.

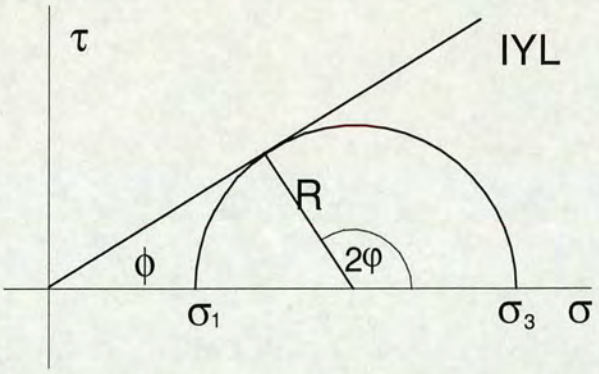

Fig. 4.2 Mohr's circle and the angle 2φ associated with plastic deformation

The choice of values for the material parameters also relates to the material model. The values of the parameters of shear viscosity (μ) and bulk viscosity (κ) were set as $\mu = 1\times10^5$ Pa and $\kappa = 9\times10^5$ Pa respectively (Karlsson, 1998), though no tests are known from which they have been deduced. These parameters are chiefly needed to keep the calculations numerically stable, and the values cannot be very high for a granular material.

The values of the other parameters are measurable, and were chosen as a bulk density of ρ = 606 kg/ m^3, internal friction angle of φ = 31.9° and wall friction angle ϕ_w = 21.8°. The values of these parameters for the material all remained unchanged throughout the calculations unless it is stated otherwise in specific situations.

4.3.3 Applications of the program SILO to a small scale silo with different inserts

4.3.3.1 Modelling of silo and inserts in SILO

The geometry of the silo used in the simulations was chosen to be that of the silo used in the experiments. It was axisymmetric, 1500 mm in height and 750 mm in diameter, with a hopper of 470 mm in height and a 34.7° cone half angle (Fig. 4.3). This cone angle is, of course, relatively steep, so it can be expected to be not too far from producing mass flow conditions for some solids. The outlet was 100 mm in diameter.

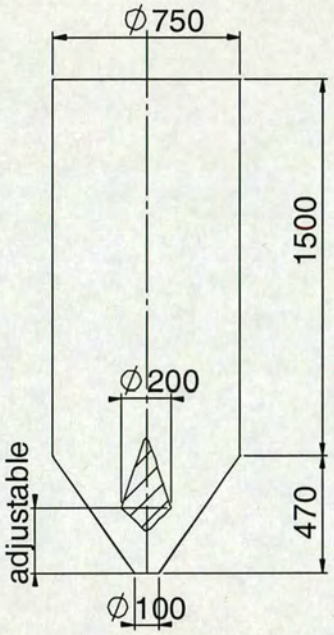

Fig. 4.3 An example configuration of an insert within the model silo

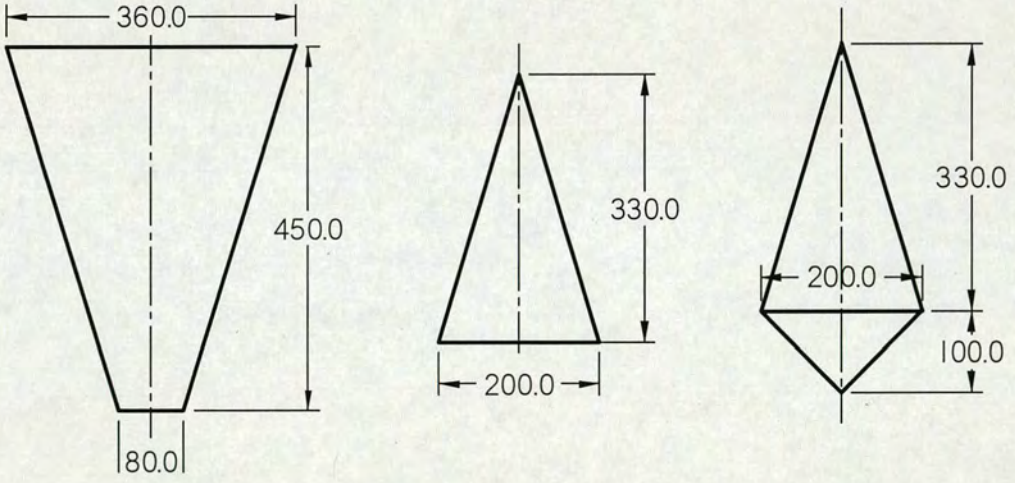

Fig. 4.4 Geometries of different inserts: (a) cone-in-cone, (b) inverted cone (c) double cone

The inserts were a cone-in-cone, an inverted cone and a double cone; the geometries are given in Fig. 4.4. They were all axisymmetric, and were fitted into the silo, aligned with the axis of the silo. Fig. 4.3 shows an example configuration of a double cone insert within the silo. The other possible configurations of silos and inserts are shown

in Table 4-1, which gives the distances of the lowest edge of each insert to the outlet. Details may also be found in the text when specific simulations are described.

Table 4.1 Configuration of inserts in the silo

Configuration between silo and insert		Config. 1	Config. 2
Distance of lowest edge of insert from outlet (mm)	Double cone	90	210
	Inverted cone	180	300
	Cone-in-cone	90	210

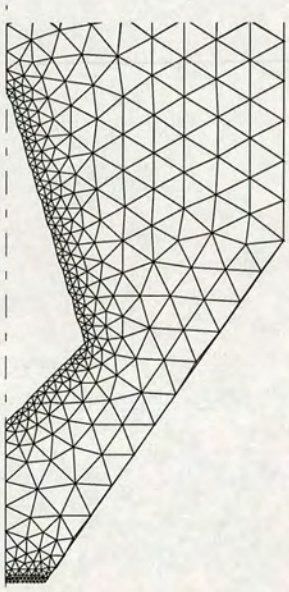

Fig. 4.5 Typical mesh used, with second-order triangular elements, including mesh refinement near zones of rapid change

A second order triangular element was used in the finite element meshes in the region 500 mm below the top of the silo. This region represented the material region confined by the silo and inserts, and formed the element domain. The governing equations and their boundary conditions were formulated and implemented in this domain accordingly. The reader is also referred to the texts by Nellson (1989) and Zienkiewicz (2002) for a fuller description of the standard parts of the formulation, and to Klisinski (1989, 1996) and Karlsson (1996) for specific descriptions concerning the

implementation and programming. An example mesh used is shown in Fig. 4.5, which includes a finer mesh in the region of the outlet and around the insert.

4.3.3.2 Numerical results from the simulations

4.3.3.2.1 Preliminary tests

Preliminary simulations were first carried out on a silo with no insert. In this preliminary work, an automatic and adaptive algorithm for time integration was used (Karlsson, 1998). The purpose was to increase the length of each time step when convergence in the iteration was achieved rapidly, and decrease the time step length when the iteration process converged slowly. The maximum number of iterations in each time step was chosen to be 10. When convergence was not reached, the length of the time step was cut in half to continue the iteration process. The minimum time step length allowed was set as 1.0×10^{-10} s. If a smaller time step was required, the program terminated. Convergence was harder to obtain after the inserts had been introduced, as can be seen later in discussion of the specific calculations.

The program permitted the introduction of tracer particles in the continuum (effectively tracing the movements of identified parts of the modelled continuum). Such tracer particles were here seeded into the mesh to visualise the numerical results as paths and locations of material movement. Using this technique, the results are given in the form of tracer particle movements as shown in Fig. 4.6 (a). In the figure, the dotted lines represent the original positions of the tracers assigned at three chosen levels, and the asterisks, also forming three lines accordingly, represent the tracer locations in the last step of the simulation. As seen in Fig. 4.6 (a), the particles near the centre and close to the wall at the upper level moved down, but the particles close to the wall at the transition level did not. The velocity distributions in Fig. 4.6 (b) show further that the material in the centre region moves faster than that close to the wall region, where no material movement occurs around the transition level. Obviously, a stagnant zone developed around the transition area in the silo, especially in the hopper.

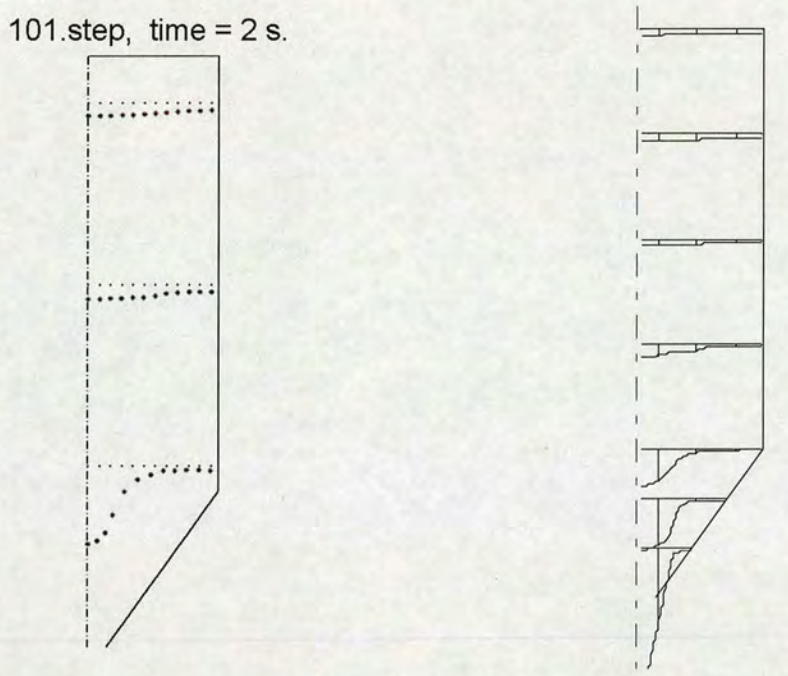

(a) Tracer particle positions at the last step of simulation

(b) Velocity distributions

Fig. 4.6 Funnel flow silo and its stagnant zone

4.3.3.2.2 Effect of inserts on flow patterns

In this funnel flow silo, different inserts as shown in Fig. 4.3 were then modelled within the silo. In the first step, the inserts were installed at a low level (referred to in Table 4.1 as Config. 1). In this Low Level placement, the lower edge of the cone-in-cone and the lower tip of the double-cone insert were both 90 mm above the outlet, leaving the base of the double cone insert 280 mm below the silo transition level; the inverted insert had its base at the same level as that of the upper cone of the double cone insert. For such installations of different inserts, finer meshes were designed in the region around the inserts and the outlet. An example was given in Fig. 4.4 in the configuration of the double cone and silo.

Using such configurations, simulations of effects of the inserts on the flow were carried out. However, the program always diverged for the case of the inverted cone insert. This was overcome by redesigning the insert and the finite element meshes in the region under its base. The redesign included transforming the inverted cone into a double cone. The upper part of this double cone was identical to the intended one,

whilst its lower part had a very small slope on its base giving only 10 mm in height. This left the bottom tip of this revised cone 180 mm above the outlet. This lower part of the cone's surface was regarded as frictionless. After this modification, all simulations were successful. They are shown in Figs 4.7 a, b, c for the conditions of the cone-in-cone, the inverted cone and the double cone, in the form of tracer locations and velocity distributions similar to those in Fig. 4.6.

Overall (Fig. 4.7), these inserts made the material in the whole silo move. The cone-in-cone insert caused the material to be discharged more evenly in the cylinder section (Fig. 4.6 (a)), but caused the material inside the insert to move faster than that outside in the hopper (Fig. 4.7 (a)). Both the inverted insert and the double cone insert, as shown in Figs 4.7 (b and c), improved the evenness of the flow pattern. They caused the material to be discharged quite evenly in the cylinder section, and made the material in the hopper move in a manner similar to a mass flow.

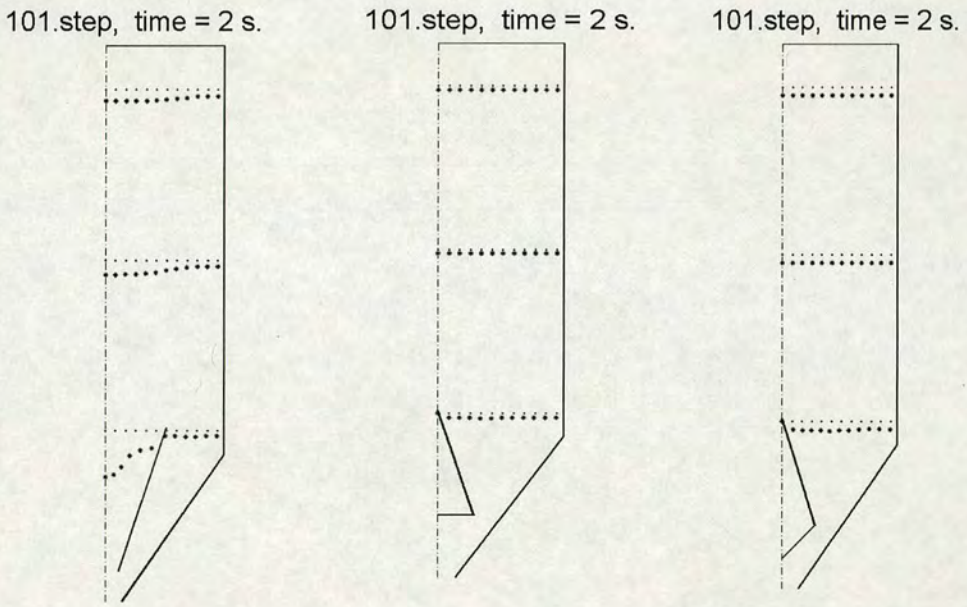

Tracer particle positions

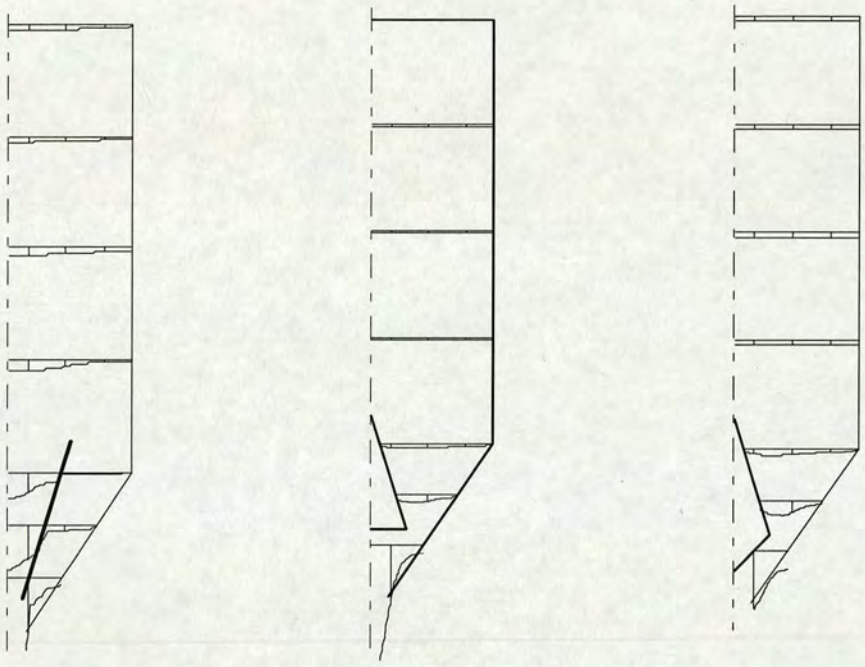

Fig. 4.7 Influence of inserts on flow pattern: (a) cone-in-cone, (b) inverted cone, (c) double cone

In the next calculations, the inserts were lifted to a position 120 mm higher. Here, the lower tips of the cone-in-cone and double cone inserts were raised to 210 mm from the outlet. At this level, the bases of the double cone and the inverted cone were both 160 mm below the silo transition level. Finer meshes were designed in the region around the inserts and the outlet, and care was taken to try to avoid divergence problems in the case of the inverted cone. Similar simulations, with all other parameters held constant, were carried out and the predictions are shown in Fig. 4.8. It can be seen in this figure that lifting the inserts changed the discharge flow pattern of the solid, with the material still being discharged quite evenly in the cylinder section in all three cases, but still not quite even in the hopper.

One very clear feature of all the simulations in Figs 4.7 and 4.8 in contrast to the predictions shown in Fig. 4.6, is that no stagnant area exists any longer; the funnel flow silo was converted to give a flow pattern that is very similar to a mass flow.

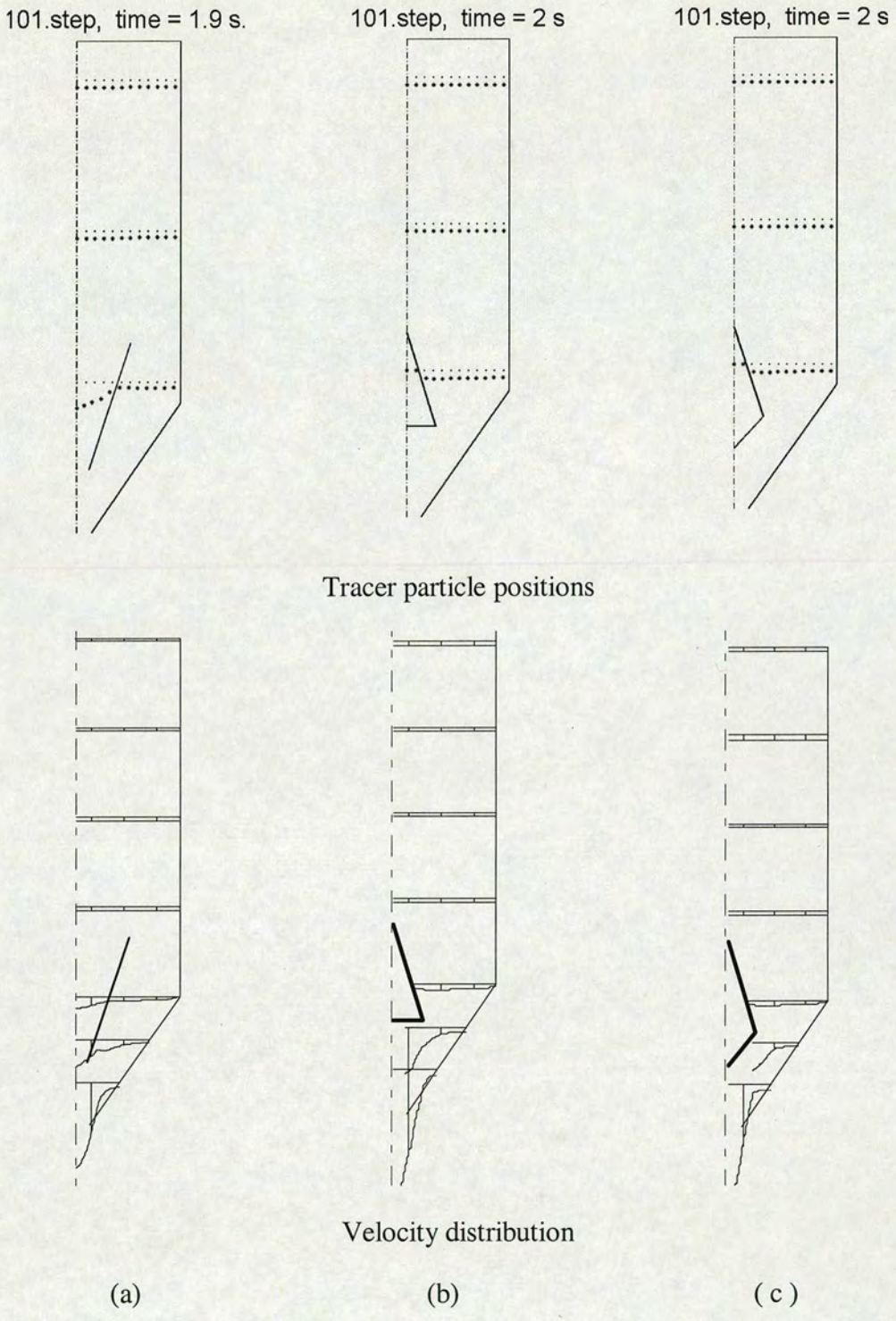

Fig. 4.8 Influence of insert position on flow pattern: (a) cone-in-cone, (b) inverted cone, (c) double cone

4.3.4 Parametric investigations into the effects of hopper angle on flow patterns in a silo with a double cone insert

4.3.4.1 A silo with shallow hopper

The next challenge was to determine how shallow the hopper could be if these inserts were still to be used to produce mass flow. For this purpose, the silo shown in Fig. 4.4 was redesigned to have a hopper, whose hopper angle was 45° to the vertical. The other dimensions remained the same.

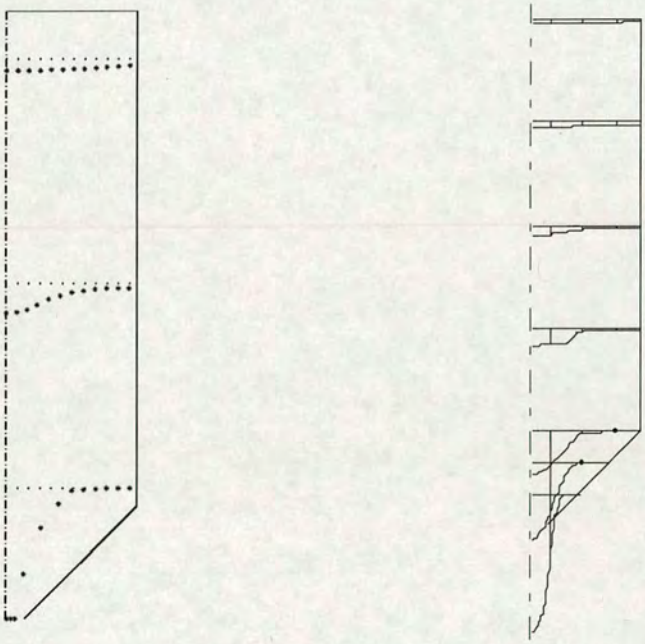

(a) Tracer particle position at the last step of simulation.

(b) Velocity distributions

Fig. 4.9 Development of a narrow channel flow in a silo with a 45° hopper and no insert

Based on these parameters, the modelling of the flow was first attempted without any insert. Tracer particles were again seeded to follow the paths and locations of material and the result is shown in the form of tracer particle movements in Fig. 4.9 (a), where the asterisks represent the tracer particles in the last step of the simulation. The particles near the centre and close to the wall at the upper level moved down, but the particles close to the wall at the transition level did not. The velocity distributions in Fig. 4.9 (b) further show that the material in the central region moved faster than that close to the wall region, where no material movement occurred around the transition

level. Clearly, a zone of stationary solid developed around the transition area in the silo, especially in the hopper.

4.3.4.2 Combination of silo and a double-cone insert

4.3.4.2.1 Location of double-cone insert

The insert was a double cone insert; identical to that as shown in Fig. 4.3. It was firstly fitted into the silo aligning with its axis. The insert was first placed with its maximum diameter 120 mm lower than the transition level, and then with its maximum diameter at the transition level; see Fig. 4.10.

Fine meshes were designed in the regions around insert and outlet. Keeping the other conditions exactly the same as those in the previous calculations, simulations were carried out and the numerical results are shown in Fig. 4.11.

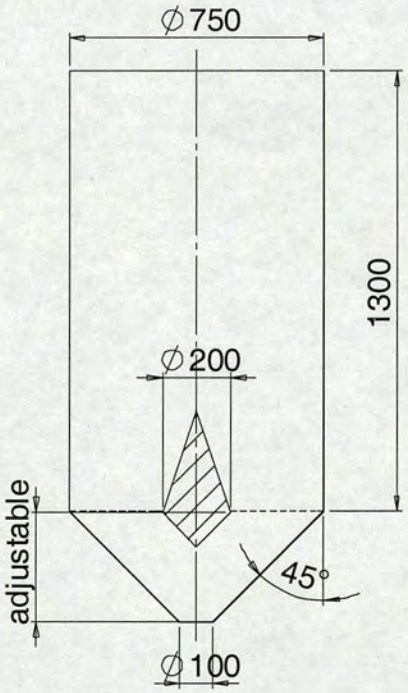

Fig. 4.10 Configuration of silo and double cone insert typical

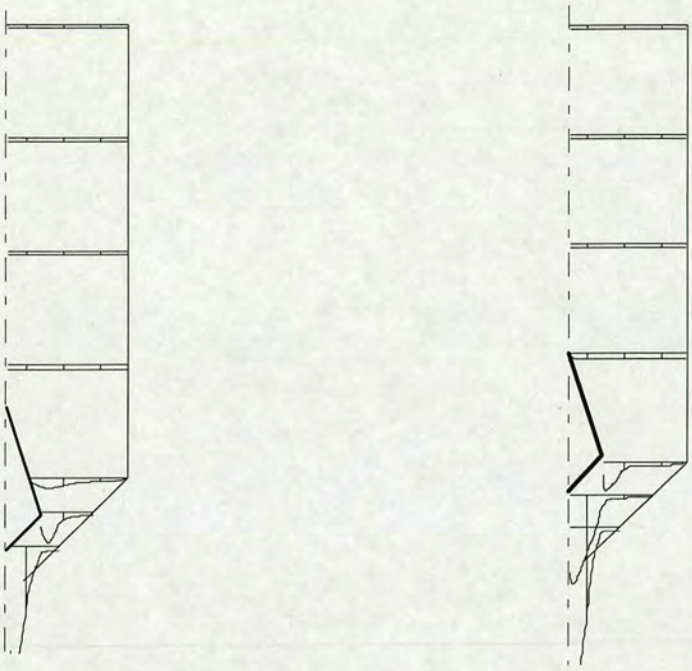

(a)Velocity distributions (insert max. dia. 120 below silo transition level)

(b) Velocity distributions (insert max. dia. at silo transition level)

Fig. 4.11 Position effect of a double cone insert on material flow in a silo with a 45° hopper

The results show that the installation of the double cone insert at this level improved the material flow pattern, i.e., with a very even movement of solid in the whole cylinder section. But below the transition level, the discharge velocity distribution was very uneven, with solid almost stagnant close to the hopper wall. To reduce the unevenness of flow pattern in the hopper, further efforts were made to focus on this portion of the silo.

4.3.4.2.2 Extensions of the insert's lower cone

Comparing the results in Fig. 4.8 (b) and (c), it is evident that there are differences induced by the lower part of the cone insert, which suggest that the length of the lower part of the cone may play an important role in the flow pattern. This was presumably understood by the inventors of such inserts, but the flow does not appear to have been examined scientifically before. It was thought that by extending the lower tip of the double cone to the outlet, the flow might be made more even and could lead to further flow improvement. This modification to the double cone insert was carried out, keeping the widest part of the cone at the same level, and its diameter unchanged.

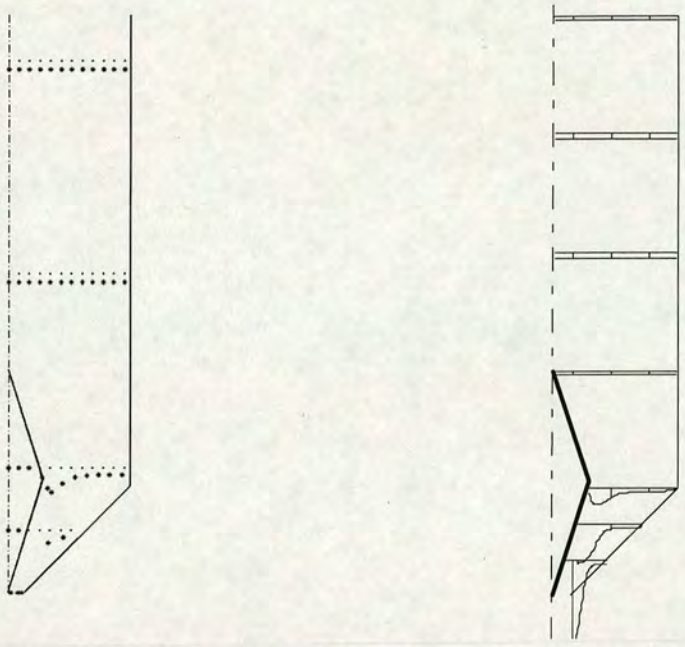

(a) Tracer particles position at the last step of simulation

(b) Velocity distributions; ϕ_w=21.8°

Fig. 4.12 Flow in a silo with a 45° hopper having an extended double cone

The results are shown in Fig. 4.12. Compared with the results shown in Fig. 4.11, the simulations show that the extension of the lower cone led to somewhat reduced unevenness of discharge in the hopper, whilst very even movement in the whole cylinder section was unaffected. The height of the lower cone thus plays an important role and the greater length of the lower cone seemed to improve discharge. However, the improvements were small under the current conditions. Other methods of flow improvement, which might include reducing the hopper wall friction, should also be considered

4.3.4.2.3 Friction contribution

There are many factors that influence the discharge flow pattern. The key parameters are the material internal friction, the hopper half angle and the wall friction between the granular material and wall. For a given material and an existing hopper, the first two parameters are set already and one is unable to do much about them. However, the wall friction can be modified by, for example, applying a coating to the silo wall. Such changes can be effected without requiring much new investment. Hence, an investigation of the effect of wall friction on the flow was carried out next.

In the zone just above the hopper, it was evident that some material remained stationary. There is therefore no obvious reason to decrease the friction along the wall of the insert and cylinder. A reduction of the wall friction between the material and the wall of the hopper alone was therefore implemented and simulations were carried out. Figure 4.13 shows the numerical results after resetting the friction between material and hopper wall to 18° and to 15° (in place for the previous 21.8°). An increase to 25° degree wall friction was also implemented as an additional comparison.

Comparing the results in Fig. 4.13 with those in Fig. 4.12, one can see that after a decrease of the wall friction on the hopper wall, the unevenness of discharge in the hopper was reduced and the velocity distribution was improved. It is also evident from the three different wall friction conditions calculated, as the hopper became smoother, the flow pattern became progressively better. In the higher wall friction hoppers, there is a slice of almost stationary solid adjacent to the hopper wall which does not move much. Since this silo is axisymmetric, a slice at the outer diameter like this represents a very significant proportion of the total material that is being discharged, so it is evident that the hopper wall friction is very important when inserts are used to improve the flow pattern.

Nevertheless, although the reduction in wall friction has improved the uniformity of flow velocities in the hopper, it should be noted that the material moving against the lower part of the double cone insert still flows at a much higher velocity than that against the hopper wall (Fig. 4.13a).

One question remained concerning the role played by the extension of the lower cone of an insert when the hopper wall friction is low. To explore this question, a further calculation was carried out in which the lower cone was returned to its original geometry, but the hopper wall friction angle was kept at 15°. The numerical results are shown in Fig. 4.14.

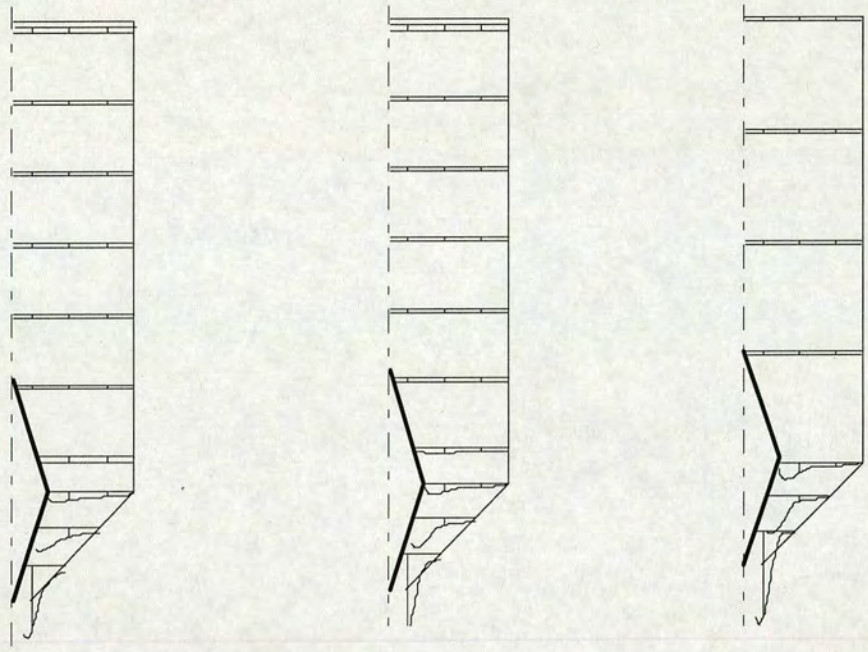

(a) ϕ_w=15°　　(b) ϕ_w=18°　　ϕ_w=25°

Fig. 4.13 Velocity distributions with different hopper wall friction

Velocity distributions (ϕ_w=15°)

Fig. 4.14 The effects of the lower cone extension

The unevenness of the flow velocities on discharge with this higher friction wall was similar to that found when the double cone insert was not extended to the outlet (Fig. 4.11(b)). Comparing the result again with that for the smoothest hopper wall (Fig. 4.13(a)), it is clear that the extension of the lower cone to the outlet is a valuable change, but it is important that the wall friction is also made low at the same time; perhaps at 18° for the present example case.

4.3.4.2.4 The width of the insert

So far, this study has concentrated on investigating the effect on the flow pattern of changing the vertical extent of a double cone. In the same manner, it is possible that changing the maximum diameter of the double cone may also change the flow pattern considerably.

Consequently, the next investigation explored the effect of an increase or decrease in the maximum diameter of the double cone on the flow patterns. This study was carried

(a) Velocity distribution (insert max. dia. =150 mm)

(b) Velocity distribution(insert max. dia. = 175 mm)

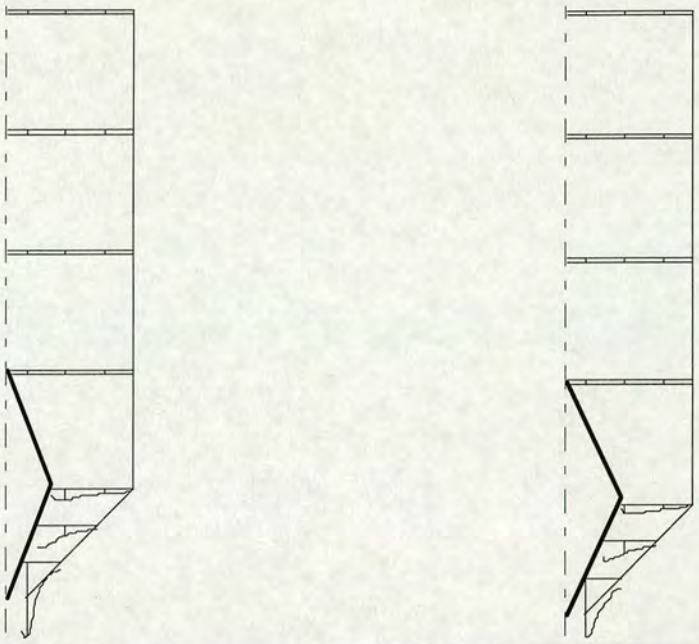

(c) Velocity distribution (insert max. dia. = 220 mm)

(d) Velocity distribution (insert max. dia. = 250 mm)

Fig. 4.15 Effect of double cone insert size on material flow (ϕ_w= 18°)

out by setting the maximum diameter of the double cone to 150 mm, 175 mm, 220 mm and 250 mm (compared with the original 200 mm). In all these changes, the tip of the lower cone of the insert was kept at the level of the outlet, and the friction between the material and the hopper wall was kept at 18°. The results are shown in Fig. 4.15.

Comparing velocity distributions caused by different diameters of the insert as shown in Fig. 4.15 with that in Fig. 4.13 (b), it is firstly evident that all the investigated diameters of insert produce good mass flow in the cylinder. However, it is clear that a decrease in the maximum diameter of the insert makes the velocity distribution in the hopper less even, and that the increase of this parameter makes only slight improvements. This suggests that it is important to keep a proper ratio between the maximum diameter of the insert and the diameter of the silo, and that it is also important to keep the cone angle at a certain level. In the conditions of this investigation, the ratio was 0.267, and the half angle of the upper cone was 17.5° (angle to the vertical).

4.3.5 Concluding remarks on this part of the investigation

The simulations described above have shown that the cone-in-cone, the inverted cone, and the double cone inserts were all able to change the material flow pattern in the cylindrical part of the silo from funnel flow to mass flow in this silo whose hopper has an inclination angle larger than that of the critical value for mass flow. Of these alternative inserts, the double cone insert performed best in this silo for hopper half angles up to a certain value. Beyond this point, mass flow could not be obtained without changing the location, vertical extension and hopper wall friction coefficient. These effects were all explored.

Locating the inserts at a proper level was found to be important in achieving an even flow. In a silo with a hopper inclination angle below a certain value, the inserts should be installed at higher levels, close to the transition rather than at a lower position close to the outlet, especially when a cone-in-cone insert or inverted insert is used. However, in a silo with a flatter hopper, where mass flow was only obtained in the cylindrical section with the double cone insert, the position of the double-cone insert had relatively little influence on flow in the hopper, where the uneven discharging remained.

It has been also shown that vertical extension of the lower cone of a double-cone insert to the outlet would improve the silo discharge pattern, but its effect is hardly noticeable if the hopper wall friction is high. This suggests that using such an insert to obtain mass flow from a funnel flow silo has a limitation with regard to the maximum hopper angles that can be permitted. But since, at worst, this extra extension did no harm to the flow pattern, it could be used in practice to facilitate axial location of the double cone, which is crucial in obtaining an even discharge.

A combination of this extension of the lower cone and a decrease of friction between the material and wall would eventually improve the silo discharge mode, and permit an increase of the hopper half angle. Also, to ensure that such improvements are effective, a proper ratio between the maximum diameter of the insert and the diameter of the silo is very important.

4.4 Experimental investigations

The experiments described here are confined to studies of the double cone insert, and the purpose of these experiments was twofold: 1) to investigate experimentally the effect of a double cone on flow ; and 2) to seek some validation of the numerical results of the above calculations.

4.4.1 Previous relevant test results

The inserts investigated at POSTEC (Enstad, 1996, 1997) consisted of a cone-in-cone, an inverted cone and a double cone insert. These have been investigated extensively for flow promotion, mostly in an axi-symmetrical model silo, but also in a plane symmetrical model silo. The geometries of the axi-symmetrical silo were adopted in the numerical model at Section 4.3. The stored solids used were a cohesive hydrated lime powder and a free flowing PVC powder. Measured using the Jenike method, the lime had an effective internal friction angle of 32.8° and a wall friction angle against the silo wall of 25°. The PVC powder had an effective internal friction angle of 32.9° and a wall friction angle of 21.8°. These parameters have a critical influence on the silo discharge flow pattern, and these values were used in the numerical models described earlier.

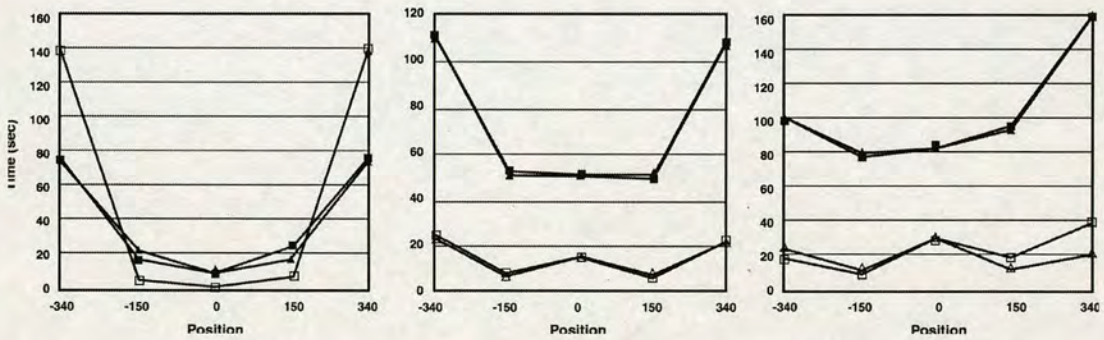

(a) Silo discharging without insert

(b) Silo discharging with an inverted cone

(c) Silo discharging with a double cone insert

Fig. 4.16 Experimental observations of the effect of an insert on silo discharge time, as shown by markers seeded at different levels (Enstad, 1996, 1997)

The results from these tests (Enstad, 1996, 1997) provide some important clues to good decisions on the insert geometry, such as the height of the cone, its diameter and angles, and its relative position in the hopper. For example, for the inverted cone, the best

results were obtained when the insert cone angle was 17.5° to the vertical and its base was 240 mm below the silo transition. One of these test results is shown in Fig. 4.16 (b), which indicated that there was flow against the wall from the start of the discharging process, and that the material around the transition zone was discharged quite evenly. Similarly with the double cone, mass flow was obtained when the cone half angle was 17.5° in the upper cone and 20° in the lower cone, with its maximum diameter at 200 mm and with that maximum diameter placed 195 mm below the silo transition.

But these tests also showed that it was still very difficult to attain symmetrical flow with free flowing powder when a double cone insert was used. The flow resembled mass flow but was rather skewed (Fig. 4.16 (c)). Mass flow was close to being obtained only when the base of the double-cone was placed 195 mm below the silo transition level.

It was also discovered that a cause of the skewed pattern noted above was that the insert had not been very carefully centred in the tests. To avoid a skewed discharge, it is clearly very important that the double cone is accurately centred.

From the above outline of the previous test results, it is clear that a cone insert can provide a valuable method of achieving mass flow in a silo that might otherwise exhibit funnel flow.

4.4.2 Investigations into the effects of a double cone on flow in a small scale silo

4.4.2.1 Experimental set-up and the solid used

The experimental set up used in the present test series is shown schematically in Fig. 4.17. It consisted of the experimental silo, a belt feeder, a screen and a collecting bag. The stored solid was fed into the silo from a container carried by a crane; so the container and the crane could be regarded as external parts of the set up. The belt feeder was used to control the discharge rate when necessary. The screen was used to filter the markers out from the discharged solid. The bag collected the solid which was carried away by a folklift.

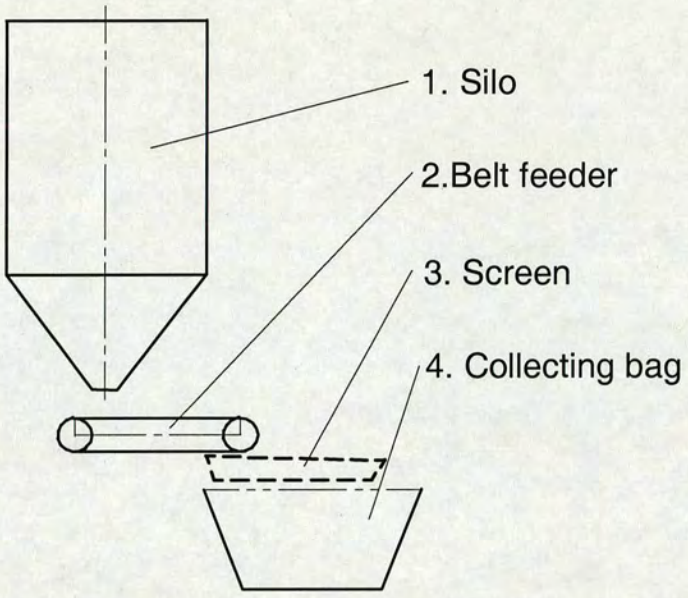

Fig. 4.17 Schematic diagram of the experimental arrangement

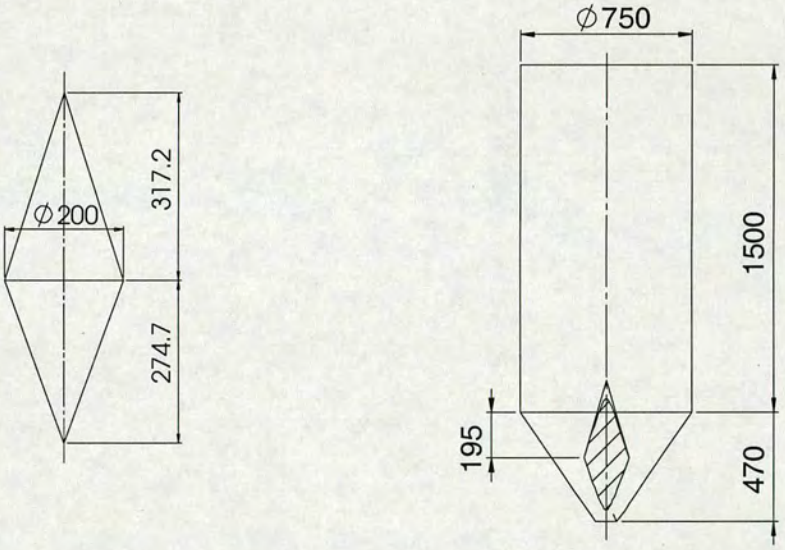

Fig. 4.18 The double cone insert and configuration with silo

The small scale experimental model silo had the dimensions shown in Fig. 4.4. The insert was a double cone insert; its dimensions are shown as in Fig. 4.18. The lower cone was extended vertically as a result of the numerical predictions described above. It was accurately placed axially in the silo using a centring tool. From the indications given by the numerical model and the previous experimental results, the insert was

placed with its base 195 mm below the silo transition, with the bottom apex reaching to the level of outlet (Fig. 4.18).

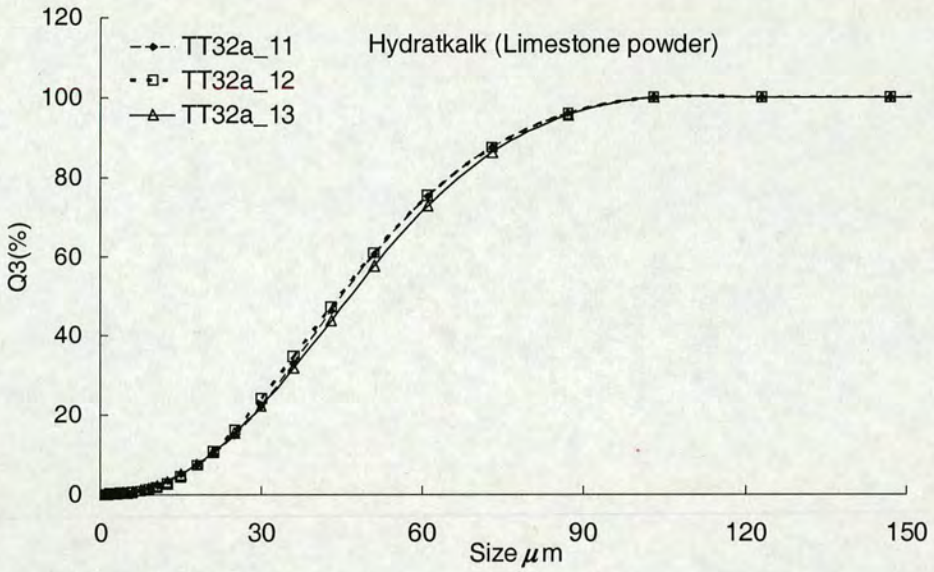

Fig. 4.19 Particle size distribution

The stored solid used was a limestone powder with the particle size distribution shown in Fig. 4.19. Its bulk density was 606 kg/m^3. As measured by a Jenike Cell, this limestone powder had an effective internal friction angle of 32.8° and a wall friction angle against the silo wall of 25°. These values are quite close to those adopted in numerical predictions.

4.4.2.2 Testing procedures

The tests were originally designed to investigate the effect the double cone insert on the material flow pattern. To ensure that the effect of the insert was properly understood, it was necessary to begin the investigations with measurements without an insert.

Discharge was investigated under conditions where it was either a free discharge or a discharge controlled by the feeder. The solid was discharged after being stored for either 1 hour or 24 hours. After these tests, the double cone insert was put into position as shown in Fig. 4.18, and a similar set of tests were carried out.

Table 4.2 Conditions of different experiments

	1 hour	24 hour	1 hour	24 hour
Without insert	Free discharge		Controlled discharge	
With insert				

The arrangements for the experiments are listed in Table 4.2: different measurements were made according to the presence or absence of the insert or the feeder:

- free discharge with no insert,

- controlled discharge with no insert,

- controlled discharge with the insert,

- free discharge with the insert.

At least two tests were performed under each condition.

4.4.2.3 Observations and results

Flow phenomena were observed both from the top and the bottom of the silo. The flow pattern of the solid was measured using tracers seeded at the transition level during filling. The tracers were placed as described below.

4.4.2.3.1 Filling of the material

With the outlet closed, the solid was filled into the silo from the top. The silo was filled to a level 300 mm below the top edge of the cylinder. The solid formed a flat surface. It settled down by about 170 mm in the first half hour. After that, the surface remained at almost the same level. This indicated that in the as-filled condition, the solid contained a lot of entrained air, which was expelled under gravity.

4.4.2.3.2 Observations from the top during discharge

4.4.2.3.2.1 Free discharge with no insert

Following the scheme as shown in Table 4.2, the tests were first carried out to observe the material behaviour under free discharge conditions without a feeder or insert.

When the outlet was opened, a little help (in the form of external shocks) was needed to start the discharge. Once initiated, some of the material discharged by gravity alone. The flow pattern after 1 hour of storage was different from that after 24 hours of storage.

In the tests after one hour of storage, it was seen from above that the material started to drop in the middle, but remained stationary in the region close to the wall. The flow pattern could be described as funnel flow from the very beginning. As discharge proceeded, the material slipped or even collapsed into the middle from the edge. When the level dropped to between 500 mm to 800 mm above the transition level, a rathole was formed, and the discharge stopped (Fig. 4.20).

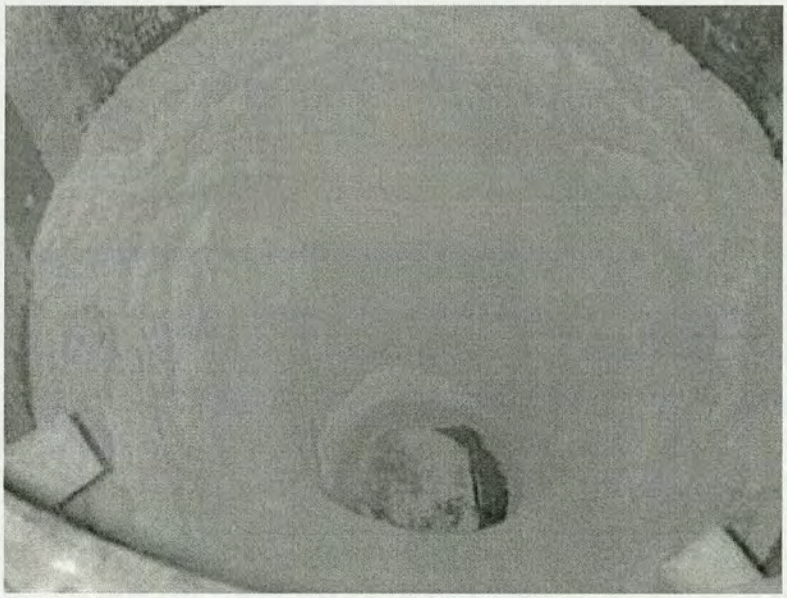

Fig. 4.20 A well developed rathole ended the discharge process (one hour storage)

In the tests after 24 hour of storage, it was seen from the top that the whole surface of material started to drop, material started to discharge in what looked from above like mass flow. This movement continued until the surface was around 300 mm above the transition, when the material close to the wall stopped moving, whilst that in the middle continued to drop. The stored solid formed a falling slope dip but no slips or collapses of the material were seen. A rathole was formed at the transition level. It was

similar to an intermediate flow. In the case for both storage periods, once a rathole had formed, the process of discharge ended.

The limestone used in the tests entrained a lot of air. The air was mostly expelled in the first half hour after filling into the silo. The limestone underwent consolidation under storages. Its properties must have changed considerably from a one-hour storage to a 24-hour storage. The change of its properties would cause the difference of discharge pattern.

4.4.2.3.2.2 Discharge with feeder but no insert

The tests using the belt feeder showed that the material discharge patterns were quite similar to those without a feeder for both storage durations. However, some small differences were observed: when the feeder was used, the movement of the surface was not as even as that without a feeder. A small slope was formed on the surface, indicating that the material was probably not discharged as evenly as that with a free discharge.

4.4.2.3.2.3 Discharge with insert

After the insert was installed, the flow patterns were observed to be different from those without an insert. The solid could be discharged completely and continuously without interruption.

After the insert had been fitted, the view from above showed that, in all cases, the solid in the parallel part dropped downwards as a plug, step by step with a pulse-like motion, until the top surface reached the transition level . Below that level, the material in the centre moved faster than that close to the wall. As a result, a dip began to form, the material near the wall fell or slid towards the centre, while at the same time it kept on sliding down the walls of the hopper. Sometimes, the material at one side dropped faster, leading to some asymmetry. This occurred even when material continued sliding at the other side. In the end and in most cases, the material was all discharged fairly evenly and the silo was completely emptied.

4.4.2.3.3 Observations from the bottom during discharge

It was hard to make observations from the outlet when a feeder was used beneath the silo. But when the feeder was moved away, some observations were made.

When there was no insert, it could be seen that the material dropped piece by piece, braking down block by block, forming and enlarging a semi-spherical arch upwards. This arch moved higher and higher in the hopper, and when it had grown large enough, the material in the hopper dropped suddenly downwards to fill the vacant space where the spherical arch had been. When there was an insert, the material dropped more or less similarly but the size of the pieces or blocks were smaller, and the height or the size of the semi-spherical arch was lower and smaller than those formed when there was no insert. With the insert present, the material discharged in this way during most of the discharge time, more continuously and smoothly, but it was still interrupted with some pulses caused by large chunks of the material being suddenly broken and some local collapses of solid.

4.4.2.4 Measurements of tracer residence time

4.4.2.4.1 Arrangement of tracers

It is impossible to observe the flow pattern inside a silo directly, since the solid is opaque. Tracers were used to monitor whether there were any dead zones inside the silo. The tracers used were spherical wooden balls. They were coloured and numbered, and were placed in two circles as shown in Fig. 4.21 on a level surface at the transition level. The ball in the centre was however placed 340 mm higher than the others, to avoid contact with the insert. It was assumed that the tracers would follow the movement of the material adjacent to them during the discharge.

The density of the wooden was 680 kg/ m^3, the limestone density was 606 kg/ m^3. It was therefore regarded that there would no relative movement between the wood tracers and limestone during discharge, i.e. , the tracer wood's movement reflected the limestone movement (Enstad, 1996, 1997).

4.4.2.4.2 Measurement results

It was expected that the markers would all be discharged with the stored solid. When they came through the outlet, the powder passed through a screen, but the markers

were retained on the screen and so separated from the powder. The sequence and the time for each marker to come out were noted down as in Table 4.3.

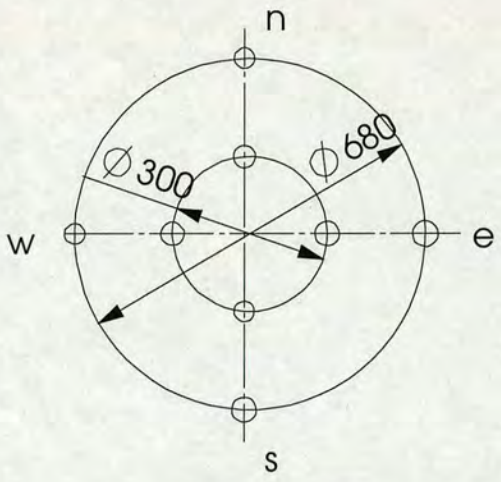

Fig. 4.21 Tracers seeded around two rings at the transition level

In the table, the initial location of each marker was identified by the radius of the ring and the orientation as indicated in Fig. 4.21. The measured residence times are shown for the two conditions: no insert and the double cone insert. In each group, the residence times were classified further according to the storage times (one hour and 24 hours) and for the outlet conditions (with belt feeder and without belt feeder). As seen in the visual observations, when there was no insert a rathole formed during discharge and the markers seeded in the larger ring did not come out. As a result, no times were recorded for those markers. The complete duration of each experiment (T1) was used to note the relative times of discharge of markers, which are entered in the table at the corresponding positions. The complete duration T1 was defined as the time from the beginning of discharge to the termination of discharge when no insert was used: the termination occurred at the moment when the rathole was formed. The complete duration T2 was defined as the whole period of the discharge for the cases where there was an insert: all the solid had emerged.

The measured time noted in Table 4.3 is the real time that each marker took to travel from its starting position to the screen where it was separated from the powder. Naturally, the distance travelled by each marker was different for the markers in the centre, the markers in the ring close to the wall and the markers in the intermediate ring. To interpret the times in a better manner, these times were modified as follows.

Table 4.3 The locations of seeded tracers and the time measured for each tracer to reach the exit

Orientation	n-s	w-e	n-s	w-e	n-s	w-e	n-s	w-e
	with a double cone insert				no insert			
	Prior storage time							
	24 hours		one hour		24 hours		one hour	
	Travel time in seconds (no feeder)							
-340	220	238	180	184			480	480
-150	200	180	99	73			203	200
0	380		310				340	
150	182	195	99	74			100	114
340	240	307	140	150			280	480
	Travel time in seconds (with a belt feeder)							
-340	192	217	420	440	540	540	540	540
-150	155	156	180	180	168	169	120	123
0	525		720		236		146	
150	183	180	330	315	189	200	128	125
340	202	242	290	360	540	540	540	540
	Travel time in second (With a belt feeder)							
-340	172	170	190	220				
-150	92	100	112	112				
0	523		352					
150	105	110	120	140				
340	183	220	200	230				

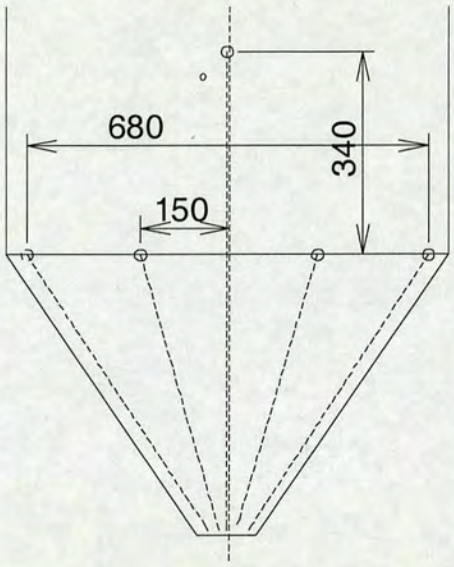

Fig. 4.22 Assumed tracer paths

It was assumed that each marker followed a path as shown in Fig. 4.22. The length of each path was characterised in terms of a time for each marker to travel this distance from its own starting point. The converted times were then divided by the full discharge times T1 and T2 for the situations without insert and with insert respectively. The results after such modifications are shown in Fig. 4.23 and Fig. 4.24 (a and b).

It should be noted that because the marker in the centre lagged far behind the other markers when an insert was present, the modified times were not used in Fig. 4.24; instead, the average value of the two adjacent neighbours on the same line were entered in Table 4.3. The fact that the tracers above the insert came out far behind the others indicated that the material in a certain zone above the insert might move much slower than the rest of material.

It is thought that the results in Figs. 4.23 and 4.24 reflect the relative relationship of movements of the markers at the transition level, so they were used to judge the evenness of the movement of the solid.

With no insert present, Fig. 23 has some blank spaces because the markers in the larger ring did not come out at all when the storage time was either 1 hour or 24 hours. This is a clear indication of the development of the ratholes as observed.

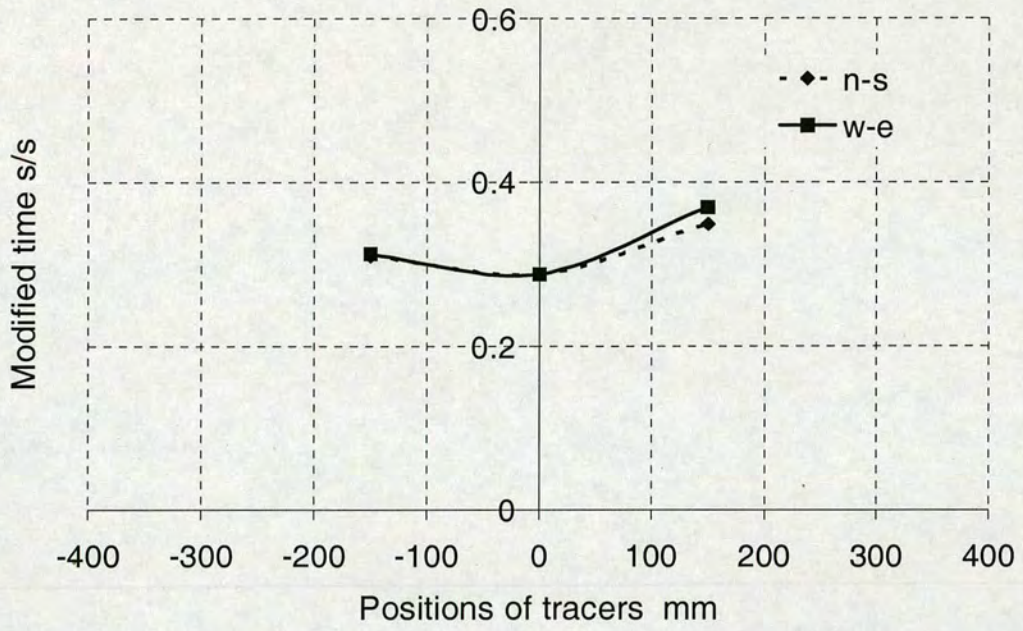

(a) Material left in silo for 24 Hours, discharged with feeder.

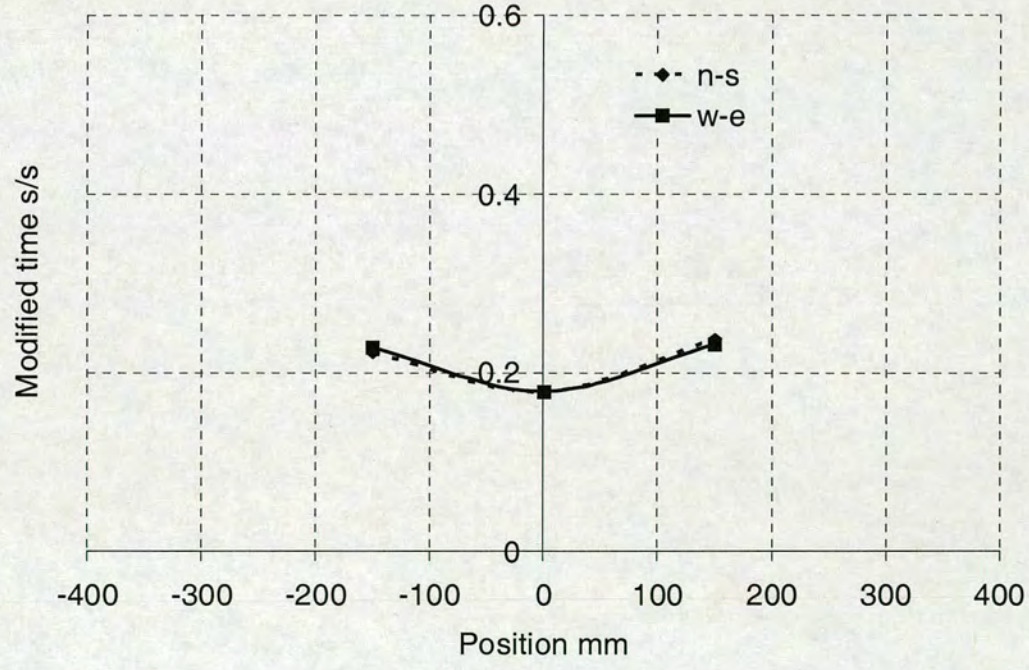

(b) Material left in silo for 1 hour, discharged with feeder.

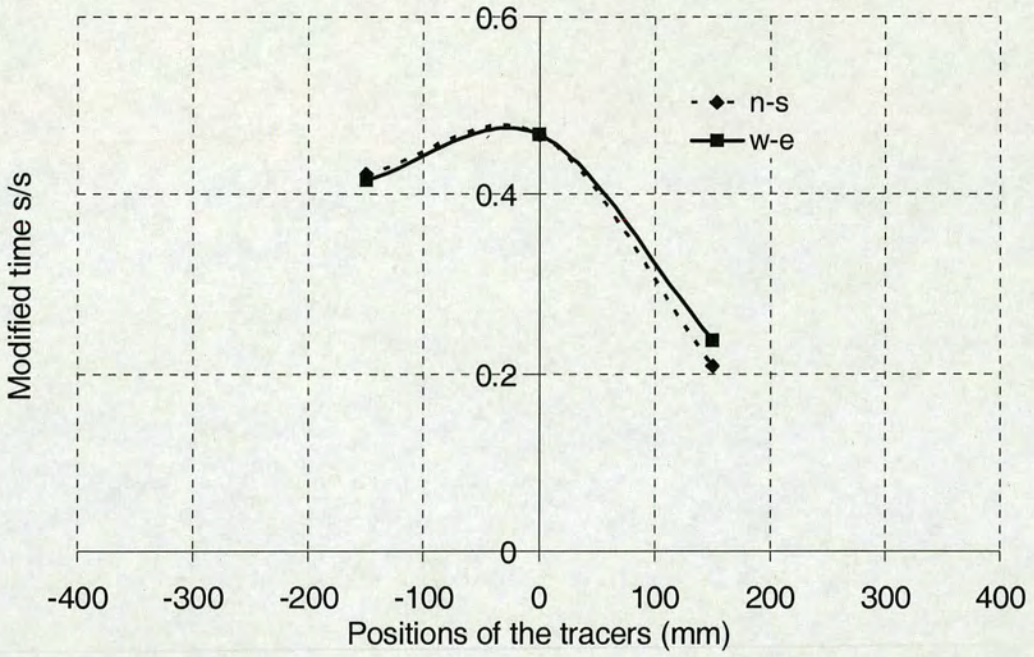

(c) Material left in silo for 1 hour, discharged without feeder.

Fig. 4.23 Tracer discharge times: no insert (expressed as the ratio of the time an individual tracer took to the whole duration of the discharge operation)

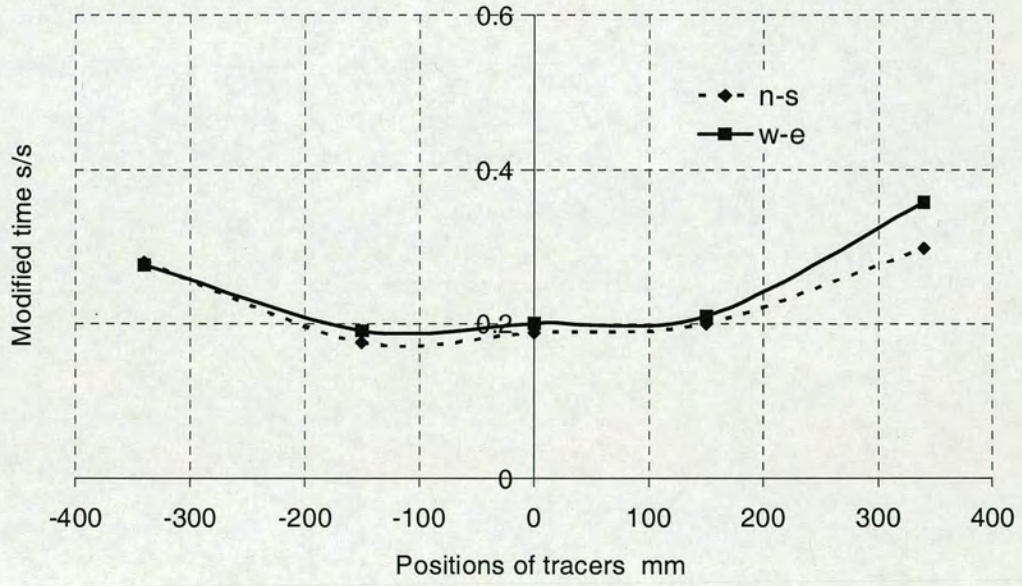

(a) With feeder

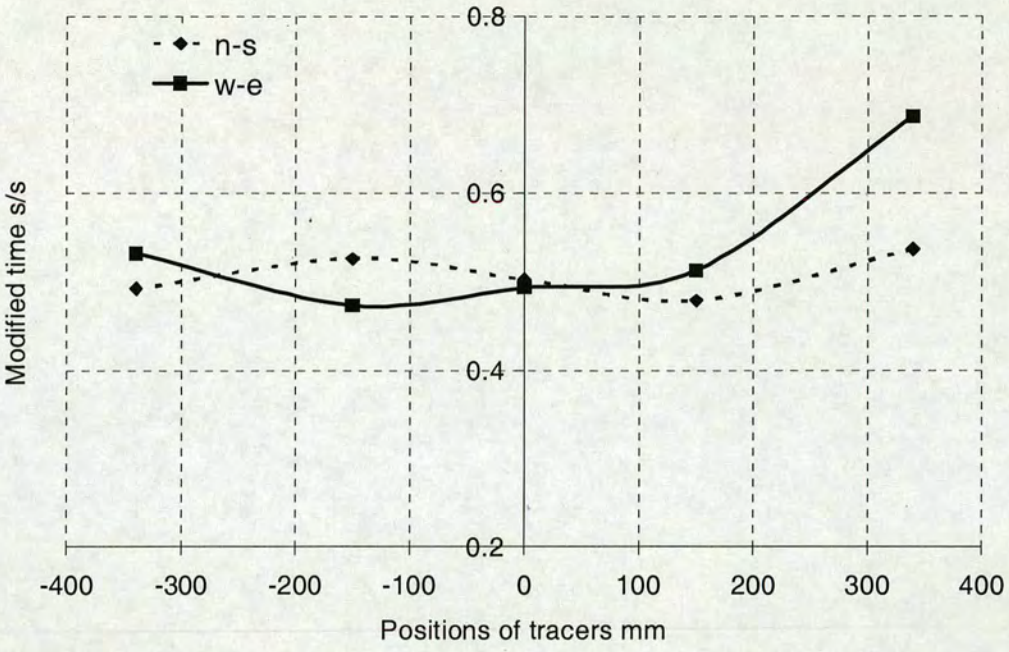

(b)Without feeder

Fig. 4.24 (a) Tracer discharge times: double cone insert, 24 hour prior storage (expressed as the ratio of the time an individual tracer took to the whole duration of the discharge operation)

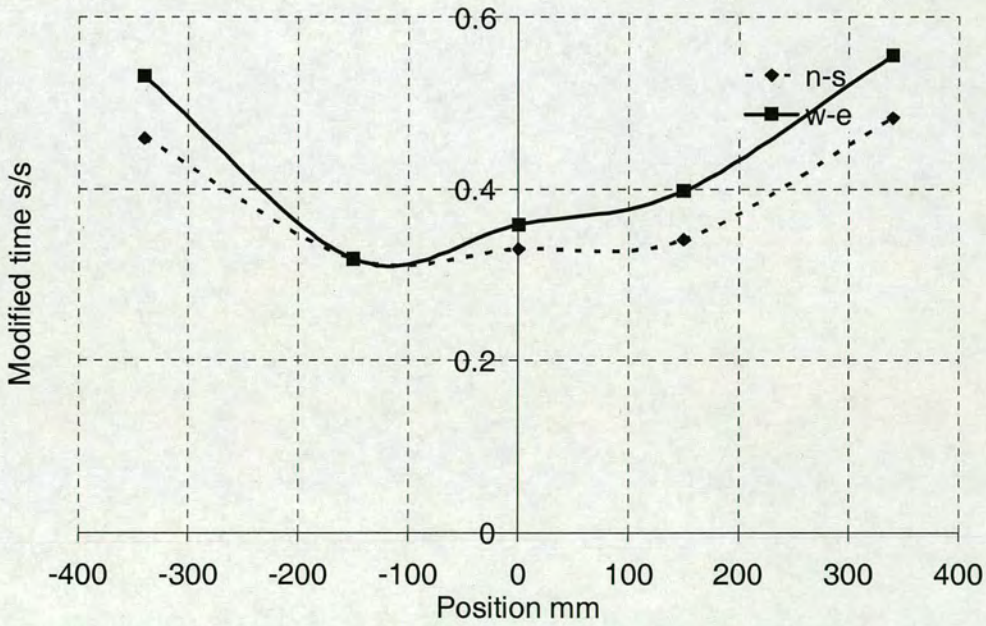

a.) With feeder (first test)

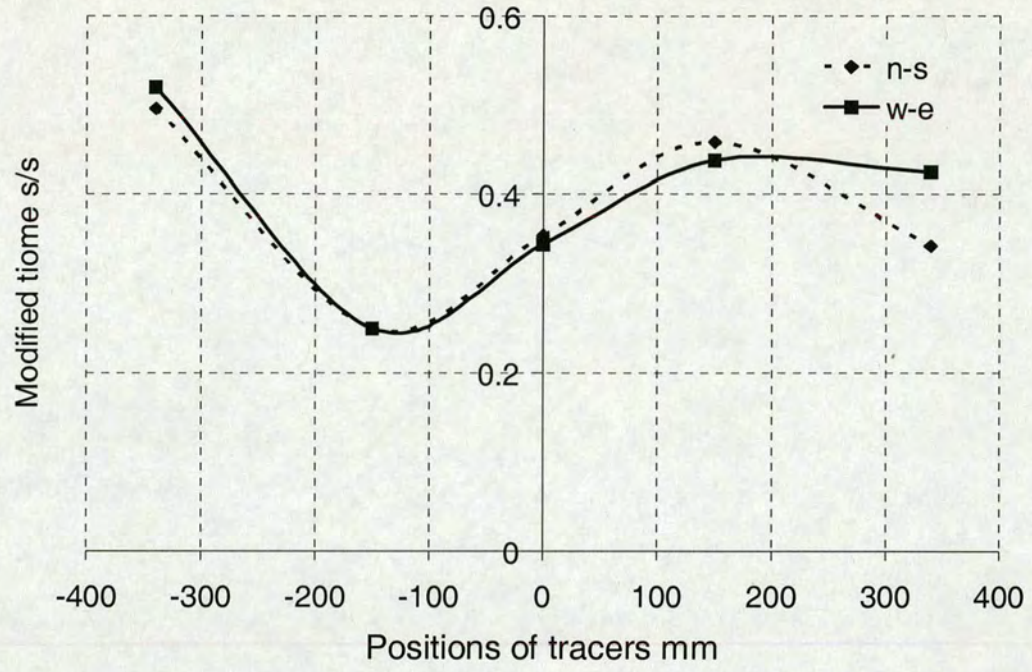

b) With feeder (second test)

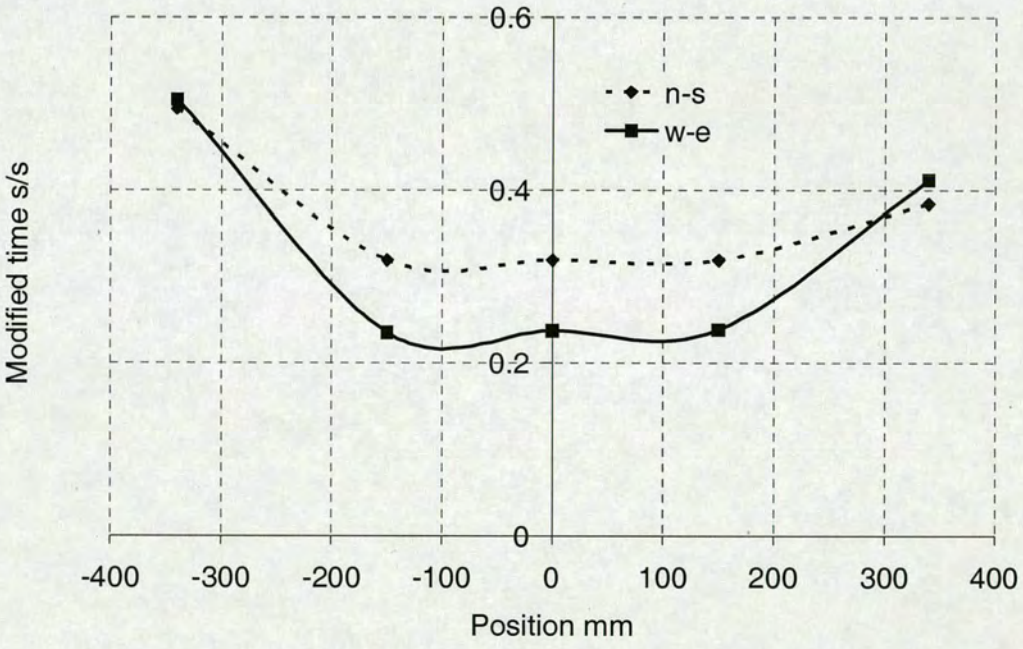

c) Without feeder

Fig. 4.24(b) Tracer discharge times: double cone insert, 1 hour prior storage (expressed as the ratio of the time an individual tracer took to the whole duration of the discharge operation)

It is a clear indication of funnel flow, in line with the existence of the ratholes as observed. One may notice also that in this funnel discharge the flow pattern could be skewed severely, and the application of a feeder did help to reduce it.

Figure 4.24 shows the measurements when the double cone insert was installed. Figure 4.24 (a) shows the results measured after a 24 hour storage; and Fig. 4.24 (b) those after a one hour storage. All markers came out under both conditions. Comparing the results in Fig. 4.24 (a) with those in Fig. 4.24 (b), it appears that the material moved more evenly after a 24 hour storage than after a one hour storage.

4.5 Closing remarks

The program SILO predicted that the flow mode in a silo with a hopper half angle of 34.7° (inclination to the vertical) to be funnel flow, and indicated the presence of a stagnant zone during discharge. Observations from the top and measurements of material movement by tracers in experiments demonstrated that the flow mode was indeed of this kind. Moreover, the items that were able to be observed were largely in agreement with the predictions from the computer program. However, there are a number of questions that are not able to be addressed by the comparison, which may be outlined as follows.

First, it was seen in the tests on solid that had been left in the silo for an hour that there had been funnel flow from the beginning. By contrast, after the material had been left there for 24 hours, the flow appeared to be more like mass flow before changing into funnel flow at the end. The tests also showed that the flow mode was more stable if the material was left in storage for a longer period. Since only a single set of material properties was used in the program SILO, such differences could not predicted: further work would be required to determine what changes in the material parameters might be appropriate to represent the change in storage time.

The same may be said of the size and shape of the ratholes that formed at the end of discharge: these were different for a 1 hour storage and a 24 hour storage. The program only predicted the initial flow of the solid, so the formation of a rathole was not explored using it.

It is not possible to know whether there was good agreement between the experiments and the predictions of the program on velocity fields early in the discharge, since this data cannot be obtained from the experiments. Thus, whether there was a stagnant zone early in the discharge, as indicated by the program, cannot be deduced in the tests, even from the marker observations, since it cannot be known whether markers moved uniformly towards the outlet, or remained stationary for a period before moving to the outlet.

The program SILO did predict that this silo would be converted to a mass flow silo by the installation of a double cone insert, and this appears to have been in agreement with the experimental results, though it cannot really be known if mass flow occurred in the test (the top surface may move down uniformly in semi-mass or mixed flow).

Both the computer predictions and the experiments confirmed that the double cone insert improved the silo discharge mode.

The program SILO has the power to provide predictions concerning the silo discharge mode under different conditions, which may be a valuable guide in situations where complex geometry is involved and the classic methods cannot be applied. Possible methods of improving the silo discharge flow pattern by means of inserts or similar devices can be explored using it. It could also be used to modify the insert itself for optimum effects. Simulations conducted showed some such results as summarised already in section 4.3.5. However, at present, the predictions of the program cannot be said to be verified in this project in more than a qualitative sense.

Finally, since the model used in SILO is axisymmetric, it cannot address issues of the loss of symmetry in flow pattern which was observed during the measurements. Conditions of asymmetry in the flow and pressures occurring in an axisymmetric silo in the presence or absence of an insert is investigated in the next chapter.

5 THE EFFECT OF A DOUBLE CONE INSERT ON SOLIDS FLOW AND LOADS IN A FULL SCALE SILO

5.1 Introduction

A silo is normally designed to mass flow if circumstance permits. Otherwise, flow promotion devices such as inserts are sometimes used to improve the flow pattern (e.g. to convert a funnel flow into a mass flow silo). There is concern about how the application of an insert affects the loads on the silo and hopper walls.

As reviewed in Chapter 2, the original purpose of the installation of an insert in a silo was for blending material and reducing segregation through its influence on flow. Studies were carried out also to investigate the possibility of changing a funnel flow silo into a mass flow silo with the aid of inserts, as demonstrated in the previous chapter. The influence of an insert on the silo wall pressures has also been investigated to some degree. This will be discussed further in this chapter.

This Chapter describes numerical and experimental investigations into the effects of inserts on the wall loads in a full scale silo. The numerical simulations to study the effect of an insert on flow in the full scale silo were performed using the ABAQUS finite element code. The full scale experiments were conducted to overcome scale effects which had been identified as significant in earlier investigations. The high costs required to set up and run the full scale test facility were funded by the Research Council of Norway (NFR: Norges Forskningsråd).

5.2 Finite element investigation into solids flow and wall pressures in a full scale silo

Many attempts have been made recently to model computationally the behaviour of granular stored solid in a silo. One of the most commonly used methods has been the

finite element method. The advances thus far established by this method have been substantial (Rombach, 1998; Rotter, 1998).

The limitations of the method have also been highlighted (Rotter, 1998; Rotter et al, 1998). For instance, a finite element analysis is unable to explore the behaviour of stored solid that occur at a scale of individual particles. One common difficulty encountered in a process such as silo discharging is how to represent the mesh being distorted massively by large deformations, and an abrupt change of direction at the transition from cylinder section to hopper section (Ooi and Rotter, 1990; Ragneau et al. 1998).

In this section, a description is given of an attempt to computationally model the discharging process for a silo, and to tackle the difficulties caused by the large deformations and abrupt direction changes in a silo. The flow modes were investigated. Predictions of the loads exerted on the walls were also made.

5.2.1 Investigation into flow in a silo using ABAQUS

5.2.1.1 Silo geometry and its content

Two axisymmetrical silos were modelled. Both had the same cylindrical section: one had a steep hopper, whilst the other had a shallow hopper. A double cone insert was introduced in the shallower hopper.

The cylinder was 6 m in height and 2.5 m in diameter, its wall was 6 mm in thickness. The steep hopper had a hopper half angle of 15°, with a height of 3.94 m and an outlet 0.41 m in diameter (Fig. 5.1-a); its wall was 6 mm in thickness. The shallow hopper had a hopper half angle of 35°, with a height of 1.50 m and an outlet 0.41 m in diameter (Fig. 5.1-b); its wall thickness was also 6 mm. In this shallow silo, a double cone insert was installed as shown in Fig. 5.1-c, centred on the axis of the silo. The dimensions of this insert are also shown. The stored solid was filled to a height 2 m below the top of the silo, with a surcharge of a 25° conical heap on top.

5.2.1.2 Finite element modelling

In the finite element model:

1) rigid elements were used to represent the insert;

2) axi-symmetrical shell elements were used to represent the wall; and

3) the granular stored solid was treated as solid elements using continuum axi-symmetrical elements.

The silo wall was fixed at its transition level between the hopper and the cylinder section, and constrained horizontally at its top. The loading on the granular stored solid was due to gravity, but the wall of the silo was assumed to be weightless.

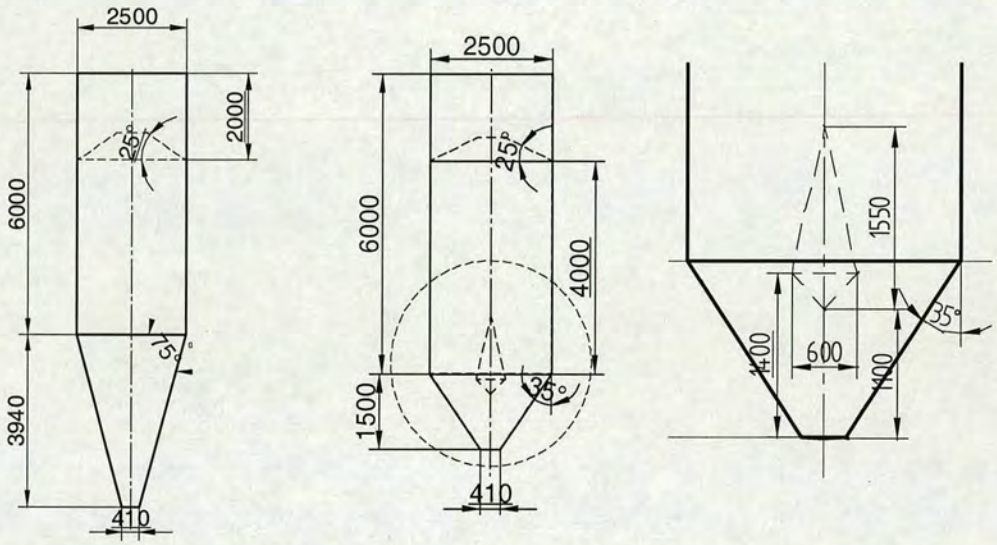

(a) Silo with steep hopper

(b) Silo with shallow hopper

(c) Double cone insert

Fig. 5.1 Configurations of silo and double-cone insert

In the model, the silo wall was assumed to be made of steel and modelled as an elastic stored solid, with a Young's modulus $E_w = 2 \times 10^{11}$ Pa and Poisson's ratio $\nu_w = 0.25$. Granular material is known to display rather complicated behaviour. This study utilised the elastic-plastic model with of Mohr-Coulomb limitation was.

The interaction between the stored solid and the silo walls was modelled as a simple Coulomb interface, as used in earlier studies in Chapter 3. The same treatment was used to model the contact between the stored solid and the insert surfaces. A constant friction coefficient was chosen as $\mu = 0.3$, and implemented in the model.

5.2.1.3 Lagrangian-Eulerian approach

In the discharging process, the amount of stored solid left inside the silo decreases; as a result, the boundaries of the stored solid body are changing. In this study, the Lagrangian-Eulerian formulation approach in Abaqus was used to model this process. At the outlet, the stored solid is discharged either freely or in a controlled way by prescribing a fixed geometry to the outlet boundary that could be given a forced displacement; an Eulerian approach is better suited here. In other regions, the boundaries are moving with the discharge and a Lagrangian approach is more appropriate (Abaqus, 2002, 2003).

In the finite element simulation, an adaptive mesh was used for the stored solid domain. At the boundary to the silo outlet, a zero movement of the adaptive mesh constraint and an Eulerian surface region were applied. By doing so, the element mesh at the outlet was fixed. A Lagrangian region type was applied to the other boundaries in order to ensure that the rest of the element mesh follows the movement of the stored solid. The finite element mesh is shown in Fig. 5.2. The application of the adaptive mesh proved to be an effective technique to deal with the difficulty of the mesh distortion caused by the large deformation in the process of discharging in the regions near the outlet and at transition.

5.2.1.4 Convergence and determination of parameter

For a finite element analysis, it is important to check the convergence of the solution. In the present study, the issues that may affect convergence include mesh design, contact definition and the large deformation undergone during discharge.

Both coarser meshes and finer meshes have been tested. In an attempt to improve the mesh, partition was used to devise finer mesh in key regions near the outlet and around the transition. The abrupt geometry change from the cylinder to the hopper at the transition presents a serious numerical problem and leads to a mathematical singularity (Ooi and Rotter, 1990; Ragneau et al. 1998). A smoothing technique was therefore conducted to avoid any sharp corners. The silo transition was curved into a smoothed curvature (filleting) with radii of 0.5 m and 1 m for two different operations, and a

0.1m radius was used at the corner of the insert base. An example of the mesh around these smoothed corners is shown in Fig. 5.2.

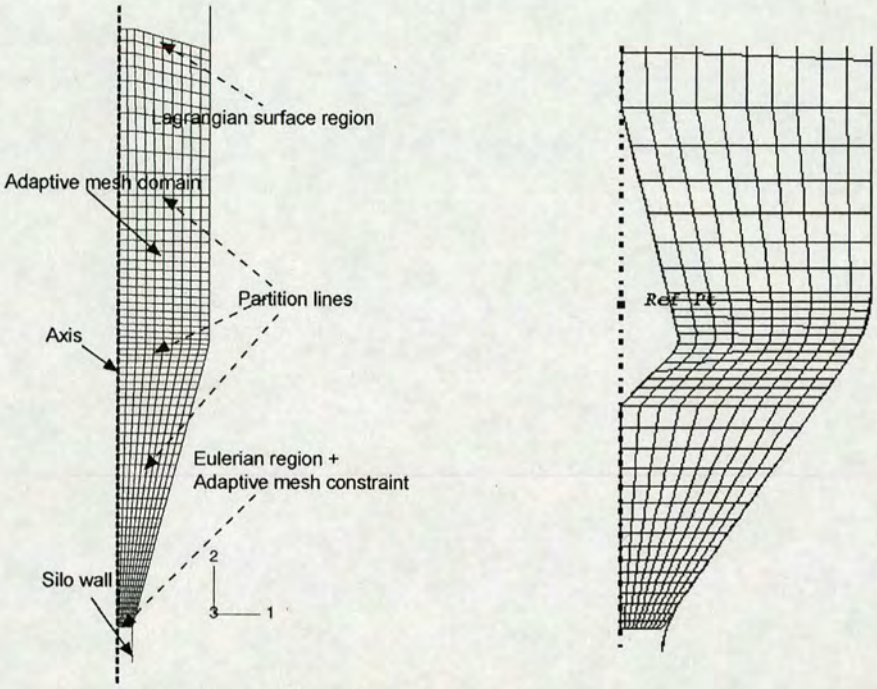

(a) Lagrangian-Eulerian approach

(b) Filleting applied to areas with abrupt changes in geometry

Fig. 5.2 Finite element mesh

The interaction between wall and stored solid was defined using Coulomb friction occurring along the contacting surfaces of elements. The implementation of contact model was rather complicated. At first, the default kinematic method of frictional constraint was imposed. This resulted in many warnings being issued with the running of the program interrupted right at the beginning. This problem was overcome by changing the kinematic method of frictional constraint to the penalty method restraint as described in Abaqus for different contact modelling (2002, 2003).

The deformation of the stored solid naturally depends on the chosen parameters for the stored solid. The gravity loading (defined through the mass density) in combination with the material Young's modulus E_w, Poisson's ratio and its internal friction, makes the stored solid deform. The deformation may have some effect on the numerical convergence.

In this investigation, the material parameters were based on the Mohr-Coulomb (M-C) model for a granular solid. They were: the stored solid internal friction angle φ, and its friction angle with the wall ϕ, set as 30°and 18° respectively. The Young's modulus E_p was taken from references for granular solid, and specified later, and the Poisson ratio ν_p was assumed to be 0.33.

Convergence tests were carried out using a density of ρ = 1000 kg/ m^3 for the particulate solid. Convergence was achieved when the Young's modulus E_p was higher than 7.0×10^5 Pa in a preliminary simulation where the material was assumed as elastic-plasticity model with a M-C criterion. In the further tests with the same material but with the kinematic hardening limitation (a used-defined model for material which is described in Abaqus 2003), the Young's modulus could be as low as 4.3×10^5 Pa. The other parameters had little effect on the convergence.

Among the investigations carried out and reported hereafter, the results were based on those from the finer meshes (in Fig. 5.2). The parameters used were: stored solid density ρ = 1000 kg/m^3, Young's modulus E_p= 10^6 Pa ; Poisson ratio ν_p = 0.3; the stored solid internal friction angle φ = 30° and the wall friction angle ϕ = 18°.

5.2.1.5 Discharging flow pattern

Using a Lagrangian-Eulerian approach to simulate silo discharge, one issue was to prescribe an initial condition for the stored solid state of stress during storage. As described in Chapter 4, attempts to import the stress distribution developed at the end of filling were not successful. A straightforward initial condition was prescribed instead in the present analysis: the stresses calculated from the theoretical formula for the silo active state of stress, was applied directly to the solids, i.e. a zero stress was defined along the top surface, the calculated stress values (refer to Appendix 1) were defined along the outlet for the steep silo and shallow silo respectively, and a stress field with a linear distribution of the values applied along the top surface and outlet were prescribed for the solids in between. Admittedly, this is not a good prescription, and problems are to be expected.

With adaptive meshes, the movement and deformation of the mesh did not by definition represent the stored solid's movement any longer. Tracers were seeded along the partition lines to monitor the stored solid movement. Since tracers require significant computational effort, only limited numbers were used (Abaqus, 2002, 2003).

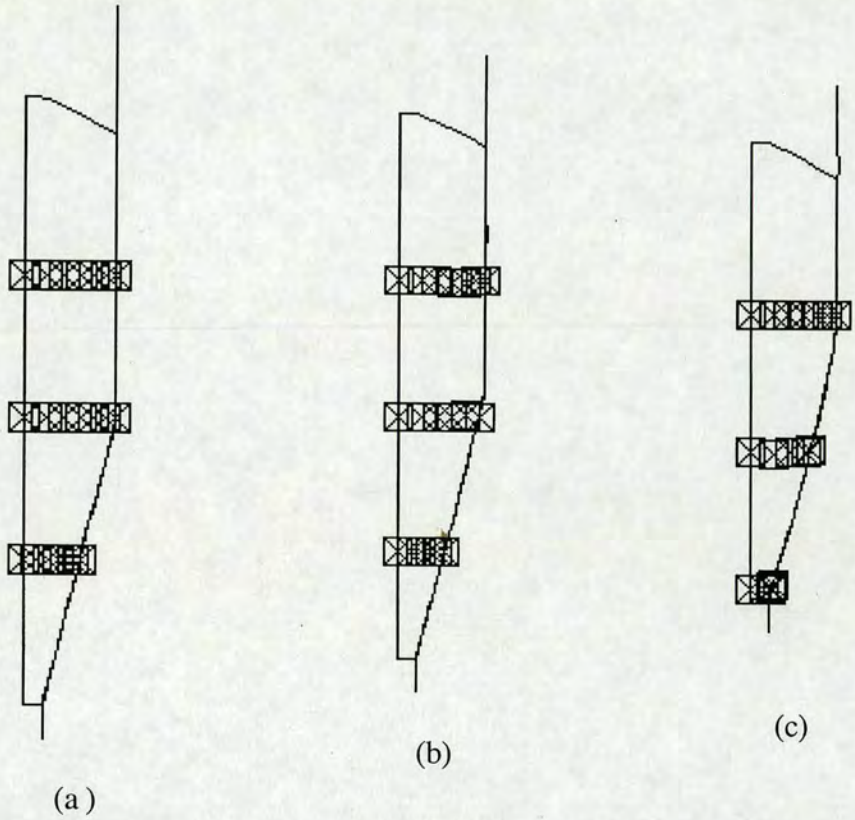

Fig. 5.3 Movement of tracers at different stages of discharge in silo with a steep hopper (a) at the beginning; (b) in middle stage; (c) at the last stage

A gravity discharge process was simulated. Several simulations were carried out. The stored solid model first implemented was the elastic-plastic M-C model. Satisfactory results were achieved for the steep silo as shown in Fig. 5.3 for the movement of the tracers. The tracer in the hopper moved faster than those in the cylinder; the traces closer to the centre moved faster than those closer to the walls of the hopper, while the tracers moved with the same speed when they were in the cylinder. Different wall frictional coefficient values were used, but they produced no difference to the flow patterns. The tracer movements indicated that mass flow was achieved.

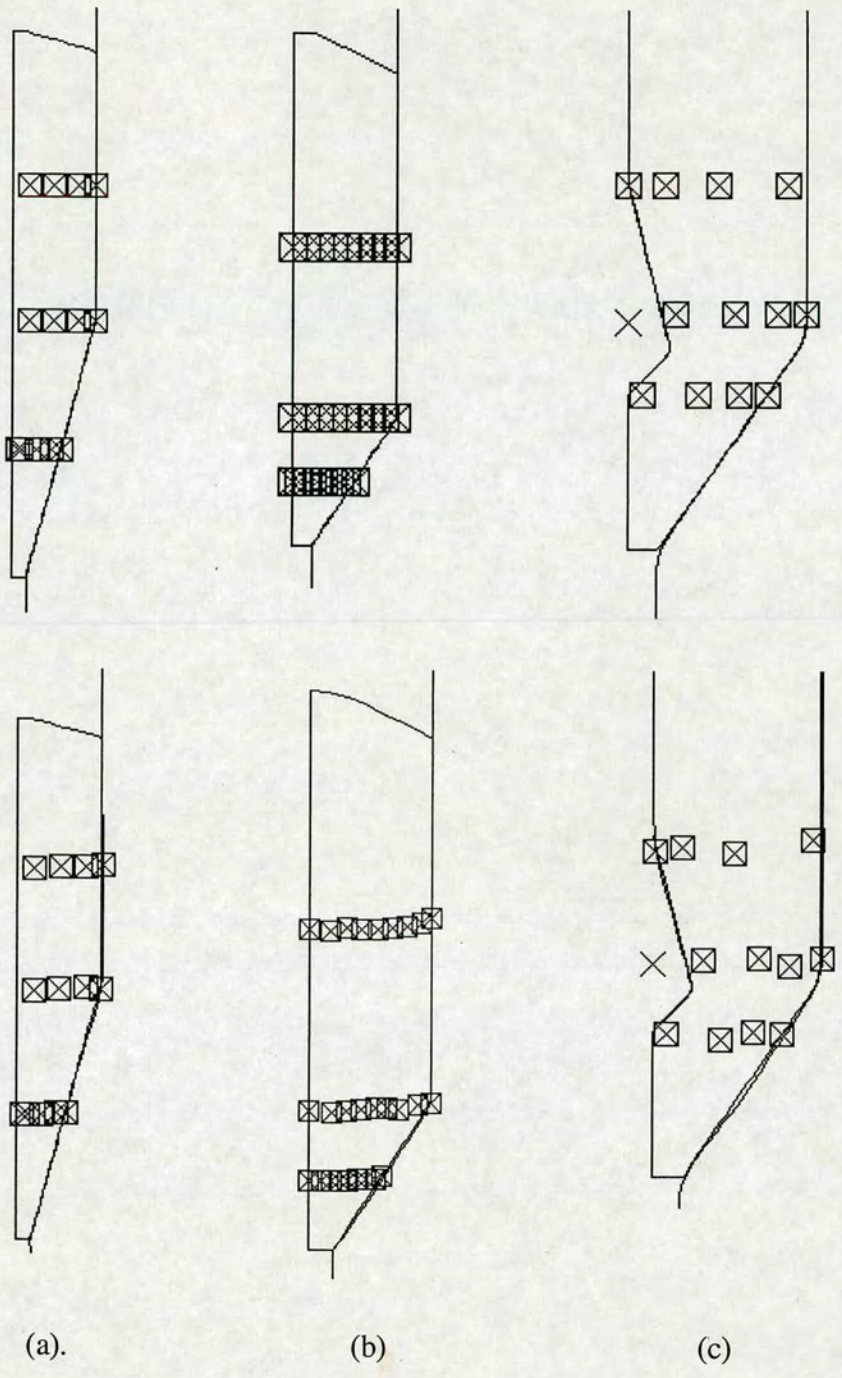

Fig. 5.4 Movement of tracers at the beginning of discharge (upper) and at different stages in the simulation (lower) for different silo geometries (wall friction at 0.6 for all cases)

The tracer movements in the shallower hopper (with or without insert) were however not very realistic in similar attempts, some tracers even moved upwards. Further simulations were then carried out after implementing the elastic-plastic model with kinematic hardening. Some of the results are shown in Fig. 5.4 for the tracers'

movement in both silos, and the shallow silo with an insert. Similar results as described above were achieved for the silo with the steep hopper, indicating that kinematic hardening have no noticeable effect on the tracers' movement. In the silo with the shallow hopper, the tracers adjacent to the wall did not move, the others did move, and the tracers close to the centre were faster than those close to the wall, but the tracers on the higher level moved faster than those on the lower level. This was asserted to be caused by the prescriptions of the initial stresses. Different initial conditions were tried out, but without decisive achievement. With the installation of the double cone into the shallow hopper, all tracers moved but with only small movements. The tracers in the middle moved faster than those close to the wall and the insert. Again the tracers on the higher level moved faster than those on the lower level. Different initial conditions were also tested, but such attempts did not give any different outcome. One can see that mass flow was achieved for the silo with a steep hopper, and might also be obtained for the silo with a shallow hopper in the presence of an insert.

5.2.2 Prediction of load with ABAQUS

Regarding the determination of wall loads for silo structural design, considerable uncertainty remains. Up to now, there is little international agreement on a unified standard, even though currently many such attempts are being made (Roberts, 1987; Rotter, 1993, 2001). The most common theory is the Janssen theory (Janssen, 1895) and its modifications. When mass flow is obtained, the Janssen formula is reasonably satisfactory for predicting the loads of granular solids on the walls of a silo with a simple geometry. But when more complex situations are involved, for example the presence of an insert, an operation commonly adopted to convert a funnel flow silo into a mass flow silo, the Janssen formula appears to be inadequate.

With the precondition that a mass flow pattern was achieved as deemed for the cases in Fig. 5.4, simulations were carried out to predict the loads exerted by the stored solid on the wall and on the insert. In a mass flow silo, all particles started to move at the commencement of discharge. At that moment, there is a significant pressure shift, and developed into a condition known as "Full Condition" (Rotter, 2001). At this moment, the largest pressure will develop most likely when the flow channel is fully activated.

An analysis was carried out in order to cover the change occurring during this condition.

Using the finite element meshes as shown in Fig. 5.2, ABAQUS analyses were performed by applying the gravity loading of stored solid when the outlet was initially opened. Severe deformation was observed at the transition. The deformation led to a separation of the stored solid from the wall. Figure 5.5 shows examples of such separations, which occurred at the transition of the steep silos with no fillet radius in (a) and with a 0.5 m fillet in (b).

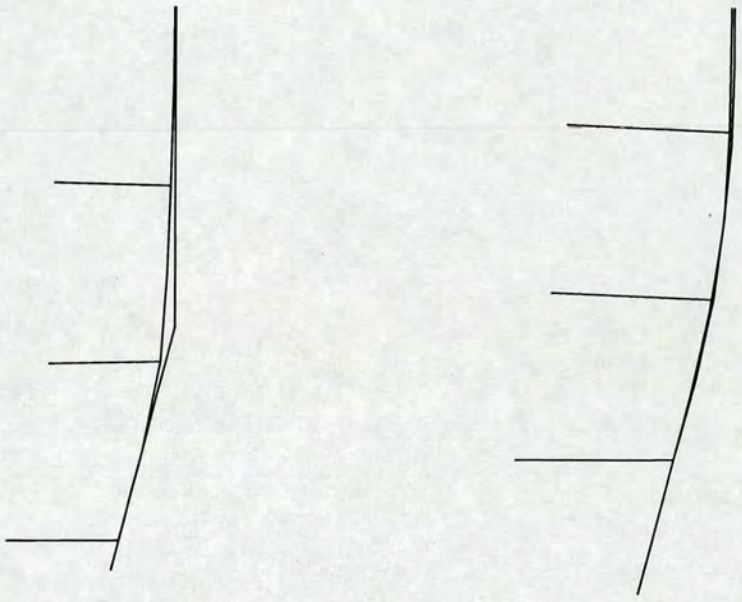

(a) (b)

Fig. 5.5 Separation of stored solid from the wall at the transition during discharge, responsible for high pressure peak

Below the separation, contact pressure peaks were predicted. The data in the output showed these peaks could be very high (8×10^5 Pa for the shallower hopper and 5×10^5 Pa for the steep hopper) due to point (line) contact between the stored solid and the wall when there is no fillet at the transition. These line contacts were modified into surface contacts by the application of filleting of the internal corners as described earlier and shown in Fig. 5.5. After such modifications, the peaks dropped close to and even lower than the theoretically predicted peaks as shown in Fig. 5.6 and Fig.5.7.

Figures 5.6 and 5.7 show the normal wall pressures in a steep hopper and in a shallow hopper with an insert. The predictions from the classic theories (presented in Appendix A) are shown for comparison. The ABAQUS predictions for the two filleting radii of 0.5 m and 1 m are largely similar, except at the transition where a smaller fillet radius produced a larger and more concentrated peak. Before reaching the peaks, the predicted pressure dropped to zero because of the separation, as shown in Fig. 5.5. On the whole, the finite element results agreed quite well with the theoretical results in the cylinder section, but differences exist in the hopper section, especially for the shallower hopper with an insert. Since the theoretical formulae were developed only for hoppers without insert, the comparison for this type of hopper is not entirely valid.

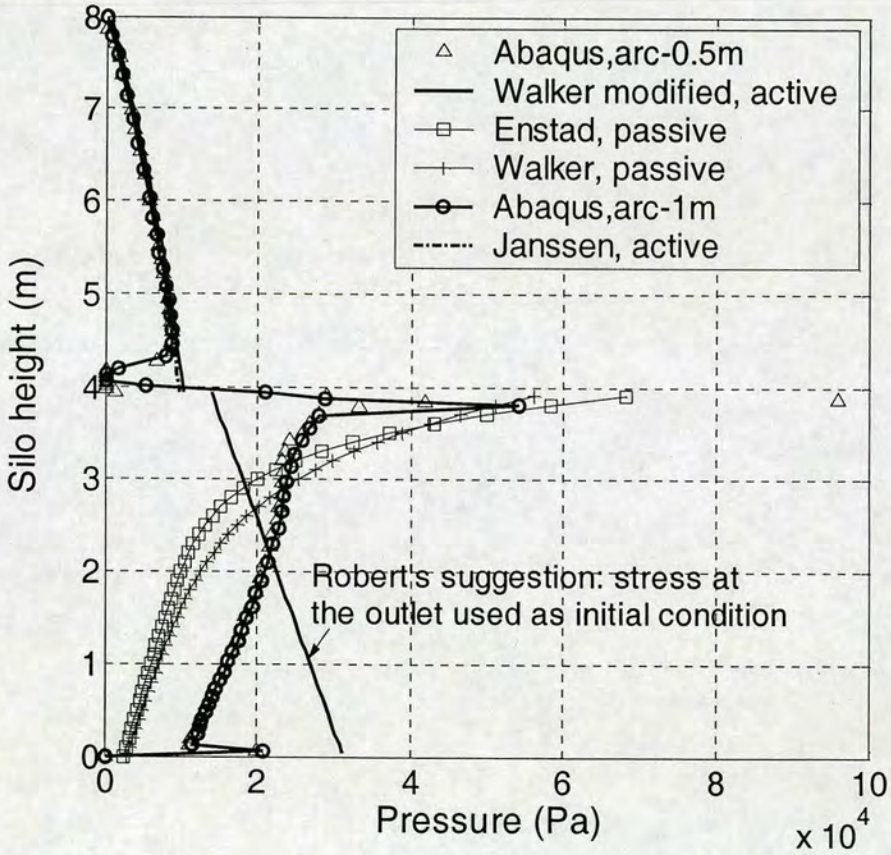

Fig. 5.6 Comparison between ABAQUS and theoretical predictions for a silo with steep hopper

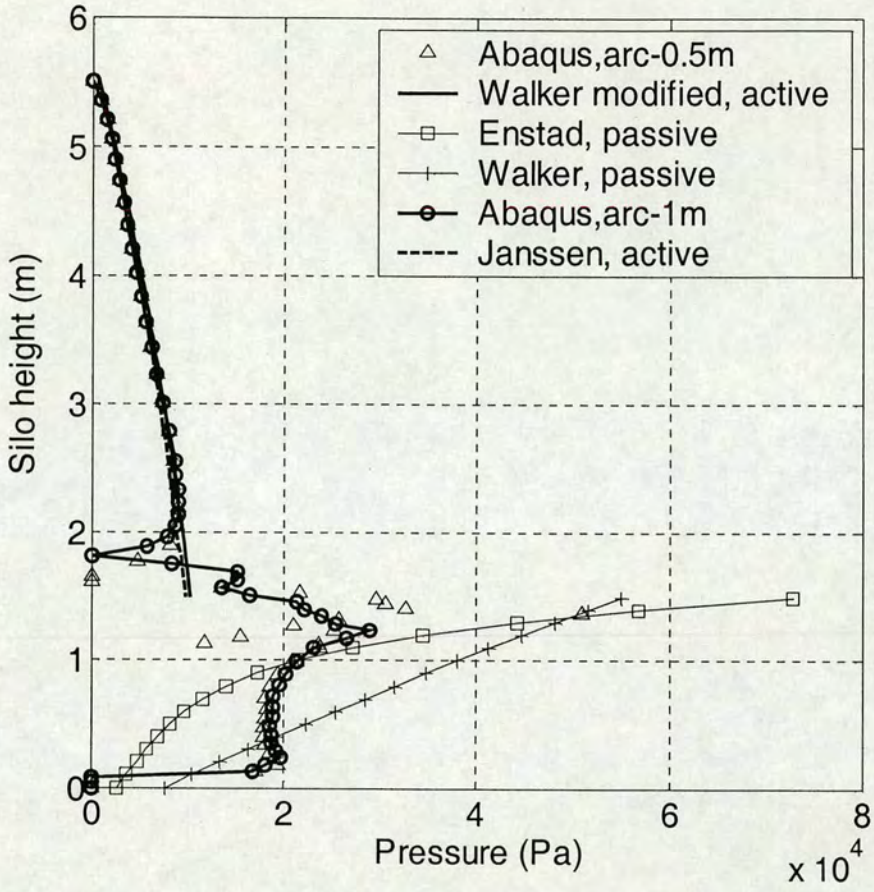

Fig. 5.7 Comparison between ABAQUS and theoretical predictions silo for a silo with a shallow hopper fitted with a double cone insert

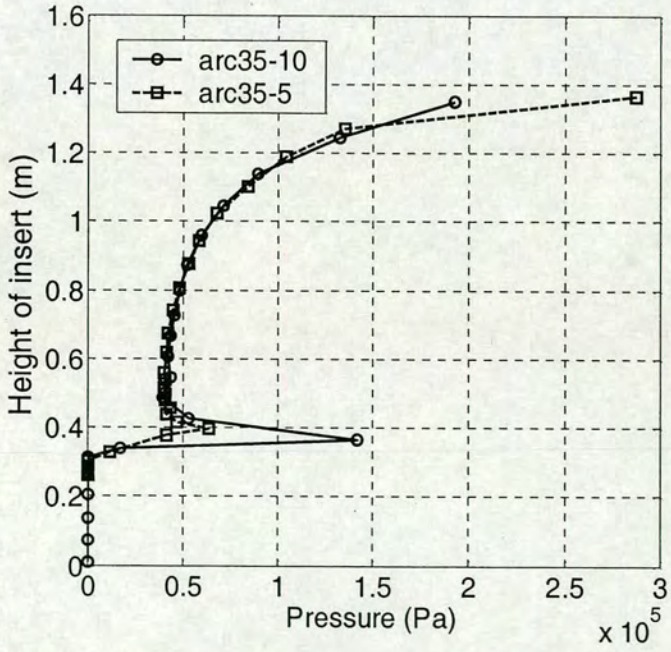

Fig. 5.8 Pressure on the insert (arcX_Y represents a X° inclination of hopper wall with a fillet radius of 0.1Y m)

The predicted load on the surface of the insert is shown in Fig. 5.8. The size of filleting at the transition appears to have little effect. It would be interesting to explore if the presence of an insert has a significant effect on the wall pressure distribution. The results on insert pressures shown in Fig. 5.8 might suggest that the insert carried a significant part of the load.

5.2.3 Concluding remarks

Finite element analysis was carried out to predict the flow and the pressure in a full scale silo using a Lagrangian-Eulerian approach. The study shows that the application of an adaptive mesh was effective in dealing with a process involving a large deformation. By defining an adaptive mesh for the stored solid and employing suitable constraining boundaries or the mesh, the approach to simulate the silo discharging process is successful to a certain degree. It was found that the crucial factors to obtain satisfactory predictions are: choosing an appropriate material model and a proper determination of the relevant parameters including prescribing the initial stress state after filling. By contrast, an Eulerian approach might have some advantages over a Lagrangian-Eulerian method, resulting in successful prediction of double cone insert effects on flow patterns as demonstrated in the previous chapter.

The simulation results have shown that (1) the insert took on a significant part of the load, but it remains to be open for further verification from experiments; and (2) the predicted pressures along the walls were in good agreement with the theories in the cylinder section, but the agreements were not always good in the hopper section. The discrepancy in the hopper section between simulation and theory grows larger when the hopper becomes shallower. Such differences support the argument that the theoretical formulae are no longer suitable when the hopper becomes too shallow or when an insert is present. This argument does not prove that the simulation results are correct. Some experiment verification is necessary.

It has also been shown to be important to apply filleting to regions with sharp corners in the geometry to avoid mathematical singularities and thus improve the condition to achieve convergence in the FE analysis.

5.3 Experimental investigation into the effect of double cone insert

Earlier studies of silo pressures generally suggested that wall pressures would be symmetrical if the filling and discharging were both symmetrical. However more careful measurements showed that wall pressures can vary significantly around the circumference and can be unsymmetrical even in symmetrical silos which appear to be symmetrically filled and discharged (Ooi and Rotter 1990; Nielsen, 1998). The loss of symmetry may be traced back to in-homogeneity and anisotropy developed in the initial packing during filling. An axi-symmetrical silo is no guarantee to obtain an axi-symmetric discharging pattern. In some cases, even a minor disturbance of the flow pattern can cause a serious loss of symmetry in the wall pressures (Rotter et al., 1998; Nielsen ,1998).

There is concern about how an insert might affect the symmetry of a silo. In this section, the influence of an insert on the loading during silo filling and the loading and flow pattern during discharge is investigated. For example, as shown in the last chapter, the presence of an insert enlarged the stored solid moving zone during discharge. It is necessary to examine whether such an enlargement of moving zone will significantly affect symmetry, and what effect it may impose on pressure distribution. Because of the complexities involved, these issues have seldom been addressed. The numerical models presented thus far are axi-symmetric two dimensional in character, and are incapable of dealing with these challenges.

The experimental investigation was carried out firstly in a pilot scale silo. This silo had a hopper with a 45° inclination angle, and was fitted with a double cone insert. This configuration is based on the numerical outcomes obtained in Chapter 4. The wall pressures were measured using pressure transducers mounted at designated locations on the walls. The test results are reported as follows.

5.3.1 Tests in a pilot scale silo

5.3.1.1 Experiment setup and testing stored solid

The experimental setup is shown in Fig. 5.9. It consisted of two parts: the material handling system (Mat) and the data acquisition system (Data).

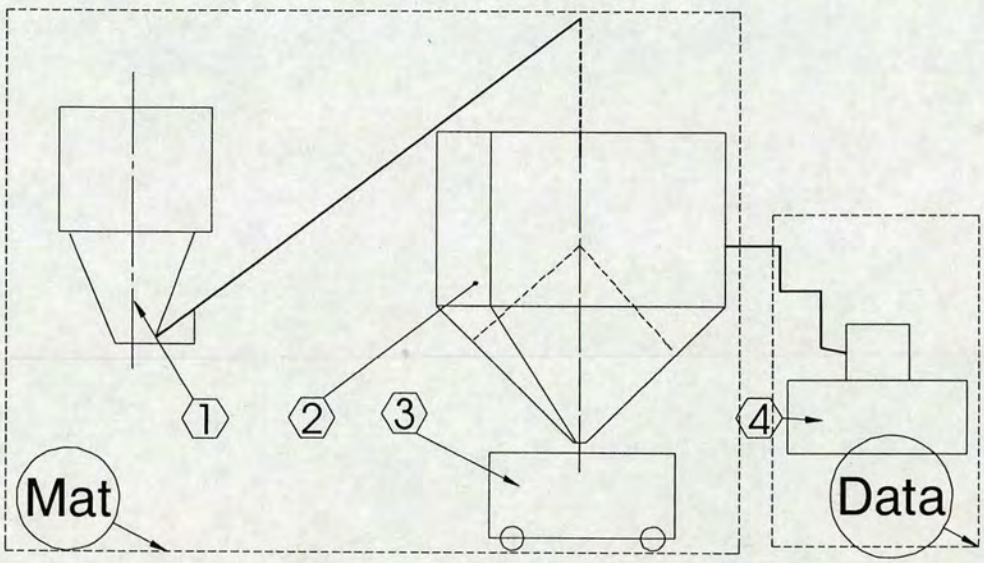

1. Rope and disc conveyor
2. The full-scale silo
3. Material collecting bag used in discharge
4. Data logger Hydra and PC

Fig. 5.9 Experimental setup

The material handling system included a material feeding unit, a full scale silo and a material discharging unit. The feeding unit was a rope and disc conveyor and was designed for carrying out a concentric filling. The discharging unit was in the form of collecting bags for free discharge, and could be interrupted so that the flow pattern could be monitored. The core part in the material handling system was a pilot scale silo as shown in Fig. 5.10. It consisted of a cylinder of 2.5 m in diameter and 1.5 m in height, made of normal mild steel; and a conical hopper with a 45° inclination angle, 1.2 m in height with ϕ 2.5 m inlet and ϕ 0.10 m outlet, made of stainless steel. The bottom of the cylinder had the same reinforced structure and rested on the same supporting frame as that described in section 3.3.3 in Chapter 3.

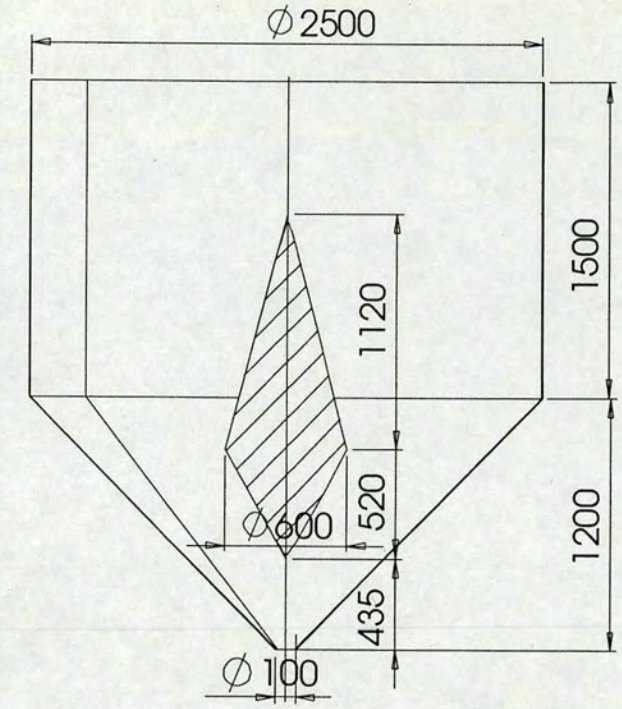

(a) Config. 1

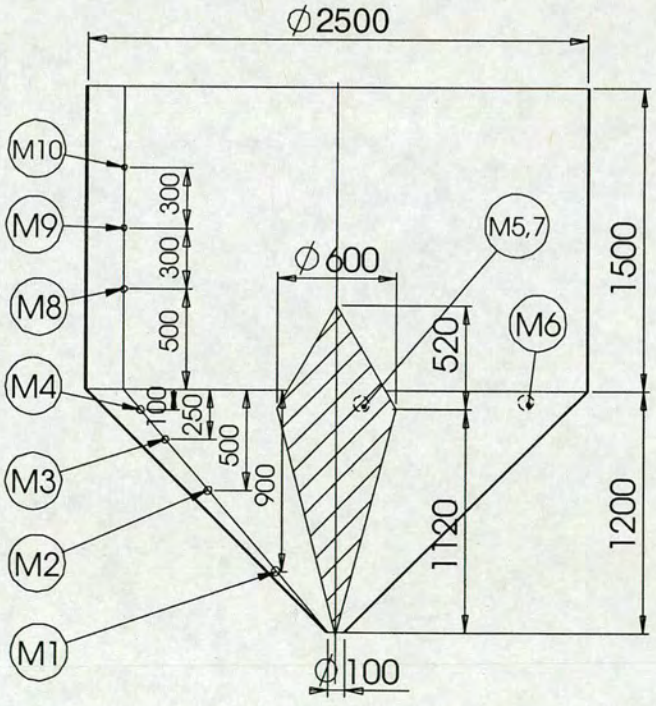

(b) Config. 2

Fig. 5.10 One installation of double cone insert into silo

Inferring from the investigation results presented in Sections 4.3 and 4.4, a double cone insert was fitted into the silo, aligned with the central axis of the silo. There were two different configurations as illustrated in Fig. 5.10. The dimensions of the insert are also shown.

The data acquisition comprised the data logger Hydra, a PC and the pressure transducers mounted on the wall. In addition to the seven transducers already in the hopper as shown previously in Fig. 3.29 (Chapter 3), three more transducers were mounted at locations on the cylinder along the same generating line as M1- M4 (Fig. 5. 10 (b)). They were named M8, M9 and M10. All of them had an interacting area of ϕ 0.12 m. Calibrations were carried out for all transducers and these are outlined in Appendix B. Hydra scanned electronic signals from the pressure transducers at a frequency of around 1 Hz and transferred them to the PC.

The sand used as the test solid had a bulk density of 1370 kg/m^3 with a particle size ranging from 0.6 to 2 mm. It was a free flowing material. The measured angle of repose was 36°. The friction angle measured was 26.5° with the steel used to construct the cylinder and 21.8° with the stainless steel used for the hopper.

5.3.1.2 Measurement procedure

Measurements focused on the effect of the double cone insert on the loads imposed on the walls by the stored solid in the processes of both filling and discharging. For comparison purposes, parallel measurements of filling and discharging were also carried out in the absence of the double cone insert. Two configurations of the insert and silo were investigated (Fig. 5.10).

5.3.1.3 Central filling and loads measurement

In these experiments, a concentric filling was carried out with the rope and disc conveyor. To secure concentric filling, the outlet of the conveyor was arranged in such a position so that the sand could be fed directly into the silo from a fixed height on the axis of the silo with a certain feeding rate. Minor adjustments were required during filling and these were made accordingly. The feeding rate has been shown to have

some effects on wall loads (Ding, and Enstad, 2003), and this was kept between 60 - 80 kg/min. A more precise control of the feeding rate was difficult to achieve.

An amount about 13.5 tonnes of sand was used for the control test without an insert. Taking into account the volume of the insert, about 13 tonnes of sand were used when the insert was installed to achieve the same final height of fill.

The final height of fill (from the bottom edge of the cylinder (i.e. the transition) around the circumference where M4 to M7 were located) for each test is shown in Table 5.1. Even with the significant effort in ensuring a concentric filling, one can see there existed some differences in the heights of fill for the tests (Fig. 5.11). The difference was as large as 13 cm (5 % of filled height) when there was no insert, and 5 cm (2%) when there was one. Consequently such differences might contribute to a loss of loads symmetry on the wall.

Table 5.1 Height of fill around the circumference (cm)

Transducers no.		M4	M5	M6	M7
No insert	Test 1	126	134	129	121
	Test 2	136	127	134	125
Config. 1	Test 1	124	120	125	129
	Test 2	124	127	126	122
Config. 2	Test 1	135	132	133	130
	Test 2	132	134	131	134

The normal wall pressures developed on transducers M4, M5, M6 and M7 for the three test configurations are shown in Fig. 5.12. It is clear from Fig. 5.12 that the loads induced on the transducers varied from one transducer to another in each individual test. The mean values for each of the three configurations of no insert, Config. 1 and Config. 2 are shown in Fig. 5.13. Comparing with the differences in the fill height

around the circumference as shown in Fig. 5.11, it is noted that the variation of normal pressure around the circumference appears to be great

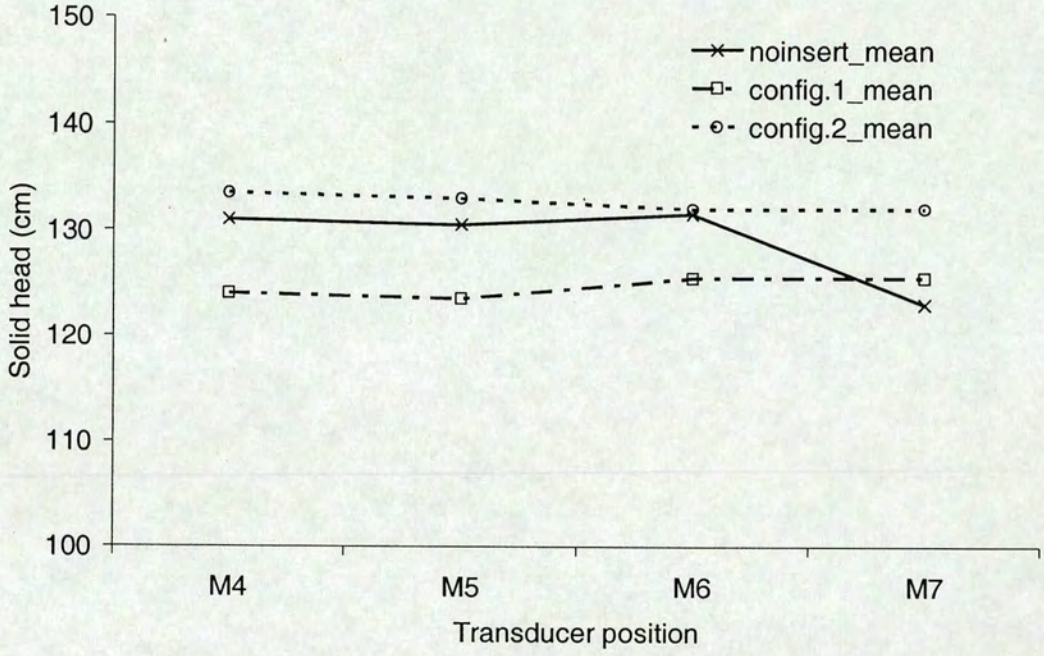

Fig. 5.11 Height of fill at four positions around the circumference

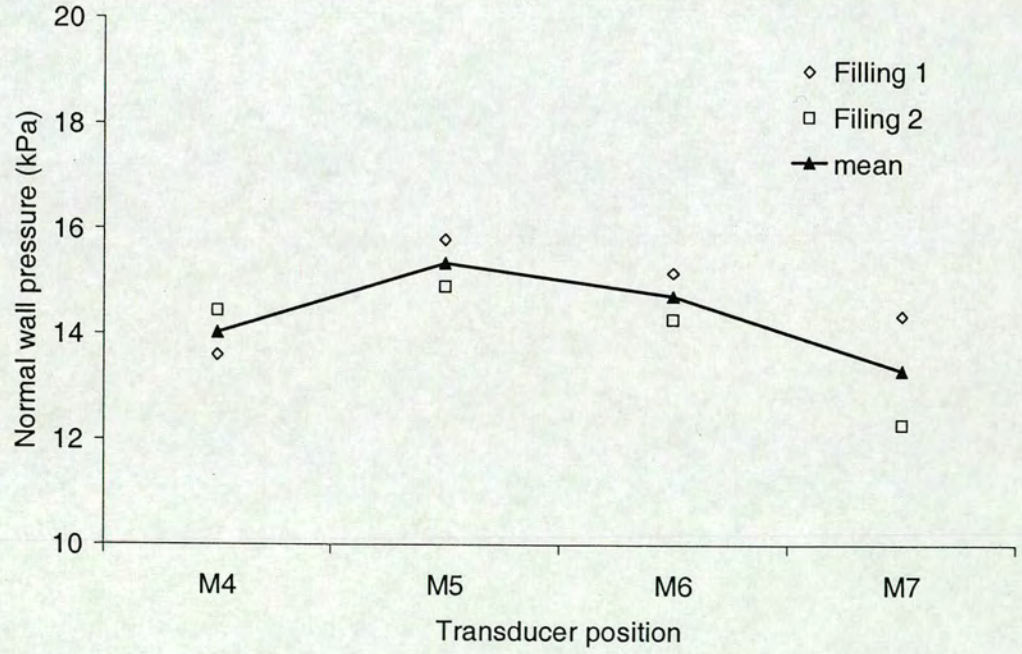

(a) No insert

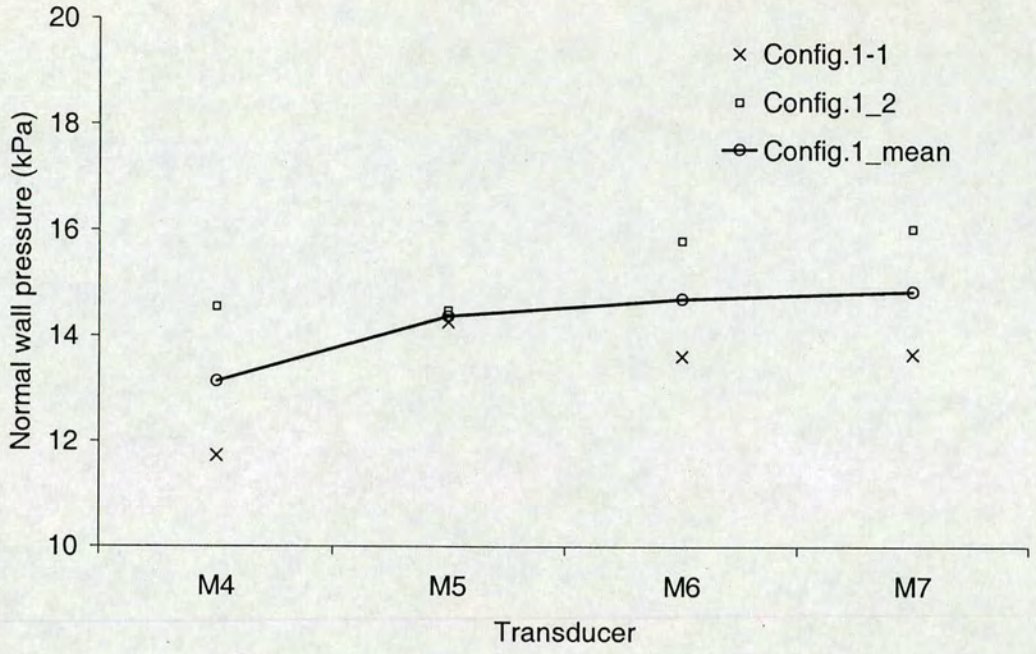

(b) Config. 1

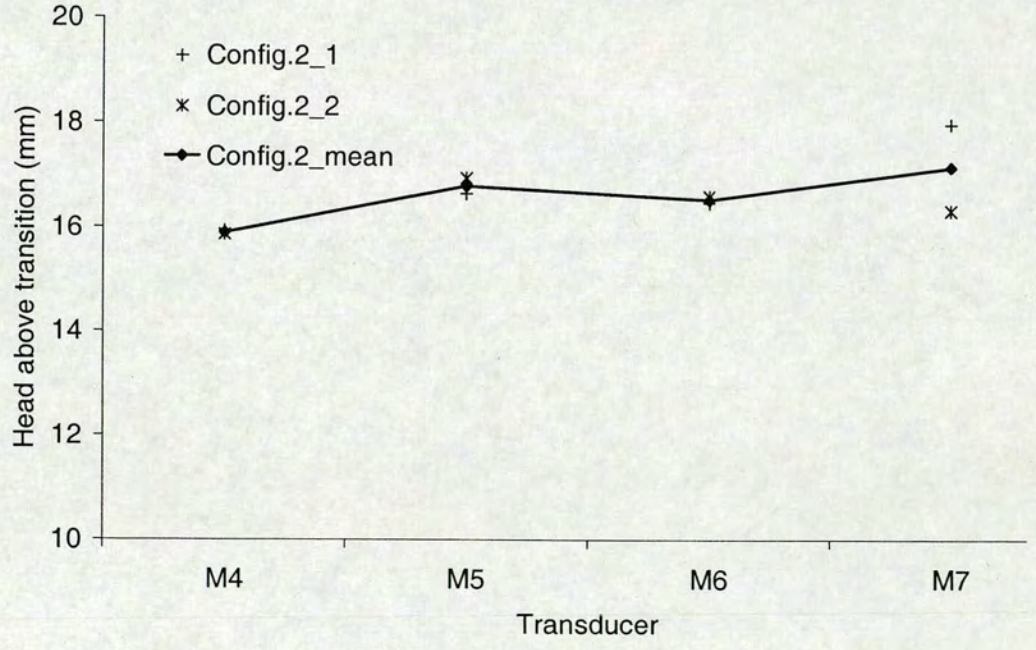

(c) Config. 2

Fig. 5.12 Normal pressures on transducers mounted just below the transition

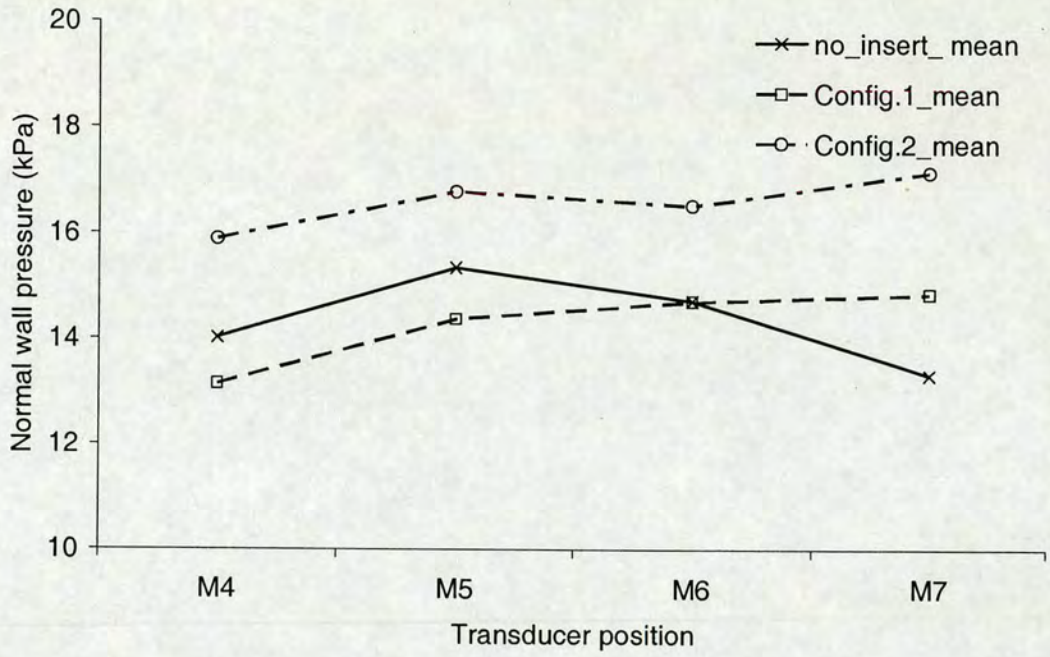

Fig. 5.13 Comparison of normal pressure developed under different conditions

5.3.1.4 Measurements during discharging

5.3.1.4.1 Surface movement measurement

The sand was discharged under free gravity. The discharge was interrupted to take measurement of the surface movement. It was observed that the movement of the surface differed from test to test.

At the beginning of discharging, the top surface of the sand started to drop. The drop was different for each of the three test configurations. When there is no insert, the drop was reasonably even with a small moving zone in the centre. Under Config. 2 insert setup, the drop appeared to be less even with a larger moving zone compared with that without the insert, whereas under Config. 1 insert setup, the drop became quite skewed to the side close to M6 .

As discharging progressed, the conical heap at the surface gradually turned into a dip (Fig. 5.14a). Under Config. 2 setup, it was observed that the sand close to wall experienced some slip movement against the wall, as shown in Fig. 5.14b. No such movement was seen in the tests for the other two conditions.

As the dip on the surface progressed to the point that the surface was sufficiently steep, the sand started to slide. When there was no insert, the sliding was rather symmetrical along the surface of the dip; the diameter of the dip gradually increased. Overall, the stored solid appeared to discharge fairly evenly. Under the condition of Config. 1, the skewed pattern to the M6 side caused the sand in the other parts to slide into the dip formed by the skewed flow. Under the condition of Config. 2, two dips developed, into which the adjacent sand slid.

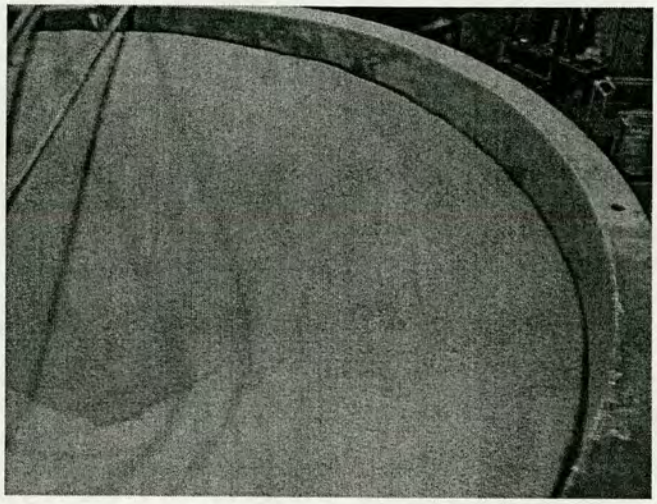

(a)

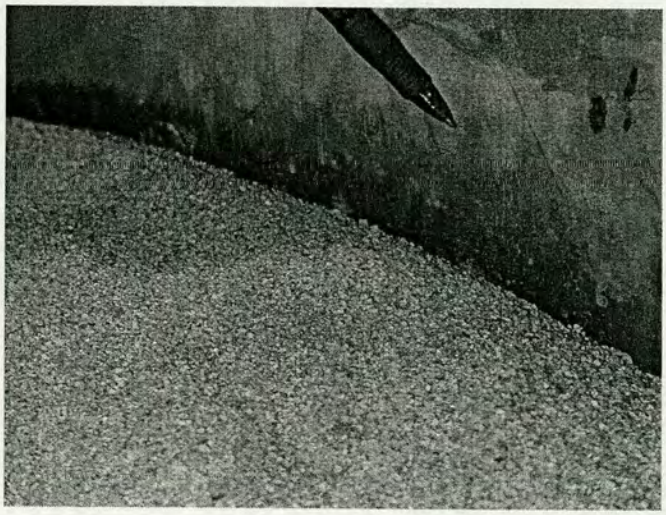

(b)

Fig. 5.14 Sand movement along the wall before the sliding along the dip started during discharge in configuration 2. (left: an overview; right: a zoom-in view)

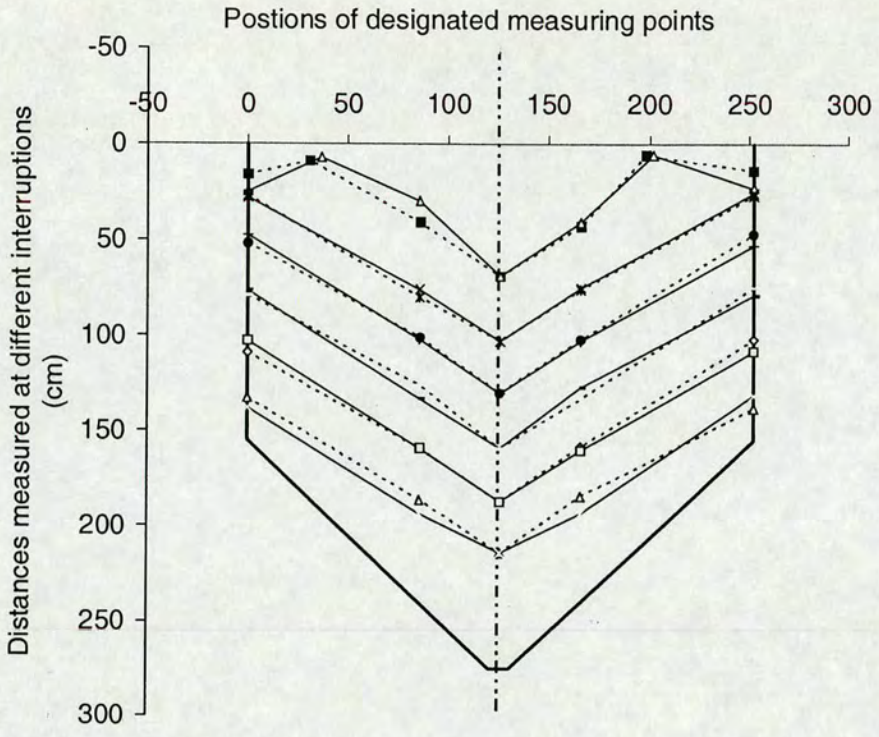

(a) No insert

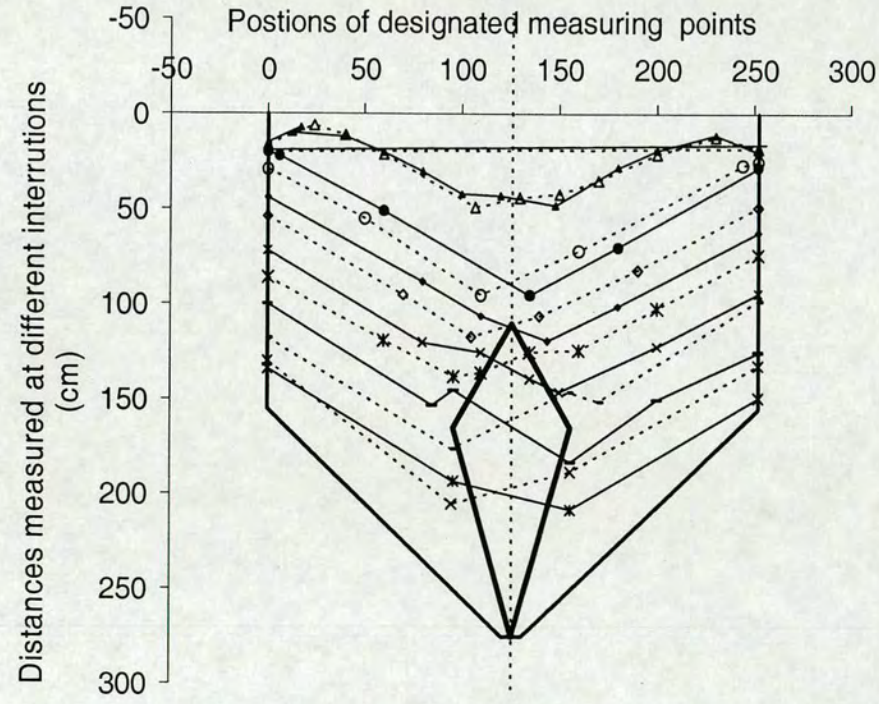

(b) Insert extended to outlet

Fig. 5.15 Measurements of surface profiles during discharge

The differences of flow pattern between Config. 2 and Config. 1 showed that Config. 2 has functioned better, that is config. 2 enlarge the move zone and retain the symmetry of discharge. Config. 2 was chosen as candidate in the further investigation in a full scale silo. The investigation on a configuration of this insert and a full scale silo similar to Config. 2 are to be carried out, and would be reported accordingly later.

The discharge process was interrupted to measure the profiles of the solid surface. This was done by measuring the vertical distances between the newly formed surface of sand and the top plane of the cylindrical section at several designated positions along two perpendicular directions. Fig. 5.15 a and b show the measured surface profiles for when there was no insert and for Config. 2 respectively.

5.3.1.4.2 Wall loads during discharging

The wall pressures developed during the discharge were measured. Figure 5.16 show typical measurements results from transducers M1, M2, M3, M4 M8, M9 and M10 (along a vertical generator) for the tests when there was no insert and with insert of Config. 2.

From Fig. 5.16, one can see that at the commencement of discharge, there were sudden increases in pressures in all transducers except for M2 and M1 where there was a drop.

The increases were larger in the hopper than in the cylinder, and the largest increase occurred just under the transition (Position M4). It is noted that the presence of an insert caused much larger increases of the pressures in the hopper. This effect also featured in the cylindrical section but much less obvious (Positions M8 to M10).

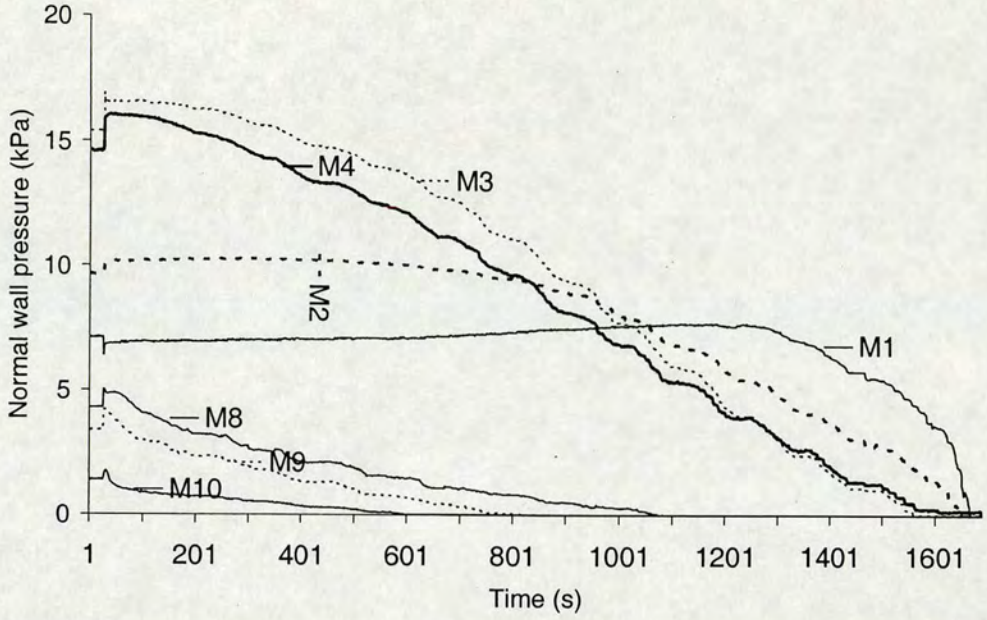

(a) No insert

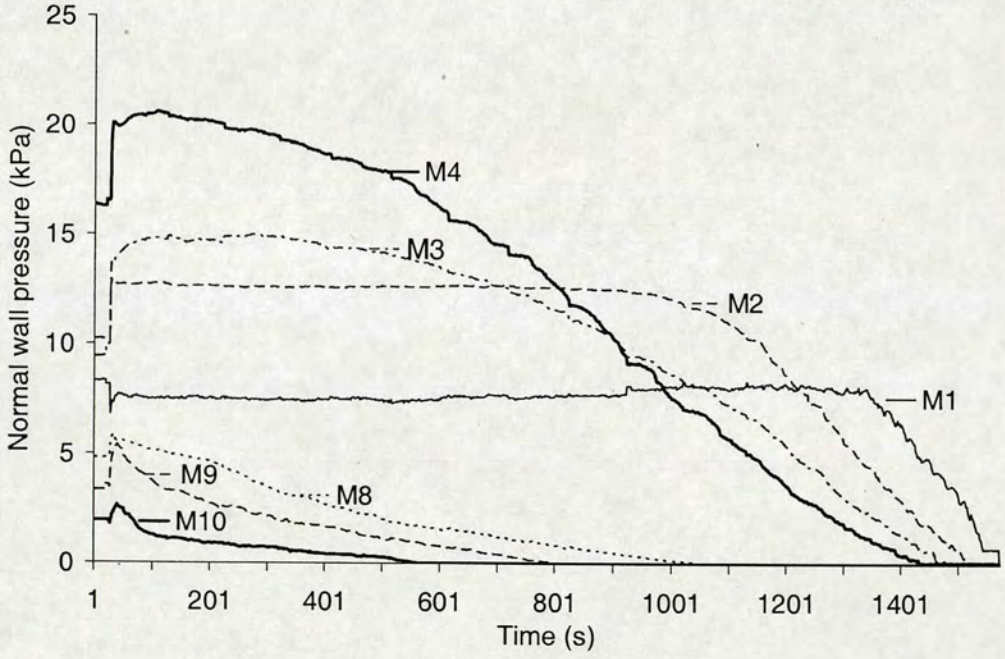

(b) With insert (Config. 2)

Fig. 5.16 Normal pressures for transducers M1-M10 during discharge

After the initial increase, the observed pressures then started to decrease in the process of further discharging. Figure 5.16 shows that the insert had little effect on the decreasing pressures in the cylinder, but had some effects in the hopper, especially on the loads measured on M1 and M2. These loads maintained their levels and even

slightly increased until the very last stage and then suddenly dropped rapidly afterwards. The insert appears to prolong this pattern.

Figure 5.17 show the normal pressure time trace for each of the four transducers around the circumference just below the transition (M4-M7). The trend of decreasing pressure with time is as expected. When there was no insert (5.17a), the sand moved down reasonably evenly. The load symmetry on Transducers M4–M7 was maintained and any slight non-symmetry caused by filling may even decrease (Fig. 5.17 (a)). However the skewed flow in Config. 1 led to stronger unevenness, causing further loss in symmetry of pressure (Fig. 5.17 (b)). The situation was better in Config. 2 setup (Fig. 5.17 (c)), but the non-symmetric character was still present. Watching the load changes on M4 –M7 closely, one can also find that the larger the increase of load a transducer had at the commencement of discharge, the stronger the tendency the sand adjacent was about to move, and as a result, the quicker the load decreased.

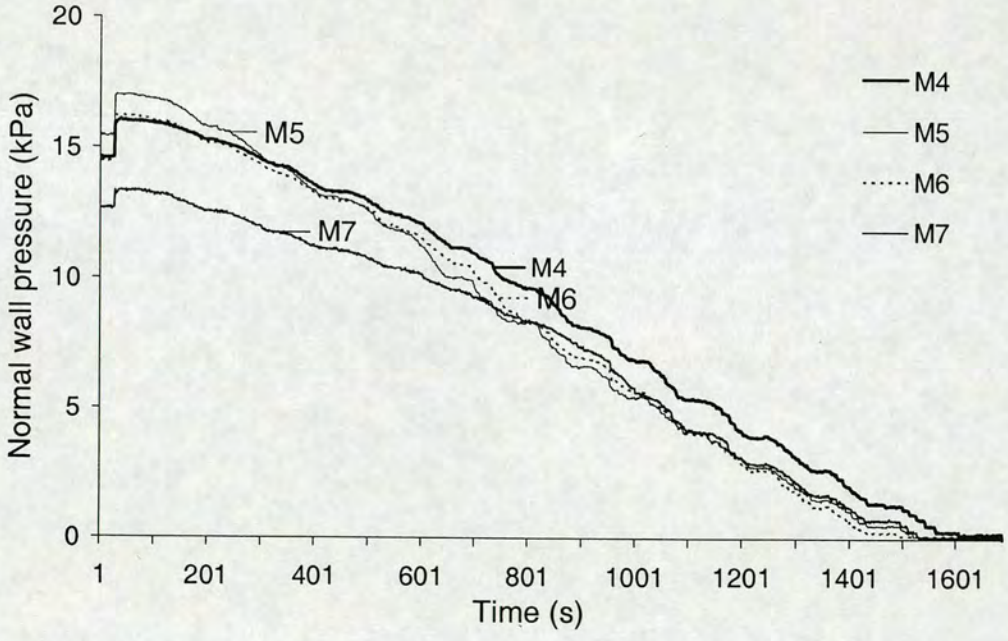

(a) No insert

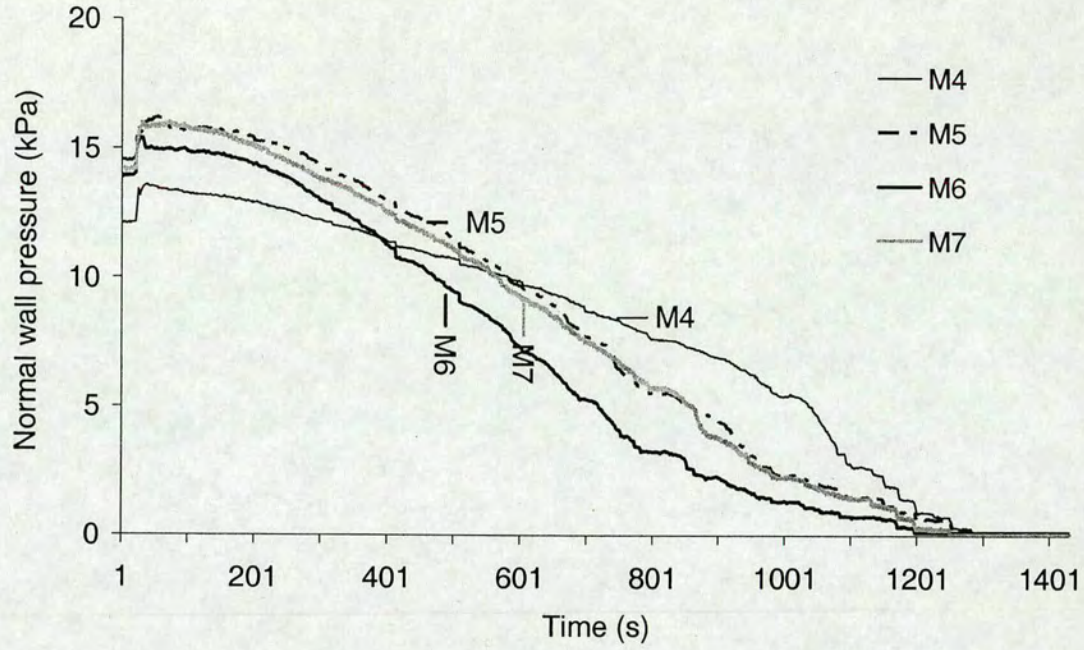

(b) With insert (Config. 1)

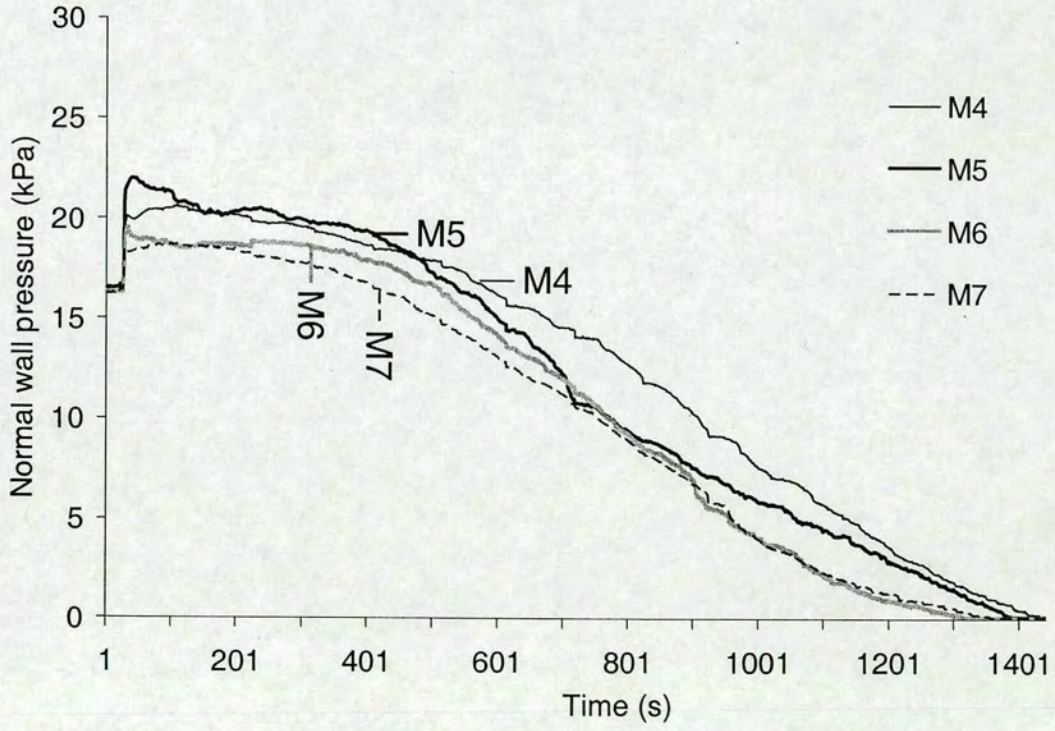

(c) With insert (Config. 2)

Fig. 5.17 Variation of normal pressure just below the transition during discharge

5.3.1.5 Concluding remarks

Measurements of pressures during filling and discharging in an axi-symmetrical pilot scale silo were carried out with and without a double cone insert. Measurements showed that even though the geometry of conical pile formed during filling appeared to be close to axi-symmetrical, the loads would not be necessarily symmetrical. A loss of load symmetry started during filling. Measurements also showed that a proper installation of the insert (Config. 2) enlarged the stored solid moving zone while retaining the symmetry of both the discharge flow pattern and the resultant loads on the walls. An improper installation of such an insert may lead to skewed discharge flow and a loss of load symmetry. Insert Configuration 2 was selected as a configuration in the further measurements in a full scale silo reported below.

5.3.2 Tests in a full-scale silo

5.3.2.1 Full scale silo facility at Porsgrunn

A full scale silo facility was designed by Prof. S. R. Sunil and Prof. G. G. Enstad. The setup was shown in Fig. 5.18. It consisted of a cylindrical silo and a rectangular silo, each with a 50 m^3 storing capacity, and was supported by a steel frame. It was fabricated by BSS AS, Porsgrunn, Norway and erected alongside the POSTEC Hall, Tel-Tek, University College Telemark, Porsgrunn, Norway.

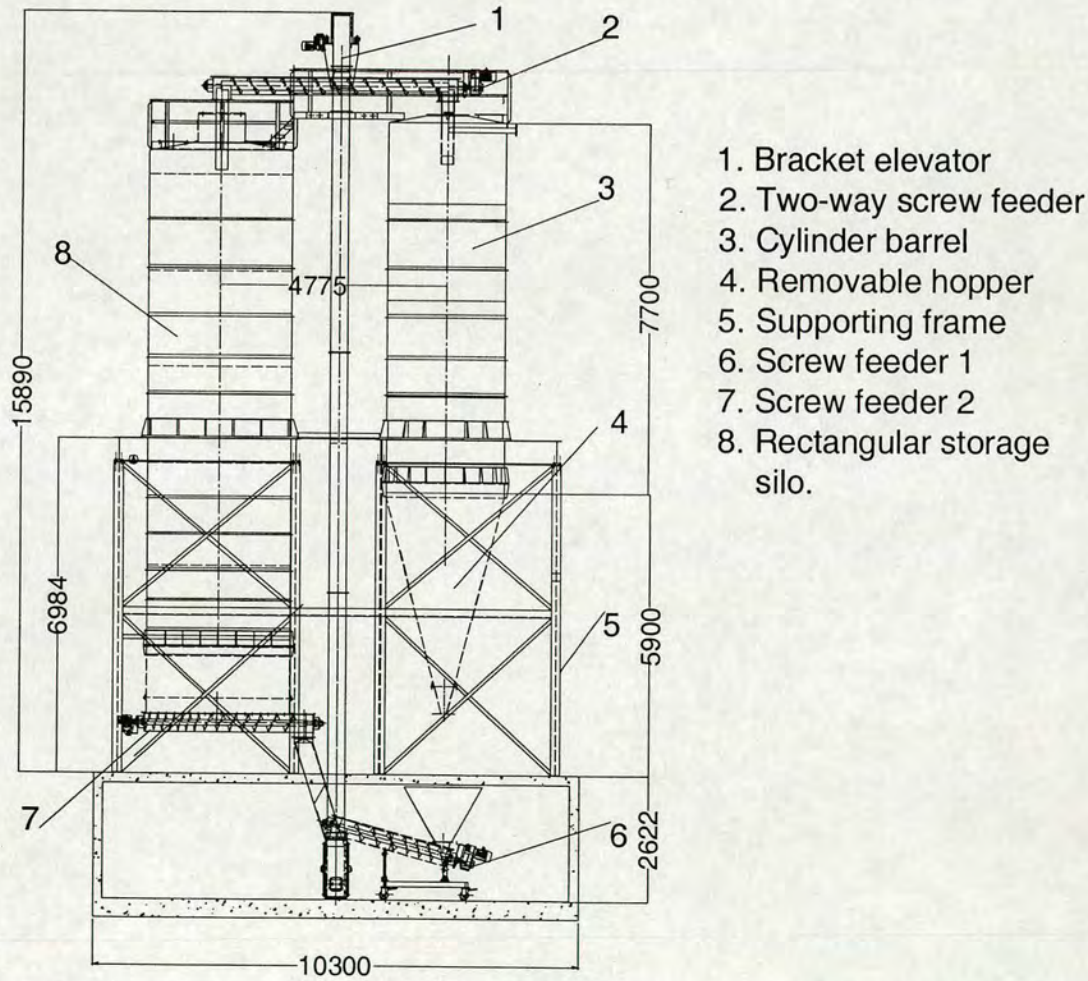

Fig. 5.18 Full scale silo test facility (dimensions in mm)

The initiative was to establish a full scale research test facility, capable of undertaking full scale experiments with both flow pattern and wall pressure measurement. It was expected that the facility, once established, would be used in many future experiments.

Several problems arose in the design, organisation and construction. However, these problems were surmounted. This section reports on the setup and the first set of full scale tests conducted.

5.3.2.1.1 Material handling system and sequence

As shown in Fig. 5.18, the material handling system for the two silos consists of a bucket elevator, a two way screw feeder and two other screw feeders. The specifications for these equipments and the corresponding driving motors are listed in Table 5.2.

Table 5.2 Specifications for units shown in Fig. 5.18

Item	Model	Motor (power / cosφ)	R /min
1. Bucket elevator	FH 67 DT 100 I4 / RS	3kW / 0.83	1400 / 41
2. Two way screw feeder	FH 87 DV 112 M4	4 kW / 0.85	1420 / 25
6. Screw Feeder 1	FH 77 DV 112 H4	3 kW / 0.84	1420 / 21
7. Screw Feeder 2	KH 87 DV 132 M4	5.5 kW / 0.84	1430 / 20

The bulk solid was delivered firstly into the small hopper mounted above Screw Feeder 1. It was then conveyed from Screw Feeder 1 into the bucket elevator and lifted to a height above the two silos. The solid was then fed into the two way screw feeder on top of the silos. Depending on the rotating direction of the motor, the bulk solid would be delivered into either the rectangular storage silo or into the cylindrical silo. The solid in the rectangular silo would be discharged via Screw Feeder 2 into the bucket elevator. In the cylindrical silo, the solid would be discharged via a valve mounted on the outlet of the hopper.

The motors were designed to be operational only in a specific sequence to avoid blockages likely to happen during the process of material handling. The motor for the

bucket elevator could start only after the motor of the two way screw feeder started, while the motor of Screw Feeder 1 (or 2) could start only when the motor of the bucket elevator was running.

In the present study, the material was handled in a sequence as follows. For the filling process, the test material stored in the rectangular silo was discharged with a constant feeding rate via Screw Feeder 2 into the bucket elevator, and then into the cylindrical test silo via the two way screw feeder. For the discharging process, the test solid in the cylindrical silo was discharged under gravity and fell into the hopper sitting above Screw Feeder 1. The solid was then returned to the rectangular storage silo via the bucket and elevator and the two-way screw feeder.

5.3.2.1.2 The cylindrical silo

As the rectangular silo was used only for storage, its specification is not described. The details about the cylindrical silo are given here. An aspect ratio (H/D) of about 3 for the silo barrel was designed to ensure that the flow channel makes contact with the silo wall (a rule of thumb assessment is generally accepted as a height to diameter ratio in excess of 2). The barrel was 7850 mm in height, 2500 mm inner diameter and 6 mm thick wall. Five external ring stiffeners were welded at positions as shown in Fig. 5.19 to reinforce the silo wall. The roof had an observation hatch to permit measurement of the solids surface profile, and provide an access to the solids in the silo if necessary. A double ring was designed at position 1100 mm above the bottom of barrel. It was reinforced with 18 ribs as shown in Fig 5.20 (view A-A in detail), and was used to support the barrel on the platform of the supporting frame structure (Fig. 5.21). Another double ring was designed and positioned 200 mm above the bottom of barrel. It was reinforced with ribs as shown in Fig. 5.20 (view B-B), and used to connect to the hopper beneath.

The same shallow hopper as the one shown in Fig. 3.26 was attached to the bottom of the barrel, connected with its upper ring to the lower ring of B-B as shown in Fig. 5.20, with a 200 mm overhang of the cylinder section.

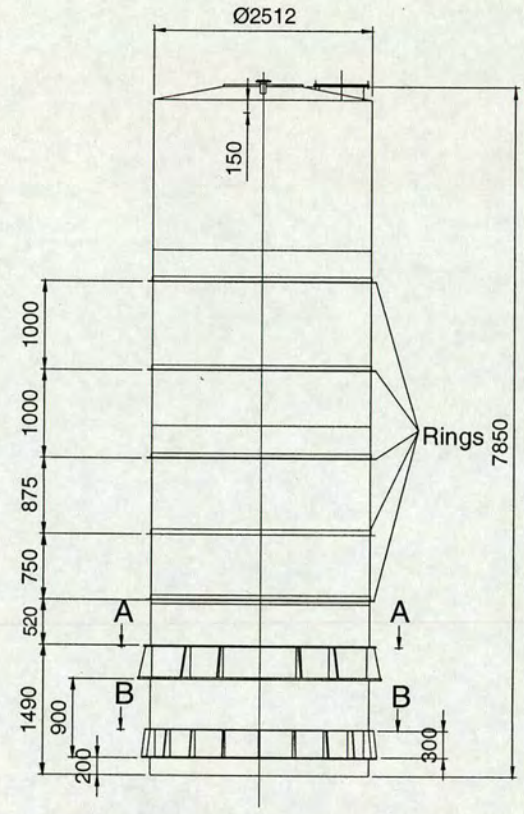

Fig. 5.19 Silo barrel (dimensions in mm)

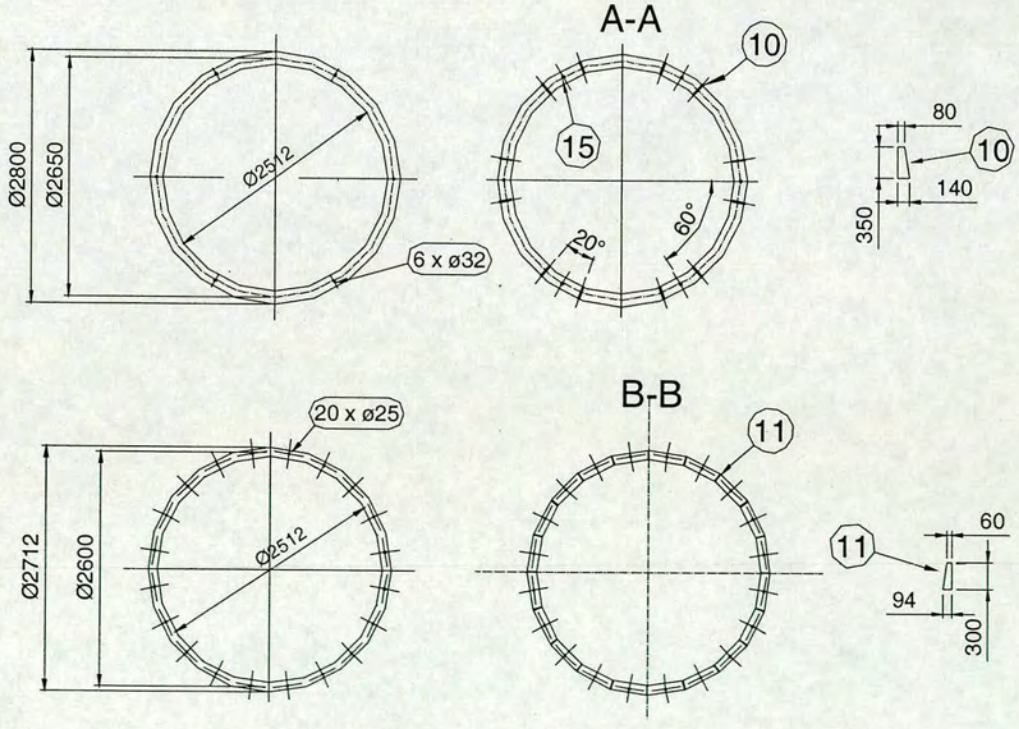

Fig. 5.20 Double rings and ribs (A-A for supporting the silo; B-B for connecting to a hopper; dimensions in mm)

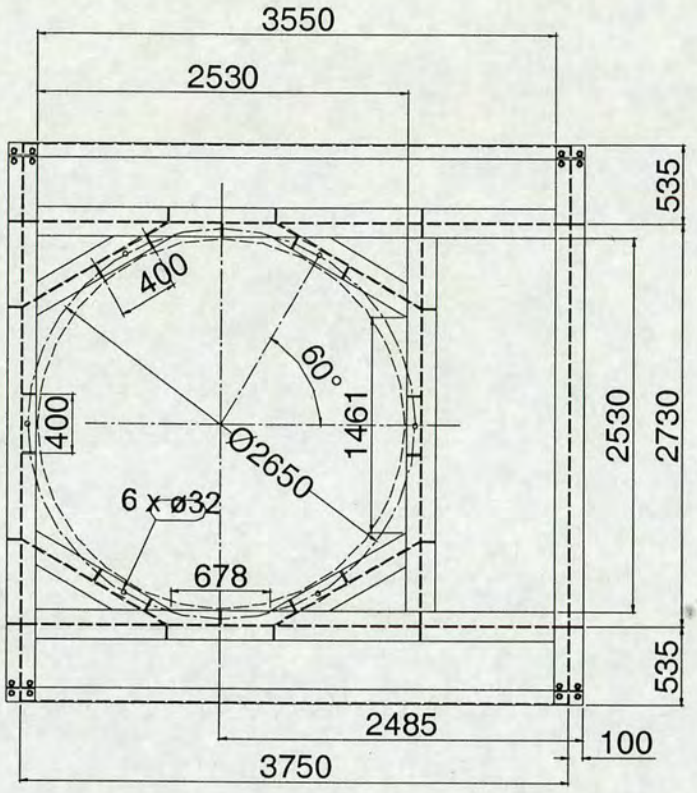

Fig. 5.21 Arrangement of supporting platform (dimensions in mm)

The same double cone insert as used at Section 5.3 was fitted into the silo. Based on the results from investigations presented thus far, in particular the results in Section 5.3, the double cone insert was placed in a position as shown in Fig. 5.10 (b) (c.f. Config 2 position), aligning with the axis of the silo with its lower tip extending to the outlet.

5.3.2.1.3 Concentric filling

Previous studies (Moriyama et al, 1983; Hartlen et al, 1984; Munch-Andersen and Nielsen, 1990; Zhong et al. 2000) have shown that the mode in which a silo is filled has a strong influence on the packing state of the stored solids, and that this in turn may influence the flow pattern during discharge. Two filling modes, namely a distributed filling (uniform raining down on the entire area of the silo cross-section) and a concentric filling (a point filling at the centre of the silo cross section) are usually regarded as producing two very different packing states. In this study, a concentric filling mode was chosen.

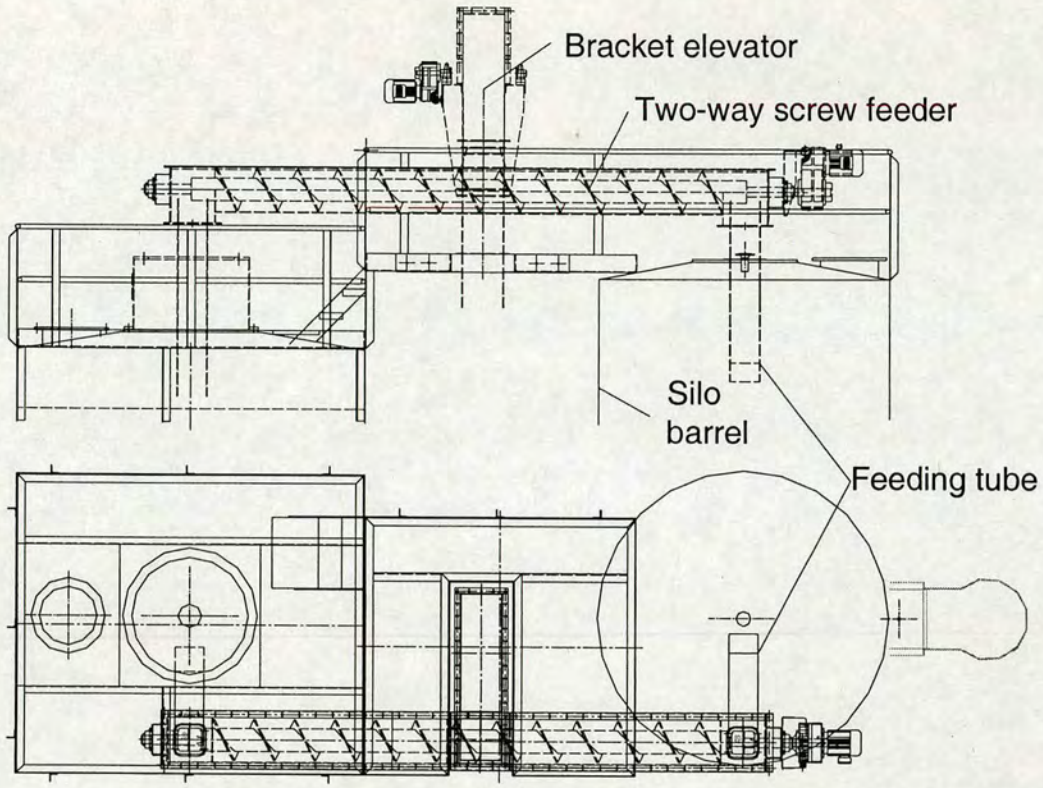

Fig. 5.22 Filling mode in original design (solids were fed into silo eccentrically)

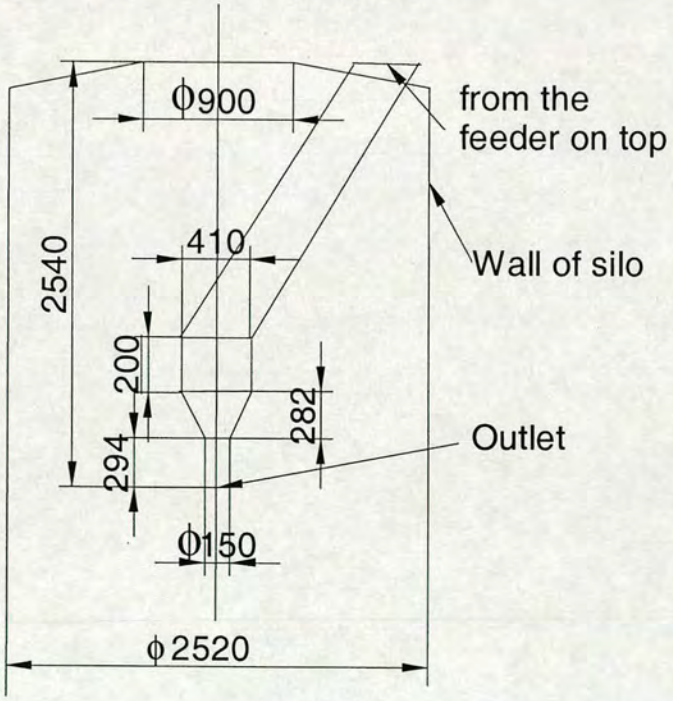

Fig. 5.23 Modified filling tube (Concentric filling mode)

From the original design as shown in Fig. 5.22, the solids entering the silo were fed through a tube. This tube had dimensions of 300 x 400 mm. It linked to the outlet of

the two way screw feeder, and protruded into the silo. As seen, the filling mode via this tube was neither a distributed filling nor a concentric filling. To produce a concentric filling, this tube was extended with an additional vertical section as shown in Fig. 5. 23.

Discharge was designed to be controlled by a valve. This valve was an air driven valve, with an effective diameter of ϕ 120 mm (as shown in Fig. 5.24). To install this valve, a tube with a diameter ϕ 120 and a height of 300 mm was first connected to the outlet of the hopper. Using such an arrangement, it was considered unlikely that the valve may affect the silo discharge pattern.

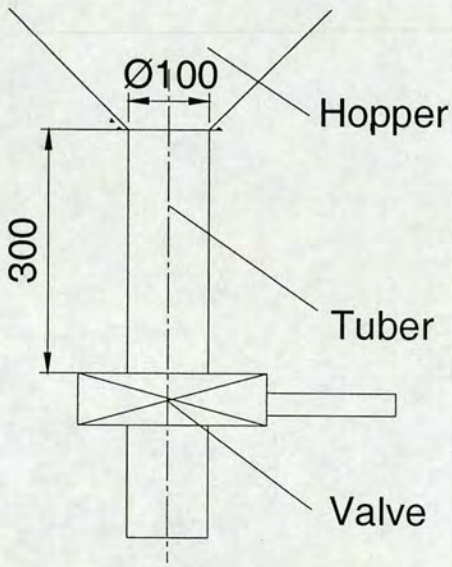

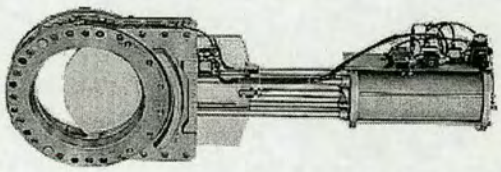

WEY® Filter Discharge Valve

Fig. 5.24 Arrangement for discharge

5.3.2.2 Load measurement instrumentation- pressure transducer and data logger

The measurement of loads included the pressure measurement on the wall via pressure transducers, and the load measurements on the insert via strain gauges. The present description concentrated on the measurement on the wall pressure, instrumentation systems employed for this purpose are briefed below – the systems used for the loads measurement on insert is going to be presented somewhere else.

The seven transducers mounted in the hopper as shown in Fig. 3.26 were left intact when the hopper was moved and connected to the silo barrel; the transducers M8, M9 and M10 were dismounted from the locations as shown in Fig. 5.10 (b), and were mounted in new locations on the wall of the cylinder barrel. They had the same generator line as M1- M4. Great care was taken to ensure the interacting face of the transducer presented a minimum protrusion into the sand. The new arrangement of all the ten pressure transducers is shown in Fig. 5.25 (Transducers M1 to M7 remained the same as those shown in Fig. 3.26). All of them had a circular interacting surface of ϕ 0.12m with the solid.

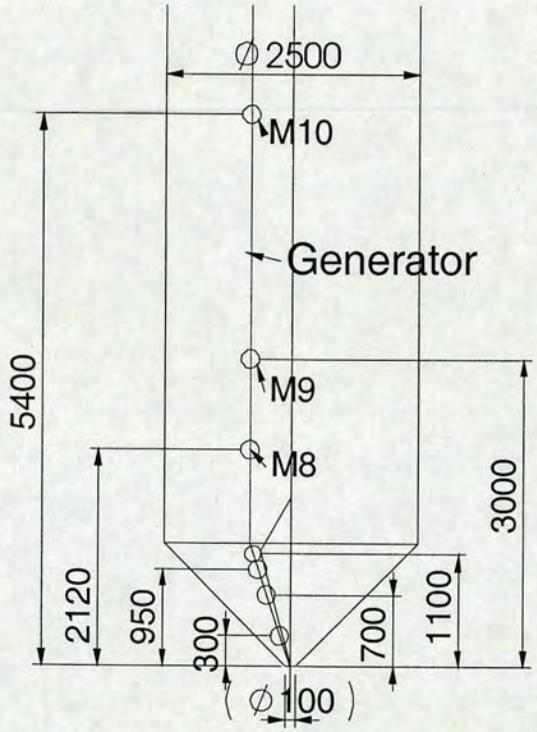

Fig. 5.25 Arrangement of pressure transducers on the wall of silo (locations of transducer M1 to M7 were identical to those shown in Fig. 3.26)

Unfortunately the amplifiers for channel of the normal force at M9 and for channel of friction force at M10 were burned out in setting up the electronic system. Considerable effort was made to recover the amplifiers but with no success. Further delays were not affordable, and decision was taken to 1.) leave the friction channel blank at M10, and 2.) to change amplifier from channel friction to channel normal force, and leave the

friction channel blank at M9. Recalibrations were carried out on all working channels (Appendix 2).

The data acquisition comprised the data logger Hydra and PC: the same as those used earlier. The logger scanned the pressure transducers at a frequency of around 1 Hz, amplified them and transferred them to the PC.

5.3.2.3 Material properties

The sand used in previous tests was not sufficient, and extra sand was purchased. The sand employed in this stage had a bulk density of 1370 kg/m^3 with a particle size ranging from 0.5 to 2 mm. It was a dry free flowing material. When it was dry, the measured repose angle was 36°. The friction angle with the wall of silo was 21.8° (μ = 0.4). Because there were some leaks through the silo roof, some water did enter the silo and mix with the sand. Material property measurements from the samples taken during some tests revealed that the water content due to the rainwater was approximately 0.2% in the sand and the friction angle with the silo wall was around 26.9° (μ = 0.51).

5.3.2.4 Experiment arrangement

Experiments were carried out to measure loads on pressure transducers for both filling and discharging. The sand was left in a state of storage for 24 hours before being discharged. Measurements of surface movement were conducted by interrupting the discharging process at certain intervals. To find what effect the insert had on the loads, parallel measurements were also performed for comparisons after removing the insert from the silo. The measurement results are reported as follows.

5.3.2.5 Measurement results from filling tests

5.3.2.5.1 Concentric filling without insert

Three filling tests were conducted. The sand was fed into the cylindrical silo at a stable feeding rate, lasting about four hours. An amount of about 45 tonnes of sand was used to fill the silo, equivalent to a height of 4500 -4700 mm high along the wall above the transition. The solid heights (measured from the transition along the generating lines where M4, M5, M6 and M7 were located) are shown in Table 5.3 when the filling

ended (see section 5.3.2.6.1 in advance). They are presented also in Fig. 5.26, which shows measurement results and their variation from the average values. The systematic lower value in the test 1 than the other two (there was a difference of 1.8% as greatest between the maximum head in test 3 and minimum head in test 1) may be due to the different shape of surcharge formed, or the sand consolidated in different fillings, or mostly likely slightly less sand was used. Table 5.3 and Fig. 5.26 indicate that even though there were some differences from test to test, the solids were fed into the silo rather concentrically in each individual filling. It was assumed therefore that, with the modification of the feeding tube (Fig. 5.23), a concentric filling was achieved.

Table 5.3 Solid head on M4 to M7 above transition (mm) (no insert)

Transducers no / Test sequences	M4	M5	M6	M7
Test 1	4517	4558	4568	4568
Test 2	4609	4660	4681	4650
Test 3	4691	4681	4629	4660

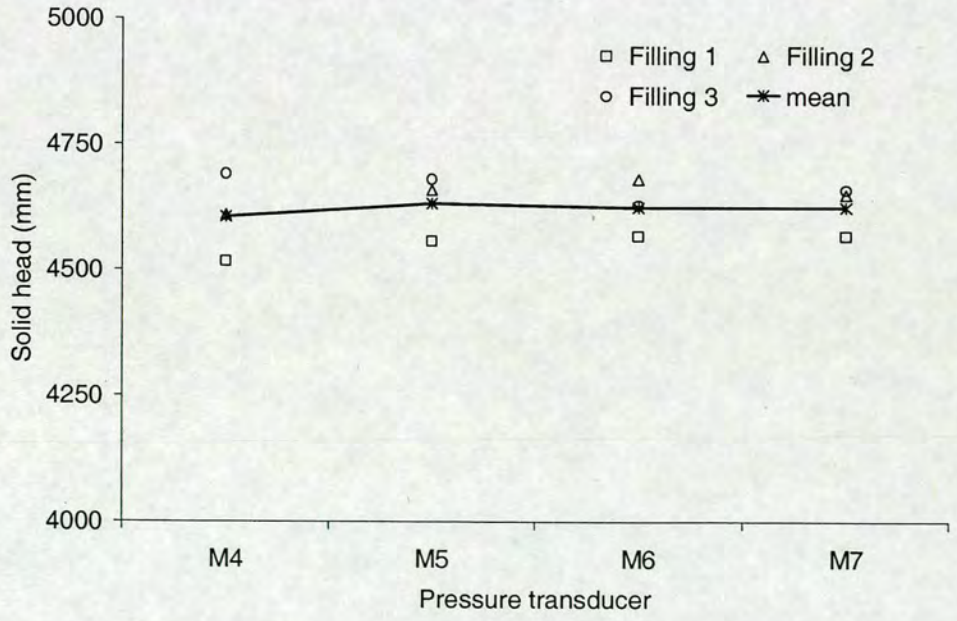

Fig. 5.26 Solid head above transition at end of filling (no insert)

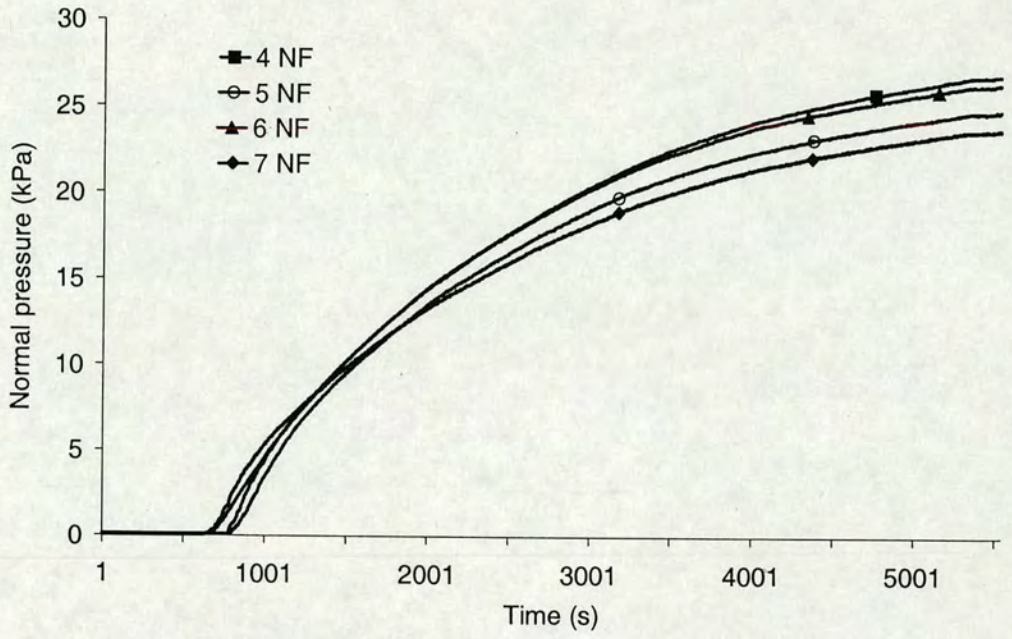

Fig. 5.27 Normal pressure development on M4 to M7 (no insert)

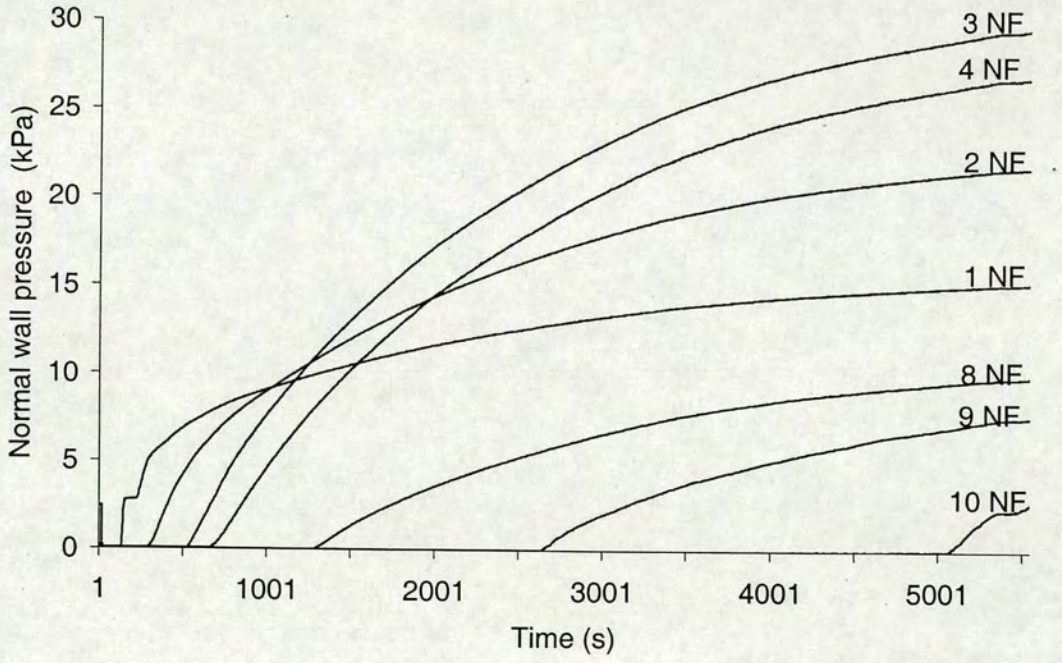

Fig. 5.28 Development of normal pressure along a generator (no insert)

Loads developed on the transducers were measured and recorded accompanying the process of filling. As an example, the data recorded for Test 2 are plotted in Fig. 5.27 for the development of normal pressure on transducers M4, M5, M6 and M7, and in Fig. 5.28 for those of normal pressure along a generator on transducers M1 to M4 and

M8 to M10. They showed the development paths of normal pressure when the sand was filled progressively into the silo.

It is clear from Fig. 5.27 that the loads induced on the M4, M5, M6 and M7 transducers, though mounted at the same level, followed different paths and reached different final values - a sign of unsymmetrical load development in a concentric filling.

The normal pressures measured at the end of filling for all three tests on transducers M4-M7 and along a generator are shown in Fig. 5.29 and Fig. 5.30 respectively, with the mean values drawn as solid lines.

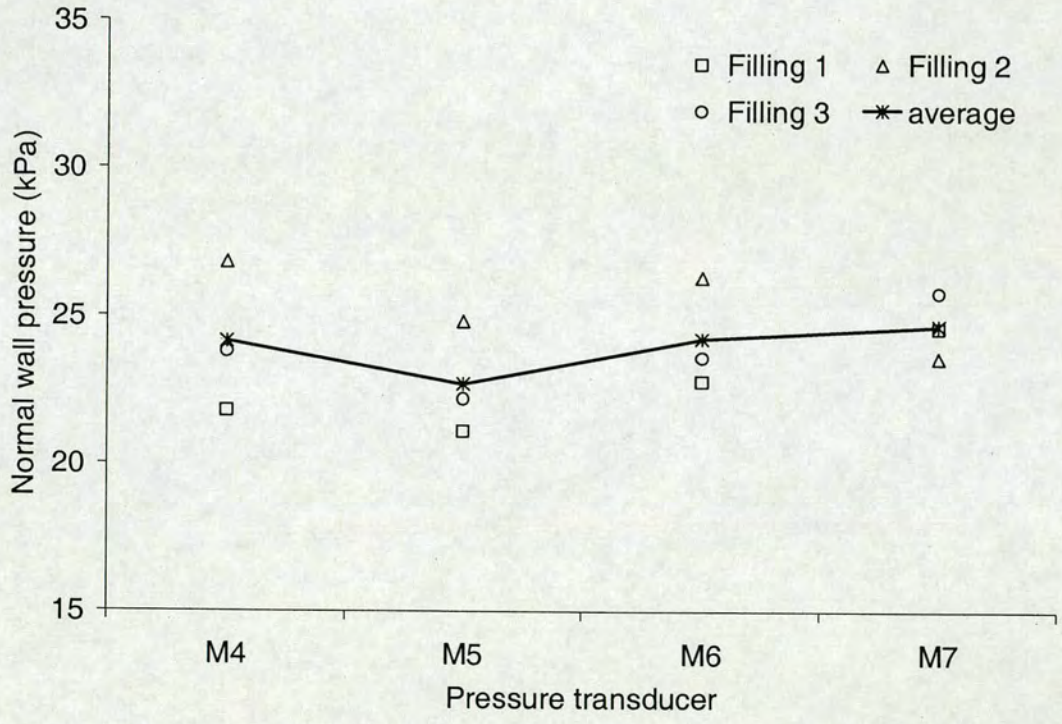

Fig. 5.29 Normal pressure on M4 to M7 at end of filling (no insert)

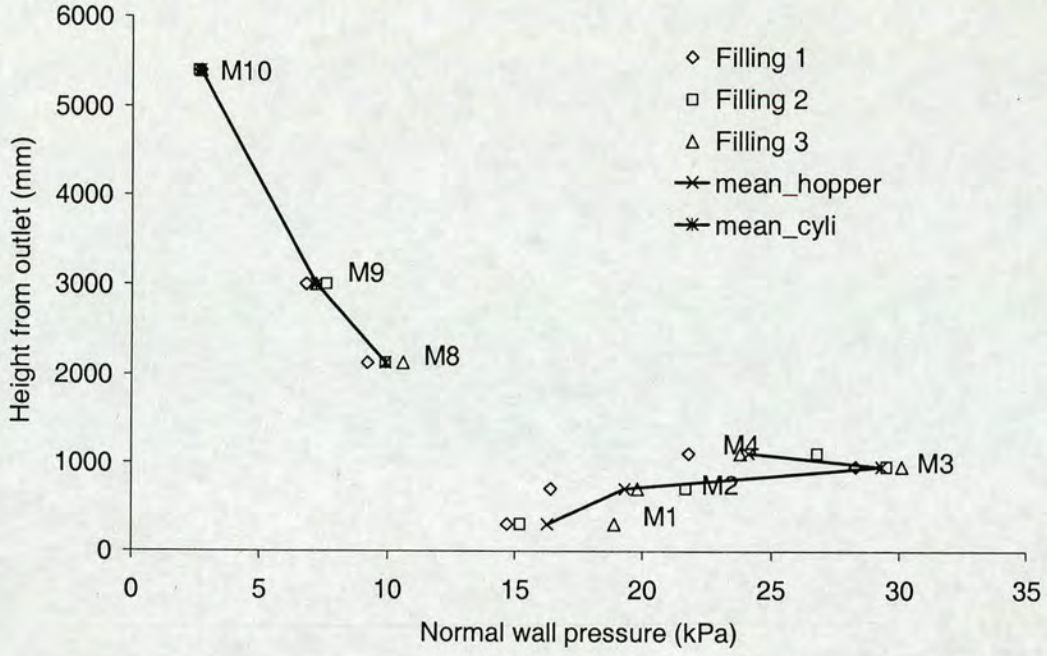

Fig. 5.30 Normal pressure along a generator at end of fillings (no insert)

From Fig. 5.29 one can see that the variation in normal pressures in each test was indeed significantly larger than the variation of solid heights (Fig. 5.26). Looking closer at the differences between the height distributions in Fig 5.26 and normal pressure distributions in Fig. 5.29, one may notice also that it was not necessary that the greater the height, the greater the load would be. For instance, the head was greater above M4 (M5) in test filling 3 than in test filling 2, while the normal pressures measured on M4 (M5) were higher in Filling Test 2 than in Filling Test 3; the head in Filling Test 1 was always lower than those in the other two fillings, but its normal pressures were however higher than those in Filling Test 2 measured on M7.

From the result as shown in Fig. 5.30, one can also see that the normal pressures in the barrel of the silo were quite different from those developed in the hopper. The normal pressure appeared to be approximately linear with head in the barrel; this trend did not exist in the hopper. Quite the contrary, the pressure was greater in the higher level than in the lower level of the hopper. From Fig. 5.30 one can see that it was not on M1 but on M3 that the maximum normal pressure was developed. It was obvious also that the load on the hopper part was much higher than that on the cylinder.

Corresponding to the normal wall pressure measurements as shown in Figs. 5.29 and 5.30, the shear stress on the transducers were also measured. Since the shear stress transducers were at fault at transducer positions M9 and M10, they are excluded in the following description.

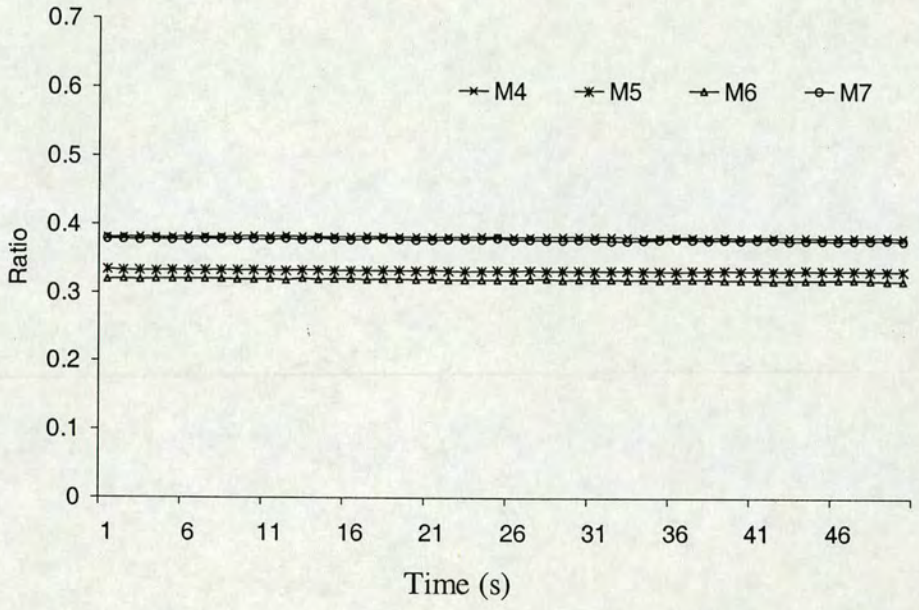

(a) Around the circumference just below the transition (at the last stage of experiment)

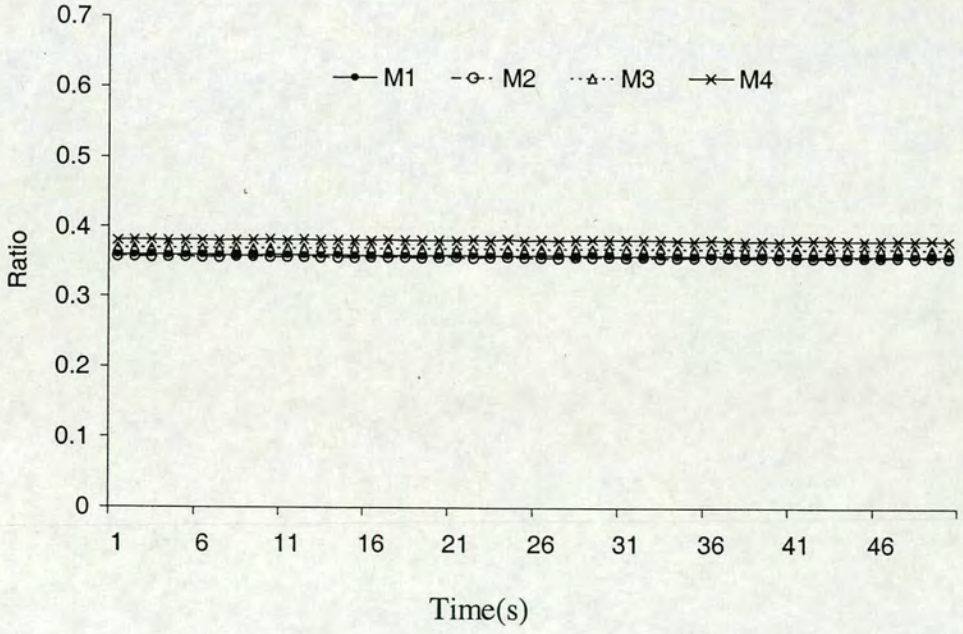

(b) Along a vertical generator (at the last stage of experiment)

Fig. 5.31 Ratio of frictional traction to normal pressure at different transducer positions (Filling Test 2, No insert)

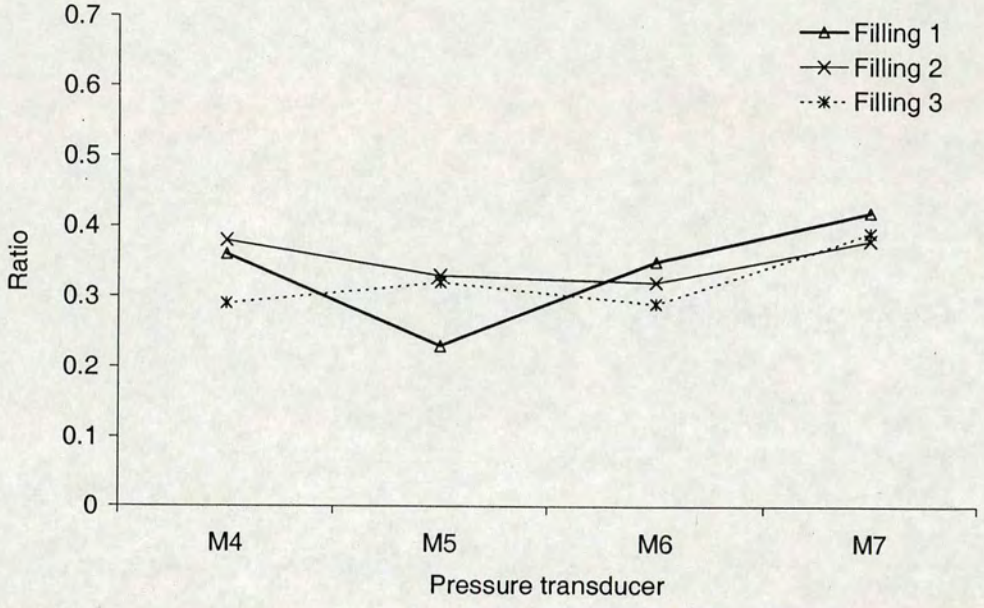

(a) Around the circumference just below the transition

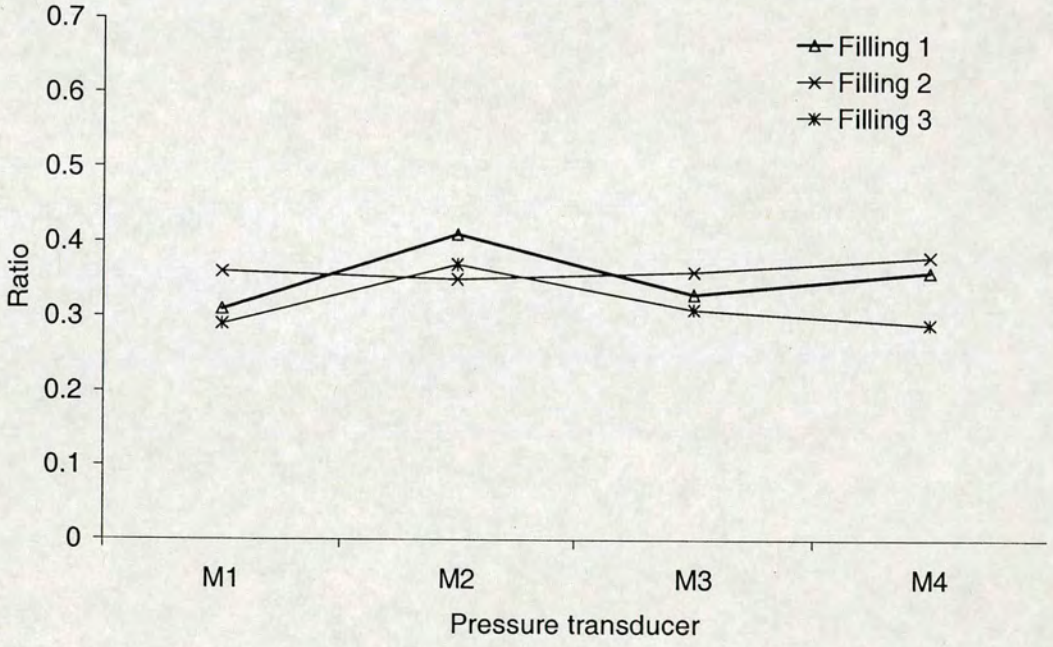

(b) Along a generator

Fig. 5.32 Ratio of frictional traction to normal pressure on transducer positions (no insert)

Sample results as recorded in the final stage of Test 2 are shown in Fig. 5.31 (a) as ratios between frictional and normal forces on transducer positions M4, M5, M6 and

M7 below the transition, and in Fig. 5.31 (b) for those on transducer positions M1, M2, M3 and M4 along a generator. Such ratios for all three tests as read at the end of filling are shown in Fig. 5. 32.

It is interesting to see from Fig. 5.31 that the development of shear stress on each individual transducer was rather stable. All of the values measured were below a value of friction coefficient 0.4 to 0.5, indicating that the limiting friction might not have been mobilised fully during filling. It was clear also that there existed some differences from transducer to transducer in each test, and from test to test as well. Among the three parallel tests, the difference may be rather small for instance as in Test 2, and may be also rather considerable for instance as in Test 1 for the values just below the transition, indicative of a potential to lose load symmetry in a concentric filling.

5.3.2.5.2 Concentric filling with insert

Four filling tests were performed with an insert. The same operating procedure, the same amount of solids and the same filling rate were used as those in the tests without an insert. Four hours were needed in each filling. The final fill heights (measured from the transition along the generating lines where M4, M5, M6 and M7 were located) are shown in Table 5.4.

Table 5.4 Solid head on M4 to M7 above transition (mm) (with insert)

Transducer no. / Test sequences	M4	M5	M6	M7
Test 1	4629	4599	4763	4711
Test 2	4640	4640	4681	4681
Test 3	4650	4640	4681	4681
Test 4	4640	4650	4650	4619

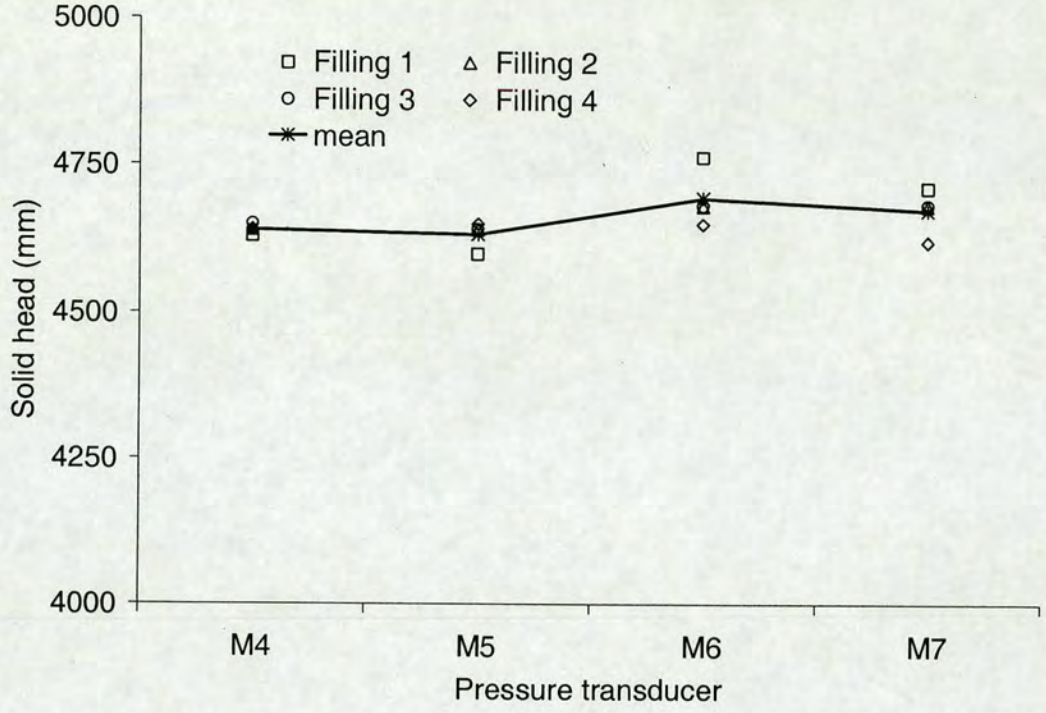

Fig. 5.33 Head above transition at end of filling (with insert)

They are presented also in Fig. 5.33, which shows their variation from the average values. From Table 5.3 and Fig. 5.33, it is seen that the solid head in each filling were close to the mean value: it was regarded that a concentric filling was achieved.

Normal pressures at the end of filling for all four filling tests at transducers M4, M5, M6 and M7 and along the generator are shown in Fig. 5.34 and Fig. 5.35 respectively, with mean values shown in solid lines.

From Fig. 5.34 one could see that the normal pressure exerted at M4, M5, M6 and M7 was not symmetrical either. The values of mean normal pressures had also some differences from one transducer to another. Referring to the solid head as shown in Fig. 5.33, one might find also that it was not always the case that the greater the sand head, the higher the normal pressure. For instance, the heads were quite close to each other above M4 in all four filling tests, the normal pressure measured was, however, noticeably lower in Filling 1 than in the other three (which were very close). Above M7 the head was highest in Filling 1 and at the average in Filling 2, but the normal pressure measured was lowest in Filling 1 and greatest in Filling 2.

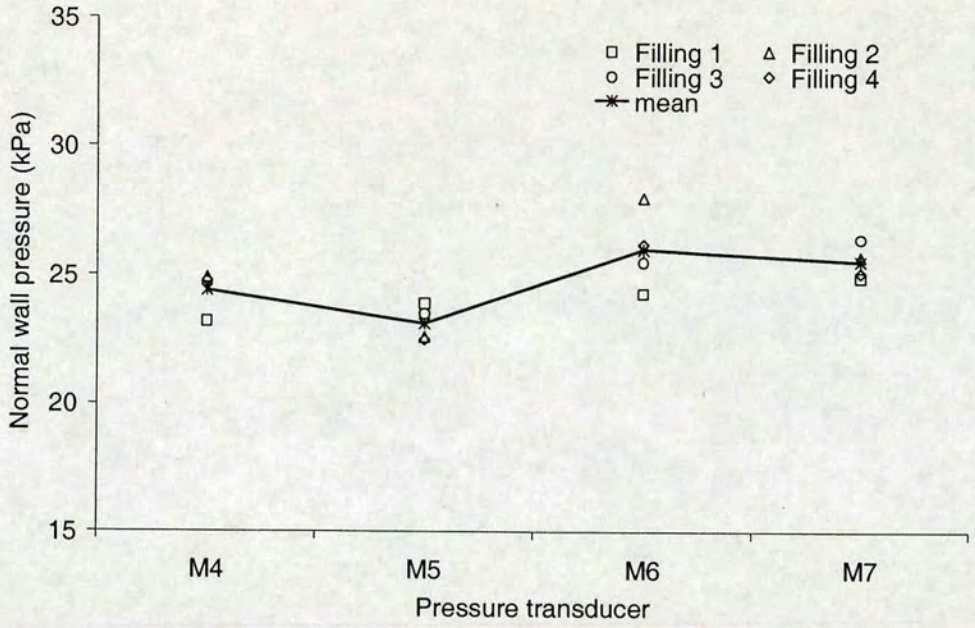

Fig. 5.34 Normal pressure on M4 to M7 at the end of filling (with insert)

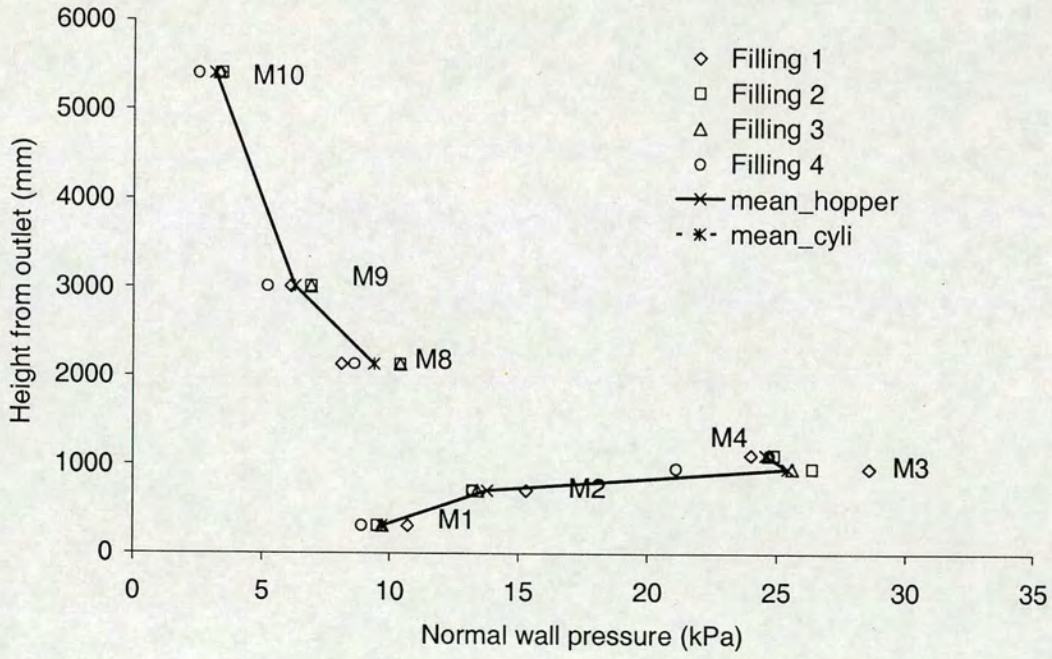

Fig. 5.35 Normal pressure along a generator at the end of filling (with insert)

It is seen also that the normal pressure development in the barrel of the silo was quite different from those developed on the hopper walls, as shown in Fig. 5.35. The normal pressure appeared to increase with solid depth in the barrel; there was not such a trend

in the hopper; on the contrary, the pressure was greater at the higher levels than the lower. From Fig. 5.35 one can see that pressure on M3 remained the greatest with a wide range of variation. The hopper endured much higher normal pressure than the barrel of cylinder.

Accompanying the measurements of normal wall pressure, the shear stresses on the transducers were also measured. As an example, the ratio of frictional and normal force measured in the final stage of Filling 4 is plotted in Fig. 5.36 (a) for transducer positions M4, M5 M6 and M7, and in Fig. 5.36 (b) for transducer positions M1, M2, M3 and M4. Such ratios as read at the end filling in all four tests on M4, M5, M6 and M7 and on M1, M2, M3 and M4 are shown in Fig. 5.37 (a) and (b).

The difference between the ratios measured from one transducer to another are noticeable (Fig. 5.36), even though in an individual transducer, the ratio was rather stable. Also it is quite obvious that there existed some differences from test to test (Fig. 5.37). The ratio varied considerably along the generator, and lost symmetry even in a concentric filling carried out carefully in the current tests.

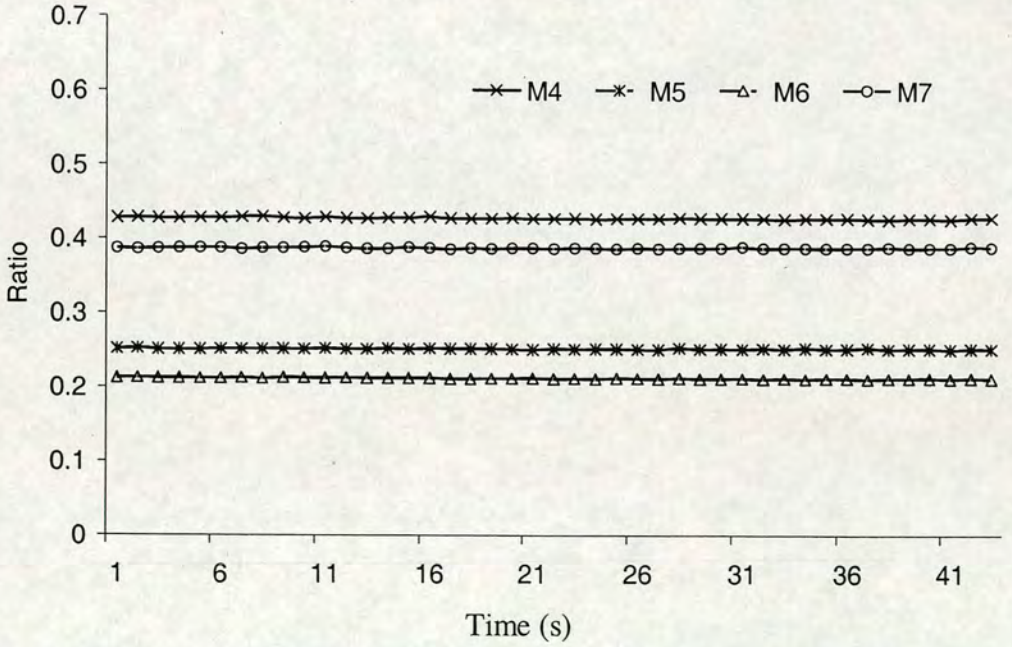

(a) Around the circumference just below the transition (at the last stage of experiment)

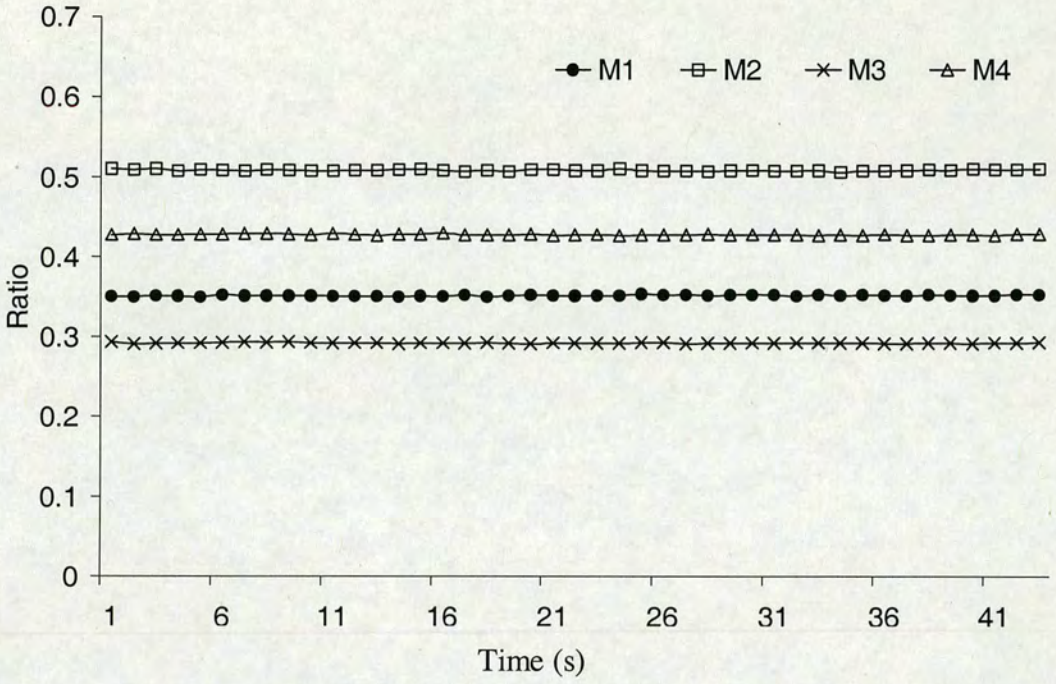

(b) Along a generator

Fig. 5.36 Ratio of frictional traction to normal pressure (Filling 4, with insert)

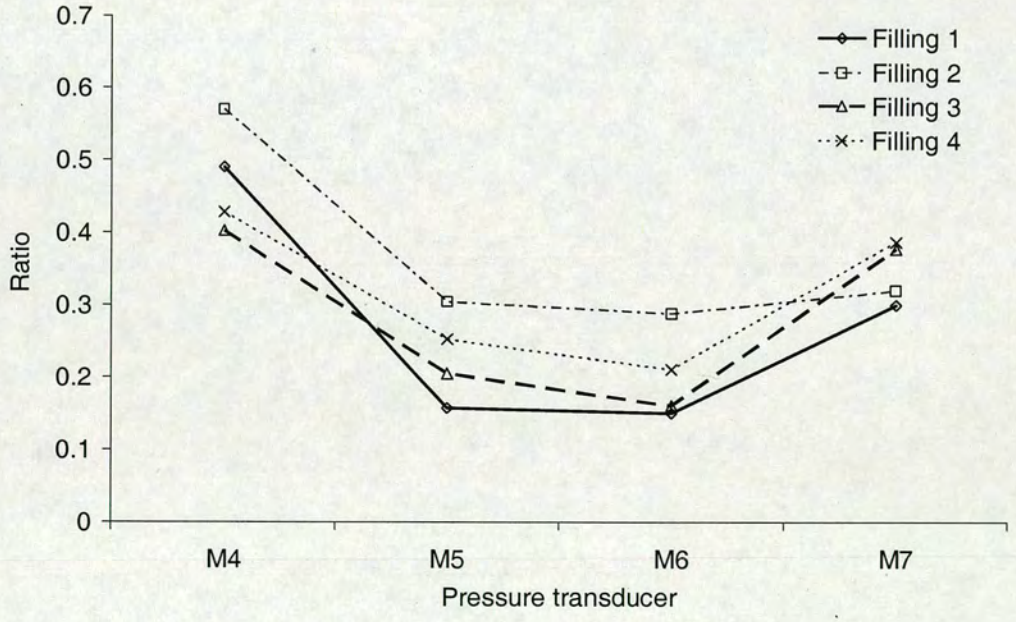

(a) Around the circumference just below the transition

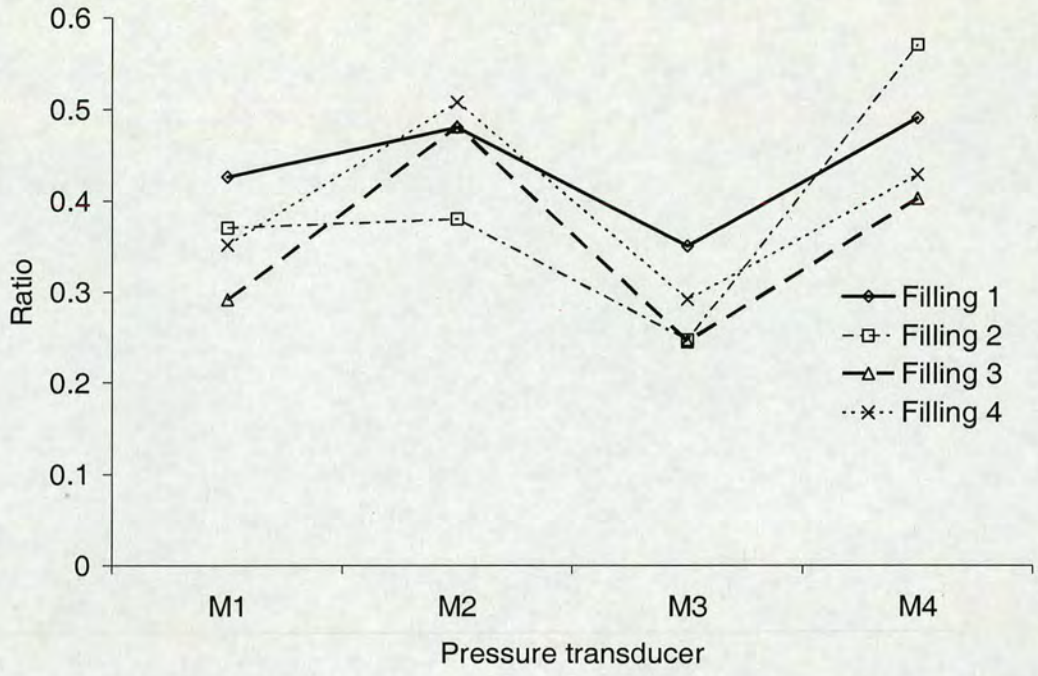

(b) Along a generator

Fig. 5.37 Ratio of frictional traction to normal pressure at the end of filling (with insert)

5.3.2.5.3 Comparison

Since the same amount of sand was used in all the tests whether there was an insert installed or not, the volume of this insert could contribute to some differences of the solid head built up during filling. In addition, the sand fed into the silo would hit the insert first and then spread and redistribute around at the beginning of filling, a process which is different from the one in the absence of an insert. This process could last until the insert was buried. As a result, the installation of an insert could affect the building up of the solid head during filling as shown Fig. 5.38, which shows the average head above the transition of three filling tests in the absence of insert and of the four filling tests in the presence of insert. From Fig. 5.38, one can see that the installation of an insert might lead to a slight loss of solid head symmetry even under the same concentric filling condition.

Starting from the difference caused by the insert in the process of filling, the load developed along the wall when there was an insert installed certainly would be different from those exerted on the wall when there was no insert. Such differences of

normal wall pressure just below the transition and along a generator are shown in Fig. 5.39 and Fig. 5.40, while the ratio of frictional traction and normal pressure is plotted in Fig. 5. 41.

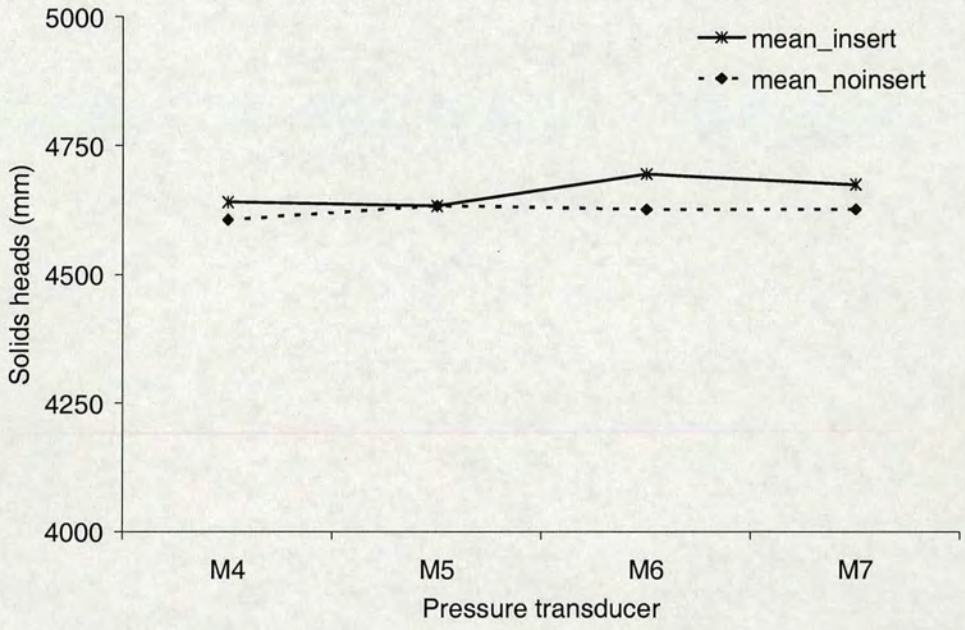

Fig. 5.38 Head difference in presence / absence of insert

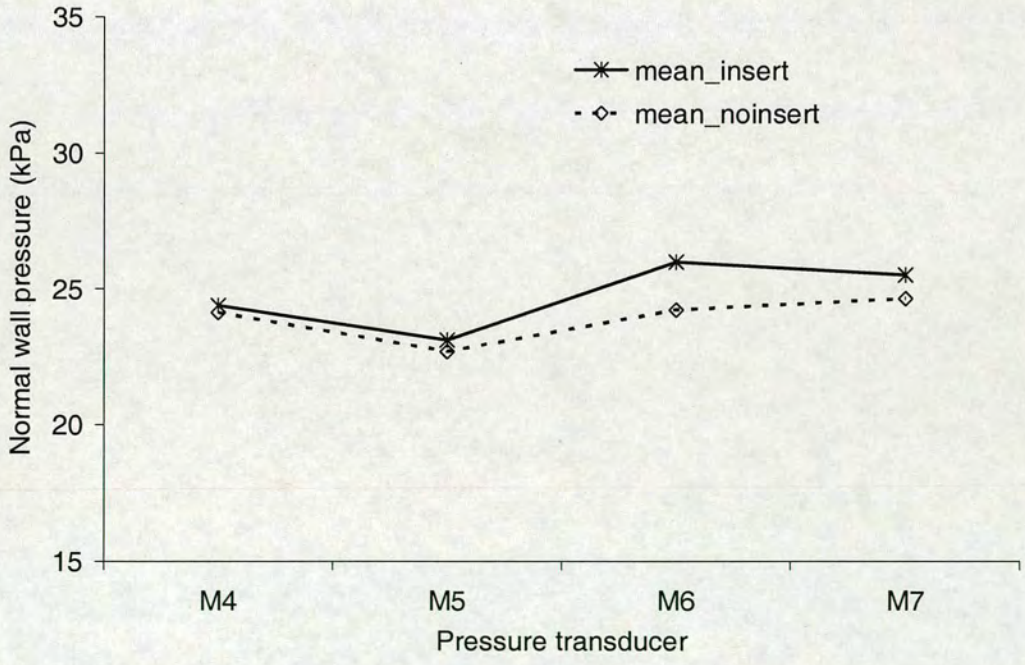

Fig. 5.39 Effect of insert on normal pressure on M4-M7 at the end of filling

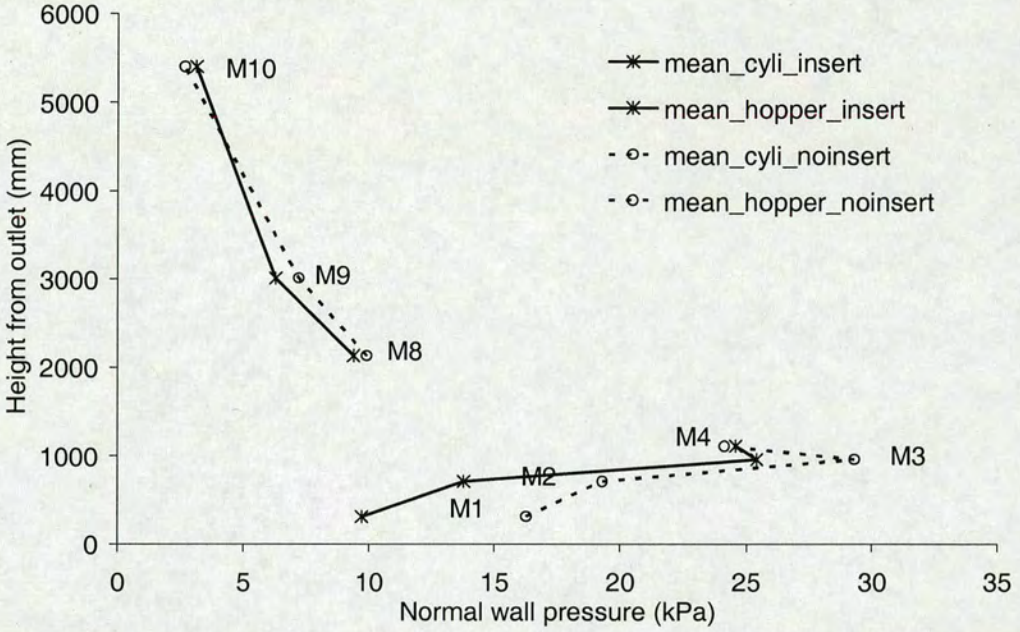

Fig. 5.40 Effect of insert on normal pressure along a generator at the end of filling

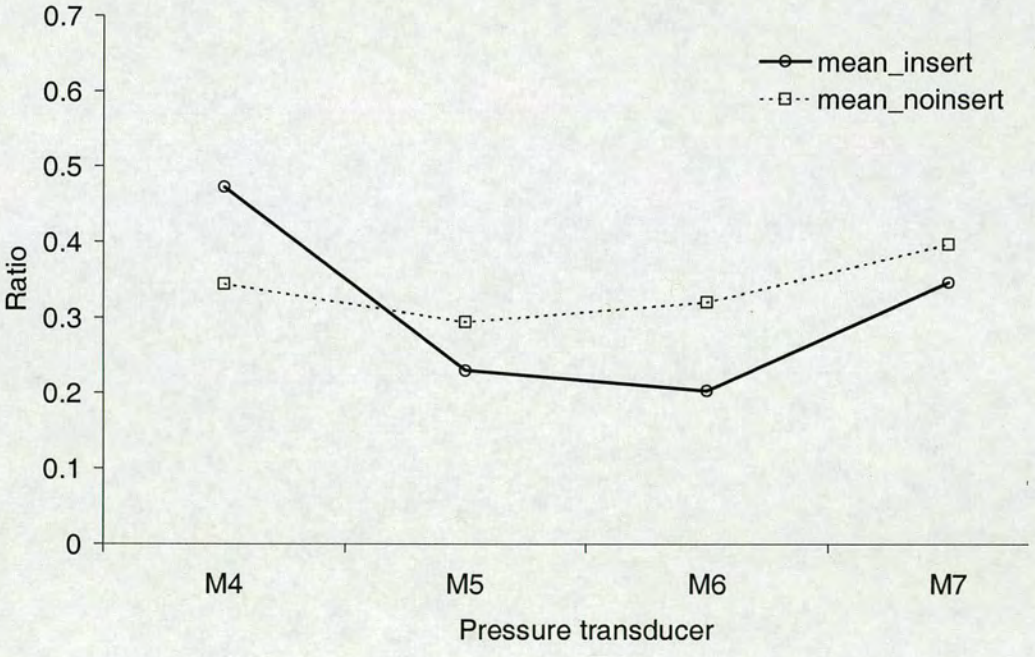

(a) Around the circumference just below the transition

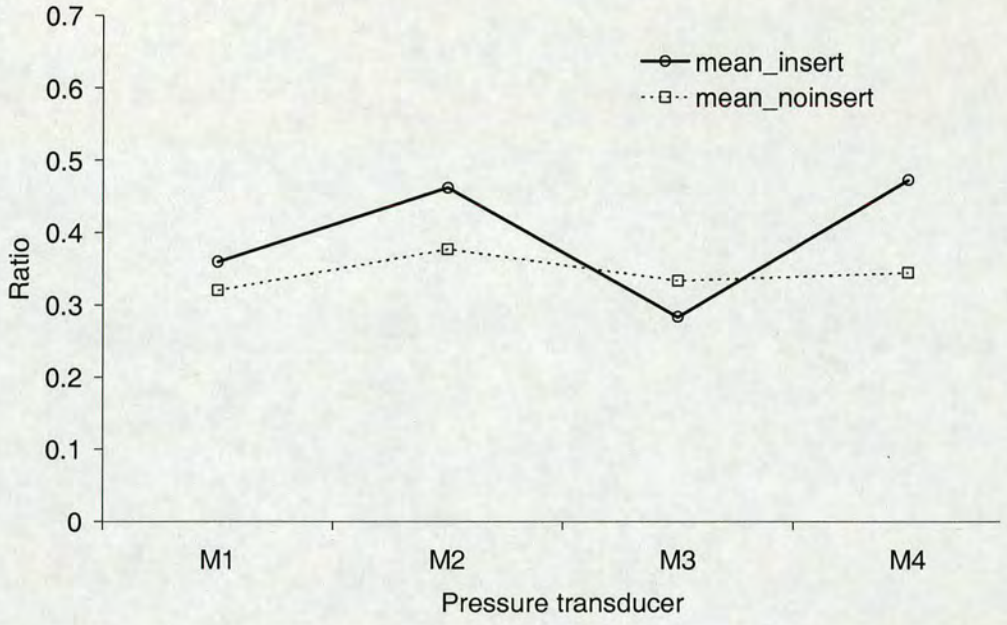

(b) Along a generator

Fig. 5.41 Effect of insert on ratio of frictional traction to normal pressure at end of filling

Figure 5.39 is in fact showing the average value of normal wall pressure given in Fig 5.29 for the three fillings in absence of an insert and the average value of normal wall pressure given in Fig. 5.34 for the four fillings in presence of an insert based on results from the transducers M4, M5, M6 and M7. It could be inferred from Fig. 5.39 that installation of an insert under the current configuration (see Fig. 5.25) might lead to a slight increase of normal pressure at the transition level, and its unevenness as well.

Similarly, Fig. 5.40 consists of the average value of normal wall pressure given in Fig 5.30 and Fig. 5.35 on the transducers mounted along the generator. It is clear from Fig. 5.40 that while the influence of the installation of an insert on the normal pressure on the wall was quite limited in the barrel of silo (a small increase), the effect of such an insert were great on the normal pressure in the hopper of the silo (a dramatic decrease). One may speculate that the insert must have taken a considerable portion of solid load, and therefore reduced the loads directly exerted on the walls of the hopper.

Figures 5.41 (a) and (b) show respectively the average value of ratio between frictional traction and normal wall pressure on transducers M4, M5, M6 and M7 below the

transition and on transducers M1, M2, M3 and M4 along a generator in absence / presence of an insert. It is evident form Fig. 5.41 (a) that, while the friction was not mobilised, the ratio of frictional traction and normal pressure appeared to be in some degree symmetrical in a concentric filling without an insert. However, this symmetry was hard to retain in the presence of an insert. As demonstrated in Fig. 5. 41 (b), the frictional traction/normal pressure ratio was rather stable along a generator line in absence of insert, but might vary considerably in presence of insert.

5.3.2.6 Measurement result during discharging

The solid in the silo was discharged when the valve (Fig. 5.24) opened. The valve was opened fully, and the solid was regarded to be discharged freely. The solid discharged was transported by the screw feeder 1, the bucket elevator and the two way screw feeder and fed back into the rectangular silo. The surface movement of solid and the loads on walls in the cylindrical silo were both measured during discharge.

5.3.2.6.1 Surface profile measurement during discharge

Depending on the flow pattern, which itself required investigating, the solid dropped down and could form different surfaces. Such a surface profile was measured in anticipation of gaining information about a possible flow pattern. Admittedly such information is rarely enough to interpret the flow pattern a silo might cause. Never the less, the surface profile measurement was carried out.

The possibility of automated systems for such measurements was investigated. For example using sound distance measurement system was vetoed due to the cost involved. A manual approach was adopted.

Closing the valve, the discharge was interrupted. The profile of the sand surface formed at that moment was obtained by manually measuring with a laser meter (Leicha DISTO Classic, right) the vertical distances between the newly formed surface of solid (surface S_s) and the plane of hatch (P_h) at the silo top at some designated positions A and B (see Fig. 5.42).

As shown in Fig. 5.42, A represented the intersection points by

the edge of hatch with P_g (P_g were planes created by generators of M4 and M6 (or M5 and M7, diametrical opposite)); B the intersection points of radius (the OB on the silo top) with the intersection line of P_g and the inner surface of silo barrel; C intersection points by the inner surface of silo barrel, P_g and S_s, and D the intersection points by lines shot down vertically from A with S_s.

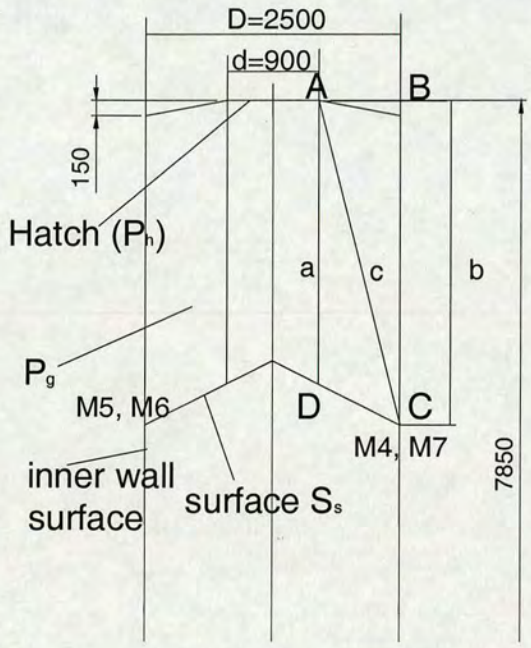

Fig. 5.42 Method for surface profile measurement

The depths AD (*a*) and BC (*b*) were measured directly or indirectly. AD (*a*) was measured directly by DISTO, while BC (*b*) was obtained by measuring AC (*c*) first according to

$$b = \sqrt{c^2 - \left(\frac{D-d}{2}\right)^2}$$

The values of *a* and *b* measured in different stages of discharge were then used to build a surface contour (C-D) to represent surface profiles of discharge. Before the discharge started the values a and b were measured. They were used to identify the head of filling (that I 7850 – b mm) as in Table 5.2 (Fig. 5.26) for the tests without insert and in table 5.3 (Fig. 5.33) for the tests with insert.

At the beginning of discharge, the solid started to move. Observation showed that this movement occurred only in a small zone in the centre when there was no insert; it was reasonably uniform. By contrast, when there was an insert present, this movement appeared to have a larger moving zone compared with that without insert.

Eventually such movements turned the heap (formed during filling) into a dip. Before the dip developed deep enough, it was observed that the solid close to wall had some downward movement when the insert was installed; it was hard to see such movement when there was no insert in position.

When the angle of the dip increased, the surface became steeper and steeper, the sand started to slide. When there was no insert, the sliding was rather even along the surface of the dip and the diameter of the dip gradually increased. Overall, the stored solid was to some degree discharged evenly. When there was an insert, an uneven surface was observed, the solid tilted to one side (mostly M4, M7), and a gentle skewed pattern developed.

Interrupting the discharges, the movement of surface was monitored, and the surface profile was obtained by measuring the depths a and b at certain intervals. Examples are shown in Fig. 5.53 as representatives for the discharging 3 in the tests with no insert (left) or with an insert (right). There were respectively five such measurements in each example, marked with surfaces profiles at five levels from 1 to 5 downwards.

In Fig. 5.43, the values a and b measured in diametrically opposite positions were plotted in same plane, i.e. the a, b measured at M4 side were axi-symmetrical to the a, b measured at M6 side, marked with a solid line to represent the surface on either side; similarly, the a, b measured at M5 side were axi-symmetrical to the a, b measured at M7 side, but marked with a dash line to represent surface on either side. The a, b measured at M4, M7 were at the same side, and those measured at M5, M6 shared another side. The average angle was the mean value of the acute angles of the solid and dash lines with the horizon ($\alpha_s = \tan^{-1}\frac{2(b-a)}{D-d}$).

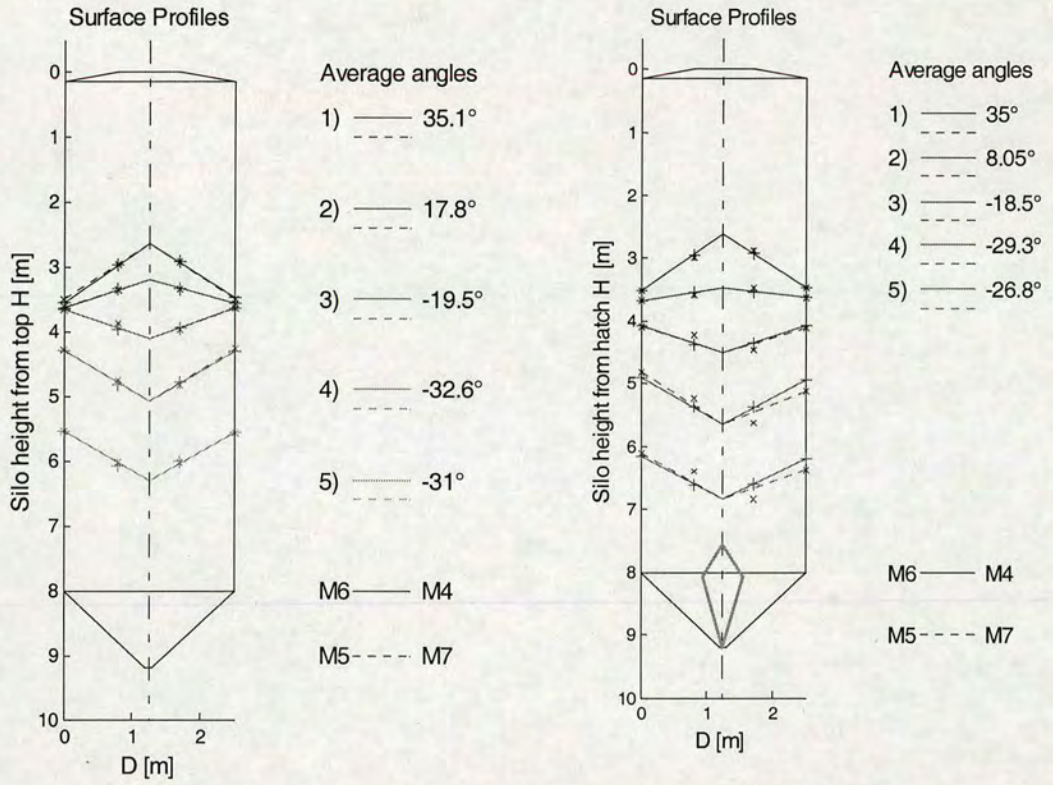

(a) No insert (discharging 3)

(b) Insert present (discharging 3)

Fig. 5.43 Surface created during discharge (numbered as 1 to 5 downwards)

Surface 1 represented a heap formed at the moment of filling (before discharge); with a surface angle very close to the repose angle. This heap surface moved downwards when discharge started. Before the heap turned into a dip represented as surface 2 in Fig. 5.43, the solid close to the wall had also some movements in the presence of the insert, a movement remarkably different from that when no insert was in position. After a dip was formed as represented by surfaces 3, 4 and 5, one may see that 1.) the surface angle of this dip was greater in absence of insert than that in presence of insert; 2.) the movement of surface remained symmetrical in the tests with no insert; such a surface movement, however, turned asymmetrical in the tests when an insert was in position as shown in Fig. 5.53 (right), skewed to M4 and M7 side in the example given.

From the measurement results described above, one may speculate that the installation insert might have enlarged the solid moving zone in discharge while at the same time causing an unevenness of such discharge. However, to what degree it may have affected the flow pattern of discharge it is difficult to say since the information provided by the surface measurements are barely enough or far from convincing.

5.3.2.6.2 Loads measurement at commencement of discharge

It has been recognised that the state of stress developed within solid undergoes a change at beginning of discharge. Such a change causes a redistribution of stress within solid and leads to a shift of load on the wall accordingly. The experiment at this stage concentrated on monitoring and measuring such a load shift.

5.3.2.6.2.1 Insert absent

The solids filled into the silo was discharged after 24 hour storage. There were in all three fillings when there was no insert, and three discharges were carried out. Normal pressure measured on M4, M5, M6 and M7 and on M1, M2, M3, M4, M8, M9 and M10 at the initiation of discharge are shown respectively in Fig. 5.44 and Fig. 5.45 for all three discharges, with the mean values in solid lines. In a similar category, the average values of normal pressure at the end of the three fillings as given in Fig. 5. 29 and Fig. 5.30 are shown also in Fig. 5.44 and Fig. 5.45 in dash line for comparison purpose.

It is seen in Fig. 5.44 that the variations of normal pressures exerted on the M4, M5, M6 and M7 transducers at the commencement of discharge were also considerable in each test, a sign of unsymmetrical load development during discharge. Comparing the average value (solid line) with the one of filling (dash line), it is apparent there was an increase of such loads at the start of discharge, along with a similar tendency of asymmetric character.

As shown in Fig. 5.45 the normal pressure developed in the barrel of the silo were quite different from those developed on the silo hopper at the beginning of discharge. The normal pressure appeared to be linear with head in the barrel; however, this normal pressure, quite the contrary, appeared approximately to be linear with head in

reverse in the hopper, with the maximum located in a region around M3. It was obvious also that the load on the hopper part was much higher than that on the cylinder. Comparing the average value (solid line) with the one of filling (dash line), one may see that normal pressure had some increases in the barrel, but remained unchanged in the hopper (except in M4 region close to the transition).

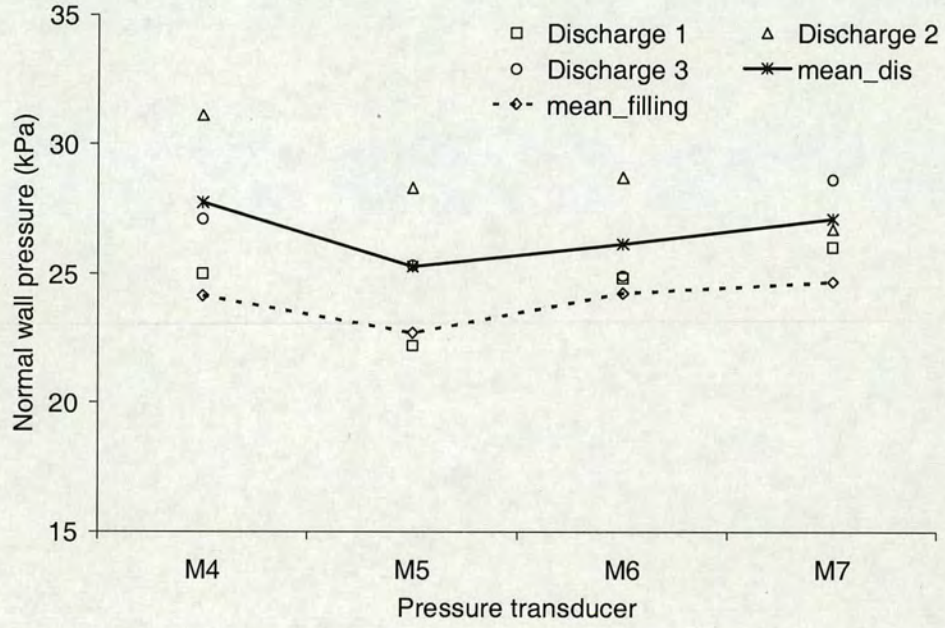

Fig. 5.44 Normal pressure on M4-M7 (no insert)

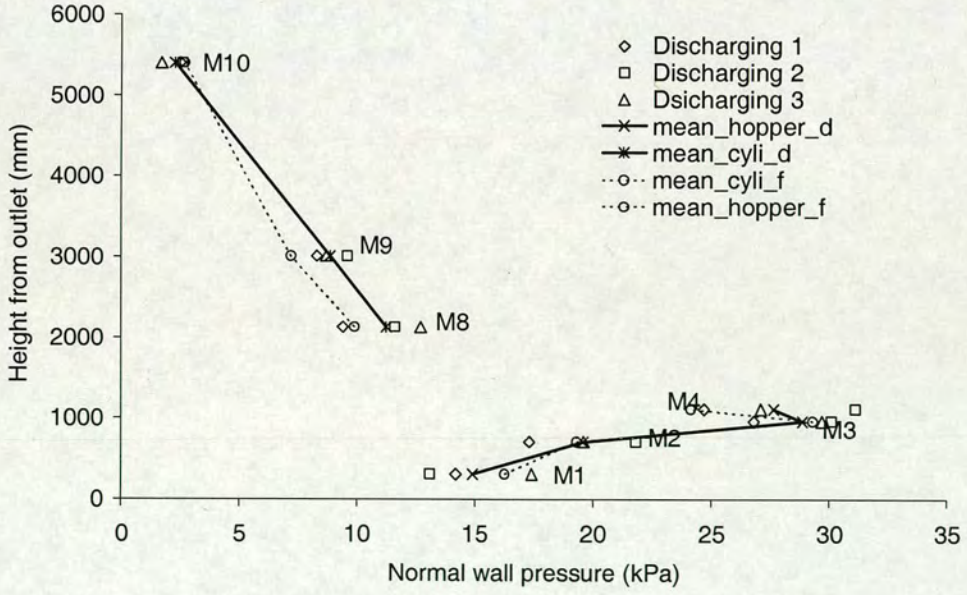

Fig. 5.45 Normal pressure along a generator (no insert)

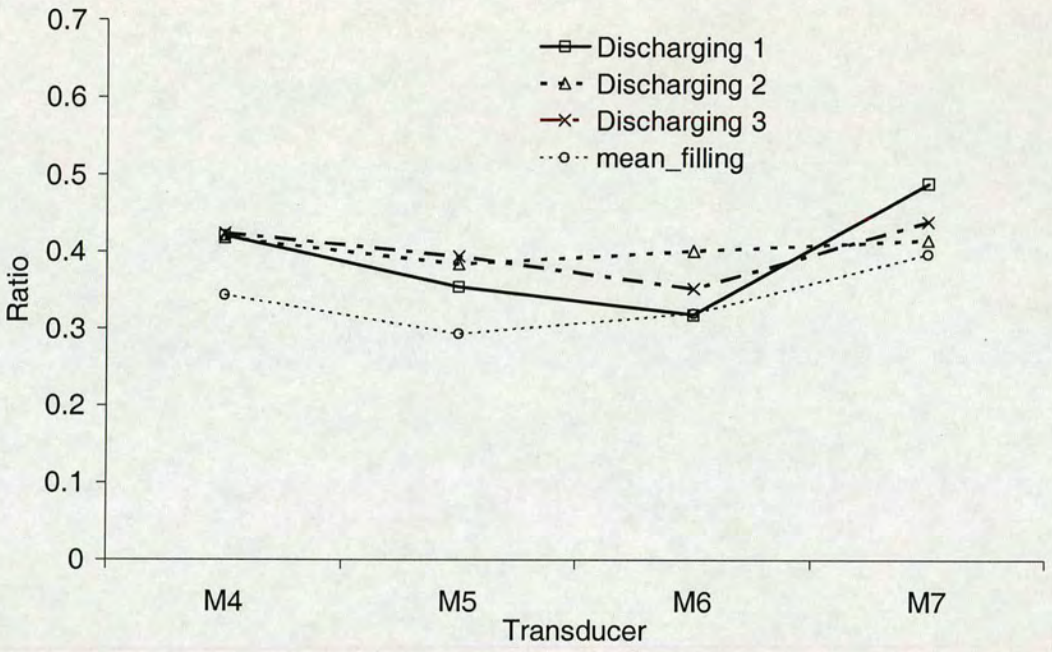

(b) Around the circumference just below the transition

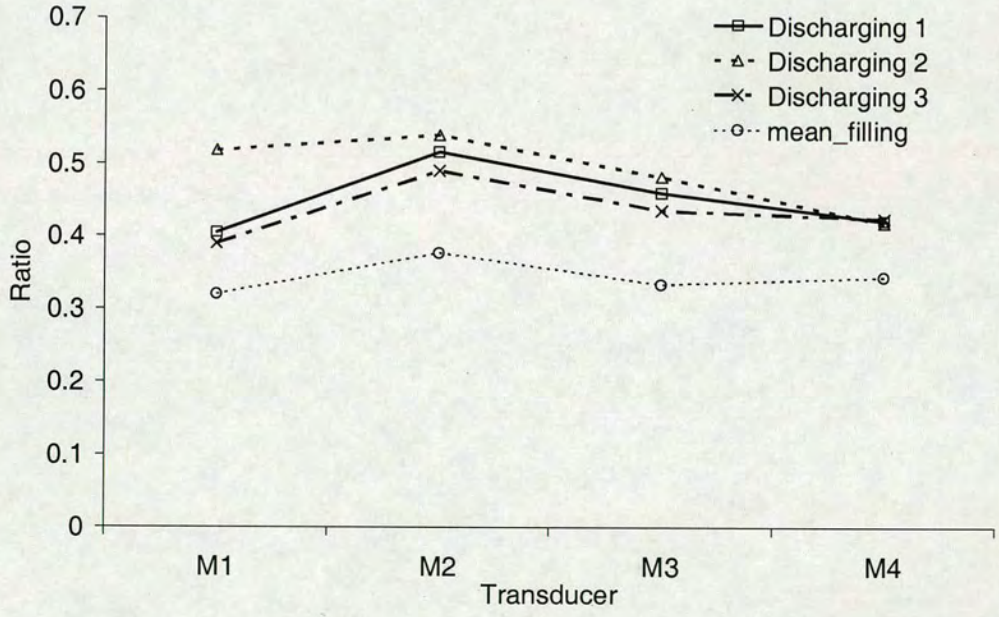

(b) Along a generator

Fig. 5.46 Ratio of frictional traction to normal pressure (no insert)

Also the shear stress on the transducers was measured. Results are shown in Fig. 5. 46 (a) as ratios between developments of friction and normal forces on transducers M4, M5, M6, M7 and in Fig. 5.46 (b) for those on transducers M1, M2, M3 and M4. For

comparison the average ratios of the frictional traction and normal pressure, as in Fig. 5.32, are fitted into Fig. 5.46 in a similar way.

It is interesting to see from Fig. 5.46 that, although there were some increases for ratios measured in all transducers, all values were still below the friction coefficients (0.51). The friction remained immobilised, indicating that there would be no movement for the solid close to the wall. It was clear also that there existed some differences from transducer to transducer in each test, and from test to test as well. Among the three parallel tests, the difference may be rather small for instance as in test 2, and may be also rather considerable for instance as in test 1, indicative of a potential for a loss of load symmetry in a concentric filling.

5.3.2.6.2.2 Insert present

Matching the four fillings in a configuration of silo with an insert, four discharges were carried out. The results measured at initiation of discharge are shown in Fig. 5.47 and Fig. 5.48 for the normal pressure developed on M4, M5, M6 and M7 and on M1, M2, M3, M4, M8, M9 and M10, with the mean values in solid lines. The average values of normal pressure at the end of the four are shown in Fig. 5.47 and Fig. 5.48 (in light dash line) similar to those in Fig. 5.34 and Fig. 5.35.

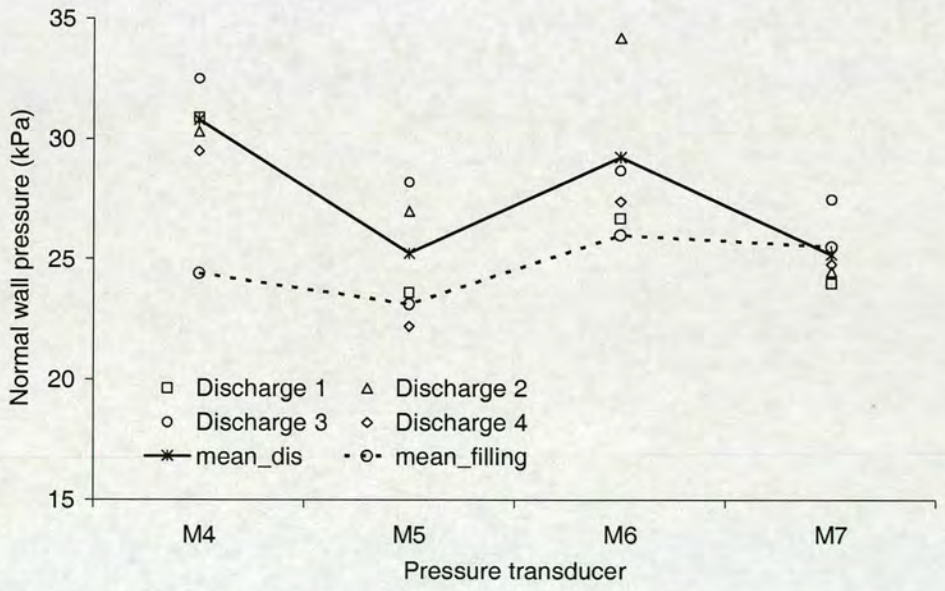

Fig. 5.47 Normal pressure on M4-M7 (with insert)

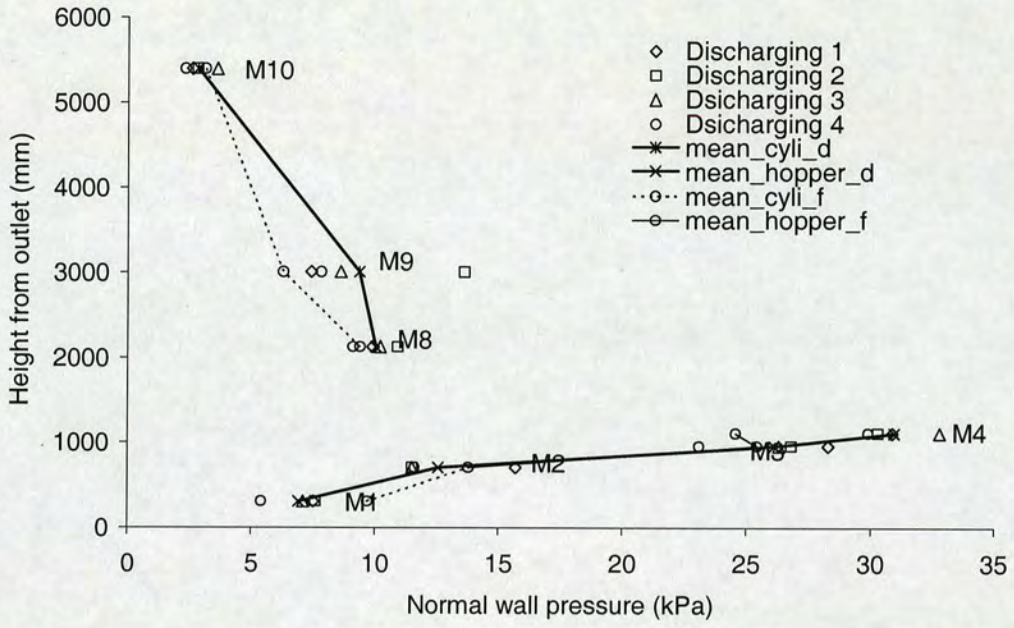

Fig. 5.48 Normal pressure along a generator line (with insert)

Comparing the average value (solid line) with the one of filling (dash line) as in Fig. 5.47, it is clear that there were increases of normal pressure on M4, M5 and M6 at the start of discharge. The asymmetric nature of filling loads was developed further during discharge. One may see also that the variations of normal pressures exerted on transducers M4, M5, M6 and M7 were sometime quite great in each test as for example during discharge 2. An unsymmetrical load is very likely during discharge.

As shown in Fig. 5.48, it is easy to notice that, compared with the results measured without insert, there were considerable increases of normal pressure on M9 and M4, while almost no changes on M1, M2 and M3. The pressure exerted on M4 became the greatest. The load on the hopper part remained much higher than that on the cylinder.

A presentation similar to that in Fig. 5.37 is used in Fig. 5.40 for the results of shear stress on the transducers, namely as ratios between developments of friction and normal forces on transducers M4, M5, M6, M7 and the transducers M1 to M4, along with the average ratio of the frictional traction and normal pressure as in Fig. 5.37.

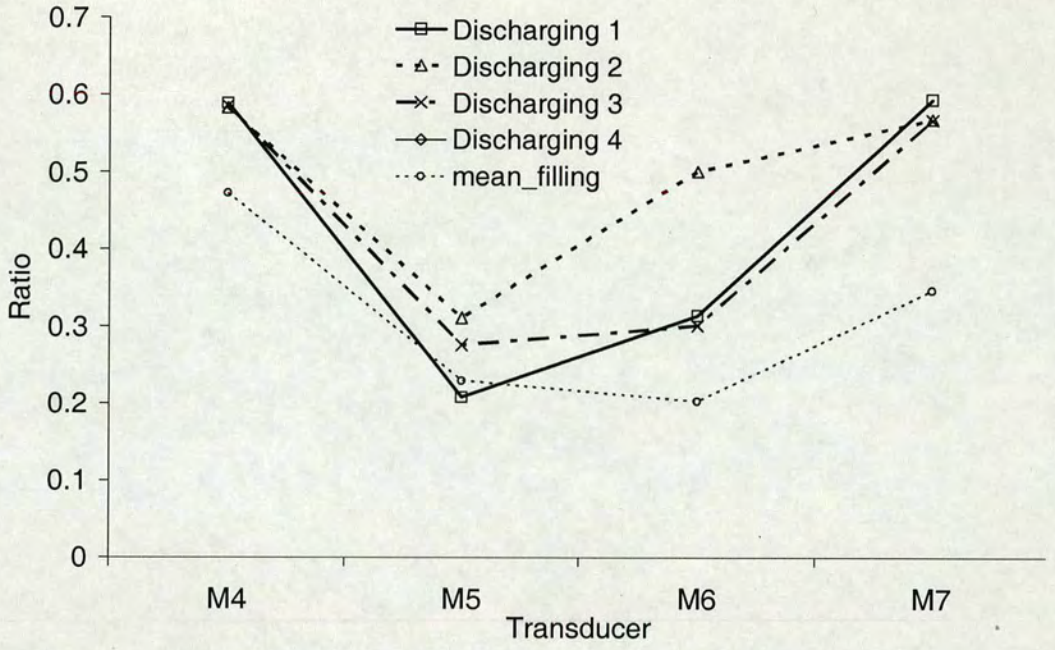

(a) Around the circumference just below the transition

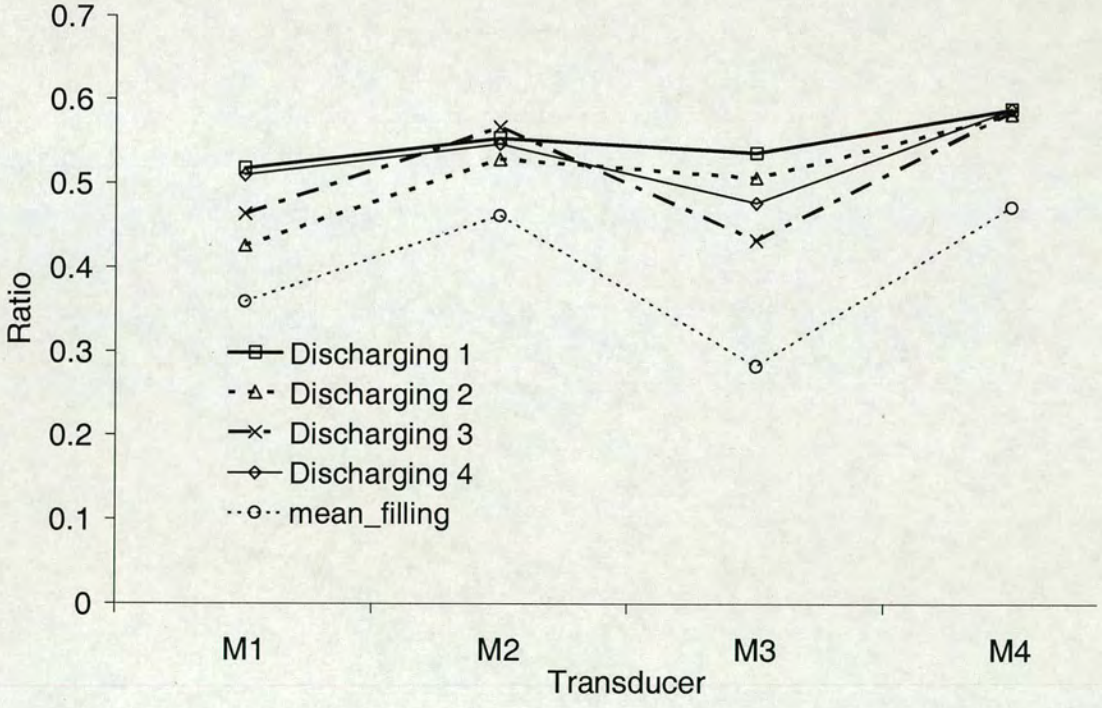

(b) Along a generator

Fig. 5.49 Ratio of frictional traction to normal pressure (with insert)

The striking feature in Fig. 5.49(a) is the unevenness of the ratio between frictional traction and normal pressure developed circumferentially below the transition. In the region where M4 and M7 were located, the friction might have been well mobilised, while in the region where M5 and M6 were located, it was far below the friction coefficient value. Such unevenness indicated an uneven discharge tendency, and might well lead to a skewed discharge, a consequence as has been seen already in the surface measurement, see Fig. 5.43.

The ratio between the frictional traction and normal pressure in the hopper (on M1 to M4 specifically) could vary substantially along a generator. In the present study it was found that there were some increases of such ratios on M1, M2, M3 and M4; the increases were greater in some cases than others, depending on the side to which the discharge might may be skewed. For instance, the ratios in discharge 1 were all higher than the friction coefficient (0.51), indicating to a potential for the solid close to the wall to move along the wall- to which the discharge might have skewed, while in the other three discharges, such ratios were not always greater than the friction coefficients (0.51) - it was unlikely for the solid to have movement along the wall.

5.3.2.6.2.3 Comparison

As a result of the differences built up in a process of filling in absence / presence of insert, as shown in Fig. 5.39, Fig. 5.40 and Fig. 5.41, the normal wall pressure and frictional traction might develop further in the process of discharging. Comparisons of such developments are shown in Fig. 5.50 and Fig. 5.51 for normal pressure as measured on transducers at the commencement of discharge, and in Fig. 5.52 for the corresponding ratio between frictional traction and normal pressure.

Figure 5.50 shows the average normal wall pressure of Fig 5.44 in absence of insert and the average normal wall pressure of Fig. 5.47 in presence of insert on the transducers M4, M5, M6 and M7. It is demonstrated by Fig. 5.50 that the installation of an insert led to an unevenness in distribution of normal pressure at the transition level.

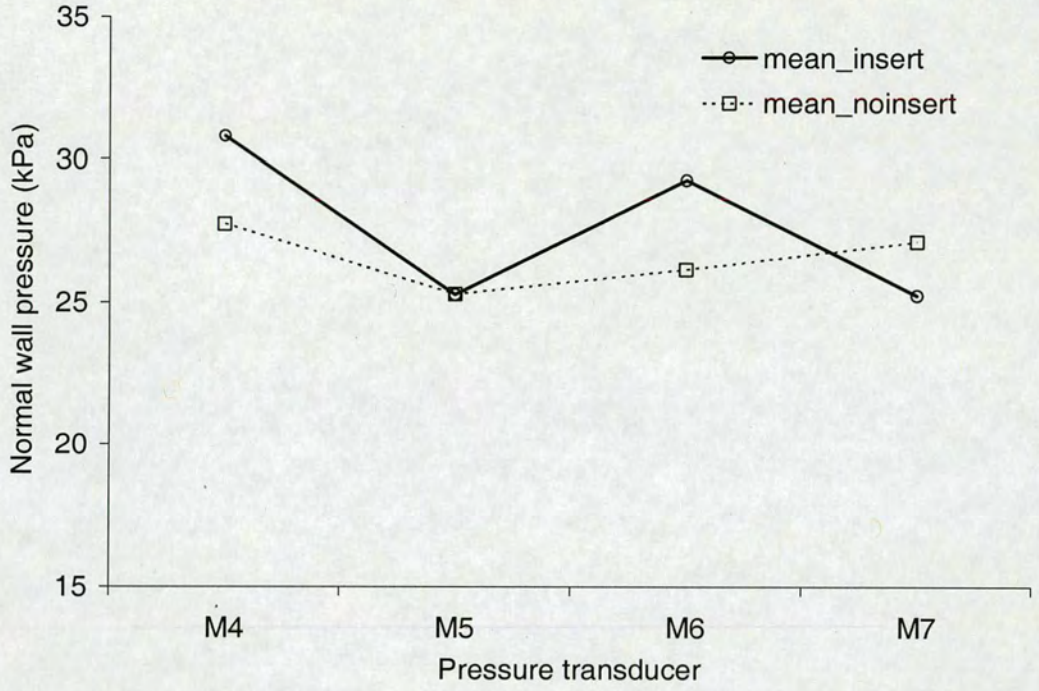

Fig. 5.50 Effects of insert on normal wall pressure on M4-M7 (at commencement of discharge)

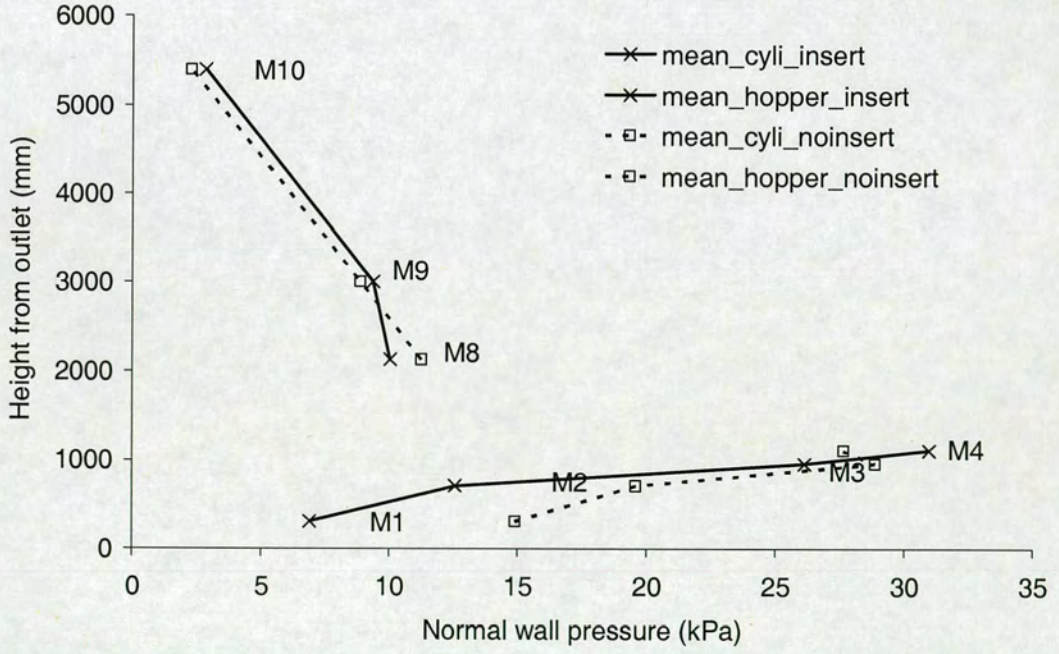

Fig. 5.51 Effect of insert on normal pressure along a generator (at commencement of discharge)

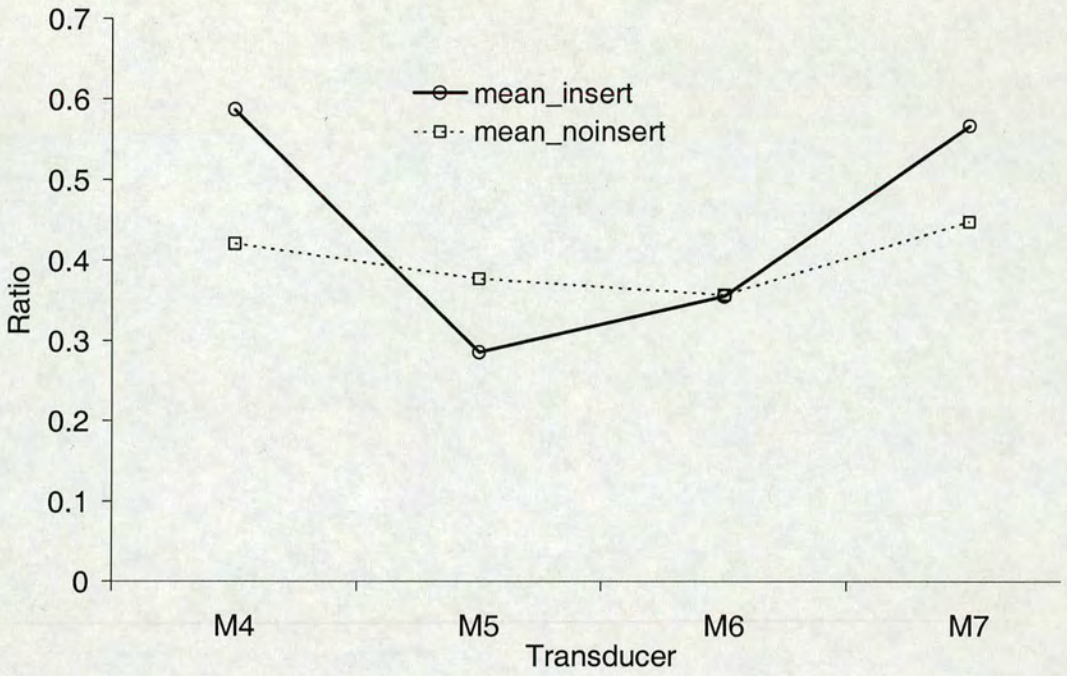

(a) Around the circumference just below the transition

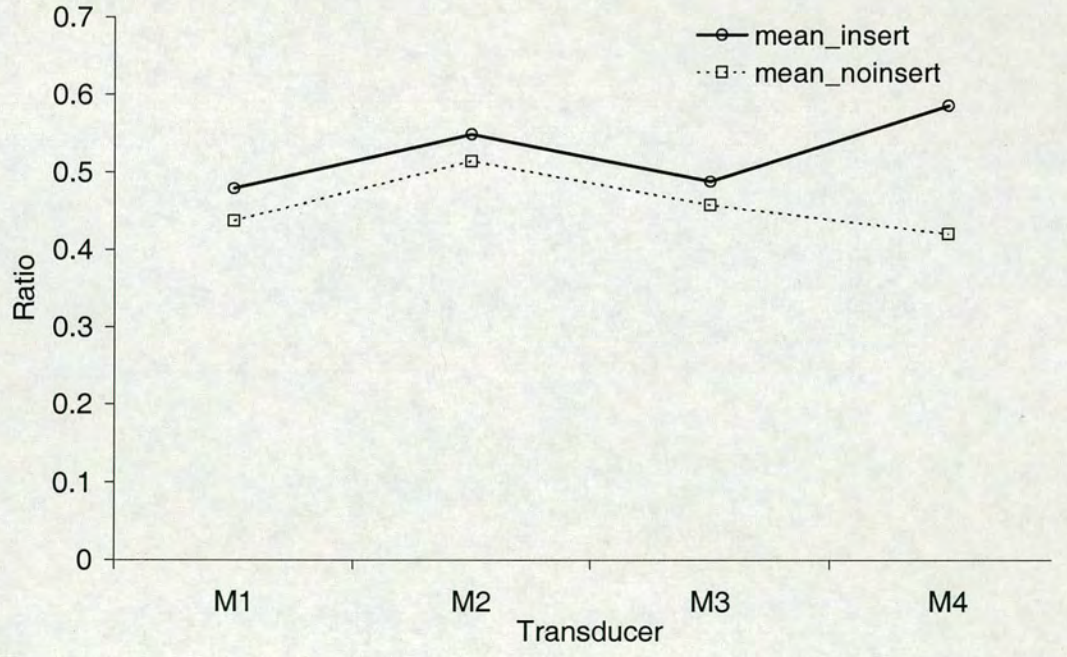

(b) Along a generator

Fig. 5.52 Effect of insert on ratio of frictional traction to normal pressure (at beginning of discharge)

Figure 5.51 consists of the average normal wall pressure of Fig 5.45 in absence of insert and the average normal wall pressure of Fig. 5.48 in presence of insert on the transducers M1, M2, M3, M4, M8, M9 and M10. it can been seen from Fig. 5.51 that the installation of an insert, while raising only slightly the normal pressure on the wall in the barrel of silo, increased substantially such pressure in a region close to the transition in the hopper. Also insert presence reduced considerably such pressure in the lower part of hopper. One may speculate that the insert must have taken a considerable portion of solid load, and therefore reduced the loads exerted directly on the hopper walls.

Figures 5.51 (a) and (b) show respectively the average value of ratio between frictional traction and normal wall pressure on transducers M4, M5, M6 and M7 and on transducers M1, M2, M3 and M4 in absence / presence insert at the initiation of discharge. From Fig. 5.52 one may see that the friction along the wall was not mobilised in the absence of insert; it might have been mobilised in presence of insert, but appeared to be limited in certain regions. The ratio of frictional traction and normal pressure developed without insert tended to be more symmetrical than that developed with insert. In fact, it is likely that a very uneven distribution of this ratio in presence of an insert could put the process of discharge at risk of losing symmetry.

5.3.2.6.3 Load measurement during discharge

With the identification of surface profiles, the loads developed during the discharge were measured. Data recorded indicated that, after the increase at the starting moment, the loads started to decrease in the process of further discharging. Samples from the measurements carried out are shown in Fig. 5.53 for the development of normal pressures on transducers M4, M5, M6 and M7 and in Fig. 5.54 for those on transducers M1, M2, M3, M4, M8, M9 and M10.

Figure 5.53 (a) shows the normal pressure development on the transducers M4, M5, M6 and M7 in a test where there was no insert. For almost half the period of discharge, the pressure declined slowly before starting to decrease quickly; the relative symmetry of normal pressure, consistent with the surface movement as in Fig. 5.43, was retained. In Fig. 5.53 (b) it is seen that the normal pressures exerted on individual transducers

were relatively stable for long periods after initial increases. The asymmetry stemming from the initial jumps persisted during a large part of discharge. A closer examination of the developments of normal pressure reveals that the unevenness was greater in the early stages.

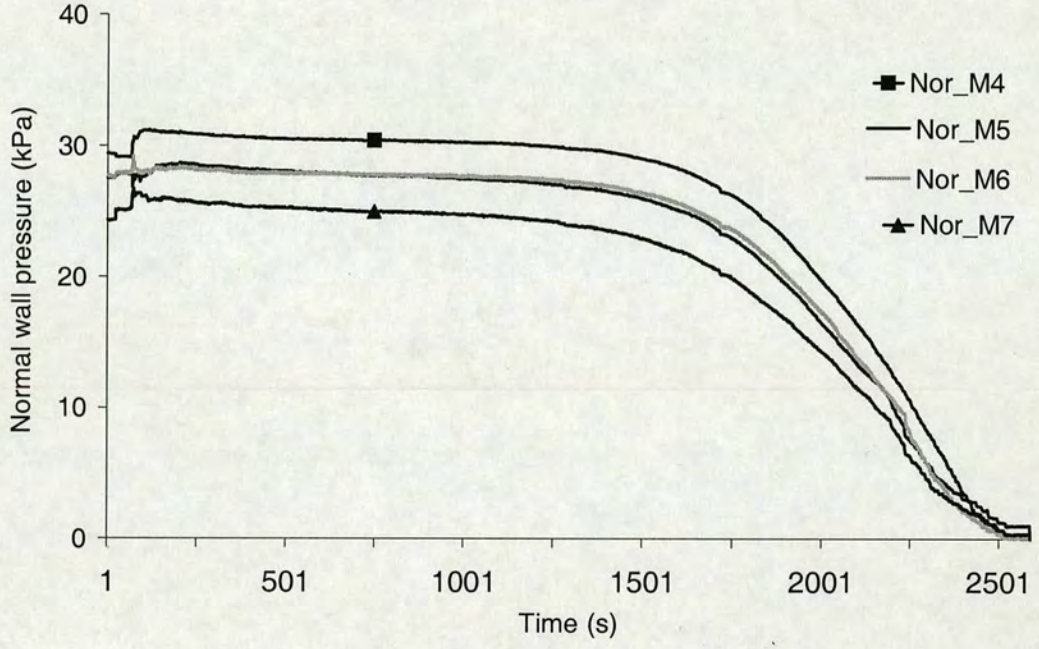

(a) No insert (Test 3)

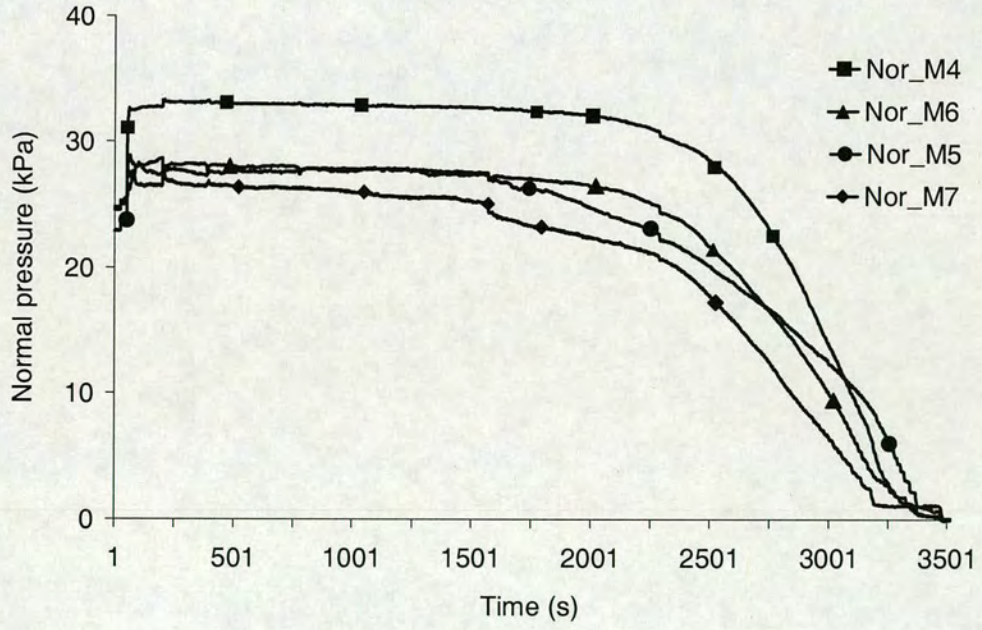

(b) Insert present (Test 3)

Fig. 5.53 Development of normal pressure just below transition during discharge

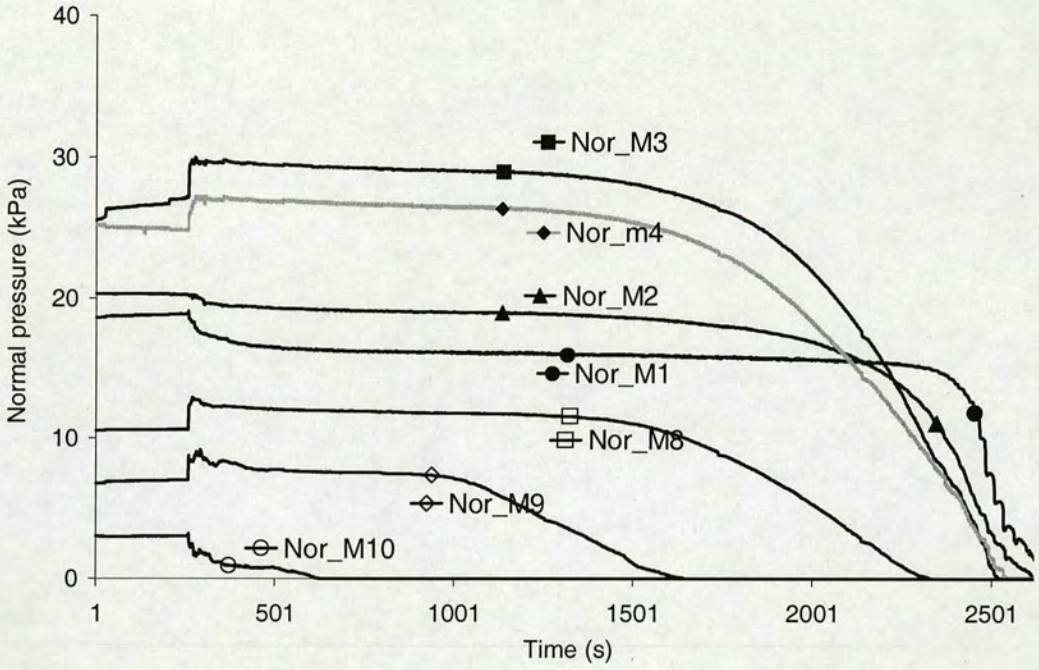

(a) No insert

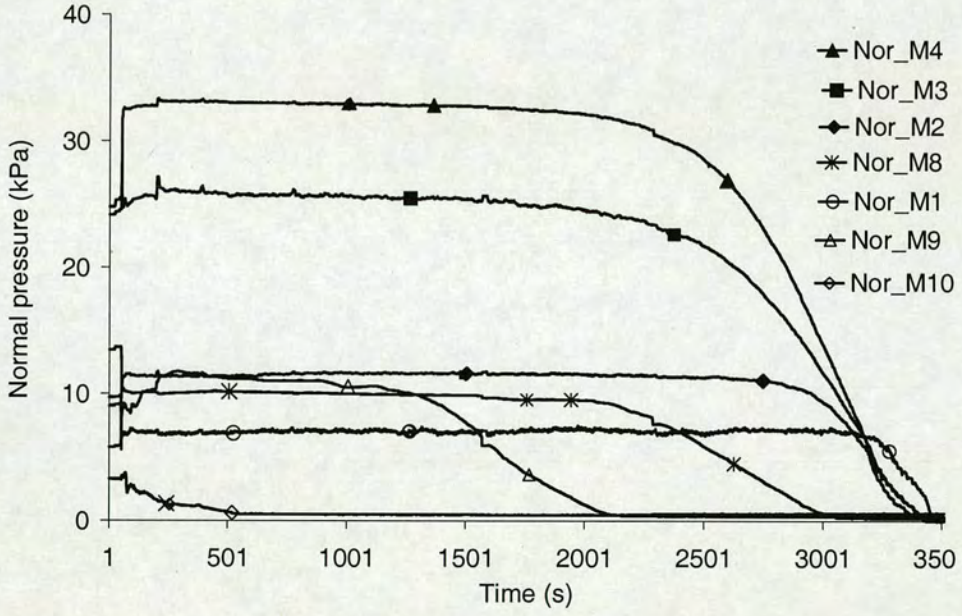

(b) Insert present

Fig. 5.54 Development of normal pressure along a generator during discharge

Figure 5.54 shows the developments of normal pressures on transducers along a generator. The most distinguished differences an insert caused might be the loads on M3 and M4: after the initial increases, the pressure on M3 developed to be greater than that on M4 when there was no insert; whereas when an insert was installed, the

pressure on M4 was greater than that on M3. The pressures on M1, M2 (lower part of hopper), after experiencing slight decreases at the beginning of discharge, remained rather stable for most of the time before decreasing rapidly in the very last stage of discharge, no matter whether or not an insert was presented. However, in value they were both lower in the presence of insert than in absence of insert. This was consistent with the pressures developed during filling (Fig. 5.40). Also shown in Fig. 5.54 is that the effect of an insert on the pressure imposed along the wall of the barrel of a silo might be limited.

The developments of frictional traction during discharge as measured on the pressure transducers mounted in the hopper are shown in Fig. 5.55 (a) when no insert was present and in Fig. 5.55 (b) when an insert was in installed. These results are presented in the form of the ratio between frictional traction and normal wall pressure, with the values highlighted at the commencement of discharge. Such ratio as measured in an individual transducer was rather stable throughout for most of discharge period.

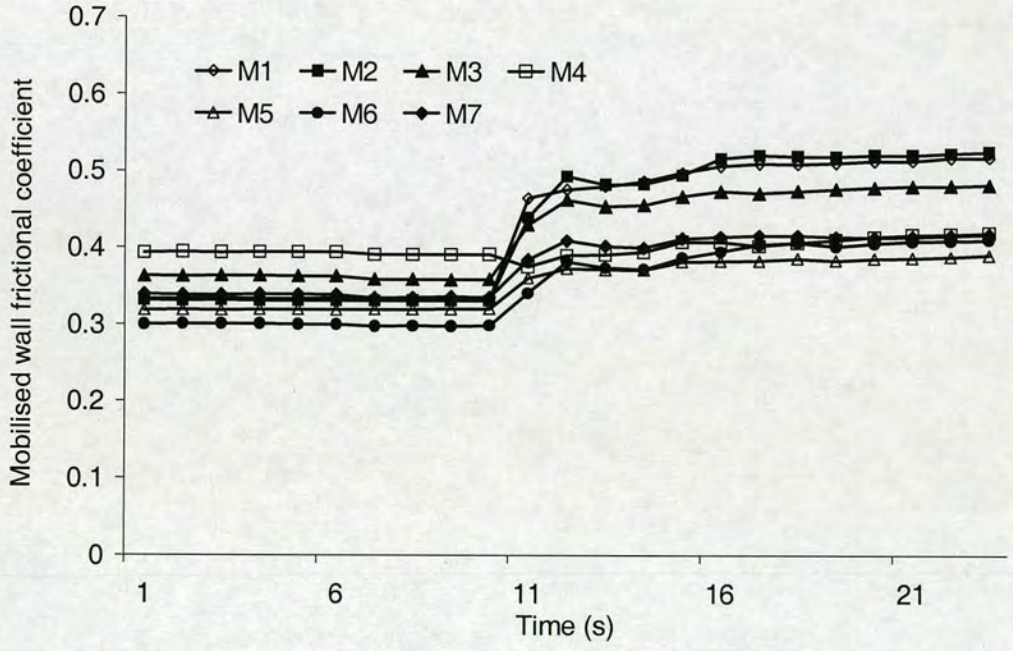

(a) No insert (Test 3)

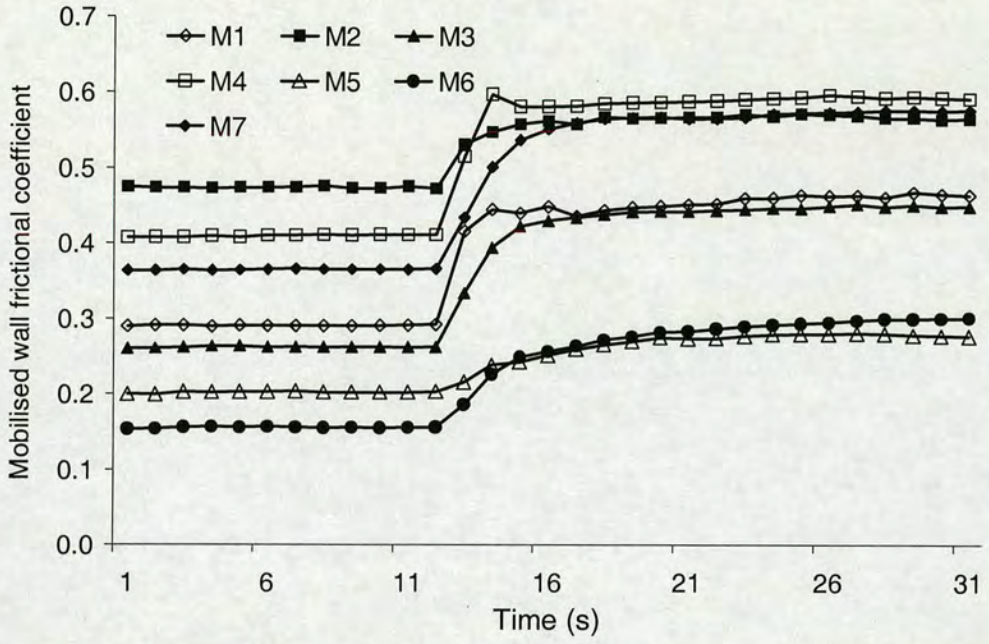

(b) Insert present (Test 3)

Fig. 5.55 Hopper frictional traction as a ratio to normal pressure during discharge

In particular Fig. 5.55 (a) shows that, in the absence of insert, the friction along the wall was not mobilised. The ratios between the frictional traction and normal pressure varied along the generator, and looked to be greater in the lower part than in higher part. Such ratios, appearing to be relatively close to each other, were far below the friction coefficient value (0.51) in the region below the transition, indicating that a stagnant zone there could persist for most of the period of discharge.

In Fig. 5.55 (b), it is apparent that in the presence of an insert the friction was very different from location to location. Under the transition, the friction could have been mobilised fully in the area on M4 and M7 side, whereas in opposite side, it was far from the case. The result of such differences could be an asymmetrical discharge, consistent with the surface profile measurement displayed in Fig. 5.44. Along a generator in the hopper, the ratios between the frictional traction and normal pressure appeared also different from place to place; most remained with friction not mobilised fully.

5.3.2.7 Concluding remarks

Measurements carried out on the full scale silo in absence / presence of a double cone insert during filling showed that:

The normal pressures developed in the barrel of the silo were quite different from those developed on the hopper of the silo, the pressure on the hopper part was much higher. The pressure was greater in the higher level than in the lower level of the hopper, whereas the maximum pressure was not just below the transition, but located somewhere lower. The development of frictional traction was rather stable in a specific location, but appeared to be different from location to location, and was not mobilised fully.

The installation of an insert might lead to a slight loss of solid head symmetry even under the same concentric filling condition. It may also lead to a slight increase of normal pressure at the transition level, and its unevenness as well. It has also been found that the effect of the installation of an insert had on the normal pressure was quite limited in the barrel of the silo (a small increase), but was great on the normal pressure in the hopper of the silo (a dramatic decrease). The ratio of frictional traction and normal pressure appeared to be in some degree symmetrical in a concentric filling without an insert. However, this symmetry was hard to retain in the presence of an insert.

As a result of the differences built up in a process of filling in absence / presence of insert, the normal wall pressure and frictional traction might develop differently in the process of discharging. Measurements carried out on the full scale silo in absence / presence of a double insert during discharge confirmed that:

The installation of an insert, while raising only slightly the normal pressure on the wall in the barrel of the silo, increased substantially the normal pressure in a region close to the transition in the hopper, but reduced considerably such a pressure in the lower part of the hopper.

At the commencement of discharge, the installation of an insert led to an unevenness of distribution of normal pressure as measured at the transition level. The friction along

the wall was not mobilised in the absence of insert, and appeared to be more symmetrical than that developed with insert. This friction might have been mobilised in presence of insert, but was limited in certain regions. While the mobilization of friction in the presence of the insert indicated an enlarged solid moving zone in silo discharge, the unevenness of the distribution of this ratio in the presence of an insert could put the process of discharge at risk of losing symmetry.

6 CONCLUSIONS

The research in this thesis has been carried out to investigate the solids flow and wall pressure in silos, and the effects of inserts on flow and pressure during filling and discharge. This chapter summarises the conclusions drawn in the previous chapters, and sets out some relevant topics for future study.

6.1 Filling pressures acting on the walls of a hopper

FE modelling and experiments as presented in Chapter 3 investigated the development of wall pressure in relation to the process of filling of a steep and a shallow hopper. The FE calculations have been used to explore the role of progressive filling on the pressures developed on the walls, while the experiments have provided some limited validation of the FE calculations of filling pressures. The key conclusions that can be drawn are as follows.

1. During the whole process of filling, the maximum normal wall pressure in the hopper did not occur at the outlet. The maximum normal pressure increased in magnitude and moved progressively upwards during the filling process. The normal pressures acting at the outlet also increased initially, but tended to approach a constant value.

2. The development of the frictional traction on the surface of the hopper wall followed the same pattern as the normal pressure. The wall friction was fully mobilised everywhere in the steep hopper except very close to the outlet. This pattern of friction mobilisation matches the model of Rotter proposed for a steep hopper.

3. The FE predictions of normal pressure along the walls for both the progressive and switch-on filling in a steep hopper have the general form proposed by

Walters, MacLean and Rotter; the predictions of Rotter's theory seems to be closest and lie between the two FE predictions.

4. Compared with switch-on filling, progressive filling increased the maximum normal pressure and moved the location of the maximum pressure downward. In the lower part of the hopper walls, the normal pressures increased with a corresponding decrease in the higher part of the walls.

5. For the case of the shallow hopper, the agreements on normal wall pressure were poor between the FE predictions and the algebraic models, with the Rotter's model giving the closest comparison. However, the experimental observations are in quite good agreement with the FE predicted pressures for the progressive filling case. It is evident that modelling progressive filling has improved the FE prediction and produced a better match with the experimental results. It also showed that Rotter's formula for predicting the normal wall pressure in a shallow hopper by adopting the effective wall friction coefficient (μ_{eff}) is a good approach. The relatively close match between the experiments and the FE calculations using progressive filling justified the more extended use of the FE calculations to explore a wider range of features of hopper pressures.

6. FE calculations showed that the wall friction has not been fully mobilised in a shallow hopper. The predicted mobilised friction from the FE calculation for both the switch-on filling and the progressive filling are all in good agreement with each other, and in reasonable agreement with the algebraic prediction of Rotter's formula using the effective friction coefficient (μ_{eff}).

7. Discrepancies exist in the development of mobilised wall frictional coefficient using different approaches. First, when the filling process is modelled using switch-on gravity, there is a zone near the top of the hopper which is predicted to have a higher level of mobilised friction: this is not matched by the progressive filling calculations or by the experiments. Second, the two experiments show a rather low mobilised friction along the wall. Further work is needed to investigate these differences.

6.2 Improvement of flow pattern with the application of an insert

Simulations using the FE program SILO to investigate the effects of different inserts on solids flow in silo were presented in Chapter 3. For the double cone insert, a parametric study and some experimental observations were also made in a small scale hopper. The key conclusions that can be drawn are as follows.

1. FE simulations showed that the cone-in-cone, the inverted cone and the double cone inserts were all able to change the material flow pattern in the cylindrical part of the silo from funnel flow to mass flow in a silo whose hopper has an inclination angle larger than that of the critical value for mass flow. Of these alternative inserts, the double cone insert appeared to perform best in this study for hopper half angles up to a certain value. Beyond this value, mass flow could not be obtained without changing the location of the insert, a vertical extension of the lower cone of the double cone insert, and the friction of the hopper wall.

2. Locating an insert at a proper level was found to be important in achieving an uniform flow. In general, an insert should be installed at a higher position, close to the transition rather than at a lower position close to the outlet, especially when a cone-in-cone insert or an inverted cone insert is used. However, in a silo with a flatter hopper, where mass flow was only obtained in the cylindrical section with the double cone insert, the position of the double-cone insert had relatively little influence on flow in the hopper, where the uneven discharging remained.

3. The vertical extension of the lower cone of a double-cone insert to the outlet would improve the silo discharge pattern, but its effect is hardly noticeable if the hopper wall friction is high. This suggests that using such an insert to obtain mass flow from a funnel flow silo has a limit with regard to the maximum hopper angles that can be permitted.

4. A combination of the extension of the lower cone of the double-cone insert and a decrease of the friction of the hopper wall would improve the silo discharge mode, and permit an increase of the hopper half angle. Also, to ensure that such

improvements are effective, maintaining the ratio between the maximum diameter of the insert and the diameter of the silo is important.

5. The program SILO predicted that the flow mode in a silo with a hopper half angle of 34.7° (inclination to the vertical) to be funnel flow, and the presence of a double cone insert improved the silo discharge mode. The observations from the top and measurements of material movement by tracers in experiments demonstrated and confirmed that the flow mode was indeed of this type.

6. The program SILO has the capability to provide predictions concerning the silo discharge mode under different conditions, which may be a valuable guide in situations where complex geometry is involved and the classic methods cannot be applied. Possible methods of improving the silo discharge flow pattern by means of inserts or similar devices can be explored using it. It could also be used to optimise the insert configuration.

7. However, the predictions using the program cannot be at present said to be verified in more than a qualitative sense in this project. A number of questions as highlighted in the closing remarks in Chapter 3 are not able to be addressed in this study.

6.3 Pressure measurements on a full scale silo

The FE models used in this study were confined to two dimensional axi-symmetric models. They cannot therefore address the issue of the loss of symmetry in flow pattern observed during the measurements. The loss of symmetry in the flow and pressure occurring in an axi-symmetrical silo in the absence or presence of an insert was investigated in Chapter 5 by making experimental measurements in a full scale silo. The key results can be summarised as follows.

1. The filling pressure was not necessarily symmetrical even though the geometry of the conical pile formed during filling appeared to be close to axi-symmetric. The loss of load symmetry started during the filling.

2. The normal pressures developed in the barrel section of the silo were quite

different from those developed on the hopper, with much higher pressures observed in the hopper section. The hopper pressures appear to increase from the outlet towards the transition, with the maximum pressure was not just below the transition, but located someplace lower.

3. The mobilisation of wall friction was rather stable in each measurement location, but appeared to be different from location to location, and was not fully mobilised.

4. A proper installation of a double cone insert as config. 2, i.e. the insert should strictly aligned with the axis of the silo, and with the long cone of the double cone pointing downwards and reaching to the outlet, enlarged the material moving zone while somehow retaining the symmetry of both the discharge flow pattern and the discharging loads on the walls. An improper installation of such an insert,. i.e., for instance as in config. 1, where there was a slight misalignment of the cone away from the central axis of silo, may lead to skewed discharge flow and a loss of load symmetry. A downward long cone to the outlet ensures an insert to be properly installed.

5. The installation of an insert appeared to result in a slight loss of symmetry in the height of fill around the circumference, even under careful concentric filling. It appeared to have also led to a slight increase in the normal pressure at the transition level, and its unevenness circumferentially. It was also observed that the insert had only a little effect (a small increase) on the normal pressure in the barrel section, but caused a significant decrease in the normal pressure in the hopper.

6. The ratio of frictional traction and normal pressure appeared to be largely symmetrical in a concentric filling without an insert. However, this symmetry was much harder to retain in the presence of an insert.

7. At the commencement of discharge, the installation of an insert, whilst raising only slightly the normal pressure in the barrel section, produced a substantial increase in the normal pressure at the region close to the transition in the

hopper. There was a corresponding significant pressure reduction in the lower part of the hopper. The hopper wall pressure near the transition level also became more uneven around the circumference.

8. The wall frictional traction was not fully mobilised in the absence of an insert, and appeared to be more symmetrical than that developed with an insert. This friction might have been mobilised in presence of an insert, but appeared to skewed. While the mobilization of friction in the presence of an insert indicated an enlarged solid moving zone in silo discharge, the unevenness of the distribution of this ratio in presence of an insert could put the process of discharge at risk of losing symmetry.

6.4 Recommendations to further study

Considerable efforts were made using ABAQUS to model silo discharging process using an Arbitrary Lagrangian-Eulerian (ALE) approach. Numerical problems were accounted when prescribing initial stresses in the solid by importing the stress field developed in a numerical model of silo filling. The ABAQUS analyses were performed by a straightforward prescription of initial stresses calculated using a theoretical formula. The numerical predictions were not as good for the case of a shallow hopper or in the presence of an insert. The reason might be that the prescription of initial stresses based on the theoretical formula is not accurate in the case of a shallow hopper or in the presence of an insert. With the more advanced version of ABAQUS, it is worth attempting again to define the initial stress state in solid by importing the stress field predicted from a proper numerical model of silo filling, and then to investigate the discharge process in a silo with a shallow hoper and in the presence of inserts.

Of the experiments conducted, attention has been principally focused on the wall pressure measurements during filling and discharge in the absence and presence of a double cone insert. Some effort was made to investigate the mode of silo discharge by measuring the surface profiles during discharge, but the information gathered was sparse and not as useful as one would have wished. Further measurements for instance

of the tracers residence time should be carried out to measure the flow pattern around the insert more directly, and to correlate with the pressure measurements.

While the measurements did reveal the effect of the double cone insert on the wall pressure, the loads on the insert itself has not been observed. Numerical investigation showed that the double cone insert took on a significant part of the overall loads. Measurement of loads acting on an insert is required to provide some verification. This information is needed for the design of a proper support structure for an insert.

7 References

ACI 313 (1991), Standard Practice for Design and Construction of Concrete Silos and Stacking Tubes for Storing Granular Materials, ACI 313-91, with Commentary (ACI313R-91) American Concrete Institute, Detroit, 27 pp.

ACI (1989), Alternate Design Procedure, Discussion document before ACI Committee 313 on Concrete Bins, Silos and Bunkers for Storing Granular Materials, ACI, Detroit.

Anand, L. and Gu, C., 2000, Granular materials: Constitutive equations and strain localization, *Journal of the mechanics and physics of solid, 48*, 1701-1733.

Antes, H., Lehmann, L. and Strusch, J., 1995, The Effect of Insert's Characteristics on the Stress Distribution in Silos, Storage and flow Particulate Solid, Neremberg, Germany, p. 173- 182.

Aoki, R. and Tsunakawa, H., 1969, The Pressure in a Granular Material at the Wall of Bins and Hoppers, J. Chem. Eng. Japan, 2, pp126-129.

Aoki, R. and Tsunakawa, H., 1972, Recent works in Japan on Silo Loads, J. Chem. Eng. Japan.

Aribert, J. M. and Ragneau E., 1990, Stress Calculations in Silos by Finite Element Method Using Different Behaviour Laws for Ensiled Material, 2nd European Symposium CHISA'90, paper No. 1669, Prague, August.

Aribert, J.M. and Ragneau E., 1990, "Stress Calculations in Silos by Finite Element Method Using Different Behaviour Laws for Ensiled Material", 2nd European Symposium CHISA'90, paper No. 1669, Prague, August.

Arnold, P.C., McLean, A.G. and Roberts, A. W., 1980, Bulk Solids: Storage, Flow and Handling, Tunra Bulk Solids Handling Associates, University of Newcastle, Australia, September.

Arteaga, P. and Tuzun, U., 1990, Flow of Binary Mixtures of Equal-Density Granules in Hoppers- Size Segregation, Flowing Density and Discharge Rates, *Chemical Engineering Science*, 45(1), p.205-223.

AS 3774, 1990, Lads on Bulk Solids Containers, Australian Standard with Commentary, Standards Association of Australia, Sydney, August 1990.

Askari A. H. and Elwi. A. E., 1988, Numerical Prediction of Hopper-Bin Pressures, *Journal of Engineering Mechanics* ASCE, 342-352.

Askegaard, V. and Munch-Andersen, J., 1984, Results from Tests with Normal and Shear Stress Cells in Medium Scale Silos (in English), Report R191, Department of Structural Engineering, Technical University of Denmark, 10 pp.

Askegaard, V., Nilsen, L. O. and Wiche, S., 1990, "Measurement of Contact Stresses on a Thin Silo Wall", 10th Int. Congress. of Chem. Engng, Chem. Equipment Design and Automation, Praha, Czechoslovakia, Aug.

Askegaard, V., Bergholdt, M. and Nielsen, J. (1971) "Problems in Connection with Pressure Cell Measurements in Silos" (in English), Bygningsstatiske Meddeselser, Vol. 42, No. 2, pp 33-74.

Askegaard, V. and Andersen, E Y (1982) "Consequence of Loading History and Mounting Procedure on Stress Cell Measuring Error", Euromech 157: Quality of Mechanical Observations on Particulate Media, Copenhagen, August 1982, pp A1-A7.

Askegaard, V. (1986) "Consequence of Loading History on the Measuring Error of Embedded Stress Cells", Proceedings, Second International Conference on Bulk Materials Storage, Handling and Transportation, Institution of Engineers, Australia, Wollongong, July 1986, pp 138-142..

Ayuga, F. Guaita, M. Aguado, P. J. and Couto, A. 2001, Discharge and Eccentricity of hopper Influence on the Silo Wall Pressures, *Journal of Engineering Mechanics*, 127(10), Oct, p.1067-1074.

Bardenhagen S. G., Brackbill J. U. and Sulsky D., 2000, The material-point method for granular materials, *Computer Methods in Applied Mechanics and Engineering*, 187, 529-541.

Bardet, J. P., 1993, Numerical Test with Discrete Element Method, in Modern Approaches to Plasticity (ed. D. Kolymbas), Elsevier, Amsterdam, 179-198.

Baxter G. M. and Behringer, R. P., 1989, Pattern formation in flowing sand, *Physical Review Letters*, 62 (24), 2825-2828.

Baxter, G. M. and C. Yeung, 1999, The rotating bucket of sand: Experiment and theory, Chaos, 9 (3), p. 631-638.

Bates, L., Ajax LynFlow Inserts, The use of inserts in Hoppers, AJAX Equipment, http://www.ajax.co.uk/inserts.htm & http://www.powderandbulk.com/pb_services/ask_joe_archive/use_of_inserts_in_hoppers.htm

Bemrose, C. R., Fowles, P., Hawkesworth, M. R. and O'Dwyer, M. A., 1988, Application of Positron Emission Tomography to Particulate Flow, Measurement in Chemical Engineering Processes, Nucl. Instr. Meth. Phys. Res. A273, p. 874-880.

Beynon, T. D., Hawkesworth, M. R., McNeil, P.A., Parker, D. J., Bridgewater, J., Broadbent, C. J. and Fowles, P., 1993, Positron-Based Studies of Powder Mixing, Powders and Grains 93, Thornton (Ed.), Balkema, Rotterdam, p.377-382.

Bishara, A.G. and Mahmoud, M.H., 1976, Using Finite Elements to Analyse Silo Pressure, Agricultural Engineering, 57(6), p. 12-15.

Blair-Fish, P. M. and Bransby, P. L., 1973, Flow Patterns and Wall Stresses in a Mass Flow Bunker, Journal of Engineering for Industry, ASME, 95 (1), p. 17-26.

Blight, G. E. and Midgley, D., 1980, Pressure Measured in a 20 m Diameter Coal Out-load Bin" Proc., Int. Conf. on Design of Silos for Strength and Flow, Univ. Lancaster, Sep.

Blight, G. E., 1983, Performance of a 20m Diameter Steel Maize Storage Bin", Second International Conference on Design of Silos for Strength and Flow, Stratford upon Avon, Nov., p.179-191.

Blight, G. E., 1986, "Pressures Exerted by Materials Stored in Silos: Part I, Coarse Materials", Geotechnique, 36 (1), p.33-46.

Blight, G. E., 1987, Strains Measured in a 7500t Sugar Silo", Bulk Solids Handling, 7, p. 573-582.

Blight, G. E., 1988, A Comparison of Measured Pressures in Silos with Code Recommendation, Bulk Solids Handling, p. 145-153.

Blight, G. E., 1989, Behaviour of a Reinforced Concrete Coal Silo under a Design Overload", Bulk Solids Handling, 9, p. 21-25

Blight, G. E., 1990, Defects in Accepted Methods of Estimating Design Loading for Silos", Proc. Instn Civ. Engrs, Part 1, Dec., 88, p.1015-1036.

Blight, G. E., 1990, Lateral Pressures and Frictional Wall Loads in Corrugated Steel Silos as Revealed by Strain Measurements", 10th Int. Congr. of Chem. Engng, Chem. Equipment Design and Automation, Praha, Czechoslovakia, Aug.

Blight, G. E., Schaffner, R. H. and Gilbert, I., 1982, Strains in a Reinforced Concrete Silo during Rapid Filling with a Fine Powder, J. Powder and Bulk Solids Technology, 6(2), 17-27.

BMHB, 1987, Silos: Draft Design Code for Silos, Bins, Bunkers and Hoppers, British Materials Handling Board and British Standards Institution, London.

Bosley, J., Schofield, C. and Shook, C. A., 1969, An Experimental Study of Granule Discharge from Model Hoppers, Transactions of the Institute of Chemical Engineers, 47, p. T147-T153.

Bransby, P. L., Blair-Fish, P.M. and James, R. G., 1973, An Investigation of the Flow of Granular Materials, Powder Technology, November-December, 8 (5-6), p. 197-206.

Bransby, P. L. and Blair-Fish, P.M., 1974, Wall Stress in Mass Flow Bunkers, Chem. Engng Sci., 29, p.1061-1074.

Briassoulis D., 1987, Author's Closure to Discussion of 'Design Friction Loads for Concrete Silos', ACI Structural Journal, 84 (2) Mar.-Apr., p. 178-179.

Briassoulis D., 1991, Limitations in the Range of Applicability of the Classical Silo Theories, ACI Structural Journal, 88 (4), July-August, p. 437-444.

Brockbank, R., Huntley, J. M. and Ball, R. C., 1997, Contact force distribution beneath a three dimensional granular pile, *J. Physique* II **7**, 1521-1532.

Brown C. J., Jarrett N. D. and Moore D. B., 1996, Pressures in a square planform silo during discharge. Proceedings IMechE, Vol. 210, Part E, Journal of Process Engineering, p. 101–108, July

Brown C. J., Lahlouh E. H., Rotter J. M., 2000, Experiments on a square planform silo. *Chem. Eng. Sci.* 55(20):4399–413.

Brown, R. L. and Richards, J.C., 1965, Kinematics of the Flow of Dry Powders and Bulk Solids, Rheologica Acta, Band 4, Heft 3, October, p. 153-165.

Carson, J. W., Goodwill, D. J. and Bengtson, K. E., 1991, Predicting the Shape of Flow Channels in Funnel Flow Bins and Silos, presented at the American Concrete Institute Convention, Boston, Massachusetts, U.S.A, March.

Carson, J.W., Goodwill, D. J. and Bengtson, K.E., 1991, Predicting the Shape of Flow Channels in Funnel Flow Bins and Silos, presented at the American Concrete Institute Convention, Boston, Massachusetts, U. S. A, March.

Carson, J. W. and Royal, T. A., 1992, In-bin blending improves process control, Powder handling & Processing, 4 (3), 310-307.

Cates, M. E. and J.P. Wittmer, 1998, Stress Propagation In Sand, PHYSIC A, 249 (1-4), P. 276-284.

Cates, M. E., Wittmer, J. P., Bouchaud, J. .P. and Claudin, P., 1999, Jamming and Stress Propagation in Particulate Matter. Physica A, 263(1-4): P. 354-361..

Cates, M. E., Wittmer, J. P., Bouchaud, J.P. and Claudin, P., 1998, Development of Stresses in Cohesionless Poured Sand. Philosophical Transactions of the Royal Society of London Series A-Mathemat, 356(1747): P. 2535-2560.

Chatlynne, C. J. and Resnick, W., 1973, Determination of Flow Patterns for Unsteady-State Flow of Granular Materials, *Powder Technology*, 8(3-4), p.177-182.

Chen, J. F., Yu, S. K. Ooi, J. Y. and Rotter, J. M., 2001, Finite-Element Modelling of Filling Pressure in a Full-Scale Silo, *Journal of Engineering Mechanics*, 127(10), Oct, p.1058-1066

Chen, J. F., Rotter, J. M. and Ooi, J. Y. (1998), Statistical inference of unsymmetrical silo pressures from comprehensive wall strain measurements, Thin-Walled Structures, Vol. 31, p 117-136.

Chen, J. F., 1996, Interpretation of flow and pressures in full scale silos, PhD. Thesis, University of Edinburgh

Cleaver, J. A. S and R. M. Nedderman, 1993, Measurement of velocity profiles in conical hoppers, Chemical Engineering Science, 1993 48(21), p.3703-3712,

Cleaver, J. A. S and R. M. Nedderman, 1993, Theoretical prediction of stress and velocity profiles in conical hoppers, Chemical Engineering Science, 1993 48(21), p.3693-3702,

Cleaver, J. A. S.,1991, Velocity Distributions in Conical Hoppers, PhD thesis, Department of Chemical Engineering, University of Cambridge, May.

Cundall, P.A., 1971, A Computer Model for Simulating Progressive Large Scale Movements in Blocky Rock Systems", Proceedings of the Symposium of the International Society of Rock Mechanics, Nancy, 129-136.

Cundell, P. A. and Strack, O. D. L., 1979, A Discrete Numerical Model for Granular Assemblies", Geotechnique, Vol. 29, No. 1, p.47-65.

Cutress, J. O. and Pulfer, R. F., 1967, X-ray Investigations of Flowing Powders, *Powder Technology, 1*, p. 213-220.

Deka (2002), Specification of pressure transduers used in silos, Norway: Beschreibung der Montage der Transducer und der Kalibriervorrichtung, DEKA Sensor & Technologie GmbH, Teltow, Germany

Dürr M., Control of flow of bulk material in silos by means of inserts, Tel-Tek Report, (1995) Nr. 410015-1,

Deutsch, G. P. and Schmidt, L.C., 1969, Pressures on Silo Walls, *Journal of Engineering for Industry*, ASME, 91, p.450-459.

Deutsch, G. P. and Clyde, D. H., 1967, Flow and Pressure of Granular Materials in Silos, *Journal of Engineering Mechanics*, ASCE, December, Vol. 93, No. 6, pp 103-125.

DIN 1055, 1987, Design Loads for Buildings: Loads in Silo Bins, DIN 1055 Part 6, Deutsches Institut fur Normung, Berlin, May.

Ding S., Enstad, G. G. and Silva, S. R., 2003, Effect of passive inserts on the granular flow from silos using numerical solutions, *Particulate Science and Technology* 21(3), p.211-226.

Ding, S. and Enstad, G. G., 2003, Effects of feeding rate on the loads measured along the wall of a full-scale hopper during filling, in: *Proceedings of the Measurement & Control of Granular Material*, Aug. 20-23, Shanghai.

Ding, S., Enstad, G. G. and Silva, S. R., 2003, Development of load on a hopper in process of filling with granular material, *Particulate Science and Technology* 21(3), p.259-270.

Ding, S., Ooi, J. Y. and Rotter, J. M., 2002, Simulation of silo discharge flow pattern and predictions of loads on walls and inserts, *15th International Congress of Chemical and Engineering, CHISA 2002*, Prague, 08.

Drescher, A., 1991, Analytical Methods in Bin Load Analysis, Developments in Civil Engineering, Elsevier, Amsterdam, Netherlands, 36.

Drescher, A., 1992, On the criteria for mass flow in hoppers, *Powder Technology*, 73, p. 251-260.

Drescher, A., 1998. Some aspects of flow of granular materials in hoppers, *Philosophical Transactions of the Royal Society of London: Series A-Mathemat*, 356 (1747),p.2649-2666.

Drescher, A., Cousens, T. W., Bransby, P. L., 1978, Kinematics of the Mass Flow of Granular Material through a Plane Hopper, Geotechnique, Vol. 28, No. 1, pp 27-42.

Drescher, A., Waters, A. J., and Rhoades, C.A., 1995, Arching in Hoppers .1. Arching Theories and Bulk Material Flow Properties: .2. Arching Theories and Critical Outlet Size, *Powder Technology*, 84(2), 165-176-183.

Ebert, F. and Dau, G., 1993, Residence Time Measurements in Bulk Solids Handling Devices, *Reliable Flow of Particulate Solids II: Proceedings*, ed. by Enstad, G. G. et al., Oslo, Norway, August, pp 897-909.

Edwards, S. F., and Mounfield, C. C., 1996, A Theoretical Model For The Stress Distribution In Granular Matter 1. Basic Equations. *Physica A*, 226(1-2), P. 1-11,.

Eibl, J. and Rombach, G., 1987, Numerical Computation of Velocity and Stress Fields in Silos - Theory and Applications, Scientific Papers of the Institute of Building Engineering of the Technical University of Wroclaw, SILOSKY, Sklarska, Poland

Eibl, J. and Rombach, G., 1987, Stress and Velocity Fields at Discharging of Silos, Proc. of NUMETA Conference, Swansea, p. D1-D12

Emanuel, J. H., Mahmoud, M. H., Best, J., and Hasanain, G. S. 1983, Initial Strain Analysis of Silo-Material Interaction, *Powder Technology*, 36, 235-243.

Emanuel, J. H., Mahmoud, M. H., Best, J., and Hasanain, G. S., 1983, Parametric Study of Silo-Material Interaction, *Powder Technology*, 36, 223-233.

Enstad, G. G., 1981, A Novel Theory on the Arching and Doming in Mass Flow Hoppers, Dr. techn. Thesis, Norwegian Institute of Technology, Bergen.

Enstad, G. G., 1996, Investigations of the use of inserts in order to obtain mass flow in silo, POSTEC- Newsletter 15, P13-16.

Enstad, G. G., 1997, Use of inverted cone and double cones as inserts for obtaining mass flow, POSTEC- Newsletter 15, P15-16.

Evesque P. and Adjemian 2002, Stress fluctuation and macroscopic stick-up in granular materials, *The European Physical Journal E*, **9**, 252-259.

Firewicz, H., 1988,. Kinematics of the gravity flow of granules from a bin. Aufbereitungs Technik, 2, 61–70..

Fitz-Henry, J. O .D., 1986, Buckling Failure of Eccentrically Discharged Silos, B. E. Thesis (Hons), University of Sydney.

Gardner, G. C., 1966, The Region of Flow when Discharging Granular Materials from Bin-Hopper Systems, *Chemical Engineering Science*, 21(3), p. 261-273.

Giunta, J. S., 1969, Flow Patterns of Granular Materials in Flat-Bottom Bins, *Journal of Engineering for Industry*, ASME, May, 91(2), p. 406-413.

Goodey, R. J. , C. J. Brown, Rotter J. M., 2003, Verification of a 3-dimensional model for filling pressures in square thin-walled silos, *Engineering Structures 25* 1773–1783.

Graham, D. P., Tait, A.R. and Wadmore, R.S. (1987) Measurement and Prediction of Flow Patterns of Granular Solids in Cylindrical Vessels, *Powder Technology*, March, 50(1), p. 65-76.

Gunies, D., Ragneau, E. and Kerour, B., 2001, 3D Finite element simulation of a square silo with flexible walls, *Journal of Engineering Mechanics*, 127(10), Oct., 1051-1057.

Handley, M. F. and Perry, M. G., 1965, Measurements of Stresses in Flowing Granular Materials, *Rheological Acta*, 4, Heft 3, pp 225-235.

Handley, M. F. and Perry, M. G., 1967, Stresses in Granular Materials in converging Hopper Sections, *Powder Technology*, 1, p.245-251.

Hartlen, J., Nielsen, J., Ljunggren, L., Martensson, G. and Wigram, S. (1984) The Wall Pressure in Large Grain Silos, Swedish Council for Building Research, Stockholm, Document D2:1984.

Haussler, U., and Eibl, J., 1984, Numerical Investigation of Discharging Silos, *Journal of Engineering Mechanics*, 110(6), P. 957-971.

Heege, A., Alart, P. and Onate, E., 1995, Numerical modelling and simulation of friction contact using a generalized Coulomb Law, *Engineering Computations*, 12, P 641-656.

HIBBITT, KARLSSON & SORENSEN, INC, 2001, ABASQUS: Manual.

Hjelmstad K, D. and Taciroglu E, 2000, Analysis and implementation of resilient modulus models for granular solids, *Journal of Engineering Mechanics-Asce*, 126, (8), Aug., 821-830.

Hogue, C., 1991, Computer Simulation of Ballistic Separation", Proc., International Conference: Bulk Materials - Towards the Year 2000, Institution of Mechanical Engineers, October 29-31, London, 217-224.

Holst, J. M. F. G., Ooi, J. Y. and Rotter, J. M., 1999, Numerical Modelling of Silo Filling: I: Continuum Analyses, *Journal of Engineering Mechanics-ASCE*, 125(1), 94-103.

Horne, R. M. and Nedderman R. M., 1978, Stress distribution in hopper, *Powder technology*, *19*, 235-241.

Horne, R. M. and Nedderman, R. M., 1976, Analysis of the Stress Distribution in Two-Dimensional Bins by the Method of Characteristics, *Powder Technology*, 14, 93-102.

Ibrahim, A.G. and Dickerson, R. P. (1983) "Analysis of Silo-Material Interaction for Powdered Coal", 2nd Int. Conf., Design of Silos for Strength and Flow, Stratford, 1983.

ISO, 1990, Loads due to Bulk Materials, Draft ISO Code, Karlsruhe, July 1990.

Jaky, J., 1948, Pressures in Silos, Proceedings, 2nd International Conference on Soil Mechanics and Foundation Engineering, Rotterdam, June 21-30, 1, 103-107.

Janssen, H. J., 1895, Verssuche uber Getreidedruck in Silozellen, Zeitschrift des Verein Deutscher Ingenieure, 39(35),1045-1049.

Jenike, A. W. and Johanson, J. R., 1962, Stress and Velocity Fields in Gravity Flow of Bulk Solids, Bulletin No. 116 of the Utah Engineering Experiment Station, May.

Jenike, A. W. and Johanson, J. R., 1968, Bin Loads, *Journal of the Structures Division*, ASCE, April, 94(ST4), p. 1011-41.

Jenike, A. W. and Johanson, J. R., 1969, On the Theory of Bin Loads, *Journal of Engineering for Industry,* ASME, May, Series B, 91(2), p. 339-44.

Jenike, A. W., 1961, Gravity Flow of Bulk Solids, Bulletin No 108, Utah Engineering Experiment Station, University of Utah, Salt Lake City, Utah, October , Vol. 52, No. 29, 309 pp.

Jenike, A. W., 1964, Steady Gravity Flow of Frictional-Cohesive Solids in Converging Channels, *Journal of Applied Mechanics*, ASME, March, pp 5-11.

Jenike, A. W., 1964, Storage and Flow of Solids, Bulletin No 123 of the Utah Engineering Experiment Station, Vol. 53, No. 26, November 1964, University of Utah, Salt Lake City, Utah, 197 pp.

Jenike, A. W., 1967, Denting of Circular Bins with Eccentric Drawpoints, *Journal of the Structures Division*, ASCE, February, 93(ST1), p.27-35.

Jenike, A. W., 1987, A Theory of Flow of Particulate Solids in Converging and Diverging Channels based on a Conical Yield Function, *Powder Technology*, 50(3), 229-236

Jenike, A. W., Johanson, J .R. and Carson, J. W., 1973, Bin Loads - Part 3: Mass Flow Bins, *Journal of Engineering for Industry*, Trans. ASME, February 1973, 95, Series B, No. 1, pp 6-12.

Jenike, A. W., Johanson, J .R. and Carson, J. W., 1973, Bin Loads - Part 4: Funnel-Flow Bins, *Journal of Engineering for Industry*, ASME, 95, Ser. B, No. 1, p.13-16.

Jenike, A. W., Johanson, J .R. and Carson, J. W., 1973, Bin Loads - Part 2: Concepts, *Journal of Engineering for Industry*, ASME, 95, Ser. B, No. 1, pp 1-5.

Jenkyn, R. T. and Goodwill, D. J., 1987, Silo Failures: Lessons to be Learned, Engineering Digest, Sept., pp 17-22.

Jenkyn, R. T. and Goodwill, D. J., 1987, Silo Failures: Lessons to be Learned, Engineering Digest, Sept., pp 17-22.

Jofriet, J.C., LeLievre, B. and Fwa, T.F., 1977, Friction Model for Finite Element Analyses of Silos, Trns. ASAE, 2C(4), 735-744.

Johansen J. R., 1982, Controlling flow patterns in bins by use of inserts, *Bulk solid handling* 2 (3), 495-498.

Johanson J. R. and Kleysteuber W. K., 1966, Flow corrective inserts in Bins, *Chemical. Engineering Progress* 11 (62), 79-83.

Johanson J. R., 1967 - 68, The placement of inserts to correct flow in bins, *Powder Technology* 1, 328-333.

Johanson, J. R., 1964, Stress and Velocity Fields in the Gravity Flow of Bulk Solids, *Journal of Applied Mechanics*, ASME, September, p. 499-506.

Johanson, J. R., 1970, In-bin Blending, *Chemical Engineering progress* 66, p.6

Karlsson T., Klisinski M., and Runesson K., 1998, Finite Element Simulation of Granular Material Flow in Plane Silos with Complicated Geometry, *Powder Technology*, 99(1), P. 29-39.

Karlsson, T., 1996:8L, Finite Element Simulation of Flow in Granular Materials, Licentiate Thesis, Luleå University of Technology.

Keiter T. W. R. and Rombach G. A., 2001, Numerical aspects of FE simulation of granular flow in silos, *Journal of Engineering Mechanics*, **127**(10), Oct., 1044-1050.

Ketchum, M.S. (1907) Design of Walls, Bins and Grain Elevators, 1st edition, McGraw-Hill, New York (2nd edition 1911, 3rd edition 1919).

Khakhar, D. V. and Orpe, A. V., 2001, Andresen and J. M. Ottino, Surface flow of granular material: model and experiments in heap formation, J. Fluid Mech. 441, p. 255-264.

Kmita, J. 1991,. An experimental analysis of internal silo loads. *Bulk Solids Handling,* 11(2), 459–468.

Kmita, J., 1985, Silo as a System of Self-induced Vibration. *Journal of Structural Engineering*, III(1), 190–204.

Kmita, J.,1992,. A study on the self-induced vibration in silos. Bulk Solids Handling, 12(l), 25–30.

Knodel, P. and Schulz, U., 1992, "Buckling of Cylindrical Bins - Recent Results", Proc., International Conference: 'Silos-Forschung und Praxis', Universitat Karlsruhe, Oct., 75-82.

Koenen, M., 1895, Berechnung des Seitenund Bodendrucks in Silos (Calculation of Side and Floor Pressure in Silo Walls), Zentralblatt der Bauverwaltung, 16, 446-449.

Kolb E., Mazozi T. Clement E. and Duran J., 1999, Forces fluctuations in a vertically pushed granular column, *The European Physical Journal B*, **8**, 483-491.

Kroll, D., 1975, Untersuchungen uber die Belastung Horizontaler uganker sowie vertikaler Hangependel und Gehange durch Schuttguter in Silozellen, Diss., Techn. Univ. Braunschweig. Germany.

Lee, J., Cowin, S. C. and Templeton, J.S., 1974, An Experimental Study of the Kinematics of Flow through Hoppers, Trans. Soc. Rheology, 18:2, pp 247-269.

Lenczner, D., 1963, An Investigation into the Behaviour of Sand in a Model Silo, The Structural Engineer, December, 41(12), p. 389-398.

Levison, B. and Munch-Andersen, J., 1993, Shocks in Coal Silos: as Case Study, Proc., International Symposium: Reliable Flow of Particulate Solids II, EFChE Publication Series No 96, Oslo, August 1993, pp 1015-1021.

Lind, H., 2003, E-mail exchanges and discussions, ABAQUS consultations in Scandinavia.

Link, R. A. and Elwi, A .E., 1990, "Incipient Flow in Silo-Hopper Configurations", *Journal of Engineering Mechanics*, ASCE, 116, 172-188.

Link, R. A. and Elwi, A. E, 1987, Incipient Flow in Silos: A Numerical Approach, Structural Engineering Report No. 147, Department of Civil Engineering, University of Alberta, May.

Litwiniszyn, 1963, The Model of a Random Walk of Particles Adapted to Researches on Problems of Mechanics of Loose Media, Bulletin de LAcademie Polonaise des Sciences, Series des Sciences Techniques, 11(10), p. 61-70.

Luding S., Duran J. Clement E. and Rajchenbach J. 1996, Simulations of dense granular flow: Dynamic arches and spin organization, *J. Phys, I France* **6**, 823-836.

Mahmoud, A.A. and Abdel-Sayed, G., 1981, Loading on Shallow Cylindrical Flexible Grain Bins, *Journal of Powder and Bulk Solids Tech.*, 5(3), p. 12-19.

Martý´nez, M. A., Alfaro, I. and Doblare, M., 2002, Simulation of axi-symmetric discharging in metallic silos, Analysis of the induced pressure distribution and comparison with different standards, *Engineering Structures* 24, 1561–1574.

McLean, A.G. and Arnold, P.C., 1976, Prediction of Cylinder Flow Pressures in Mass-Flow Bins Using Minimum Strain Energy, Trans. of ASME, *Journal of Engineering for Industry*, November, 1370-1374.

MacLean, R. F., 1984, Safer Silos, Chapter 6, in Developments in Thin-Walled Structures-2 (eds J. Rhodes and A. C. Walker), Elsevier Applied Science Publishers, London.

Medina A., Andrade, J. and Trevino, C., 1998, Experimental study of the tracers in the granular flow in a 2D silo, *Physics Letter A* 249, 63-68.

Wojcik, M., Härtl, J., Ding, S. and Enstad, G. G., (2004), Experimental Investigations of Stresses and Flow in a Full Scale Silo of axial Symmetry - with and without Insert, Tel-Tek-report, No. 4104010 (in preparation).

Michalowski R. L., 1987, Flow of granular media through a plane parallel converging bunker, *Chemical Engineering Science,* 42 (11), 2587-2596.

Michalowski, R. L., 1984, Flow of granular material through a plane hopper. *Powder Technology*. 39, 29-40.

Michalowski, R. L., 1991 Strain localization and periodic fluctuations in granular flow processes from hoppers. *Geotechnique* 41(3), p.471-473.

Mullins, W.W., 1972, Stochastic Theory of Particle Flow Under Gravity, *Journal of Applied Physics*, February, 43 (2), p. 665-678.

Mullins, W.W., 1974, Experimental Evidence for the Stochastic Theory of Particle Flow under Gravity, *Powder Technology*, 9, p.29-37.

Mullins, W.W., 1979, Critique and Comparison of Two Stochastic Theories of Gravity-Induced Particle Flow, *Powder Technology*, 23(1), p.115-119.

Munch-Andersen J. and Nielsen J., 1990, Pressure in slender grain silos, *CHISA, 2nd European symposium on stress and strain in particular solids*, Prague, August.

Munch-Andersen J., Askegaard V. and Brink A., 1992, Silo models tests with sand, *SBI Bulletins 91*, Danish building research institute.

Munch-Andersen, J. and Nielsen, J., 1986. Size Effects in Large Grain Silos, *Bulk Solids Handling*, 6, p. 885-889.

Munch-Andersen, J. and Nielsen, J., 1990, Pressures in Slender Grain Silos, CHISA 1990, Second European Symposium on Stress and Strain in Particulate Solids, Prague, August 1990, 9 pp.

Murfitt, P. G. and Bransby, P. L., 1982, Pressures in Hoppers Filled with Fine Powders, *Powder Technology*, 31, p.153-74.

Murfitt, P. G., Bransby, P. L. and Nienow A. W., 1981, Flow in Core Flow Hoppers, I. *Chem. E. Symposium* Series No. 63, pp D3/S/1-22.

Nanninga, N., 1956, Does the Usual Method of Calculating Pressures on the Walls and Bottom of Silo Structure Give Safe Results, *Ingenieur*, 68(44), p. 190-194.

Nedderman, R. M., 1988, The Measurement of the Velocity Profile in a Granular Material Discharging from a Conical Hopper, *Chemical Engineering Science*, 43 (7), p. 1507-1516.

Nedderman, R. M., 1992, *Statics and Kinematics of Granular Materials*, Cambridge University Press.

Nedderman, R. M., 1995, The Use of the Kinematic Model to Predict the Development of the Stagnant Zone Boundary in the Batch Discharge of a Bunker, *Chemical Engineering Science*, 50(6), 959-965.

Nedderman, R. M., Tuzun, U., 1987, A Kinematic Model for the Flow of Granular Materials, *Powder Technology*, 22, 243-253.

Nguyen, T. V., Brennen, C. E. and Sabersky, R. H., 1980, Funnel Flow in Hoppers, *Journal of Applied Mechanics*, ASME, December, Vol. 47, No. 4, pp 729-735.

Nielsen J., 1998, Pressures from flowing granular solids in silos. *Philosophical Transactions of the Royal Society of London: Series A-Mathemat*, 356(1747), 2667–84.
Nielsen, J. and Andersen, E.Y.,1982, Loads in Grain Silos, Bygningsstatiske Meddelelser, 53 (4), p.123-135.

Nielsen, J. and Kristiansen, N. O., 1979, Pressure Measurements on a Silo in Karpalund (in Danish), Nordic Group for Silo Research, Report No. 5, Technical University of Denmark, Department of Structural Engineering.

Nielsen, J. and Kristiansen, N. O., 1980, Related Measurements of Pressure Conditions in Full Scale Barley Silo and in Model Silo, Proc., Int. Conf. on Design of Silos for Strength and Flow, University of Lancaster, September.

Nielsen, J., 1983, Pressure Measurements in a Full Scale Fly Ash Silo, Fine Particle Society, Pacific Region Meeting, August.

Nilsson, L., 1986, The Effect of Imperfections on the Pressure in Grain Silos, Bulk Solids Handling, 6 (5), p. 899-901.

Nothdurft, H., 1976, Schuttgutlasten in Silozellen mit Querschnittsvergengungen, Diss., Techn. Univ. Braunschweig, Germany.

Novosad, K. and Surapati, K.,1968, Flow of Granular Materials: Determination and Interpretation of Flow Patterns, *Powder Technology*, 2, p. 82-86.

Ooi J. Y., Rotter J. M. and Pham L., 1990, Systematic and random features of measured pressures on full-scale silo walls, *Engineering Structures* 12 (2), p. 74–87.

Ooi, J. Y. and Rotter, J. M.,1990, Wall Pressures in Squat Steel Silos from Finite Element Analysis, *Computers and Structures*, Vol. 37, No. 4, p. 361-374.

Ooi, J. Y. and She, K. M., 1997, Finite Element Analysis of Walls Pressure in Imperfect Silos, *International Journal of Solids and Structures*, 34(16), p. 2061-2072.

Ooi, J. Y. Chen, J. F. and Rotter, J. M., 1998, Measurement of Solids Flow Patterns in Gypsum Silo, *Powder Technology*, 99(3), p.272-284.

Ooi, J.Y. and Rotter, J. M., 1991, Elastic Predictions of Pressures in Conical Silo Hoppers, *Engineering Structures*, January, Vol. 13, No. 1, p. 2-12.

Ooms, M. and Roberts, A. W., 1985, Significant Influence on Wall Friction in the Gravity Flow of Bulk Solids, *Bulk Solids Handling*, 5(6), 1271-1277.

Otto M., Bouchaud J. P Claudin P. and Socolar J. E. S., 2003, Anisotropy in granular Media: classical elasticity and directed-force chain network, *Physical Review E*, 67, 031302.

Ottosen, N. S. and Petersen, H., 1992, Introduction to the Finite Element Method, Prentice Hall.

Pariseau W. G., 1969-70, Discontinuous velocity fields in gravity flows of granular materials through slots, *Powder Technology* 3, 218-226.

Parker, D. J., Broadbent, C. J., Fowles, P., Hawkesworth, M. R. and McNeil, P., 1993, Positron Emission Particle Tracking - A technique for studying flow within engineering equipment, *Nucl. Instr. and Meth.* A326, p.592-607.

Perry, M. G., Rothwell, E. and Woodfin, W. T., 1976, Model Studies of Mass Flow Bunkers, 2 - Velocity Distributions in the Discharge of Solids from Mass Flow Bunkers, *Powder Technology*, 14 (1), p. 81-92.

Perry, M. G., Rothwell, E. and Woodfin, W. T.,1975, Model Studies of Mass Flow Bunkers, 1 - Development of the Radio Pill Technique for Dynamic Pressure and Velocity Measurements, *Powder Technology*, 12, p. 51-56.

Pfiste J. and Eberhard, 2002, Frictional contact of flexible and rigid bodies, *Granular Matter* 4, p. 25-36.

Pieper, K. and Wenzel, F., 1963, Comments on DIN1055: Design Loads for Buildings Loads in Silo Bins, Beton und Stahlbetonbau, 1963, p.6-11.

Pieper, K., 1969, Investigation of Silo Loads in Measuring Models, *Journal of Engineering for Industry*, Trans ASME, May, p.365-372.

Pieper, K., 1969, Investigation of Silo Loads in Measuring Models, *Journal of Engineering for Industry*, Trans ASME, May, p. 365-372.

Pitman, E. B., 1986, Stress and velocity fields in two- and three-dimensional hoppers. *Powder Technology*. 47, 219-231.

Polderman, H. G., Scott, A. M. and Boom, J., 1985, Solid Stress in Bunkers with Inserts, *Int. Chem. Eng. Symp. Ser.* 91, p. 227-240.

Poschl, T., 1992, Recurrent Clogging and Density Waves in Granular Material Flowing Through a Narrow Piper, preprint HLRZ 67/92, Julich, Germany.

Qu Q., Negi S. C. and. Jofriet J. C., 2001, Storage of Cohesive material in Silos, Part 2: Parametric Study, *Powder Handling Processing*, **13**(1), Jan/March, 27-30.

Ragneau, E., Ooi, J. Y. and Rotter, J. M., 1998, Finite Element Models For Specific Applications, (in SILOs ed. by Brown C. J. and Nelsen, J., E &FN SPON.

Rahim, H. A. E., 1989, Effect of Constructional Imperfections on the Internal Forces on Silo Walls, *Bulk Solids Handling* 9, 205-206.

Rankine, W.J.M., 1857, On the Stability of Loose Earth, *Phil. Trans. Roy. Soc.*, London, 147, p 9.

Rao, V. L. and Venkateswarlu, D., 1973, Determination of Velocities and Flow Patterns of Particles in Mass Flow Hoppers, *Powder Technology*, 7(5), p. 263-265.

Reimbert, M. and Reimbert, A., 1976, Silos: Theory and Practice, Trans Tech Publications.

Reimberts, M., and Reimberts, A., 1987, Discussion of 'Design Friction Loads for Concrete Silos', *ACI Structural Journal*, 84 (2), Mar.-Apr., 178-179.

Richards, P.C. (1977) Bunker Design - Part 1: Bunker Outlet Design and Initial Measurements of Wall Pressures, *Journal of Engineering for Industry*, ASME, 99(4), p. 809-813.

Ristow G. H. and Herrmann H. J., 1995 Forces on the walls and stagnation zones in a Hopper filled with granular material, *Physica* A **213**, 474-481.

Ristow G. H., 1997,

Ristow, G. H. and Herrmann, H. J., 1995, Forces on the walls and stagnation zones in a Hopper filled with granular material, *Physica A* 213, p. 474-481,.

Roberts, A. W. ,1999,. Flow pulsations in the gravity flow of bulk solids and the influence on silo loads. *Proceedings of the Chemiecal Congress*, The Institution of Engineers, Australia.

Roberts, A. W., 1989, Loads on Bulk Solids Containers, Draft Australian Standard for Comment.

Roberts, A. W., 1990, Storage and Discharge of Bulk Solid from Silos with Special reference to the Use of Inserts, POSTEC research report, Powder Science and Technology Research R&D, Porsgrunn, Norway.

Roberts, A. W., 1996, Shock loads in silos, the silo quaking problem, *Bulk Solids Handling*, 16(1), 59–73.

Roberts, A. W., Scott, O. J., & Wiche, S. J.,1991,. 'Silo quaking', a pulsating load problem during discharge in bins and silos. Proceedings of Bulk 2000, The Institution of Mechanical Engineers, UK, p.7–12.

Roberts, A. W., Wensrich, C. M., 2002, Flow dynamics or 'quaking' in gravity discharge from silos, *Chemical Engineering Science 57,* P. 295 – 305.

Roberts, I., 1882, On the Pressure of Wheat Stored in Elongated Cells or Bins, Engineering, 27 October, 399.

Roberts, I., 1884, *Proc. of the Royal Society of London*, January.

Rombach G. A., 1991, Shüttguteinwirkungen auf silozellen –Exzentrische Entleerung, Ph. D. thesis, Karlsruhe University, Karlsrule, Germany.

Rombach, G., 1998, Comparison of existing programs, Chapter 25 in *Silos: Fundamentals of Theory, Behaviour and Design*, (Eds C.J. Brown and J. Nielsen), E & FN Spon, London, pp 584-604.

Rotter J. M., Brown C. J. and Lahlouh E. H., 2002, Patterns of wall pressure on filling a square platform steel silo, *Engineering Structure* 24, 135 – 150.

Rotter, J. M., 1999, Flow and pressures in silo structural integrity assessments, Proc., International Symposium: Reliable Flow of Particulate Solids III, Porsgrunn, Norway, Aug 1999, pp 281-289.

Rotter J. M., Holst J. M. F. G., Ooi J. Y. and Sanad A M., 1998, Silo Pressure Predictions using Discrete-Element and Finite-Element Analyses, *Philosophical Transactions of the Royal Society of London: Series A-Mathemat,*. 356(1747), 2685-2712.

Rotter, J. M., 1998, Challenges for the future in numerical simulation", Chapter 36 in *Silos: Fundamentals of Theory, Behaviour and Design*, (Eds C.J. Brown and J. Nielsen), E & FN Spon, London, pp 584-604.

Rotter, J. M., 1988, Recent Research on the Strength of Circular Steel Silos, Proc., International Conference: 'Silos- Forschung und Praxis', Universitat Karlsruhe, October 1988, 265-286.

Rotter, J. M., 1990, Structural Design of Light Gauge Silo Hoppers, *Journal of Structural Engineering, ASCE*, July 1990, 116 (7), p. 1907-1922.

Rotter, J. M., 1991, Strength Criteria for Steel Silo Structures, Proc., International Conference: Bulk Materials - Towards the Year 2000, Institution of Mechanical Engineers, October 29-31, London, p.1-6.

Rotter, J. M., 1993, The Design of Circular Metal Silos for Strength, Proc., International Symposium: Reliable Flow of Particulate Solids II, EFChE Publication Series No 96, Oslo, August 1993, p.p 217-234.

Rotter, J. M., 1998, Shell Structures: The New European Standard and Current Research Needs, *Thin-Walled Structures*, 31(1-3), 3-23.

Rotter, J. M., Ooi, J. Y., Chen, J. F. Tiley, P. J. and Mackintosh, I, 1995, Flow Pattern Measurement in Full Scale Silos, Research report R95-008, Silo Research Group, The University of Edinburgh,

Rotter, J. M., Pham, L. and Nielsen, J., 1986, On the Specification of Loads for the Structural Design of Bins and Silos, 2nd Int. Conf. Bulk Materials Storage, Handling and Transptn, Institution of Engineers, Australia, Wollongong, July 1986, p. 241-247.

Rotter. J. M., 2001, Guide for the Economic Design of Circular Metal Silos, Spon Press, London & NewYork

Rowe, R. E., 1959, An Investigation into the Cause of Cracking in a Reinforced Concrete Silo Containing Cement, Magazine of *Concrete Research*, 11(32) July, p.65-74.

Ruckenbrod, C. and Eibl J., 1993, Numerical Results to Discharge Processes in Silos, International Symposium - Reliable Flow of Particulate Solids II: Proceedings, Oslo, Norway, 23rd-25th Aug.

Runesson, K. and Nilsson, L., 1986, Finite Element Modelling of the Gravitational Flow of a Granular Material, *Bulk Solids Handling*, 6 (5), p. 877-884.

SAA, 1990, Standards Association of Australia, Loads of Bulk Solid Containers, AS No. 774-, Sydney.

Safarian, S.S. and Harris, E. C., 1985, Design and Construction of Silos and Bunkers, Van Nostrand Reinhold, New York.

Sanad, A.M., et al., 2001, Computations of Granular Flow and Pressures in a Flat-Bottomed Silo, *Journal of Engineering Mechanics-ASCE*, **127**(10), P. 1033-1043.

Savage, S. B., (1979,) Gravity Flow of Cohesionless Granular Materials in Chutes and Channels, *Journal of Fluid Mechanics*, 92, Part 1, pp 53-96.

Schmidt, L. C. and Wu, Y. H., 1989, Prediction of Dynamic Wall Pressures on Silos, *Bulk Solids Handling*, August, 9(3), p. 333-338.

Scholz, V., 1988, Untersuchungen zur Anordnung starrer coaxial Einbauten in Schuttgutbehaltern, Diss., Wilhem-Pieck-Universitat Rostock.

Schwedes, J. and Feise, H., 1993, "Modelling of Pressures and Flow in Silos", International Symposium - Reliable Flow of Particulate Solids II: Proceedings, Oslo, Norway, 23rd-25th Aug., 193-215.

Schwedes, J., 2003, Review on testers for measuring flow properties of bulk solids, *Granular matter* 5, P1-43.

Seville, J. P. K., Martin, T. W. and Parker, D. J., 1995, Particle Velocities in Hopper Discharge Using Positron Emission Particle Tracking, Proc. PARTEC 95, 3rd European Symp. Storage and Flow of Particulate Solids (Janssen Centennial), p.271-280.

Shinohara, K., Idemitsu, Y., Gotoh, K., & Tanaka, T., 1968, Mechanism of gravity flow of particles from Hopper. *Industrial Engineering, Chemistry, Process Design and Development*, 7(3), 378–383.

Smallwood and Thorpe, 1980, Flow of Granular Media, Chemical Engineering Tripos, Undergraduate final year dissertation, University of Cambridge.

Smid J. and Novosad J. 1981, Pressure distribution under heaped bulk solids, in Proc. Of 1981 Powtech Conference, *Ind. Chem. Eng. Symp.* 63, 1-12.

Smid, J., 1975, Pressures of Granular Material on Wall of Model Silo, Collection Czechoslov. Chem. Commun. 4C, 2424-2436.

Socolar J. E. S., Shaeffer D. G. and Claupin P., 2002, Directed force chain networks and stress response in static granular materials, *The European Physical Journal E*, 7, 353-370.

Spencer, A. J. M. and Bradley, 1992, Gravity flow of a granular material in compression between vertical walls and through a tapering vertical channel, *Quarterly Journal of Mechanics and Applied Mathematics*, 45, p, 733-746.

Spencer, A: J. M. and Hill, J. M., 2001, Non-dilatant double-shearing theory applied to granular funnel-flow in hoppers, *Journal of Engineering Mathematics*, 41(1), p. 55-73

Standards Association of Australia (SAA), 1990, Loads of Bulk Solid Containers, AS #774-, Sydney.

Strusch J. and Schwedes J., 1998, Wall stress distributions in silos with inserts, and loads on inserts, in *Silos* ed. By Brown C. J, and Nielsen, J., E & FN, London,

Strusch, J. Lyle, C. and Schwedes, J, 1993, The Influence on the state of stress in silos by insert, reliable flow of particulate solid 2, Oslo, Norway, 727-738.

Sugden, M. B., 1980, Effect of Initial Density on Flow Patterns in Circular Flat-Bottomed Silos, International conference on the design of silos for strength and flow, Lancaster, England.

Sugita, M., 1972, Flow and Pressures of Non-cohesive Granular Materials in Funnel Flow Bins, ASME, September, Paper No. 72-MH-20, No. 8, pp17-20.

Suzuki, M., Akashi, T. and Matsumoto, K., 1985, Flow Behaviour and Stress Conditions in Small and Medium Silos, *Bulk Solids Handling*, 5.

Takahashi, H. and Yanai, H., 1973, Flow Profile and Void Fraction of Granular Solids in a Moving Bed, *Powder Technology* 7, (4), p. 205-214.

Tejchman, J. and Bauer E., 1996, Numerical Simulation of Shear Band Formulation with a Polar Hypo-plastic Constitutive model, *Computers and Geotechnics*, 19, 221-244.

Tejchman, J. and Wu W., 1997, Dynamic Patterning of Shear Bands in Cosserat Continuum, *Journal of Engineering Mechanics-ASCE,* 123(2), 123-133.

Tejchman, J., & Gudehus, G., 1993, Silo music and silo-quake experiments and a numerical cosserat approach, *Powder Technology* 76, 201-212.

Tejchman, J., 2000, Behaviour of Granular Bodies in Induced Shear Zones, *Granular Matter* 2 ,77.

Teng, J. G. and Rotter, J. M., 1991, The Strength of Welded Steel Silo Hoppers under Filling and Flow Pressures, *Journal of Structural Engineering*, ASCE, 117, (9), p.2567-2583.

Theimer, R. 1974, Japanishe Druckversuche in Mehlsilozellen mit Nasenauslauf, Die Muhle und Mischfuttertechnik, 111(11), p. 153-159.

Thornton, C., 1989, Application of DEM to Process Engineering Problems", The 1st US Conference on Distinct Element Method", Golden, Colorado, Oct.

Thornton, C., 1991, Computer Simulated Hopper Flow", 4th World Congress of Chemical Engineering: STRATEGIES 2000, Karlsruhe/Germany 16-21 June.

Turitzin, A.M.. 1963, Dynamic Pressures of Granular Materials in Deep Bins, *J. Structural Division*, ASCE 89, p.49-73

Tuzun U, and Neddermann, R. M., 1985, Gravity flow of granular materials round Obstacles, *Chemical Engineering Science* 40(3), 1. Investigation of the effects of inserts on flow patterns inside a silo, 325-336.; 2. Investigation of the stress profiles at the wall of a silo with inserts, 337-351.

Tuzun, U. and Nedderman, R .M.,1979, A Kinematic Model for the Flow of Granular Materials, *Powder Technology*, March-April, Vol. 22, No. 2, pp 243-253.

Tuzun, U. and Nedderman, R. M., 1979, Experimental Evidence Supporting Kinematic Modelling of the Flow of Granular Media in the Absence of Air Drag, *Powder Technology*, January-February, Vol. 24, No. 2, pp 257-266.

Tuzun, U. and Nedderman, R. M.,1982, An Investigation of the Flow Boundary during Steady-State Discharge from a Funnel Flow Bunker, *Powder Technology*, January-February, 31(1), p. 27-43.

Van Zanten, D.C. and Mooij, A., 1977, Bunker Design - Part 2: Wall Pressures in Mass Flow, *Journal of Engineering for Industry*, ASME, 99, Ser. B, No. 4, pp 814-818.

Van Zanten, D.C., Richards, P.C. and Mooij, A., 1977, Bunker Design - Part 3: Wall Pressures and Flow Patterns in Funnel Flow, *Journal of Engineering for Industry*, ASME, Vol. 99, Ser. B, No. 4, pp 819-823.

Vanel L. and Clement E., 1999, Pressure screening an fluctuations at the bottom of a granular column, *The European Physical Journal B*, 11, P 525-533.

Vanel, L., Claudin, P., Bouchaud, J. P., Cates, M.E., Clement, E., Wittmer, J. P., 2000, Stresses in silos: Comparison between theoretical models and new experiments, *Physical Review Letters*, 84(7), p. 1439-1442

Walker D. M., 1966, An approximate theory for pressure and arching in hopper, *Chemical Engineering Science,* 21, p.975-997.

Walker, D. M. and Blanchard, M. H., 1967, Pressures in Experimental Coal Hoppers, *Chemical Engineering Science*, 22(8), p.1713-1745.

Walters, J. K.,1973, A Theoretical Analysis of Stresses in Silos with Vertical Walls., *Chemical Engineering Science*, 28 (3), 13-21.

Walters, J.K., 1973, A Theoretical Analysis of Stresses in Axially-Symmetric Hoppers and Bunkers, *Chemical Engineering Science*, 28 (3), p.779-89.

Waters, A. J. and Drescher, A., 2000, Modelling plug flow in bins or hoppers, *Powder Technology* 113, 168–175.

Watson, G. R., 1993, Flow Patterns in Flat-Bottomed Silos, PhD thesis, University of Edinburgh, Edinburgh, Scotland.

Watson, G. R., Rotter, J. M., 1996, A Finite Element Kinematic Analysis of Planar Granular Solids Flow, *Chemical Engineering Science*, 51(16), P. 3967-3978.

Wensrich C, 2002, Dissipation, dispersion, and shocks in granular media, *Powder Technology,* 126 (1), JUN, 1-12.

Wensrich, C. M., 2003, Numerical modelling of quaking in tall silos, *International Journal Of Mechanical Sciences* 45 (3): 541-551 MAR

Wieckowski et al., 1999,

Wieckowski, Z., Youn, S. K. and Yeon, J. H., 1999, A particle-in-cell solution to the silo discharging problem, *International Journal for Numerical Methods in Engineering*, 45, 1203-1225.

Wilms, H. and Schwedes, J. ,1985, Analysis of the Active Stress Field in Hoppers, *Powder Technology* 42, 19-23.

Wilms, H., 1985, Calculation of Stresses in Silos by the Method of Characteristics, *Bulk Solids Handling*, 5, 19-23.

Wilms, H., 1986, Homogenisation of Bulk Solids in Silos, 1986, *World Congress Powder Technology*, Nuremberg, Germany, 617-630.

Wilms, H., 1992, Blending Silos – and Overview, *Powder Handling & processing* 44 (3), p. 293-299.

Wittmer J. P., Cates M.. and Claudin, P. 1997, Stress Propagation and Arching in Static Sand-piles, *Journal De Physique I*, 7(1), 39-80.

Wittmer, J. P., Cates, M. E. and Claudin, P., 1997, Stress Propagation and Arching in Static Sand-piles. *Journal De Physique I*,. 7(1): P. 39-80.

Wood, J. G. M., 1983, The Analysis of Silo Structures Subject to Eccentric Discharge, Proc., Second Internat. Conf. on Design of Silos for Strength and Flow, Stratford-upon-Avon, 132-144.

Wu, Y. H. and Schmidt, L.C., 1992, Boundary Element Method for Prediction of Silo Pressure, *Computers and Structures*, 45(5), 315-323.

Zhang, Q. and Ansourian, P.,1990, "Stability of Silo Wall Stiffened by Particulate Solids", 10th Int. Congr. of Chem. Engng, Chem. Equipment Design and Automation, Praha, Czechoslovakia, Aug.

Zhang, Q., Puri, V. M. and Manbeck, H. B., 1986, Finite Element Modelling of Thermally Induced Pressures in Grain Bins Filled with Cohesionless Granular Materials, Trans. ASAE, 29(1), 1, 248-256.

Zhang, Q., Puri, V. M. and Manbeck, H. B., 1989, Finite Element Predicted Static and Thermally Induced Loads in Grain Bins, Trans. ASAE, 32 (6), 2131-2136.

Zhang, Q., Puri, V. M., Manbeck, H. B. and Wang, M. C., 1987, Finite Element Model for Predicting Static and Thermally Induced Bins Wall Pressures", Trans. ASAE, 30 (6), 1797-1806.

Zhong, Z, Ooi, J. Y, Rotter, M., 2001, The sensitivity of silo flow and wall stresses to filling method, *Engineering Structure*, 23, P. 756-767.

Zienkiewicz, O. C. and Taylor, R. L., 2000, The Finite element method, Butterworth-Heinemann.

APPENDIX A

A.1 Some classical analyses for hopper

Some theories have been proposed for the distribution of pressures in conical silo hoppers. The differential slice method, originally used by Janssen for cylindrical silos, was adopted by Walker, Walters etc. to derive theories to describe pressure distributions in conical hoppers. The hopper was assumed to be steep as shown in Fig. A.1 below; the theories developed are usually suitable for both filling and flow cases, distinguished by an active state for the filling and a passive state for discharging.

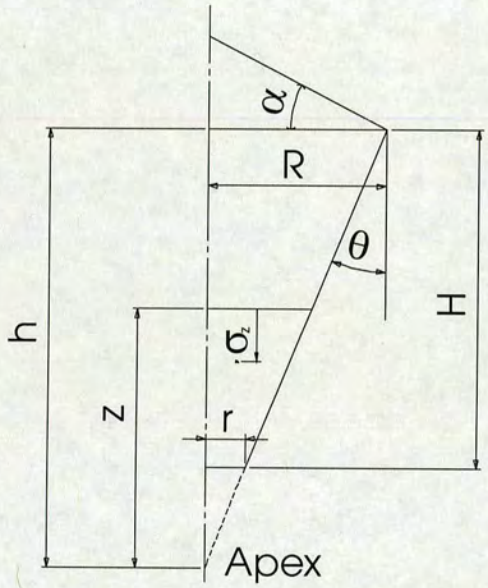

Fig. A.1 Filling pressures on steep conical hopper walls

- Linear assumption: Walker Theory

Based on an assumption made by Janssen that the major principal stress was vertical, Walker developed his pressure theory by differential slice method for hoppers.

For the initial filling/static condition he proposed a hydrostatic distribution of vertical pressure as:

$$\sigma_z = \gamma(h - z) + \sigma_{zi} \qquad A.1$$

where

σ_z: the mean vertical stress at height z above the hopper apex;

h: the vertical height between the hopper apex and the transition;

σ_{zt}: the mean vertical induce by the surcharge, taken as zero in the distributed filling and a value as $\sigma_{zt} = \frac{\gamma R \tan\alpha}{3}$ in the concentric filling, α is the angle of the repose.

Walker assumed that wall friction is fully mobilised in a steep hopper. The normal pressure distribution is given as

$$P_f = F_i \sigma_z \qquad A.2$$

with

$$F_i = \frac{\tan\theta}{\mu + \tan\theta} \qquad A.3$$

where θ is the hopper half angle. Jenike and Johanson reached quite similar results.

- The m approaches

The normal pressures P_f acting on the walls of a conical hopper after filling or storing under symmetrical filling conditions are found using the following equations, based on a generalisation of what is commonly known as Walker's theory:

$$P_f = D\, F_f\, \sigma_z$$

And the frictional traction τ acting along the hopper walls is given by:

$$\tau = \mu\, P_f$$

D is the distribution factor; the F_f is:

$$F_f = \frac{1 + \sin\varphi \cos(\phi_w + \omega)}{1 - \sin\varphi \cos(2\theta + \phi_w + \omega)} \qquad A.4$$

where:

φ: the internal friction angle;

ϕ_w: the wall friction angle;

$$\omega = \sin^{-1}\left(\frac{\sin\varphi}{\sin\phi_w}\right); \qquad A.5$$

$$\mu = \tan\phi_w.$$

The mean vertical stress at height z above the apex of the hopper cone is given by:

$$\sigma_z = \frac{\gamma h}{m-1}\left\{\frac{z}{h} - \left(\frac{z}{h}\right)^m\right\} + \sigma_t\left(\frac{z}{h}\right)^m \qquad A.6$$

where:

γ: the solid unit weight;

h: the vertical height between the hopper apex and the transition;

z: the vertical coordinate upwards from hopper apex;

θ: the hopper half angle;

σ_{zt}: the mean vertical stress impose by the surcharge, a value of zero when distributed filling and a value of $\sigma_{zt} = \frac{\gamma R \tan\alpha}{3}$ with a concentric filling.

And the m takes different values by different approaches.

- The Walker D and m

The distribution factor D, which is the ratio of the vertical stress at the wall to the mean vertical stress at any given level, is assumed by Walker to be unity.

while the m is

$$m = \frac{2B}{\tan\theta} \qquad A.7$$

where:

$$B = \frac{\sin\varphi\sin(\omega - \phi_w - 2\theta)}{1 + \sin\varphi\cos(\omega - \phi_w - 2\theta)} \qquad A.8$$

B is the ratio of vertical shear stress to vertical direct stress at the wall.

- The MacLean m

MacLean, based on the Jenike and Johanson radial stress field solution, suggested the equation derived by Walker for the flow to be used to represent the pressure distribution for initial filling. He recommended that a value of the parameter m should be deduced as

$$m = \frac{2\mu}{\tan\theta} \qquad A.9$$

F_f and D remained the same definitions.

- Walters D

Walters used the same m as Walkers', but extended Walker's analysis to allow non-uniformity D of vertical stresses on a horizontal slice of stored solid. Walters assumed that the entire mass was in a state of plastic failure, the stress state was active during filling and passive during flow; and the vertical shear varied linearly with radius. Walters' assumptions again led to D having a value other than unity.

$$D = \frac{1 + \sin^2\varphi \pm 2\sin\varphi\sqrt{1-c}}{1 + \sin^2\varphi \pm \dfrac{4\sin\varphi\left[1-(1-c)^{3/2}\right]}{3c}} \qquad A.10$$

$$c = \left(\frac{\tan\eta}{\tan\varphi}\right)^2 \qquad A.11$$

$$\eta = \tan^{-1}\left[\frac{\sin\varphi\sin(\phi_w + \omega + 2\theta)}{1 + \sin\varphi\cos(\phi_w + \omega + 2\theta)}\right] \qquad A.12$$

Where alternative positive and negative signs are indicated, the positive sign is used when the initial filling (active) condition is being considered and the negative sign for the flow (passive) condition.

- Rotter suggestions to m and F_f on steep hoppers

Rotter (2001) proposed that, for the filling conditions, the value of F_f may be taken from the experimental data as:

$$F_f = \frac{a\mu + \tan\theta}{\mu + \tan\theta} \qquad A.13$$

where:

a : an empirical constant, taken here as a = 0.8 for filling. Rotter (2001) emphases a = 0.8 gives a reasonable estimate of hopper filling and storing pressures for structural design purposes. Rotter also recommended that the m as:

$$m = \frac{2a\tan\phi_w}{\tan\theta} \qquad A.14$$

A.2 Some classical theories quoted in most common for silo

There are theories to predict silo wall pressures induced by stored material. A brief review of the most quoted theories is given here; they were used in the text for comparison purpose.

- Cylinder section: Janssen and Walker formula

Janssen's original analysis was carried out on a cylindrical bunker containing a cohensionless granular material. He derived that the pressure against the wall being expressed by:

$$\sigma_{rr} = \frac{\gamma D}{4\mu}\left[1 - \exp(-\frac{4\mu kz}{D})\right] + \frac{\gamma Dk}{6}\tan\alpha\exp(-\frac{4\mu kz}{D}) \qquad A.15$$

where γ is the granular material specific weight, [N/m^3], D the silo diameter, [m], $\mu = tan\phi_w$ is the material friction with wall, k is the Janssen constant, defined as:

$$k = \frac{\sigma_{rr}}{\sigma_{zz}} \qquad A.16$$

σ_{zz} is the average vertical stresses along a horizontal plane of z of the cylinder, z is the material height from the top, α is the angle of repose.

Walker improved the Janssen equation to some extent by reconsidering in greater detail the actual stress distribution in the wall region and the cross-section as well by modifying constant k into k_{wa} as in equation (A.17).

$$k_{wa} = \frac{1-\sin\varphi\cos(\omega-\phi_w)}{1+\sin\varphi\cos(\omega-\phi_w)} \qquad A.17$$

$$Where\ \omega = \arcsin\left(\frac{\sin\phi_w}{\sin\varphi}\right)$$

φ the solid internal friction angle.

- Hopper section: Walker, Enstad formulae

Janssen's analysis was extended to the case in the hopper by walker and Enstad. In walker's analysis, it was assumed that the vertical stress is constant across any horizontal cross-section. Using the slice element method, he gave the solution to the pressure acting on the wall as :

$$\sigma_w = (\sigma_{hh})_w \frac{1+\sin\varphi\cos(\omega+\phi_w)}{1-\sin\varphi\cos(\omega+\phi_w+2\theta)} \qquad A.18$$

$$Where\ (\sigma_{hh})_w = \Omega\left\{\frac{\sigma_{rr}}{k}\left(\frac{h}{h_0}\right)^m + \frac{\gamma h}{m-1}\left[1-\left(\frac{h}{h_0}\right)^{m-1}\right]\right\}$$

Ω is a distribution factor as the ratio of the axial stress at the wall and the mean axial stress. σ_{rr} is the result from equation (A.15); h: the height of material measured vertically from the apex of hopper, [m]; h_0: the maximum of h in the hopper, [m].

$$m = \frac{2\sin\varphi\sin(\omega + \phi_w - 2\theta)}{\tan\theta[1 - \sin\varphi\cos(\omega + \phi_w + 2\theta)]} \qquad A.19$$

And θ hopper half angle.

Enstad assumed that the minor principal stress was constant across a spherical surface spanning the hopper, and by effort derived another approximation for pressures in the hopper. Expressed in terms of the mean stress, his solution to pressure induced by material along the wall during flow is given as:

$$\sigma_w = p(1 + \sin\varphi\cos 2\beta) \qquad A.20$$

And

$$p = \frac{\gamma Y r}{X - 1} + \left(\frac{\sigma_{rr}}{k(1 - \sin\varphi)} - \frac{\gamma Y r_0}{X - 1}\right)\left(\frac{r}{r_0}\right)^X . \qquad A.21$$

Where:

$$X = \frac{2\sin\varphi}{1 - \sin\varphi}\left[1 + \frac{\sin(2\beta + \alpha)}{\sin\alpha}\right]$$

$$Y = \frac{\sin\beta\sin^2(\alpha + \beta) + 2[1 - \cos(\alpha + \beta)]\sin\alpha}{(1 - \sin\varphi)\sin^3(\alpha + \beta)}$$

$$\beta = 0.5(\omega + \phi)$$

And r is the height of material measured radically from the apex of hopper along the hopper wall,[m] and r_0 is the maximum of r in the hopper, [m].

APPENDIX B

Based on the principle of transducer, calibrations for the normal force and the friction forces were carefully carried out separately according to the instructions specified by the provider.

The loads were exerted with the extra puller rollers fixed on the special device provided by the transducer manufacturer DEKA Sensor & Technologie GmbH: an known load was imposed on the transmittal bar 1 by roller 1 in the case of the normal force, and on the transmittal bar 2 through a combination of the rollers 1 and 2 in the case of the friction force (Fig. b.1).

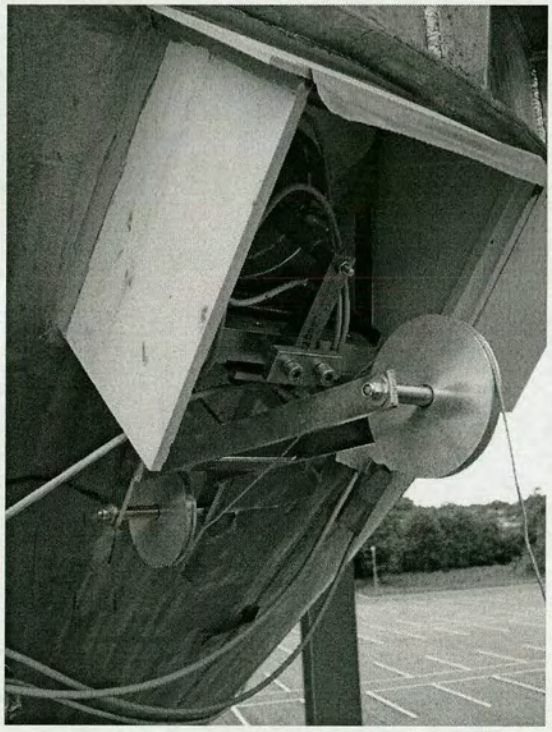

Fig. B.1 The setting up for calibration

The strengths of signal generated by the sensors are linear with the loads on the transmittal bar, the values of the signal measured when there were no load and a 269.8 N load were amplified and converted as input parameters to set up the data logger Hydra, and thereby the transducers were calibrated.

This calibration were then verified by checking up two given loads of 148.1 N and 418.9 N imposed by the same way as that carried out during calibration. The results are shown in Table B.1. One can see that the accuracy of transducers was acceptable, with a maximum error of 5.3 % on M4 on friction force component.

The reader is referred to Wojcik et al. for details (2004).

Table B.1. The result of calibrations

Transducer		Setting up Given loads (N)		Verifications Given loads (N)	Measured loads (N)	Error %	Given loads (N)	Measured loads (N)	Error %
M1	WW	0	269.8	148.1	152.4	3.0	418.9	415.1	0.9
	FF	0	269.8	148.1	141.0	4.7	418.9	over loads	
M2	WW	0	269.8	148.1	144.5	2.3	418.9	415.6	0.8
	FF	0	269.8	148.1	150.5	1.7	418.9	421.8	0.7
M 3	WW	0	269.8	148.1	144.5	2.3	418.9	421.5	0.6
	FF	0	269.8	148.1	151.7	2.5	418.9	416.0	0.7
M 4	WW	0	269.8	148.1	145.2	1.8	418.9	414.3	1.1
	FF	0	269.8	148.1	140.1	5.3	418.9	420.0	0.3
M 5	WW	0	269.8	148.1	146.7	0.8	418.9	422.4	0.8
	FF	0	269.8	148.1	147.5	0.3	418.9	417.6	0.3
M 6	WW	0	269.8	148.1	142.3	3.8	418.9	419.6	0.2
	FF	0	269.8	148.1	151.3	2.3	418.9	414.5	1.0
M 7	WW	0	269.8	148.1	145.6	1.6	418.9	420.4	0.4
	FF	0	269.8	148.1	144.7	2.2	418.9	416.7	0.5
M 8	WW	0	269.8	148.1	140.6	5.0	418.9	419.2	0.1
	FF	0	269.8	148.1	144.1	2.6	418.9	395	5.7
M 9	WW	0	269.8	148.1	145.6	1.6	418.9	417.8	0.3
	FF	0	269.8	148.1	151.8	2.6	418.9	414.2	1.1
M10	WW	0	269.8	148.1	141.2	4.6	418.9	429	2.4
	FF	0	269.8			Channel failure			
WW: Normal force; FF: friction force.					Max err %	5.3			5.7